Epigenetic regulation of lysine acetylation: targeting writers, readers and erasers in cancer

Montserrat Pérez Salvia

UNIVERSITAT DE BARCELONA

EPIGENETIC REGULATION OF LYSINE ACETYLATION: TARGETING WRITERS, READERS AND ERASERS IN CANCER

Memòria Tesi Doctoral

Montserrat Pérez Salvia

Barcelona, 2019

EPIGENETIC REGULATION OF LYSINE ACETYLATION: TARGETING WRITERS, READERS AND ERASERS IN CANCER

Memòria presentada per Montserrat Pérez Salvia per optar al títol de doctor per la Universitat de Barcelona

UNIVERSITAT DE BARCELONA – FACULTAT DE MEDICINA

PROGRAMA DE DOCTORAT EN BIOMEDICINA 2019

Aquesta tesi doctoral ha estat realitzada en el Grup d'Epigenètica del Càncer, dins del Programa d'Epigenètica i Biologia del Càncer (PEBC) de l'Institut d'Investigacions Biomèdiques de Bellvitge (IDIBELL)

Dr. Manel Esteller Badosa

Director i Tutor

Dr. Cátia Moutinho

Co-directora

Montserrat Pérez Salvia

Doctorand

CONTENTS

ABBREVIATIONS

#	
5caC	5-Carboxylcytosine
5fC	5-Formylcytosine
5hmC	5-hydroxymethylcytosine
5mC	5-methylcytosine
A	
Ac-K	Acetyl Lysine
ADN	Ácido desoxirribonucleico
AKT	Serine/threonine kinase
AML	Acute Myeloid Leukemia
AP-1	Activator Protein-1
AR	Androgen receptor
ASCL1	Achaetescute homolog-1
ASH1	Absent, Small, Or Homeotic-Like histone lysine methyltransferase
ATCC	American type culture colection
ATM	Ataxia telangiectasia mutated protein
B	
BAF	BRG1 or hbrm-associated factor
BAX	BCL2-associated X
BCAS1	Breast carcinoma amplified sequence-1
BCL-2	B-cell lymphoma 2
BCL6	B Cell CLL/Lymphoma 6
BER	Base excision repair
BET	Bromodomain and extra terminal
BIM	BCL2 Like 11 (BCL2L11)
BiP	Binding immunoglobulin protein
BPES	Blepharophimosis-ptosis-epicanthus inversus syndrome
BRCA1	Breast cancer 1
BRCA2	Breast cancer 2
BRCT	BRCA1 C-terminal domains
BRD	Bromodomain
BRD2	Bromodomain-containg protein 2
BRD3	Bromodomain-containg protein 3
BRD4	Bromodomain-containg protein 4
BRD7	Bromodomain-containg protein 7
BRD9	Bromodomain-containg protein 9
BRDT	Bromodomain testis associated
BRM	Brahma
BTK	Bruton's tyrosine kinase
C	
CCAT1	Colon cancer associated transcript 1
CCND1	Cyclin D1
CDC25B	Cell Division Cycle 25B
CDC37	Cell division cycle 37
CDH1	E-cadherin

CDK	Cyclin dependent kinases
CDK2	Cyclin-dependent kinase 2
CDK4	Cyclin-dependent kinase 4
CDK6	Cyclin-dependent kinase 6
CDK9	Cyclin Dependent Kinase 9
C-FLIP	FLICE-like inhibitory protein
ChIP	Chromatin Immunoprecipitation
CIMP	CpG island methylator phenotype
CLL	Chronic Lymphocytic Leukemia
CML	Chronic Myelogenous Leukemia
CNS	Central Nervous System
CoA	Coenzyme A
CpG	Cytosine-phosphate-Guanine
CREBBP	cAMP response element-binding protein (CBP/KAT3A)
CRPC	Castration-resistant prostate cancer
CTCL	Cutaneous T-cell lymphoma
CTD	C-terminal repeat domain
D	
DISC	Death inducing signal complex
dMSL	Drosophila Male Specific Lethal
DNA	Deoxyribonucleic acid
DNMT	DNA methyltransferase
DNMT1	DNA Methyltransferase 1
DNMT3A	DNA Methyltransferase 3 Alpha
DNMT3B	DNA Methyltransferase 3 Beta
E	
E2F	E2 factor
EGCG	Epigallocatechin-3-gallate
EGFR	Epidermal growth factor receptor
EMT	Epithelial-to-mesenchymal transition
EP300	E1A-binding protein p300 (p300/KAT3B)
ER	Estrogen receptor
F	
FASL	FAS receptor ligand
FDA	Food and Drug Administration
FISH	Fluorescence in situ hybridisation
FOSL1	FOS Like 1, AP-1 Transcription Factor Subunit
G	
GATA4	GATA-binding protein 4
GATA6	GATA-binding protein 6
GCN5	General control non-repressed protein 5 (KAT2A)
GNAT	GCN5-related N-acetyltransferases
GPS	Genitopatellar syndrome
H	
H2A	H2A histone

H2B	H2B histone
H3	Histone 3
H4	Histone 4
HAT	Histone acetyl transferase
HATi	Histone acetyl transferase inhibitors
HBO1	HAT bound to ORC (KAT7/MYST2)
HCC	Hepatocellular carcinoma
HDAC	Histone deacetylase
HDACi	Histone deacetylase inhibitors
HER2	Human epidermal growth factor receptor 2
HEXIM1	Hexamethylene Bisacetamide Inducible 1
HIF1-α	Hypoxia inducible factor 1 subunit alpha
HMGI(Y)	High Mobility Group isomers I and Y
HMT	Histone methyltransferases
HR	Homologous recombination
Hsp70	Heat Shock Protein 70
Hsp90α	Heat Shock Protein 90 Alpha

I

IC50	Fifty inhibitory concentration
IGF-1R	Insulin-like growth factor 1 receptor
IL-10	Interleukin-10
ING4	Inhibitor Growth 4
ING5	Inhibitor Growth 5
IRF4	Interferon Regulatory Factor 4

J

JAK/STAT	Janus kinase/signal transducers and activators of transcription
JAK2	Janus kinase 2

K

K	Lysine
KAT	Lysine acetyltransferase
KATi	Lysine acetyltransferase inhibitors
KDAC	Lysine deacetylase
KDACi	Lysine deacetylase inhibitors
KMT2A	Lysine Methyltransferase 2A

L

LC/MS-MS	Liquid chromatography-tandem mass spectrometry
LEUTX	Leucine twenty homeobox

M

MBD	Methyl-CpG-binding domain
MBTs	Malignant brain tumour domains
MCL	Mantle Cell Lymphoma
MDM2	Mouse double minute 2 homolog
MLL	Mixed Lineage Leukemia
MLPA	Multiplex ligation-dependent probe amplification
MMTV-PyMT	Mouse mammary tumor virus-Polyoma Virus Middle T

MOF	Males absent on the first (KAT8/MYST1)
MORF	Monocytic leukemia zinc finger protein-related factor (KAT6B/MYST4)
MOZ	Monocytic leukemia zinc finger protein (KAT6A/MYST3)
MSL	Male Specific Lethal
MSL1v1	Male-Specific Lethal 1 Homolog
MTT	(3-(4,5-dimethyl-2-thiazolyl)-2,5-diphenyl-2H-tetrazolium bromide)
MTS	(3-(4,5-dimethylthiazol-2-yl)-5-(3-carboxymethoxyphenyl)-2-(4- sulfophenyl)-2H-tetrazolium)
MYC	Proto-oncogene MYC

N

NF-kB	Nuclear factor of kappa light polypeptide gene enhancer in B-cells 1
NMC	NUT midline carcinoma
NoRC	Nucleolar remodeling complex
NPM1	Nucleophosmin 1
NSCLC	Non-small-cell lung cancer
NSL	Non specific lethal

O

ORC	Origin recognition complex

P

PARP	Poly ADP ribose polymerase
PARPi	Poly ADP ribose polymerase inhibitor
PB1	Polybromo protein (BAF180)
PBAF	Polybromo-associated BAF
PBMCs	Peripheral blood mononuclear cells
PCAF	P300/CBP-associated factor (KAT2B)
PCR	Polymerase chain reaction
PDAC	Pancreatic ductal adenocarcinoma
PDZK1	PDZ domain containing 1
PHDs	Plant homeodomains
PI	Propidium Iodide
PI3K/AKT	Phosphoinositide 3-kinase/ v-akt murine thymoma viral oncogene homolog 1
PR	Progesterone receptor
PTCL	Peripheral T-cell lymphoma
P-TEFb	Positive transcription elongation factor complex
PTM	Post-translational modification
PUMA	p53 upregulated modulator of apoptosis
PWWPs	Pro-Trp-Trp-Pro domains

R

Rb	Retinoblastoma
RNA	Ribonucleic acid
RNAP II	RNA polymerase II

S

SBBYSS	Say-Barber-Biesecker-Young-Simpson syndrome
SCLC	Small Cell Lung Cancer
SGC	Structural Genomic Consortium

shRNA	short-hairpin RNA
SIRT	Sirtuins
SMARCA2	SWI/SNF Related, Matrix Associated, Actin Dependent Regulator Of Chromatin, Subfamily A, Member 2 (BRM)
SMARCA4	SWI/SNF Related, Matrix Associated, Actin Dependent Regulator Of Chromatin, Subfamily A, Member 4 (BRG1)
Snail	Snail Family Transcriptional Repressor 1 (SNAI1)
SNP	Single nucleotide polymorfism
Slug	Snail Family Transcriptional Repressor 2 (SNAI2)
SRM	Selected reaction monitoring
SWI/SNF	Switch mating type/sucrose nonfermenting
T	
TDG	Thymine-DNA-glycosylase
TET	Ten-eleven translocation
TFGβRII	Transforming growth factor receptor II
TIF2	Transcriptional Intermediary factor 2
TIP5	TTF-1-interacting protein-5
Tip60	HIV Tat-interacting protein of 60 kDa (KAT5)
TNBC	Triple Negative Breast Cancer
TP53	Tumor protein p53
TRAIL	TNF-related apoptosis-inducing ligand-receptor
TRIM24	Tripartite motif-containing 24
TSA	Trichostatin A
U	
UPR	Unfolded protein response
V	
VHL	von Hippel-Lindau tumor suppressor
W	
WB	Western-Blot
X	
XBP-1	X-box binding protein 1
Z	
ZEB1/2	Zinc Finger E-Box Binding Homeobox 1/2
ZnF	Zinc Finger

SUMMARY IN SPANISH

INTRODUCCIÓN

El cáncer es el término que designa un conjunto de enfermedades caracterizadas por poseer células con una división incontrolada que presentan también la capacidad de extenderse a otras partes del organismo invadiendo otros tejidos (metástasis) [1].

En la actualidad, el cáncer se define como una enfermedad genética y epigenética. El concepto de epigenética fue introducido por primera vez por C.H. Waddington en 1939 [2] y posteriormente fue redefinida como los cambios heredables en la expresión génica que tienen lugar sin alteración en la secuencia del ADN [3]. En general, la epigenética consiste en diversos procesos biológicos que modifican el estado de la cromatina desde un estado abierto (eucromatina) a un estado cerrado (heterocromatina) regulando así el acceso de las diferentes maquinarias moleculares involucradas en procesos relacionados con el ADN. De esta manera se modula qué genes son expresados o inhibidos. Los mecanismos epigenéticos más estudiados son la metilación del ADN y la modificación covalente de histonas.

La presencia de alteraciones epigenéticas es común en cáncer. Es frecuente la metilación aberrante del ADN así como alteraciones en las marcas de histonas, sin olvidar las alteraciones (mutaciones, deleciones, amplificaciones…) que afectan a las enzimas reguladoras de estas marcas [4].

Los tejidos tumorales se caracterizan por tener patrones de metilación del ADN diferentes a los tejidos sanos. En tumores se ha descrito la existencia de una hipometilación global del genoma, y a su vez, la inactivación de genes supresores tumorales como consecuencia de la hipermetilación de sus regiones promotoras en las zonas denominadas “islas CpG” [5].

Las modificaciones covalentes de histonas son variadas, incluyendo la metilación, acetilación, fosforilación, ubiquitinación entre otras, siendo las dos primeras las más estudiadas. Las marcas de histonas juegan un papel importante en la transcripción y reparación del ADN. Estas marcas están involucradas en modificar el estado de empaquetamiento de la cromatina, así como en el reclutamiento en sitios específicos de otras proteínas implicadas en procesos del ADN. En general, altos niveles de acetilación están relacionados

con cromatina abierta y transcripición activa. Sin embargo, las marcas de metilación pueden provocar la activación o la represión de la transcripción, dependiendo del residuo y de la posición. Así la metilación de los residuos H3K4, H3K36 y H3K79 están relacionadas con activación de la transcripción, mientras que la metilación de H3K9, H3K27 y H4K20 están ligadas a la inhibición de la transcripción [6]. Las marcas de histonas tienen una enorme complejidad dadas las múltiples posiciones y modificaciones posibles, formando así el denominado "código de histonas". Además actúan muchas veces de forma cooperativa o dependiente del contexto celular y del tejido [7].

La acetilación, eje central de esta tesis, está regulada por tres grupos de enzimas denominadas escritoras, lectoras y borradoras: 1) las Histonas Acetiltransferasas (HATs) son las responsables de añadir grupos acetilo en las lisinas (escritoras); 2) las Histonas deacetilasas (HDACs) son las que quitan estos grupos acetilos (borradoras) y 3) los bromodominios son los que actúan como lectores, uniéndose a grupos acetilo y reclutando diversa maquinaria molecular a sitios específicos de la cromatina. Las alteraciones en estos reguladores epigenéticos son comunes en cáncer.

Es importante destacar que las HATs y las HDACs también pueden regular la acetilación de proteínas diferentes a las histonas, pero que son también muy importantes en cáncer como *tumor protein p53* (TP53) o *MYC Proto-Oncogene* (MYC) [8].

Una de las ventajas de la epigénetica frente a la genética es la naturaleza reversible de las marcas epigéneticas. Esto ha llevado en los últimos años a un creciente interés por la investigación de fármacos específicos capaces de modular y corregir los defectos epigenéticos presentes en tumores. De hecho, hay seis fármacos epigenéticos que se utilizan actualmente en clínica para el tratamiento de tumores hematológicos. Son dos inhibidores de ADN metiltransferasas y cuatro inhibidores de HDACs [9]. Además, actualmente hay múltiples ensayos clínicos con fármacos dirigidos contra enzimas escritoras, lectoras y borradoras del epigenoma.

OBJETIVOS

Teniendo en cuenta el contexto científico explicado en el apartado anterior, el objetivo general de esta tesis doctoral es el estudio de reguladores epigenéticos involucrados en la acetilación de histonas y otras proteínas en cáncer, así como su tratamiento con inhibidores específicos. Nuestra hipótesis consiste en que un estudio profundo de nuevas alteraciones o de la función de estos reguladores epigenéticos abrirá nuevas posibilidades de tratamiento. Además, también pretendemos estudiar cómo afecta su inhibición con fármacos específicos al fenotipo tumoral en diferentes tipos de cáncer.

Para ello, el proyecto fue dividido en tres líneas de estudio, marcando para cada una de ellas objetivos específicos.

Estudio I:

1. **Investigar el papel de la histona acetil transferasa KAT6B en cáncer de pulmón de células pequeñas *(Small Cell Lung Cancer, SCLC).***

1.1. Estudiar nuevas alteraciones genéticas en el gen *KAT6B* en SCLC y sus consecuentes cambios en su función proteica.

1.2. Examinar el fenotipo *in vitro* e *in vivo* causado por la alteración de KAT6B.

1.3. Estudiar los mecanismos moleculares responsables del fenotipo causado por las alteraciones en KAT6B.

1.4. Evaluar si los tumores con alteraciones en KAT6B muestran especial sensibilidad a algún fármaco epigénetico o quimioterapéutico.

Estudio II:

2. **Evaluar las implicaciones moleculares del tratamiento con el inhibidor de bromodominios JQ1 en cáncer de mama.**

2.1. Investigar el efecto de JQ1 en líneas celulares humanas de cáncer de mama luminal

2.2. Explorar qué genes están involucrados en el efecto del fármaco JQ1.

2.3. Comprobar la eficacia del tratamiento con JQ1 *in vivo* en un modelo murino de cáncer de mama luminal.

Estudio III:

3. Estudiar un nuevo inhibidor de HDAC6 (QTX125) en cáncer.

3.1. Estudiar la especificidad del nuevo compuesto QTX125 hacia HDAC6 y su proteína diana α-Tubulina.

3.2. Interrogar la potencia antitumoral de QTX125 en líneas celulares de cáncer humano.

3.3. Estudiar el efecto de QTX125 en apoptosis en líneas celulares de linfoma de células del manto *(Mantle Cell Lymphoma, MCL)*.

3.4. Investigar la eficacia de QTX125 *in vivo* en MCL.

3.5. Evaluar el efecto de QTX125 en sangre procedente de donantes sanos y en muestras primarias de pacientes de MCL.

MATERIALES Y MÉTODOS

Estudio I

Para estudiar posibles alteraciones en el número de copias de reguladores de histonas y así detectar la deleción génetica de *KAT6B* testamos diez líneas celulares humanas de SCLC utilizando el Illumina Infinium HumanOmni5 microarray, que interroga 4,301,332 polimorfismos de un solo nucleótido (SNPs) en cada muestra. Después validamos esta deleción mediante varias técnicas moleculares: reacción en cadena de la polimerasa (PCR) cuantitativa de ADN genómico, *multiplex ligation-dependent probe amplification (MLPA)* e hibridación fluorescente *in situ* (FISH). Para comprobar que esta deleción se traducía en una ausencia de ARN mensajero (mARN) y de proteína de KAT6B utilizamos PCR cuantitativa (qPCR) y Western-Blot (WB).

A continuación, para estudiar el fenotipo tumoral causado por la ausencia de KAT6B, realizamos el silenciamiento mediante *short-hairpins (shRNAs)* del gen en líneas celulares que no tenían la deleción estudiada. Con estos modelos de silenciamiento, estudiamos el crecimiento tumoral mediante ensayos de *MTT (3-(4,5-dimethyl-2-thiazolyl)-2,5-diphenyl-2H-tetrazolium bromide)*, donde se mide mediante colorimetría el porcentaje de células vivas y realizamos también ensayos de crecimiento de colonias. Para explorar el fenotipo tumoral causado por KAT6B *in vivo* realizamos tres tipos de experimentos: 1) *xenograft*, se

implantan en el ratón células tumorales de líneas celulares de SCLC (con el gen silenciado o controles), 2) ortotópico, se implanta un pequeño fragmento del tumor (procedente del tumor desarrollado en el *xenograft*) en el órgano correspondiente en el ratón, en este caso en el pulmón, 3) modelos de diseminación, se inyectan células tumorales en el bazo del ratón, y posteriormente se analiza la formación de metástasis en otros órganos como el hígado.

Para describir de forma cualitativa la posición de acetilación de KAT6B, sometimos a análisis por cromatografía líquida acoplada a espectrometría de masas en tándem (LC/MS-MS) la histona H3 digerida y extraída de una línea celular en la que sobre-expresamos KAT6B. Para confirmar la marca obtenida de forma cuantitativa utilizamos la técnica *Selected Reaction Monitoring (SRM).* Está basada en la espectrometría de masas y nos permite cuantificar la acetilación en péptidos (posiciones) concretos. La marca obtenida de acetilación mediante estas dos técnicas fue también validada mediante WB.

Comprobamos en muestras de pacientes de SCLC la existencia de la deleción de KAT6B mediante MLPA. También realizamos inmunohistoquímica en estas muestras observando la tinción de KAT6B y de H3K23Ac. A continuación, para testar si la pérdida de KAT6B confería especial sensibilidad a algún fármaco, utilizamos los modelos de silenciamiento *in vitro*. Calculamos la concentración inhibitoria media (IC50) mediante el ensayo con MTT, optimizando previamente el rango de concentraciones de droga, tiempo de exposición y número de células sembradas. Con irinotecán, la droga que presentaba diferencias de sensibilidad, realizamos un ensayo *in vivo* utilizando el modelo ortotópico anteriormente explicado.

Estudio II

Realizamos ensayos de sensibilidad al fármaco JQ1 calculando la IC50 mediante MTT en líneas celulares humanas de cáncer de mama luminal. Los niveles de mRNA y proteína de C-MYC *y Bromodomain-containg protein 4* (BRD4) los medimos mediante qPCR y WB.

Para la búsqueda de otros genes implicados en el efecto inhibitorio de JQ1, realizamos un Array de Expresión en el que interrogamos la expresión de 36.712 genes en dos líneas celulares tratadas con 1 μM de JQ1 durante 24h y comparándolas con las mismas líneas celulares no tratadas. Los resultados del array los validamos mediante qPCR.

Para analizar la contribución al fenotipo tumoral de los genes seleccionados en el Array, realizamos el silenciamiento mediante shRNAs en líneas celulares de cáncer de mama luminal y medimos la proliferación celular mediante ensayos de MTT. También realizamos ensayos de sensibilidad a JQ1 en los modelos de silenciamiento, calculando la IC50 con MTT.

En los experimentos *in vivo* con JQ1 utilizamos el modelo murino de cáncer de mama luminal *MMTV-PyMT (mouse mammary tumor virus-Polyoma Virus Middle T)*. Es un modelo de ratón transgénico cuyas hembras desarrollan espontáneamente tumores de mama a las cuatro semanas de edad. Para el tratamiento curativo, cuando los ratones tenían una suma de sus tumores entre 1000-2700 mm^3 los dividimos de forma aleatoria en dos grupos: 1) el grupo de tratamiento (n=8), al que administramos 11 dosis (25 mg/kg) de JQ1, 2) el grupo control (n=8), al que administramos solo el vehículo del fármaco. Medimos los tumores de los ratones cada 2-3 días hasta la finalización del experimento (2 días después de la última dosis). En el tratamiento preventivo, empezamos a tratar los ratones cuando todavía no tenían tumores visibles ni palpables. Los dividimos también en dos grupos: tratados (n=5) y vehículo (n=7). Les administramos JQ1 (25 mg/kg) durante tres semanas en un régimen de 5 días de tratamiento y 2 días de descanso, y el volumen de los tumores fue monitorizado hasta que la suma de todos los tumores de cada animal era de 4000mm^3. Alcanzado este volumen, los animales fueron sacrificados. Así calculamos el tiempo de supervivencia de ambos grupos representando una curva de Kaplan-Meier.

Estudio III

En este estudio testamos la capacidad antitumoral del nuevo fármaco mediante el cálculo de IC50 con MTS, ensayo basado en el mismo fundamento que el

MTT, en 48 líneas celulares de tumores humanos. La acetilación de la α-tubulina la medimos mediante Western Blot.

Para medir si el tratamiento con QTX125 inducía apoptosis en las líneas celulares utilizamos dos técnicas diferentes: WB de varias Caspasas y PARP y citometría de flujo mediante tinción de las células con Annexina V y Ioduro de Propidio (IP).

En los experimentos *in vivo*, administramos el fármaco a dos modelos *xenograft*, inyectados con dos líneas celulares de MCL. Se dividió a los ratones en cuatro grupos de tratamiento de n=8: 1) vehículo; 2) QTX125 (60 mg/kg) en régimen 5 días de tratamiento/ 2 días de descanso durante 4 semanas; 3) QTX125 (60 mg/kg) diariamente durante 4 semanas y 4) ciclofosfamida (100mg/kg durante 5 días).

Finalmente testamos el fármaco en células primarias extraídas del nódulo linfático de dos pacientes de MCL. Calculamos la IC50 midiendo el porcentaje de células vivas utilizando citometría de flujo (AnnV/PI negativas). Para testar QTX125 en sangre de donantes sanos, realizamos la extracción de las células mononucleares de sangre periférica (PBMCs) de capas leucocitarias de estos donantes mediante una centrifugación con gradiente de Ficoll. Utilizando anticuerpos específicos separamos los CD19+ (linfocitos B) y los CD3+ (linfocitos T) mediante citometría de flujo. En estas tres poblaciones calculamos también la IC50 midiendo el porcentaje de células vivas por citometría de flujo.

RESULTADOS

Estudio I

En este estudio describimos la deleción homocigota de la histona acetiltransferasa *KAT6B* en 2 de 10 (20%) líneas celulares de SCLC estudiadas. Después comprobamos que la expresión de KAT6B tanto a nivel de mRNA como de proteína era nula en las dos líneas celulares portadoras de la dicha deleción.

A continuación, investigamos el papel que jugaba KAT6B en el fenotipo tumoral. Observamos que el silenciamiento de la expresión de KAT6B en dos líneas celulares que poseían originalmente las dos copias del gen, les confería

propiedades tumorales. Mostraban un mayor crecimiento celular y la formación de mayor número de colonias que las células no silenciadas (controles). Observamos un comportamiento similar *in vivo*. Los ratones con células de SCLC con KAT6B silenciado desarrollaron tumores de mayor volumen que los ratones con células control, tanto en modelos *xenograft* como ortotópicos. Se observó también *in vivo* que el silenciamiento de KAT6B producía mayor número de nódulos metastásicos en el hígado.

Después, buscamos qué marcas de acetilación podía estar catalizando KAT6B en la histona H3, hasta ese momento no descritas. Obtuvimos que en células donde sobre-expresamos KAT6B se produce una mayor acetilación de la lisina 23 en la histona H3. Dicha acetilación fue también validada mediante WB en los modelos de silenciamiento.

Identificamos que la deleción homocigota de *KAT6B* también ocurría en 8 de 60 (13%) tumores humanos de SCLC. Y analizando los pacientes de los que disponíamos de datos clínicos, observamos que dicha deleción correlacionaba con un menor tiempo de supervivencia.

A continuación, nos preguntamos si la pérdida de KAT6B confería una especial sensibilidad hacia algún fármaco anticancerígeno. Cuando tratamos las líneas celulares silenciadas y las controles con múltiples inhibidores de HDACs, y los fármacos quimioterapéuticos comunes en el tratamiento de SCLC (cisplatino y etopósido), no observamos con ninguno de ellos diferencias de sensibilidad. Sin embargo, las células silenciadas resultaron ser más sensibles a irinotecán. Trasladamos estos resultados a nuestro modelo ortotópico *in vivo*, donde confirmamos que los ratones cuyos tumores tenían KAT6B silenciado eran también más sensibles a irinotecán.

Estudio II

Inicialmente comprobamos que líneas celulares de cáncer de mama de tipo luminal eran sensibles al fármaco JQ1, inhibidor de bromodominios. Esta inhibición del crecimiento estaba ligada a un ya descrito silenciamiento de C-MYC tanto a nivel transcripcional como proteico. Sin embargo, los niveles de BRD4 gen diana del fármaco, no se vieron alterados.

A continuación, buscamos qué genes además de C-MYC podían estar implicados en el efecto de inhibición de crecimiento celular inducido por JQ1. Cuando realizamos un Array de expresión comparando dos líneas celulares de cáncer de mama luminal tratadas con JQ1 con las mismas líneas tratadas con vehículo, obtuvimos 1149 genes de los 36712 (3.1%) interrogados por el Array que cambiaban significativamente. De ellos, 420 (36.6 %) presentaban una mayor expresión, mientras 729 (63.4%) estaban silenciados de forma común en ambas líneas celulares tratadas con el fármaco. En este segundo grupo es donde se encuentran los posibles genes diana de JQ1. De entre los candidatos con menor expresión, nos centramos en *PDZ domain containing 1 (PDZK1)* y *breast carcinoma amplified sequence-1 (BCAS1)*, por su descrita implicación en cáncer de mama. Comprobamos que el silenciamiento de la expresión de estos dos genes en nuestras líneas celulares estudiadas causaba un incremento de la proliferación celular, comportándose por tanto como oncogenes. Queríamos también comprobar si el silenciamiento de estos genes causaba alguna diferencia en la sensibilidad al fármaco. Para ello comparamos el crecimiento de las células silenciadas para PDZK1, BCAS1, y también C-MYC por separado, con las células control bajo los efectos del tratamiento con JQ1. Sin embargo, observamos que la inhibición del crecimiento era igual en ambas condiciones. Además, la inhibición del crecimiento causada por el fármaco era mucho mayor que la causada únicamente por el silenciamiento de estos genes.

Finalmente, testamos el fármaco *in vivo* en un modelo murino de cáncer de mama de tipo luminal (MMTV-PyMT) de manera curativa y preventiva. En el tratamiento curativo, observamos que los ratones tratados con JQ1 desarrollaban tumores de menor volumen que los tratados con vehículo (controles). En el tratamiento preventivo, los ratones tratados con JQ1 tuvieron un mayor tiempo de supervivencia que los ratones no tratados.

Estudio III

En este estudio nuestros colaboradores de Quimatryx y la Universidad del País Vasco sintetizaron un compuesto (QTX125) que mostró ser selectivo para la histona deacetilasa HDAC6 frente al resto de HDACs en un estudio de actividad enzimática. Nosotros observamos que funcionaba como anticancerígeno en 48

líneas celulares de varios tipos de cáncer humano, que incluía tanto tumores sólidos como hematológicos. Sin embargo, el efecto fue especialmente potente en linfoma de Burkitt, linfoma folicular y linfoma de las células del manto (MCL) y decidimos centrar el estudio en MCL. En cuatro líneas celulares de este tipo de linfoma comprobamos la inhibición de HDAC6 que ejercía el fármaco observando después del tratamiento una hiperacetilación de α-tubulina, que es un conocido gen diana de HDAC6.

A continuación, comprobamos que la inhibición de crecimiento celular causada QTX125 estaba asociada con la inducción de apoptosis. El tratamiento inducía un clivaje de caspasas (Caspasa-9, Caspasa-8 y Caspasa-3) y PARP.

Después *in vivo*, administramos el fármaco en dos modelos murinos *xenograft*, inyectados con líneas celulares de MCL. En ambos experimentos, los ratones tratados con QTX125 desarrollaron tumores más pequeños que los ratones tratados con vehículo (controles).

Finalmente, testamos el fármaco en células primarias extraídas del nódulo linfático de dos pacientes con MCL. Comprobamos que QTX125 a bajas dosis reducía la viabilidad celular. Entonces, probamos el efecto del fármaco en sangre de cuatro donantes sanos. Extrajimos PBMCs, y los separamos en CD19+ (linfocitos B) y CD3+ (linfocitos T). Observamos que todas las poblaciones celulares procedentes de sangre sana eran más resistentes al fármaco que las células de pacientes o las líneas celulares.

DISCUSIÓN

En el **estudio I** describimos por primera vez la deleción homocigota del gen *KAT6B* en cáncer de pulmón de célula pequeña. Este subtipo de cáncer de pulmón es muy agresivo y metastásico. Inicialmente responde bien a la quimioterapia, pero en la mayoría de los casos existe una recaída, siendo alta su mortalidad. Es conocida la inactivación de los genes supresores tumorales *TP53* y *proteína del retinoblastoma (RB1)* en un alto porcentaje de casos de SCLC [10], así como la más reciente descripción de mutaciones en enzimas reguladoras de histonas como *CREB-binding protein (CREBBP), EP300* y *KMT2A (Lysine Methyltransferase 2A (KAT2A/MLL)* [11]. Estos descubrimientos,

así como la necesidad de nuevos avances en el tratamiento de este tipo de cáncer, nos llevaron a investigar posibles alteraciones en genes codificantes para modificadores de histonas, encontrando esta deleción en una Histona acetil transferasa (HAT).

Además, descubrimos que la deleción genética de este regulador epigenético de la acetilación de histonas confiere a las células un fenotipo tumoral más agresivo. Es por tanto un gen supresor tumoral en SCLC. Son pocos los estudios existentes de este gen en cáncer y su función no había sido descrita anteriormente en SCLC.

Todas las demás proteínas de la familia MYST tenían una o varias marcas de acetilación descritas, excepto KAT6B [12]. En este estudio describimos que cataliza la acetilación de la lisina 23 de la Histona H3. Curiosamente, durante la revisión de este trabajo, fue publicado un estudio que reportaba que la proteína KAT6 Enok en *Drosophila*, con alta similitud a KAT6B, también catalizaba esta marca [13]. Además, CREBBP y EP300, mutadas en SCLC, son otras dos HATs que igualmente catalizan esta marca. Estos hechos sugieren que H3K23Ac puede estar jugando un papel importante en este tipo de cáncer [14].

Nos centramos también en buscar un fármaco al que la deleción de KAT6B causará un incremento de sensibilidad. En cáncer de pulmón de células no pequeñas, han sido aprobados inhibidores de EGFR porque la mutación de dicho receptor sucede en más del 60% de los casos [15]. En SCLC no hay ninguna terapia contra una alteración genética o epigenética y sería muy interesante encontrarla. Esto ocurre porque hay pocas alteraciones descritas, y las que hay son en genes supresores de tumores. Un fármaco contra la activación de un oncogén es más fácil de conseguir que uno que consiga la reactivación de un gen ausente o inactivado como pasa en SCLC. En nuestro trabajo encontramos que las células con KAT6B silenciado eran más sensibles a irinotecán. Nuestra hipótesis del posible mecanismo se basa en que la sobre-expresión de la familia MYST a la que pertenece KAT6B ha sido relacionada con la inducción del gen *ataxia telangiectasia mutado (ATM)* implicado en la reparación del daño al ADN y fosforilación de γH2AX, marca de daño en el ADN [16]. Posiblemente, los niveles más bajos de ATM que observamos en células con KAT6B silenciado incremente su sensibilidad a irinotecán, al ser las células menos capaces de

reparar el daño en el DNA que induce este agente quimioterapéutico. El irinotecán es utilizado en clínica para tratar el cáncer de colon y se encuentra en ensayos clínicos en SCLC como segunda línea de tratamiento. Nuestros resultados sugieren que los pacientes que presenten una deleción en KAT6B podrían beneficiarse de este tratamiento como primera línea, dado que presentarían una mayor sensibilidad al mismo.

En el **Estudio II**, investigamos el efecto del fármaco inhibidor de bromodominios JQ1 cáncer de mama de tipo luminal. Este tipo de cáncer de mama es el más común, y existe la necesidad de encontrar nuevos tratamientos, ya que es frecuente la aparición de resistencia. Encontramos que las líneas celulares seleccionadas de este tipo de cáncer respondían al fármaco y lo hacían con una bajada del oncogén C-MYC y sin modificar los niveles de BRD4. Estos resultados están en concordancia con otros estudios publicados [17, 18].

Además, identificamos con un Array de Expresión dos genes, *PDZK1* y *BCAS1*, implicados en la respuesta al tratamiento con JQ1. Nuestro interés en ambos genes fue porque están descritos como oncogenes en cáncer de mama [19, 20]. En nuestras líneas celulares también se comportaban así, ya que al silenciarlos observamos que incrementaba la proliferación celular. Otro de nuestros objetivos era probar si alteraciones en alguno de estos genes podían ser utilizados como biomarcadores predictivos de tratamiento, al conferir una diferente sensibilidad a JQ1. Para ello silenciamos PDZK1, BCAS1 y también C-MYC en nuestras líneas celulares y medimos si eran más sensibles o más resistentes al tratamiento que las células control. El resultado que obtuvimos fue que JQ1 causaba una disminución del crecimiento celular hasta niveles muy bajos, pero sin diferencias entre ambas condiciones. Además, la inhibición de la proliferación era mayor con el tratamiento que con el silenciamiento de un único gen. Estos resultados sugieren que JQ1 ejerce un potente efecto antitumoral inhibiendo la transcripción de muchos genes de forma global. El silenciamiento únicamente de estos genes, a pesar de ser oncogenes en nuestro sistema, no confiere una diferencia de sensibilidad, ni siquiera el silenciamiento de C-MYC, que es un conocido y potente oncogén que regula muchos otros genes en cáncer.

Respecto al uso JQ1 *in vivo*, el tratamiento curativo mostró que JQ1 es capaz de disminuir el volumen tumoral. Y el tratamiento preventivo incrementó el tiempo

de supervivencia. Estos resultados sugieren que este fármaco podría ser administrado en pacientes con mutaciones en los genes *Breast cancer 1 (BRCA1) y Breast cancer 2 (BRCA2)* que indican un alto riesgo de desarrollar cáncer de mama. De hecho, hay un estudio reciente que muestra que la existencia de deficiencias en BRCA1 incrementa la sensibilidad a inhibidores de bromodominios [21]. Además, estos inhibidores también hacen sinergia con inhibidores de PARP, aprobados para el tratamiento de cáncer de mama y ovario con mutaciones en BRCA1/2. Los inhibidores de PARP causan daño en el ADN. Esta sinergia se basa en que los inhibidores de bromodominios parecen inducir la bajada de expresión de genes involucrados en mecanismos de reparación daño al ADN [22].

En el **estudio III,** testamos un nuevo inhibidor específico de HDAC6 (QTX125) en múltiples líneas celulares de cáncer humano. Nos centramos en linfoma de células del manto (MCL), primero porque detectamos una extrema sensibilidad a QTX125, y segundo porque para este tipo de linfoma no existe una cura efectiva actual. Además, el hecho de que este fármaco sea selectivo para una única HDAC (HDAC6), probablemente evite indeseados efectos secundarios, que ya se han observado en algunos de los inhibidores no específicos de HDACs aprobados en clínica.

HDAC6 está localizada principalmente en el citoplasma y deacetila proteínas como la α-Tubulina, cortactina y Hsp90. HDAC6 juega un importante papel en cáncer participando en la regulación de la dinámica del citoesqueleto, la movilidad celular y la degradación proteica mediante la formación de agresomas [23]. Comprobamos que este nuevo inhibidor de HDAC6 inducía la hiperacetilación de su proteína diana más conocida, la α-Tubulina. Y observamos que su efecto antimoral venía ligado a una inducción de muerte celular por apoptosis. Nuestra hipótesis del posible mecanismo de acción de este fármaco se basa en estudios publicados con otros inhibidores de HDAC6 en otro tipo de linfomas [24]. La inhibición de HDAC6 podría estar impidiendo la degradación proteica inhibiendo la formación de agresomas. Esto causaría un incremento del estrés celular por acumulación de proteínas mal plegadas que terminaría con la inducción de la muerte celular por apoptosis con previa cascada de Capasas, que nosotros observamos. En el tratamiento de linfomas la inhibición de

mecanismos de degradación proteica, que son principalmente proteasoma y agresoma, está tomando especial relevancia. Esto se debe a que los linfomas tienen de forma fisiológica una respuesta a proteínas desplegadas *(UPR, unfolded protein response)* elevada debido a que los linfocitos realizan una mayor síntesis de proteína necesaria para la producción de altos niveles de anticuerpos requeridos por la respuesta inmune [25]. Algo similar ocurre en mieloma múltiple, y por ello se han aprobado recientemente inhibidores de proteasoma para su tratamiento [26].

Tuvimos la oportunidad de testar el fármaco en células primarias extraídas de nódulos linfáticos de pacientes de MCL y comprobar que también inducía apoptosis a bajas dosis. Sin embargo, PBMCs, células CD19+ (linfocitos B) y CD3+ (linfocitos T) de sangre de donantes sanos eran más resistentes al fármaco. Estos resultados son muy esperanzadores de cara a la posible futura aplicación en clínica de este fármaco.

Actualmente hay un fármaco inhibidor de HDAC6 (Ricolinostat) en ensayos clínicos en múltiple mieloma y otros linfomas. Y concretamente en MCL, existen ensayos clínicos con bortezomib, un inhibidor de proteasoma con buenos resultados. El bortezomib ha mostrado sinergia con inhibidores de HDAC6 en mieloma múltiple debido a la inhibición simultánea de las dos vías principales de degradación proteica, el proteasoma y los agresomas [27]. Por tanto, sería interesante realizar más experimentos para explorar la posible futura aplicación en clínica en MCL de QTX125 en MCL refractario solo o en combinación con bortezomib.

CONCLUSIONES

Basándonos en los resultados obtenidos, las conclusiones de esta tesis doctoral son:

Estudio I:

- La Histona Acetil transferasa *KAT6B* se encuentra delecionada de forma homocigota en cáncer de pulmón de células pequeñas (SCLC).
- En SCLC, KAT6B tiene un papel antitumoral *in vitro* e *in vivo*.

- KAT6B actúa como una histona acetil transferasa en la lisina 23 de la histona H3, siendo la primera posición de acetilación descrita de esta proteína.
- La deleción de KAT6B predice una elevada sensibilidad a irinotecán en SCLC.

Estudio II:

- JQ1 inhibe el crecimiento tumoral en cáncer de mama luminal *in vitro* e *in vivo.*
- JQ1 ejerce su efecto antitumoral mediante la inhibición de la expresión de C-MYC, PDZK1 y BCAS1 en líneas celulares de cáncer de mama.
- JQ1 provoca una mayor inhibición de la proliferación celular que el silenciamiento de C-MYC, PDZK1 o BCAS1 por separado.
- JQ1 administrado como tratamiento curativo está asociado con el desarrollo de tumores más pequeños en un modelo murino de cáncer de mama luminal.
- Como tratamiento preventivo, JQ1 aumenta la supervivencia y retrasa la aparición de tumores en un modelo murino de cáncer de mama luminal

Estudio III:

- QTX125 muestra una elevada especificidad por HDAC6 frente a otras histonas deacetilasas (HDAC1-11)
- QTX125 es un nuevo inhibidor de HDAC6.
- QTX125 incrementa los niveles de acetilación de α-Tubulina de una forma dosis-dependiente.
- QTX125 tiene un efecto antitumoral en 48 líneas celulares de cáncer humano.
- Las líneas celulares de linfoma de células del manto (MCL) son muy sensibles a QTX125.
- QTX125 induce apoptosis mediante el clivaje de Caspasas-9, 8, 3 y de PARP en líneas celulares de MCL.
- QTX125 ejerce un efecto antitumoral *in vivo* en modelos *xenografts* de MCL.
- Las células primarias de pacientes de MCL son más sensibles a QTX125 que PBMCs, CD3+ y CD19+ procedentes de donantes sanos.

INTRODUCTION

1. Cancer

Cancer is a term used to designate diseases characterized by harbouring cells with an uncontrolled division that can after spread to other parts of the body invading different tissues (metastasis) [28]. Division in normal cells is a controlled process that allow cells to growth and maintain an organism alive. Tumor development occurs due to a sequence of multiple alterations that lead to molecular aberrancies. These ones allow affected cells to divide faster, out of control and adapt better to environment when compared to normal cells, becoming progressively carcinogenic and invasive [1].

Due to the high diversity that presents carcinogenesis, Hanahan and Weinberg in 2000 proposed six hallmarks of cancer in order to rationalize the complexity of human cancer [29]. The original six hallmarks proposed include sustaining proliferative signalling, evading growth suppressors, resisting cell death, enabling replicative immortality, inducing angiogenesis, and activating invasion and metastasis (Figure 1). Together they describe six biological capacities acquired by cells in order to achieve their main objectives to become a malignant neoplasm: reproduce uncontrollably and invade other tissues [1].

In 2011, as cancer research evolve, Hanahan and Weinberg published two additional emerging hallmarks: deregulating of cellular energetics, which reprograms the cellular energy metabolism of cancer cells in order to maintain proliferation; and avoiding immune destruction, that allows cancer cells to evade immunological destruction [30].

Underlying these hallmarks there are two enabling characteristics: genome instability, and tumor-promoting inflammation, that support multiple of the hallmarks (Figure 1).

The genomic instability that confers malignancy to cancer cells affects mainly genes that activated lead to oncogenic features (oncogenes) and/or tumor suppressors genes. This occurs due to genetic and epigenetic alterations [29]. For oncogenes to be activated alterations like mutations, gene amplification or chromosome rearrangements need to occur in only one allele. In contrast, tumor suppressor genes need to inactivate both alleles leading to loss of function. It is normally produced by a loss of heterozygosity together with the inactivation of the

retaining allele by mutations or epigenetic mechanisms such as DNA methylation [31].

Together with genomic instability, after years of research, it is now clear that carcinogenic lesions are populated with immune cells that maintain chronic inflammation and promote tumor growth [32]. Inflammation contributes to the acquisition of multiple core hallmarks by supplying bioactive molecules to the tumor microenvironment such as growth factors, survival factors or proangiogenic factors [30, 33].

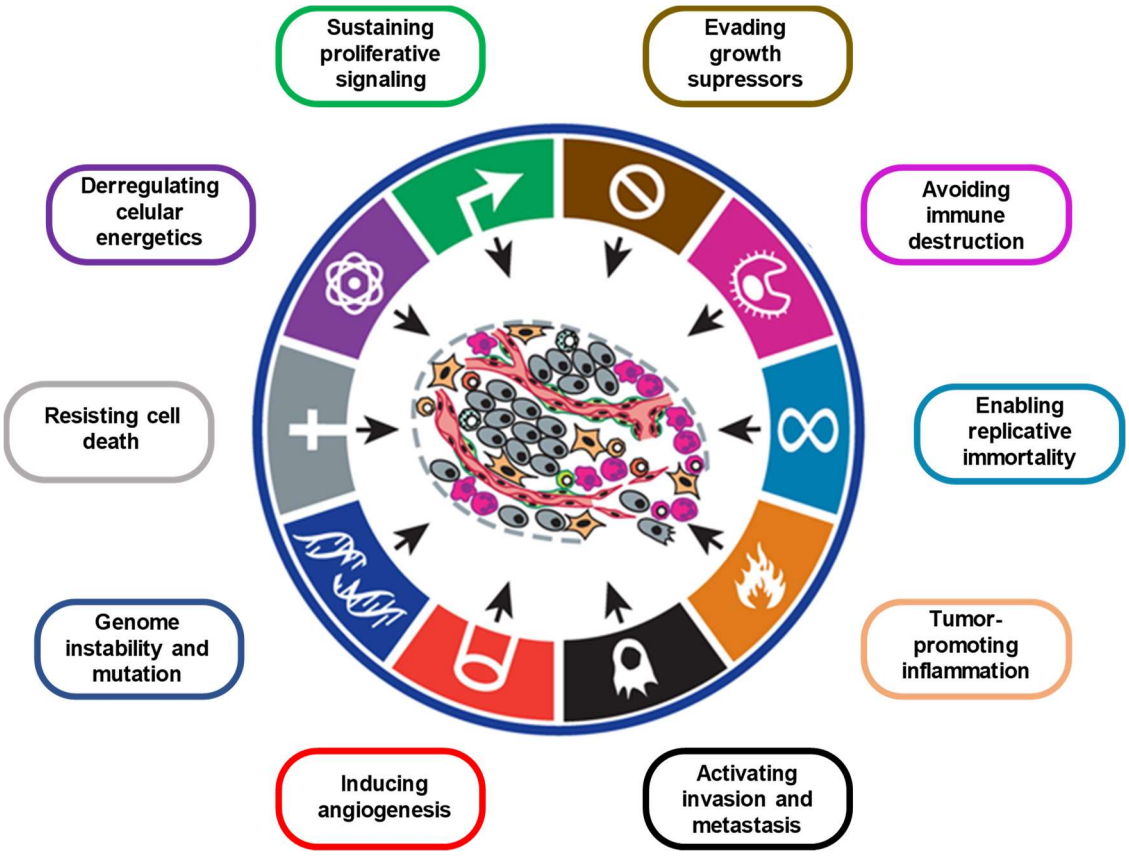

Figure 1: Hallmarks of cancer*. Eight hallmarks of cancer that cells acquire during its tumorigenic transformation and two enabling characteristics (genome instability and mutation plus tumor-promoting inflammation) that support multiple of the hallmarks. Adapted from Hanahan and Weinberg, 2011 [30].*

2. Epigenetics in cancer

Cancer is nowadays defined as a genetic and epigenetic disease. Epigenetics was first introduced by C.H. Waddington in 1939 as 'the casual interactions between genes and their products, which bring the phenotype into being' [2], and was later defined as heritable changes in gene expression that are not due to any alteration in the DNA sequence [3]. The different cells of an organism contain the same DNA sequence, however, they are able to differentiate and maintain different phenotypes as to play different biological functions. These processes are possible due to epigenetics. In general terms, epigenetics consists on different molecular mechanisms that modifies the state of chromatin to an open (euchromatin) or closed (heterochromatin) state regulating the access of different molecular machineries involved in DNA-related processes, orchestrating which genes are expressed or repressed.

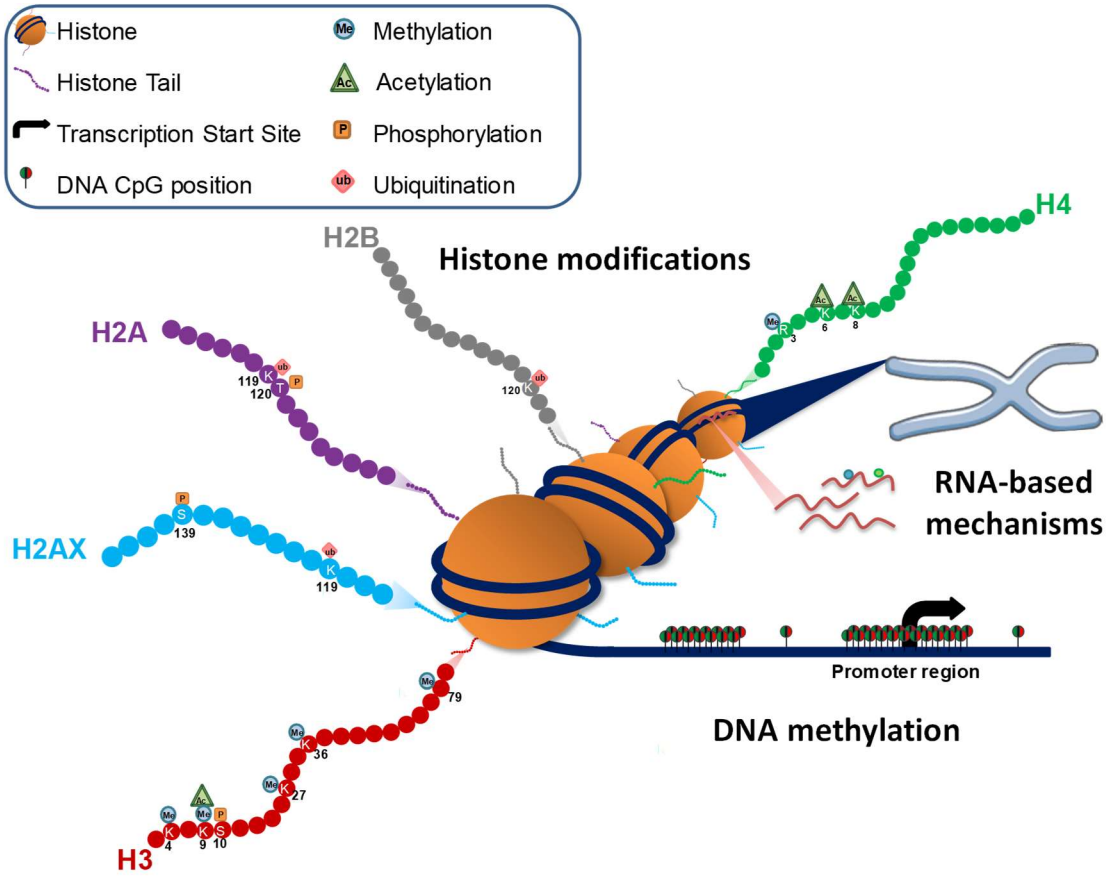

***Figure 2: Epigenetic mechanisms**. The three main epigenetic mechanisms are represented: DNA methylation, histone covalent modifications and RNA-based mechanisms. Adapted from Llinàs-Arias et al. 2017 [34].*

The classic epigenetic mechanisms are DNA methylation and covalent histone modifications, which will be further explained since they are important concepts for the understanding of this PhD thesis (Figure 2). However, it is important to mention that there are other epigenetic regulation layers such as non-coding RNAs [35] and the emerging field of epitranscriptomics, which involves the study of the RNA epigenetic patterns and the RNA-modifying enzymes [36].

Important to have in mind, that alterations in the normal epigenetic landscape as in the epigenetic regulators are found in cancer, and also in other several diseases such as autoimmune disease, neurodegenerative and phycological disorders [5].

2.1. DNA methylation

DNA methylation is the classic and best studied epigenetic mark. It usually takes place at 5' position of cytosine ring within CpG dinucleotides and the main consequence is the silencing of genes and other non-coding genomic regions. This CpG nucleotides usually are concentrated in regions called CpG islands, which are CpG rich DNA regions located in nearly 60% of human gene promoters or in regions with large repetitive sequences such as centromeres or retrotransposon elements [37].

In normal tissues CpG islands at promoters are usually unmethylated whereas CpG in repetitive sequences are highly methylated to avoid chromosome instability [38]. Gene bodies are also methylated in normal cells to avoid erroneous transcription initiation sites. Important to remember that methylation at CpG islands is also important during development in X chromosome inactivation or genomic imprinting [39, 40]. Tissue-specific DNA methylation also occurs in other regions with less CpG density and located close (- 2 kb) to CpG islands, named CpG island shores [41] (Figure 3).

The enzymes responsible of placing this epigenetic mark are the DNA methyltransferases (DNMTs). There are three DNMTs in humans: DNMT1 is the maintenance DNMT, responsible for keeping the methylation pattern upon DNA replication; DNMT3A and DNMT3B are *de novo* DNMTs that act in previously

unmethylated regions. In cancer, overexpression, mutations or deletions in DNMTs are common [42].

Although the methylation pattern in somatic cells is generally maintained, unmethylation is necessary in specific developmental stages, for example erasing paternal-origin-specific imprints [43]. The reversion to an unmethylated state can be reached by two proposed mechanism: 1) a ‘passive’ DNA demethylation that can occur when there is a failure in the methylation maintenance programme during cell division or 2) an ‘active’ DNA demethylation that is mediated by ten-eleven translocation (TET) enzymes (TET1, TET2 and TET3). They catalyse in a step-wise manner the oxidation of 5-methylcytosine (5-mC) to 5-hidroxymethylcytosine (5-hmC) and other intermediate oxidation states (5-formylcytosine (5-fC) and 5-carboxycytosine (5-caC)), then followed by TDG (thymine-DNA-glycosylase) and BER (base excision repair) results in an unmodified cytosine [44]. TET proteins are considered tumor suppressor genes and their decreased expression and mutations are common in cancer [45].

DNA methylation can inhibit gene expression by two different mechanism. It can directly prevent transcription by avoiding DNA binding proteins accessibility. Otherwise, it can promote Methyl-CpG-binding Domain (MBD) proteins that recruit chromatin remodellers and histone deacetylases and methylases to specific sites in the genome. These protein complexes usually cause transcription repression by inducing histone repression marks or nucleosome positioning that closes chromatin making it inaccessible for transcription.

Alterations in DNMTs, TETs or MDBs are potential responsible for the two most common alterations in DNA methylation in tumors: global hypomethylation of the genome and CpG island hypermethylation of tumor-suppressor genes promoters (Figure 3).

Global DNA hypomethylation in tumors was one of the first epigenetic alterations discovered [46]. It contributes to tumorigenesis by generating chromosomal instability, reactivating transposable elements and causing loss of imprinting [4]. It generally occurs in those regions of DNA with repetitive elements, transposons or other non-coding regions, allowing DNA transcription machinery to initiate transcription form erroneous sites in the genome [47].

CpG island hypermethylation in promoters of tumor suppressor genes was initially reported in the promoter of the *retinoblastoma gene (Rb)* [48] and later extended to other well-known tumor suppressor genes such as *Von Hippel–Lindau (VHL)* [49], *p16* [50] or *Breast cancer 1 (BRCA1)* [51], being then considered an epigenetic tumor-suppressor inactivating mechanism [52]. Nowadays, numerous studies report the silencing of tumor suppressors genes through this epigenetic mechanism affecting genes involved in cell division, apoptosis, metastasis and metabolism reprogramming. Moreover, the profiles of CpG island methylation in tumor suppressor genes are specific for each tumor type [53]. For that reason, there is an increasing interest in the last years for using DNA methylation profiles as cancer biomarkers for diagnosis and treatment [54].

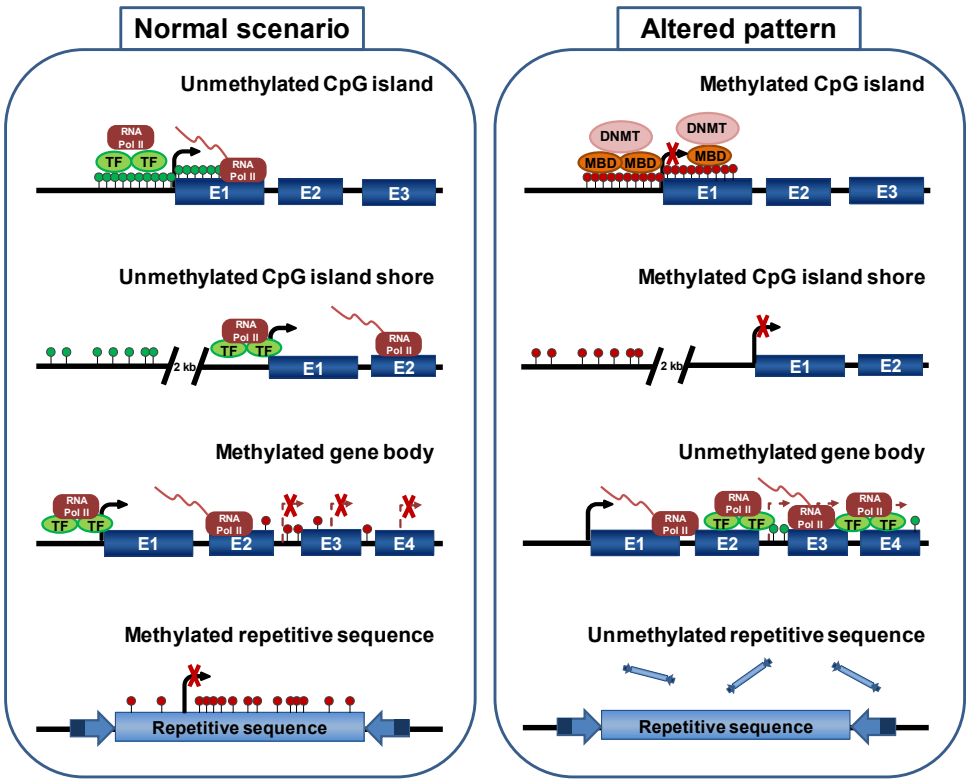

***Figure 3**: **DNA methylation patterns in different regions of genome.** Normal scenario (left) compared with cancer cells altered patterns (right). CpG island promoters are unmethylated in normal conditions whereas aberrant hypermethylation is found in cancer, causing the inactivation of tumor suppressor genes. The same occurs in island shores, located up to 2kb upstream of the CpG island. In gene body, methylation prevents incorrect transcription. In cancer, unmethylation in gene body allows aberrant transcription from incorrect sites. Repetitive sequences are hypermethylated in normal cells to avoid chromosomal instability, transposition and recombination, whereas in cancer are unmethylated. Adapted from Portela et al. 2010 [5].*

2.2. Histone covalent modifications

Histone covalent modifications are together with DNA methylation the best studied epigenetic marks. DNA is packaged in chromatin within the cells. Chromatin units are the nucleosomes that are composed of an octamer of two copies of each of the four canonical histones (H3, H4, H2A and H2B) wrapped by 147 DNA base pairs and separated by ~50 bp of free DNA. Histones are globular but they have N-terminal tails which are covalently modified. These modifications are up to sixteen [55] including acetylation, methylation, phosphorylation, ubiquitylation, sumoylation, ADP ribosylation, deimination, proline isomerization, being the most studied acetylation and methylation [56].

It is important to understand that there are several aminoacids residues at different positions in histone tails able to undergo modifications, that together with the different possible modifications mentioned above give a vast number of permutations and combinations that conform the complexity of the named 'histone code' [7].

In general, histone tails modifications play a role in transcription and DNA repair. There are mainly two described mechanism caused by histone modifications. The first is the disruption of the non-covalent interaction between DNA and histones or between nucleosomes. Of all the known modifications, acetylation is the most involved in chromatin unfolding. The second is the recruitment by certain histone marks of other proteins involved in DNA processes to specific sites [57]. Lysine methylation is more actively involved in this latter mechanism than in chromatin structure changes, since methylation does not imply a change in aminoacids charges as it does acetylation [58].

Generally, histone acetylation is associated with active transcription. However, methylation marks can provoke either activation or repression of transcription, depending on the residue and the position, being also much more specific than acetylation. Three methylation sites in histones are related with activation of transcription: H3K4, H3K36 and H3K79, whereas H3K9, H3K27 and H4K20 are involved in transcription repression [6]. In cancer, together with a global loss of H4K16Ac, there is also a loss of H4K20me3 [59].

Histone modifications are not static, they are dynamically changing depending on the cellular context [55]. It is known that some marks can influence others, meaning that histone modification act in “cross-talk” between several epigenetic modifications [60].

The enzymes that catalyse histone covalent marks are commonly named `writers´ which are responsible for depositing the mark, `erasers´ that remove the residues and `readers´ which recognize specific marks in histone tails and recruit other molecular machineries to those sites in histones (Figure 4).

In cancer it is common to found aberrancies in the histone code and also alterations in the epigenetic regulator enzymes that catalyse histone marks. In the following section we will go deep into acetylation marks and their epigenetic regulators together with their common alterations in cancer, since this is one of the main concepts of this PhD work.

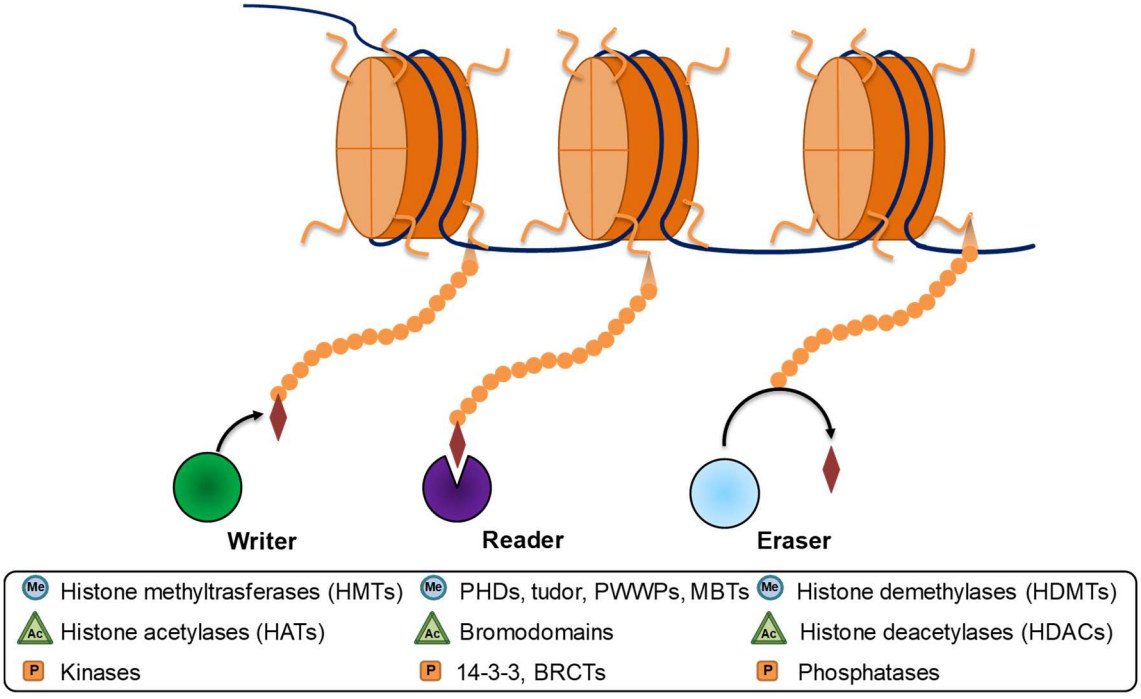

Figure 4: Writers, readers and erasers. *The epigenetic regulators of histone marks are named writers, readers and erasers. Writers catalyse the addition of marks in histone tails. Erasers are responsible for the removal of these marks. Readers recognize these marks and recruit other molecular machineries. Some common examples are shown in the figure. PHDs: plant homeodomains, PWWP: Pro-Trp-Trp-Pro domains, MBTs: malignant brain tumour domains, BRCT domains: named after BRCA1 C-terminal domain. Adapted from Filippakopoulos P et al. 2014 [61].*

3. Histone and non-histone acetylation in cancer

Acetylation of the epsilon amino group of lysine was first described in histones by Vincent Allfrey and colleagues in 1964 [62] (Figure 5). Since then it has been the most studied histone covalent modification mark together with methylation.

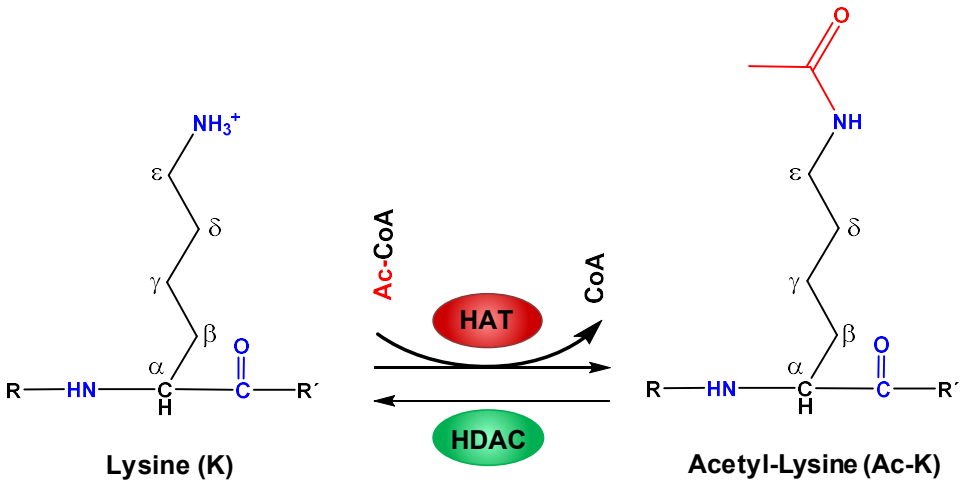

Figure 5: Lysine acetylation. *Acetylation of epsilon amino group of lysines in histone tails or in other proteins is a reversible epigenetic mark. It is added by HATs using Acetyl-CoA as cofactor. HDACs remove this acetyl groups. Chemically, the acetyl group neutralizes de positive charge of the amino group in lysine. This weakens the interaction between the negative DNA wrapped around positive charged histones. Adapted from Di Martile et al. 2016 [63].*

Histone acetylation is involved in chromatin remodeling and transcription regulation by two molecular mechanisms suggested. The first one consists on a dynamic process where chemically the negative charge of the acetyl group neutralizes de positive charge of lysine and weakens the interaction between the negative backbone of DNA with the highly positively charged histones. This causes a more relaxed state of chromatin (euchromatin), which facilitates the access to other molecular complexes involved in transcription. Conversely, low levels of acetylation are responsible of a more tighten interaction with DNA leading to a more compacted chromatin status (heterochromatin) and a repression of transcription [64]. The second mechanism proposed is that

acetylated lysines function as signals for the recruitment of regulatory factors or chromatin remodeling complexes to specific positions in the genome [65].

Although histones have been the main focus of lysine acetylation studies, in the last 30 years, it has been expanded to other proteins, involved in several cellular processes [8]. In fact, there are different studies about enzymes that modify histones but also target non-histone proteins. This makes sometimes difficult to distinguish the individual role of this chemical group in histone tails from the effects of acetylation or interactions with other proteins by theses enzymes [55].

Acetylation in histone tails is mainly involved in gene transcription regulation, promoting tumorigenesis when aberrant levels of acetylation are present. In non-histones substrates acetylation is involved in diverse molecular processes also important in cancer such as protein stability, protein-protein interaction or cellular localization. Not less important are the alterations in the epigenetic enzymes responsible of orchestrating the acetylation process, being also a common hallmark in cancer.

Lysine acetylation is a reversible post-traductional modification (PTM) orchestrated by two main groups enzymes: 1) lysine acetyl transferases (KATs), formerly named histones acetyl transferases (HATs), because they were first discovered in the context of histone and 2) lysine deacetylases (KDACs) also named histones deacetylases (HDACs). The first group ‘writes’, add the acetylation marks and the second ‘erases’, remove them. Moreover, there is a third group of enzymes that are involved in the recognition of acetylated lysines called bromodomains, being these ones the ‘readers’ (Figure 6).

Being lysine acetylation the main edge of this PhD thesis, in the next section these three groups of enzymes will be carefully reviewed both in the context of master regulators of one of the most studied histones marks and also as non-histone modifiers, always highlighting their role in cancer.

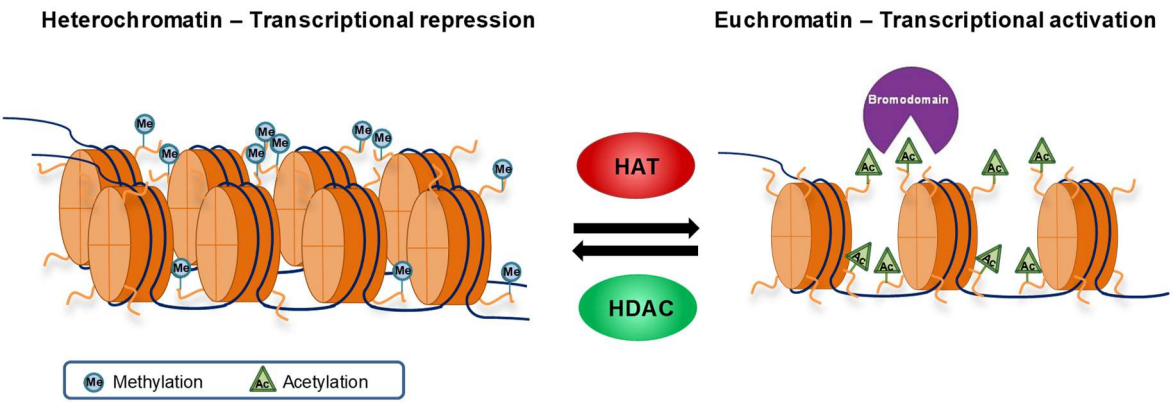

***Figure 6: Epigenetic regulators of acetylation**. Acetylation is a reversible post-traductional modification. It is regulated by HATs, enzymes that add the acetyl group (writers), HDACs remove this group (erasers) and Bromodomains recognize and bind to these acetyl marks (readers). In histones, lower levels of acetylation are linked with a closed status of chromatin (heterochromatin) causing a transcriptional repression. Contrarily, high levels of acetylation are related with an open status of chromatin (euchromatin) and transcriptional activation. Adapted from Simo-Riudalbas et al. 2015 [9].*

3.1. Lysine Acetyl Transferases (KATs/HATs)

Lysine Acetyl Transferases (KATs, also known as HATs) catalyze the transfer of an acetyl group from the cofactor Acetyl-CoA to lysine in histone tails or in non-histone proteins.

Originally HATs were classified in two general classes based on their subcellular localization: A-type HATs that are nuclear and B-type HATs that are cytoplasmatic.

Type A HATs lead to acetylation events that are involved in transcription regulation. They are divided into families based on their structure and sequence similarity. The three families better characterized in human are: 1) GNAT (GCN5 and PCAF), 2) the p300/CBP family and 3) the MYST family (MYST 1-4, Tip60) [66]. In addition to the HAT domain, some of them possess reader domains conferring specificity and diversity to these enzymes with this double function.

Type B-HATs promote acetylation events that are involved in the transport of newly synthesized histones to the nucleus to be deposited onto new nucleosomes. Only a few human B-HATs have been described, including HAT1 [67] and HAT4 [68].

Human Type-A HATs will be following explained in more detail, since they are the most studied in carcinogenesis context.

GNAT family

GCN5-related *N*-acetyltransferases (GNAT) family is composed of general control non-repressed protein 5 (GCN5, also known as KAT2A) and P300/CBP-associated factor (PCAF, also named KAT2B).

GCN5 was the first transcription-related HAT identified in 1996 [69]. Together with PCAF (KAT2B) are homologous transcription co-activators found in several human multiprotein HAT complexes [70, 71].

Several studies have demonstrated their involvement in cancer [72]. For example, GCN5 have been reported to acetylate H3K9 and H3K56, acetylation marks that are involved in DNA damage response [73, 74]. Moreover, PCAF acetylation of H4 is related with the inactivation of AKT signalling and the induction of apoptosis in hepatocellular carcinoma [75].

GNAT family members also acetylate two important non-histone proteins in cancer including MYC-protooncogene protein (C-MYC) and tumor protein p53 (TP53). PCAF acetylation of p53 tumor suppressor takes place at Lys320 and promotes the activation of p53 target genes such as p21 [76]. Furthermore, GCN5/PCAF by acetylating C-MYC [77], contribute to the stability of this potent oncogene. MYC is known to associate with GCN5/PCAF containing complexes recruiting them to chromatin at Myc-target promoters [78]. The role of GNAT family members in regulation of C-MYC and p53 may suggest their dual role in promoting and inhibiting cell proliferation. For example, GCN5 was described to act as an oncogene in human lung [79] and colon cancer [80], whereas PCAF was reported as a tumour suppressor in gastric cancer [81] and in hepatocellular carcinoma promoting cell autophagy and apoptosis [82, 83] or inhibiting metastasis by inhibition of epithelial-mesenchymal transition [84].

p300/CPB family

CREB-binding protein (CBP, also known as CREBBP or KAT3A) and E1A-binding protein p300 (EP300, also named p300 or KAT3B) acetyl transferase activity was confirmed in 1996 [85, 86]. They have in common 63% aminoacids sequence and almost 90% of the HAT domain, reason why they share most of the targets and most publications fail in differentiating them, commonly named “p300/CBP”.

CBP and p300, unlike other HATs, acetylates multiple positions in all the four histones, being important players in the dynamic process of acetylation within the histone code, mediating the activation or repression of gene transcription.

They are large proteins with multiple functional domains that acetylate and also interact with a large number of proteins bringing for example DNA-binding transcription factors into proximity to the transcription machinery. Like this they are involved in cell proliferation, cell cycle, cell differentiation and DNA damage response. In cancer, they also have a dual role as oncogenes and tumor suppressors depending on the cellular context (reviewed in [87, 88]).

They are also able to acetylate several non-histone proteins involved in tumorigenesis including p53 [89], p73 [90], Rb [91], E2F [92, 93] and High Mobility Group isomers I and Y (HMGI(Y)) [94, 95]. In most cases, acetylation of these proteins on lysine residues adjacent to DNA-binding domains increases promoter binding, resulting in activation of transcription of specific target genes.

Acetylation also affects protein-protein interactions, as occurs in the pRb pathway where acetylation of pRb by p300 increases the strength of the binding with Mouse double minute 2 homolog (MDM2) oncoprotein [91].

In addition, several mutations and translocations of these two genes have been reported, linked with hematological malignancies such as Acute Myeloid Leukemia (AML) and Mixed Lineage Leukemia (MLL) and also in solid tumors (reviewed in [88, 96]).

MYST family

This family, originally named for its four founding members in yeast and mammals, is currently composed of five human HATs: Tip60 (KAT5), MYST1 (MOF/KAT8), MYST2 (HBO1/KAT7), MYST3 (KAT6A/MOZ), and MYST4 (KAT6B/MORF). All contain a MYST domain being an acetyl-coA-binding domain and zinc finger (ZnF) motifs [97, 98].

Tip60

HIV Tat-interacting protein of 60 kDa (Tip60, or KAT5), as other HATs, can act as pro-oncogenic or anti-oncogenic depending on the cellular context.

Its HAT activity have been reported as a key player in double-strand DNA break repair and induction of apoptosis [99] being responsible of acetylation and consequent activation of ataxia-telangiectasia mutated (ATM) kinase in response to DNA damage [100]. Tip60 also acetylates p53 at Lys120, a post-traductional modification that modulates the decision between cell-cycle arrest and apoptosis [101, 102]. It is downregulated in several cancer types, such as colon, lung [103], metastasic prostate cancer [104], metastasic melanoma [105], lymphomas and AML [106].

In its pro-oncogenic role, Tip60 is a cofactor of MYC [107, 108], E2F [109] and its accumulation in the nucleus correlates with ligand-independent androgen receptor (AR) activation in prostate cancer progression [104].

MOF

Males absent on the first (MOF, also known as KAT8 or MYST1) was first identified in *Drosophila* as a the catalytic subunit of the Male Specific Lethal (dMSL) complex involved in dosage compensation [110].

Human MOF is part of different molecular complexes that modulate its substrate specificity. Thus, when MOF interacts with MSL (Male Specific Lethal) or its homolog MSL1v1 (Male-Specific Lethal 1 Homolog) acetylates H4K16, a key mark which loss is considered a hallmark of cancer [59]. However the complex of MOF with NSL (non-specific lethal) also acetylates H4 on lysines 5 and 8 [111].

MOF has also non-histone substrates like TTF-1-interacting protein-5 (TIP5) subunit of the chromatin-remodeling complex NoRC [112] and K120 of p53 [102], which acetylation is mediated by MSLv1[113]. MOF also interacts with ATM and is involved in its response to DNA damage [114].

Its downregulation is a feature of several cancers such as colorectal, gastric, renal [115], medulloblastoma, breast carcinoma [116] and ovarian cancer [117].

HBO1

HAT bound to ORC (HBO1, also known as MYST2 or KAT7) was first identified associated with ORC1, the largest subunit of the origin recognition complex [118]. Thus, it regulates S phase progression and is the main responsible of H4 acetylation [119].

HBO1 forms two different complexes with Inhibitor Growth 4 (ING4) and Inhibitor of Growth 5 (ING5) tumour suppressors. ING5 complex is essential for DNA replication [119] and ING4 recognizes H3KMe3 mark. This latter interaction recruits HBO1 and activates its acetylating activity at H3 tails. It also drives acetylation to ING4 target promoters genes, and is potentially implicated in apoptosis in response to genotoxic stress [120].

p53 interacts directly with HBO1 and negatively regulate its HAT activity upon stress signalling, suggesting that p53 could control HBO1 activity to regulate DNA replication [121].

HBO1 is found to be more abundant in testis, ovarian, breast, stomach/oesophagus and bladder cancer compared to normal tissues [122].

MOZ and MORF

Monocytic leukemia zinc finger protein (MOZ, also known as KAT6A or MYST3) and monocytic leukemia zinc finger protein-related factor (MORF, or KAT6B or MYST4) are highly homologous transcription co-activators. MOZ was initially identified as a fusion protein with CBP in AML [123], and MORF was identified some years later [124]. In fact, MOZ and MORF are found in fusion with other proteins in AML, including MOZ-CBP [123], MOZ-p300 [125], MOZ-TIF2 (Transcriptional Intermediary factor 2) [126], MOZ-LEUTX (leucine twenty

homeobox) [127] and MORF-CBP [128]. The underlaying mechanism of these chimera proteins to drive tumorigenesis in not fully understood but could potentially be due to aberrant acetylation [129].

Apart from haematological malignancies, MOZ and MORF are also altered in solid tumours. *MOZ* gene is mutated in oesophageal adenocarcinoma and *MORF* gene is altered in breast cancer [130] and castration-resistant prostate cancer [131]. However, amplification of these genes has also been found across several cancer types [12, 132]. Recent studies show that MOZ enhances phosphoinositide 3-kinase/ v-akt murine thymoma viral oncogene homolog 1 (PI3K/AKT) signalling by recruitment of Tripartite motif-containing 24 (TRIM24) in glioblastoma [133]. These findings remain unclear the role of these proteins as oncogenes or tumour suppressors in cancer.

3.2. Lysine Deacetylases (KDACs/HDACs)

The HDACs are enzymes responsible for the removal of the acetyl group of lysines, being popularly named the “erasers”.

In histones, upon deacetylation the positive charge of lysine is restored, recovering the strength of histone-DNA interaction within a heterochromatin state resulting in a transcriptional repression.

Eighteen mammalian HDACs have been discovered so far and are divided into five classes based on their phylogenetic comparison with yeast enzymes. Class I includes HDAC1, HDAC2, HDAC3 and HDAC8, it has a nuclear localization and it is ubiquitously expressed in human cell lines and tissues. Class II is subdivided in class IIa that comprises HDAC4, HDAC5, HDAC7 and HDAC9; and class IIb consists of HDAC6 and HDAC10. Class III comprises the members of the sirtuin family from SIRT1 to SIRT7 and the Class IV contains only HDAC11. HDACs are numbered according to their chronological order of discovery, being HDAC1 first reported in 1996 and then HDAC2 some months later [134, 135].

HDACs from Class I, II and IV require a zinc ion for catalysis, whereas Class III (sirtuins) are NAD+- dependent enzymes with protein deacetylase and ADP-ribosylase activity [136].

HDACs are involved in multiple stages of tumorigenesis through deacetylation of histones and non-histones proteins that are able to alter transcriptional regulation, protein stability, localization and activity together with protein-protein interactions [137].

Their involvement in cancer has been dilucidated with the help of HDAC inhibitors (HDACi), which are not always specific for a single HDAC. This means that HDACs individual role is not always fully described, together with the fact that several HDACs are involved in similar functions that can also vary depending on the context. For these reasons, more than each HDAC specific characteristics, we will next describe their role in the different hallmarks of cancer.

For instance, the important role of HDACs in cell proliferation is observed when HDAC inhibition induces cell-cycle arrest by upregulation of cyclin-dependent kinase (CDK) inhibitors or downregulation of cyclins and CDKs. HDAC1 and 2 directly bind to the promoter of *p21*, *p27* and *p57* genes negatively regulating their expression [138]. Upregulation of HDACs in several cancer types including HDAC1 [139], HDAC2 [140], HDAC3 [141], HDAC4 [142] cause a significant decrease of *p21* gene. Similarly, knockdown of HDAC1 and 2 causes cell cycle arrest in G1 phase or G2/M transition [143], and knockdown of HDAC5 induces downregulation of cyclin D1 and CDK2/4/6, resulting in cell cycle arrest in human HCC cells [144]. Loss of HDAC10 also contributes to cell cycle arrest in G2/M by loss of cyclin A2 [145]. In the same way, inhibition of HDAC with sodium butyrate increased p21 expression and decreased cyclin B1 [146].

HDACs have been reported to influence apoptosis in cancer by regulating pro-apoptotic or anti-apoptotic proteins. HDAC inhibitors have been shown to induce apoptosis by both extrinsic and intrinsic apoptosis pathways. In the extrinsic pathway HDACi upregulate cell surface death receptors or their ligands such as FAS receptor and its ligand (FASL) or tumor necrosis factor-related apoptosis-inducing ligand (TRAIL) receptors. HDACi also reduce the levels of cytoplasmic FLICE-like inhibitory protein (c-FLIP) protein and enhance the recruitment of death inducing signal complex (DISC) formation [147]. For example, inhibition of HDAC1-3 in non-Small Cell Lung Cancer (NSCLC) downregulated FLIP expression and induced apoptosis via caspase-8 activation [148]. Inhibition of HDAC1 and 2 selectively sensitizes Chronic Lymphocytic Leukemia (CLL) to

TRAIL induced apoptosis [149]. In the intrinsic pathway, where B-cell lymphoma-2 (Bcl-2) family plays an important role, HDAC inhibition is involved in decreasing the expression of anti-apoptotic proteins and increase the expression of pro-apoptotic factors [147]. Thus, HDAC3 inhibition promotes p53 upregulated modulator of apoptosis (PUMA) expression in gastric cancer cells [150]. Moreover, HDAC2 inactivation is reported to supress BCL2 and activate Bcl2-associated X protein (BAX) [151].

Epithelial-to-mesenchymal transition (EMT) is an important process in metastasis and invasion. Several studies report the role of HDACs in EMT regulation. HDACs are involved in the loss of E-cadherin and the activation of transcription factors such as Snail Family Transcriptional Repressor 1 (SNAI1/Snail), Snail Family Transcriptional Repressor 2 (SNAI2/Slug) or Zinc Finger E-Box Binding Homeobox 1/2 (ZEB1/2). For instance, Snail represses E-Cadherin expression by recruiting an HDAC1/HDAC2 complex being Trichostatin A (TSA) inhibition (a pan-HDACi) enough to block this Snail repression [152]. ZEB1 transcriptional repressor was found to recruit HDAC1 and HDAC2 to *E-cadherin (CDH1)* gene promoter in pancreatic cancer. There, HDAC1/2 deacetylation of histones H3 and H4 mediates the downregulation of *CDH1* [153]. Another HDAC that has been related with cell mobility and migration is HDAC6. This protein, unlike other HDACs, is mainly located in the cytoplasm and deacetylates non-histone proteins. It plays a key role in regulating microtubule dynamics and migration by deacetylating α-Tubulin and cortactin [154]. It is also involved in degradation of misfolded proteins through aggresome formation avoiding the toxic effects of cellular stress. It also deacetylates Heat Shock Protein 90 Alpha (Hsp90α) regulating its chaperone activity and giving a survival advantage to transformed cells [155]. HDAC6 expression is correlated with high tumor aggressiveness, occurring its overexpression in several cancers, having a potential oncogenic role [23, 156].

Concerning angiogenesis, HDACs play an important role by modulating several pro- or antiangiogenic factors. In fact, many HDACs are involved in hypoxia inducible factor 1 subunit alpha (HIF1-α) regulation and treatment with HDAC inhibitors causes its degradation and impairment. HDAC1 and HDAC4 deacetylates HIF1-α increasing its stability and transcriptional activity [157, 158].

HDAC6 inhibition leads to HIF1-α degradation due to the hyperacetylation of Hsp90 that inhibits the function of HSP70/HSP90 axis. This causes accumulation of immature HIF1-α/Hsp70 complex and HIF1-α consequent degradation by proteasome [159]. HDAC4, HDAC5 and HDAC7 increased transcriptional activity of HIF1-α by promoting its interaction with coactivator p300 [160, 161].

Tumor cells have altered or low differentiation level, keeping an immature state synonymous of malignancy. Inhibition of HDACs stimulates cells to differentiate in a normal manner in solid and haematological cancers. Downregulation of transcription factor GATA family genes which normally promote differentiation is a common event in several cancers. HDAC inhibition with TSA restore their expression in ovarian cancer. It is because it counteracts the hypoacetylation of histone H3 and H4 responsible for the loss of GATA-binding protein 4 (GATA4) and GATA-binding protein 6 (GATA6) [162]. Moreover, B Cell CLL/Lymphoma 6 (BCL6), which is involved in survival and differentiation of several cell types, is known to be repressed by class I and II HDAC containing complexes [163].

3.3. Bromodomains

Bromodomains (BRDs) are the `readers' of acetylation in histone tails. They bind acetylated lysines and recruit transcription machinery or other molecular complexes involved in chromatin remodelling to specific sites in chromatin, thus regulating gene transcription.

Bromodomains were discovered in the early 1990s in the *brahma* gene from *Drosophila melanogaster*. This family of evolutionary conserved motifs is composed of 61 bromodomains that are found in 46 different proteins. They are classified in eight subfamilies based on their structure, being the most studied the bromodomain and extra terminal (BET) family [164] (Figure 10).

Apart from BET family, other BRDs have been identified in HATs, chromatin remodelling complexes, histone methyltransferases and transcriptional coactivators [17]. Implication of bromodomains in cancer has led to the discovery of multiple small-molecule inhibitors in the last years.

BET bromodomains

BET bromodomain family is composed of BRD2, BRD3, BRD4 and BRDT, being all of them ubiquitously expressed, excluding BRDT expressed only in testis. They share two characteristics: a C-terminal extra-terminal (ET) domain and two bromodomains in tandem (BD1 and BD2) in the N-terminal.

BRD2 and BRD4 regulate gene expression. They are involved in transcription initiation and elongation by two reported mechanisms. First, they recruit through its BRDs the positive transcription elongation factor complex (P-TEFb) to acetylated sites in chromatin. BRD4 help to activate Cyclin Dependent Kinase 9 (CDK9) subunit of P-TEFb, which then phosphorylates the C-terminal repeat domain (CTD) of RNA polymerase II (RNAP II) required for transcription (Figure 7). Second, BRD4 is in charge of the release of active P-TEFb from Hexamethylene Bisacetamide Inducible 1 (HEXIM1) inactive complex [165]. Thus, BET bromodomains are highly involved in cancer with its capacity to regulate directly the expression of important tumorigenic genes, such as *c-MYC.*

BET bromodomains are also involved in cell cycle regulation [166]. BRD4 inhibition leads to cell cycle arrest in G1 phase [167]. BRD2 is reported to bind E2F1 and E2F2, key transcription factors of S phase genes in complexes with other proteins [168]. Moreover, BRD2 overexpression accelerates cell cycle by increasing the expression of cyclin A [169].

BRD4 also maintains constitutively active Nuclear factor of kappa light polypeptide gene enhancer in B-cells 1 (NF-kB) by binding to acetylated RelA/p65 in cancer [170]. Active NF-kB is found in a variety of tumors and its target genes regulate several hallmarks of cancer. RelA subunit of NF-kB is highly regulated by acetylation. Thus, p300/CBP acetylation of several lysines of RelA affects its different functions. BRD4 recognizes specifically lysine 310 acetylation and causes the transcriptional activation of NF-kB target genes [170].

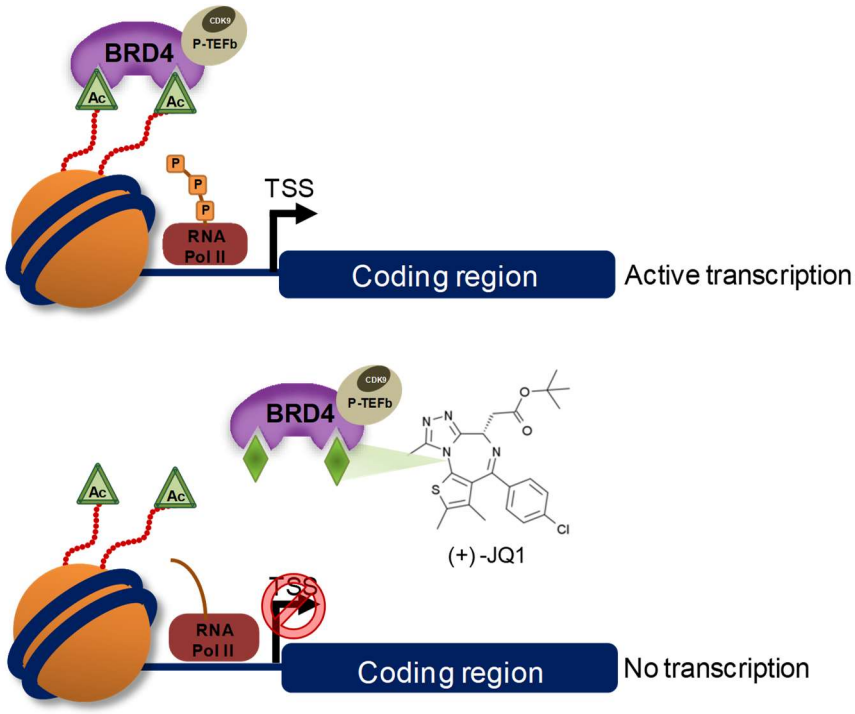

Figure 7: Schematic representation of BRD4 role in transcription. *BRD4 binds to acetylated lysines in histone tails through its bromodomains. There, BRD4 recruits P-TEFb and activates its CDK9 subunit, which phosphorylates RNA Polymerase II necessary for transcription (top). When bromodomain inhibitor JQ1 is present, it avoids BRD4 binding and the consequent recruitment of transcription machinery to acetylated sites in chromatin. This results in inhibition of transcription (bottom). Adapted from Sengupta et al. (2015) [171].*

Important to refer that BRD4 is expressed ubiquitously in a wide number of cells. However, BET inhibition shows selectivity for cancer cells over normal cells. Also, it demonstrates efficacy in cancers not bearing any alteration in BRD4. These facts, prompted researchers to ask how a general regulator such as BRD4 could selectively affect only the expression of some genes in specific cells. It seems that the answer could be in the preferential binding of BRD4 to enhancers and super-enhancers [172]. Enhancers are short cis-acting DNA sequences that can increase transcription of genes by preferential binding of transcription factors. They are characterized by the presence of certain histone marks such as H3K4me1 and H3K27Ac [173]. Super-enhancers are groups of several putative enhancers located in close genomic proximity. They are enriched in cancer cells and located in key oncogenic genes [172]. In fact, the well-known BRD4 target

C-MYC has also described a super-enhancer. In addition, super-enhancers are quite cell-type specific [174], explaining that BET inhibition could affect different genes depending on the cancer type.

Apart from enhancer binding, BET bromodomain function also depends on their binding partners which vary with the context. This is another reason why several different genes and pathways can be affected by these readers of acetylation.

Other bromodomains

Apart from BET family, bromodomains are present in other proteins involved in transcription or other molecular processes. This section will focus on the several bromodomain containing proteins that are also epigenetic regulators and play a key role in cancer, providing evidence of the cross-talk between epigenetic machineries.

There are histone methyl transferases (HMTs) and HATs that contain bromodomains, being `writers´ and `readers´ at the same time. Thus, histone methyltransferases MLL and ASH1 contain one bromodomain, and both are associated with actively transcribed genes [175]. In the group of HATs, CBP and p300 contain a bromodomain. It has been reported to bind acetylated lysine 382 of p53, important for p53 recruitment of CPB upon DNA damage. This is a crucial interaction for p53 transcriptional activation of *p21* in cell cycle arrest [176]. PCAF also has a bromodomain, although little is known about its function in cancer. Nevertheless some PCAF bromodomain inhibitors have been developed for HIV, where they act as potent inhibitors of HIV replication by avoiding the interaction between these bromodomain and acetylated HIV Tat protein [177]. GCN5 also harbours a bromodomain that seems to be involved in regulating site specificity acetylation of this HAT [178].

Bromodomains are also present in chromatin remodelling complexes, involved in their assembly and correct targeting. ATP-dependent SWI/SNF complexes have a mutually exclusive core subunit being SWI/SNF Related, Matrix Associated, Actin Dependent Regulator Of Chromatin, Subfamily A, Member 4 (SMARCA4/BRG1) or SWI/SNF Related, Matrix Associated, Actin Dependent Regulator Of Chromatin, Subfamily A, Member 2 (SMARCA2/BRM). Both contain

a bromodomain that is implicated in the recognition of acetylated lysines in H3 and H4 [179]. Moreover, bromodomain-containing protein 9 (BRD9) and BRD7 bromodomain-containg protein 7 (BRD7) are components of BAF (BRG1 or hbrm-associated factor) and PBAF (Polybromo-associated BAF) SWI/SNF complexes respectively. They are highly homologous and their functions in these complexes have not been fully elucidated, but BRD9 is over-expressed in several cancers and have been reported to be essential for sustaining MYC transcription in AML [180]. However, BRD7 has been reported as tumor suppressor in several cancers [181]. Polybromo protein (PB1 or BAF180) which is also member of PBAF SWI/SNF complex contains six BRDs and together with BRD7 have been identified as critical regulators of p53 transcriptional activity directed to induce replicative senescence [182].

4. Targeting lysine acetylation in cancer

Due to the involvement of HATs, HDACs and bromodomains in cancer and other diseases there is an increasing interest in finding specific inhibitors to modulate their activity. In this section, we will go through the main inhibitors of each class tested in cancer.

4.1. Lysine Acetyl Transferase inhibitors (KATi/HATi)

HAT inhibitors (HATi), in contrast to HDAC or bromodomain inhibitors, are less available and none of them is in clinical yet. This fact suggests that HATs are difficult to target and a new approach for inhibitors discovery is needed.

They can be classified in three main classes according to their origin and mechanism of action: **bisubstrate inhibitors, natural products** and **small molecules (synthetic products)** (Table 1 and Figure 8).

Bisubstrate inhibitors

The bisubstrate inhibitors are HAT substrate analogues consisting on two parts connected by spacers of different length: a CoA mimicking the acetyl-CoA substrate and a peptide moiety that resembles the sequence of protein substrates. The first bisubstrate inhibitors reported were **Lys-CoA** for p300 and

H3-CoA-20 for PCAF [183]. Since then other CoA derivatives have been synthesized, being useful for the study of HATs interactions [184-186].

The main limitation of these HAT inhibitors is that although they show inhibitory activity, they have poor pharmacokinetic properties, having low cell permeability and metabolic instability. This is probably due to the existence of highly polar phosphate groups in the pocket for CoA binding.

Natural Products

Several HATi have been obtained from plants or microbial extracts. They sometimes present problems of selectivity and not good physicochemical properties, but they have been a good template for further derivatization.

The first natural HAT inhibitor reported was **Anacardic acid,** extracted from cashew nutshells. It was reported as a non-selective p300/CBP and PCAF inhibitor and later activity against Tip60 inhibition was described [187]. On the cellular level, this compound caused repression of the NF-KB signalling pathway dependent on acetylation of the p65 subunit by p300 and PCAF [187, 188]. It also induces apoptosis in prostate cancer cells by androgen receptor (AR) downregulation through p300 inhibition [189]. However, this compound had problems of solubility, but based on its structure other HAT inhibitors were synthesized with better properties [190].

Curcumin is the main component of rhizome of *Curcuma longa* and is commonly used in Indian and Chinese traditional medicine. It is a p300/CBP specific HAT inhibitor [191]. Curcumin has been shown to modulate several transcription factors such as NF-kB and Activator Protein-1 (AP-1) [192]. Curcumin and analogues have been broadly studied and have reached clinical trials for diverse diseases including several types of cancer in combination with other drugs, however none of them have been completely successful due to the lack bioavailability of the compound [193].

Garcinol was isolated from *Garcinia Inidica* and identified as p300 and PCAF inhibitor. It was reported to be a potent inducer of apoptosis [194] and it has shown antitumor properties in leukemia, breast, colon and pancreatic cancer

[195]. The derivative isogarcinol lead to **LTK-14** selective for p300 and less toxic for cells [196].

There are other HATi extracted from natural products that have shown antitumoral effect in several cancer types (Table 1), including **Plumbagin**, specific inhibitor of p300 [197] and inductor of apoptosis and cell cycle arrest [198, 199]. **Epigallocatechin-3-gallate (EGCG)** [200], **Delphinidin** [201, 202] and **Gallic acid** [203, 204]**,** are pan-HATi, that inhibit p300 acetylation of p65. **Sanguinarine** is an inhibitor of p300, PCAF and G9a methylation, being able to modulate chromatin by regulating different histone marks [205, 206] and **Procyanidin B3** is a p300 inhibitor that mediates deacetylation of androgen receptor [207].

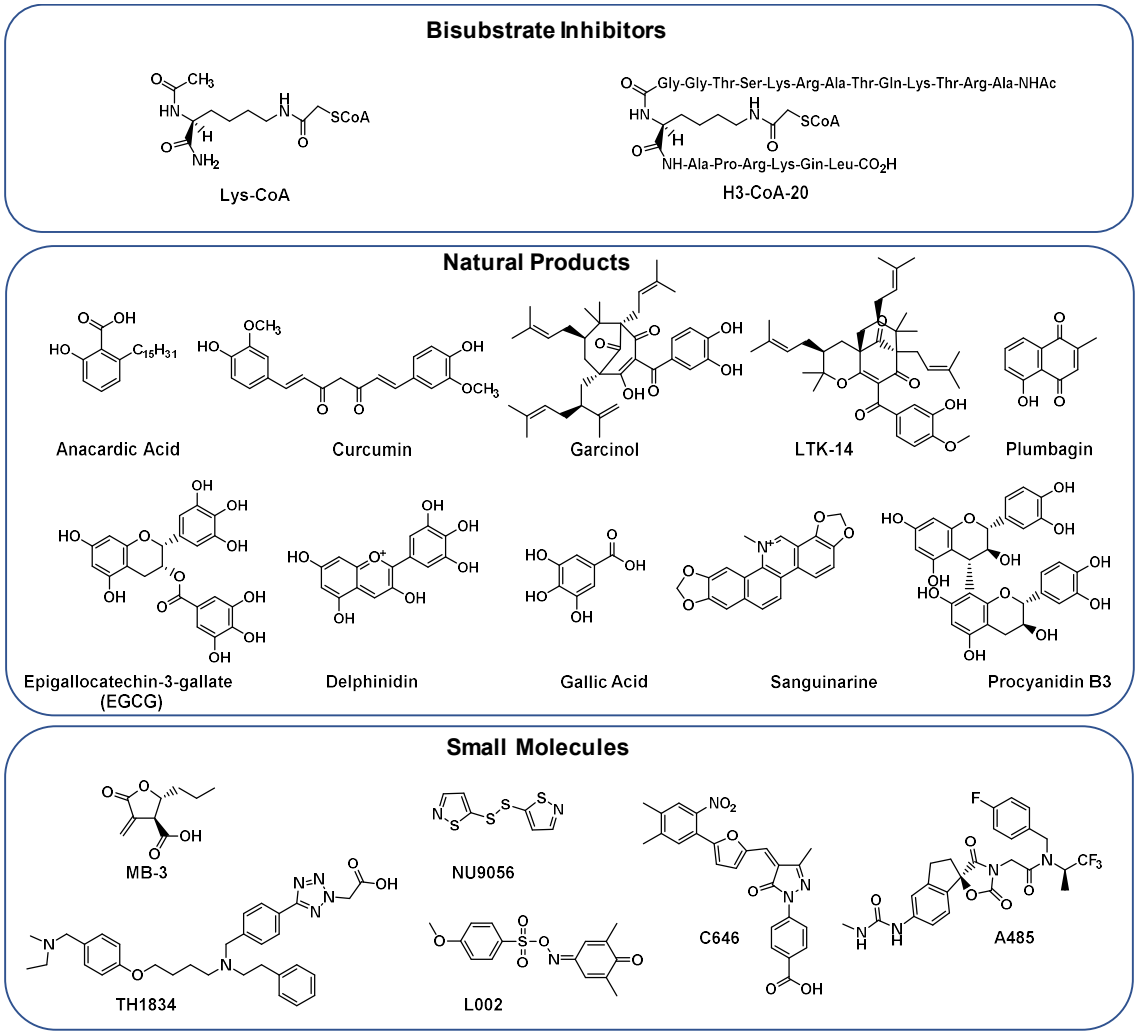

Figure 8: HAT inhibitors chemical structures. *Chemical structures available from HAT inhibitors detailed in the text.*

Small molecules (Synthetic Products)

The first synthetic small molecule HATi reported was **MB-3** in 2004, also known as γ-butyrolactone, inhibitor of GCN5 [208]. It was an important starting point for the development of other inhibitors, and years later showed antitumoral effect in acute lymphoblastic leukemia [209].

From a series of Isothiazolone compounds**,** the molecule named **NU9056** was found to be a potent and selective Tip60 inhibitor inductor of apoptosis and inhibitor of DNA damage response in prostate cancer [210]. Another Tip60 inhibitor **TH1834** was reported to be specific and inductor of apoptosis in breast cancer cells [211]. **L002** and analogues are non-specific HATi that showed inhibitory activities in leukemia and lymphoma cell lines, together with breast cancer [212].

Since the discovery of the previously described synthetic compounds, there were very few studies going deeper on their antitumoral activity. Contrarily, **C646** has been used in several studies since its report in 2010 as a selective p300 inhibitor that showed cell growth effects in melanoma and lung cancer cell lines [213]. C646 showed growth inhibition by apoptosis and cell cycle arrest in AML, especially in AML-1 ETO fusion protein (AE)-positive AML [214]. It was also effective in supressing migration in gastric cancer cell lines [215] and enhanced gemcitabine effect in pancreatic cancer [216]. In cervical cancer cells altered glucose metabolism and induces apoptosis [217]. Another recent inhibitor reported was the new p300/CBP inhibitor **A-485**. This compound selectively inhibited proliferation in lineage-specific tumours, such as several haematological malignancies and androgen receptor-positive prostate cancer [218].

Table 1: HAT inhibitors *Clinical trials from https://clinicaltrials.gov/ (accessed 2018, November 7). In the cases where there are several clinical trials reported, it will be shown the first posted (year) accompanied by the number of clinical trials reported to date for the most common cancers.*

CLASS	COMPOUND	TUMOR TYPE	STATUS	REFERENCES/ CLINICAL TRIAL IDENTIFIER
Bisubtrate inhibitors	**Acetyl-CoA derivatives**	Mechanistic studies	Preclinical	[184]
Natural products	**Anacardic Acid**	Prostate	Preclinical	[187]
	Curcumin	Colorectal	Clinical Trials	NCT00027495 (2003) + 11 other
		Breast	Clinical Trials	NCT00852332 (2009) + 7 other
		Prostate	Clinical Trials	NCT01917890 (2013) + 6 other
		Hematological	Clinical Trials	NCT00113841 (2005) + 4 other
		Pancreas	Clinical Trials	NCT00094445 (2004) + 3 other
		Lung	Clinical Trials	NCT01048983 (2010) + 2 other
		Endometrial	Clinical Trials	NCT02017353 (2013) + 1 other
		Head and neck	Clinical Trials	NCT01160302 (2010)
	Garcinol	Breast, colon, pancreatic, and leukemia	Preclinical	[195]
	LTK-14	Mechanistic studies	Preclinical	[196]
	Plumbagin	Lung, breast, ovarian, prostate, and colon	Preclinical	[199]
	Epigallocatechin-3-gallate (EGCG)	Prostate	Clinical Trials	NCT00459407(2007) + 4 other
		Breast	Clinical Trials	NCT00516243 (2007) + 3 other
		Colon	Clinical Trials	NCT01606124 (2012) + 3 other
		Lung	Clinical Trials	NCT00573885 (2007) + 3 other
		Bladder	Clinical Trials	NCT00666562 (2008)
		Multiple Myeloma	Clinical Trials	NCT00942422 (2009)
	Delphinidin	Breast, prostate, lung, liver, colon and ovarian	Preclinical	[202] [219]
	Gallic Acid	Colon, prostate, lung, cervical, glioma, leukemia	Preclinical	[204]
	Sanguinarine	Lung, colon, breast, pancreas, bladder, gastric and melanoma	Preclinical	[206]
	Procyanidin B3	Prostate	Preclinical	[207]
Small molecules	**MB-3**	Acute Lymphoblastic Leukemia	Preclinical	[209]
	NU9056	Prostate	Preclinical	[210]
	TH1834	Breast	Preclinical	[211]
	L002	Breast, hematological malignancies	Preclinical	[212]
	C646	Melanoma, lung, gastric, pancreatic, cervical and AML	Preclinical	[213-215, 217]
	A485	Hematological malignacies and prostate	Preclinical	[218]

4.2. Lysine Deacetylase inhibitors (KDACi/HDACi)

There is a broad number of HDAC inhibitors that can be classified in several major classes including **hydroxamic acids, cyclic tetrapeptides, benzamides** and **short chain fatty acids** derived inhibitors (Figure 9). Biological effects induced by these inhibitors are multiple such as cell growth arrest, induction of apoptosis or induction of terminal differentiation.

In this section the most studied HDAC inhibitors will be described and summarized in Table 2. They are being widely studied in a vast number of cancer types and in some cases in a huge number of clinical trials. Table 2 tries to give an overview of the status of each compound in the main cancers being tested.

Important to highlight that there are four HDAC inhibitors approved by the FDA for cancer treatment to date: Vorinostat, Romidepsin, Belinostat and Panobinostat. Vorinostat, Belinostat and Panobinostat belong to the hydroxamic acid class whereas Romidepsin to the cyclic tretrapeptides class.

Hydroxamic acids

Vorinostat (SAHA/Zolinza®) was the first HDACi approved by the FDA for the treatment of cutaneous T-cell lymphoma (CTCL) in 2006 [220]. It inhibits class I, II and IV HDACs and exerts its anticancer activity by inducing apoptosis and cell cycle arrest, inhibition of angiogenesis and downregulation of immunosuppressive interleukins [221]. For example it induces p21 [222] and downmodulate interleukin-10 (IL-10) expression as it also does romidepsin [223]. Actually, there are more than 200 clinical trials at different phases for vorinostat treatment in solid and hematological malignancies and other diseases such as HIV.

Belinosat (Beleodaq®) was approved in 2014 for peripheral T-cell lymphoma (PTCL) treatment [224]. It inhibits class I, II and IV HDACs inducing cell cycle arrest and apoptosis. In addition, it repressed survivin expression and increased the expression of transforming growth factor receptor II (TFGβRII) [225]. Belinostat had shown efficacy in preclinical studies in numerous solid and hematological tumors and several *in vitro* studies show that can act synergically with the proteasome inhibitor bortezomib [224].

Panobinostat (Farydak®) was approved in 2015 as combination therapy with bortezomib and dexamethasone for the treatment of patients with recurrent multiple myeloma who have received at least two previous treatment regimens [226]. This compound is a pan-HDAC inhibitor that inhibits class I, II and IV HDACs. It seems to be more potent than the other approved HDACi. It decreased proliferation in preclinical studies in several cancer types at nanomolar doses. Moreover, it showed no toxicity in normal cells. In multiple myeloma, it inhibited the aggresome protein degradation pathway and upregulated p21, resulting in apoptosis. It showed synergy with bortezomib [227]. Actually, there are more than 100 clinical trials ongoing with this drug for the treatment of hematological cancers, melanoma and glioma.

Due to the good results in the clinica of Vorinostat, an hydroxamic-acid based compound, further research was developed in this type of HDACi.

Trichostatin A (TSA) was one of the first natural hydroaxamate compound obtained [228] to which Vorinostat is structurally related. It inhibits class I, II and IV HDACs and has broad range of anticancer effects. TSA has never reached clinical trials due to negative side effects [229], however it has been broadly used in research of HDACs. **Abexinostat** is a pan-HDACi that shows induction of apoptosis as a primary mechanism of action [230]. It has shown synergy effects in combination with bortezomib in neuroblastoma [230] and with chemotherapeutic agents in soft tissue sarcoma [231]. To date there are clinical trials ongoing with this agent alone or in combination with other drugs. **Pracinostat** inhibits class I, II and IV HDACs and has shown antiproliferative features in several cancer cell lines. It shows synergy with the JAK2 inhibitor pracritinib in preclinical models of AML [232]. It is currently in clinical trials mainly for myelodisplasic syndromes and acute myeloid leukemia. **Resminostat** is a pan-HDAC inhibitor specially targeting class I HDACs. It has been mainly tested in hepatocellular carcinoma (HCC), showing good results in combination with Sorafenib, Cisplatin and Doxorubicin being in several clinical trials for HCC [233] and for other cancers. **Givinostat** is a pan-HDAC inhibitor that shows anticancer activity through inhibition of the Janus kinase/signal transducers and activators of transcription (JAK/STAT) pathway [234] in myeloproliferative neoplasms and several hematological cancers [235] being actually in several clinal trials for these

types of malignancies. **CUDC-101** was found to inhibit HDACs, the epidermal growth factor receptor (EGFR) and human epidermal growth factor receptor 2 (HER2) in cancer cells. This capacity of multitarget inhibition displayed a potent antiproliferative and proapoptotic effect [236]. It is clinical trials for solid tumors and specially in head and neck [237].

In this group of HDAC inhibitors, apart from pan-HDACi, there are also selective inhibitors including those for HDAC6 (**Tubacin, Tubastatin A and Ricolinostat**). Ricolinostat [27] is in clinical trials for multiple myeloma and other hematological malignancies. Studies in combination with other agents such as bortezomib are being investigated [27, 238].

Cyclic tetrapeptides

These group of HDAC inhibitors are the more complex in structure. The best studied is Romidepsin.

Romidepsin (Istodax®) was FDA approved in 2009 for CTCL [239] and in 2011 for PTCL [240]. This drug is a bicyclic depsipeptide [241] that inhibits mainly class I HDACs, leading to an increase of histone acetylation and an open chromatin status. It is a prodrug only activated after uptake into the cell that inhibits angiogenesis [242] and increases cell cycle arrest in early G1 phase by inducing p21, leading to inhibition of CDK and dephosphorylation of Rb [243]. It is actually in more than 60 clinical trials for the treatment of hematological malignancies and solid tumors.

Benzamides

Mocetinostat (MGCD0103) is selective for class I and class IV and showed a broad anticancer activity spectrum [244]. It is now in clinical trials mainly for hematological malignancies and some solid tumors such as lung cancer and melanoma. **Entinostat (MSC275)** is a selective class I inhibitor [245]. It is currently in several clinical trials for breast cancer, lung cancer, renal cancer, colorectal cancer and hematological malignancies.

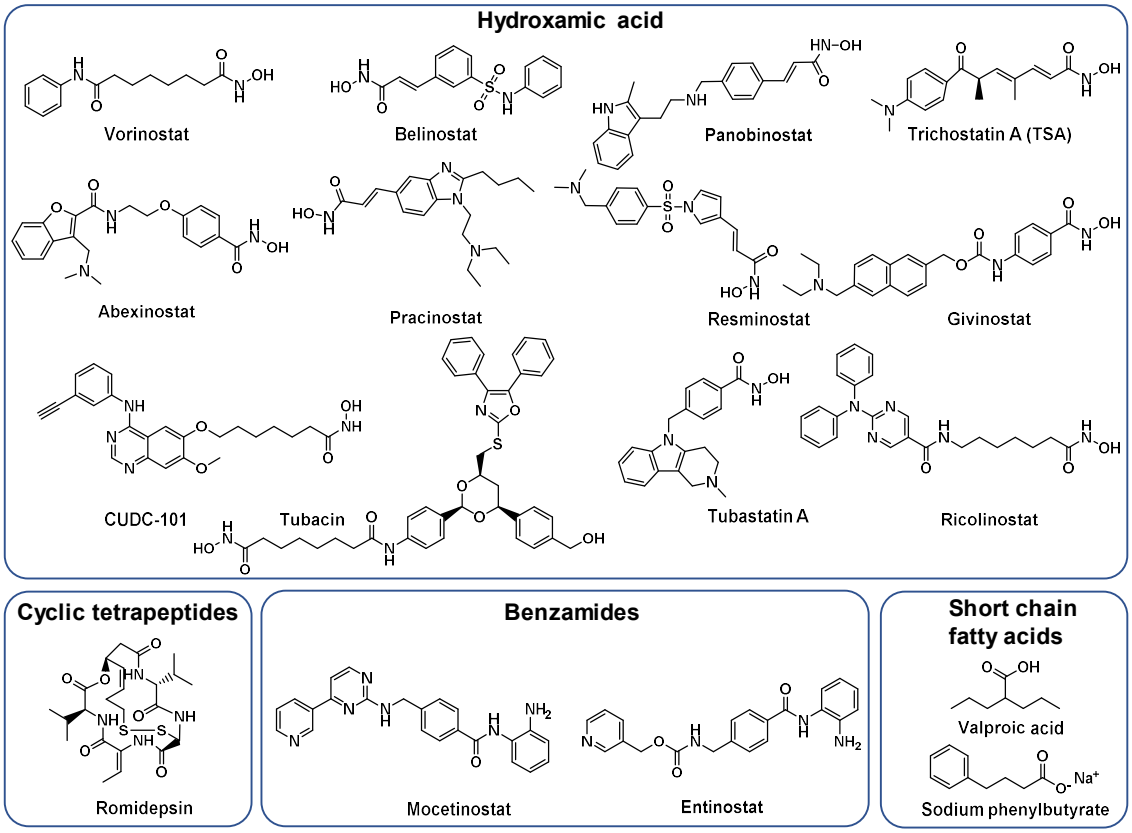

Figure 9: HDAC inhibitors chemical structures. *Chemical structures available from each class of HDAC inhibitors detailed in the text.*

Short chain fatty acids

The aliphatic acids are relatively weak HDAC inhibitors, being less attractive compounds.

Valproic acid has been used in the clinics for years for the treatment of mental diseases such as epilepsy or bipolar disorder. It was later described as a class I and IIa HDAC inhibitor with anti-cancer potency inducing apoptosis, cell cycle arrest and inhibits angiogenesis [246]. In cancer entered first in clinical trials for pediatric cancers such as central nervous system (CNS) tumors [247], but at present it is in clinical trials also for other cancers including hematological malignancies and a variety of solid tumors. **Sodium butyrate** and **Sodium Phenylbutyrate** inhibit class I and II of HDACs and possess diverse molecular functions as anti-cancer agents, such as supressing proliferation [248], inducing differentiation and senescence [249]. They have been broadly used in research for unveiling HDAC molecular functions, and sodium phenylbutyrate is in several clinical trials in cancer.

Table 2: HDAC inhibitors *Clinical trials from https://clinicaltrials.gov/ (accessed 2018, November 9). In the cases where there are several clinical trials reported, it will be shown the first posted (year) accompanied by the number of clinical trials reported to date for the most common cancers.*

CLASS	COMPOUND	TUMOR TYPE	STATUS	REFERENCES/ CLINICAL TRIAL IDENTIFIER
Hydroxamic acids	Vorinostat (SAHA/Zolinza®)	Cutaneous T-cell lymphoma (CTCL)	Approved by FDA (2006)	[220]
		Lymphoma	Clinical Trials	NCT00097929 (2004) + 57 other
		Leukemia	Clinical Trials	NCT00217412 (2005) + 42 other
		Lung	Clinical Trials	NCT00138203 (2005) + 27 other
		Multiple Myeloma	Clinical Trials	NCT00111813 (2005) + 21 other
		Breast	Clinical Trials	NCT00132002 (2005) + 19 other
		Melanoma	Clinical Trials	NCT00121225 (2005) + 5 other
		Colorectal	Clinical Trials	NCT00126451 (2005) + 4 other
		Prostate	Clinical Trials	NCT00005634 (2003) + 4 other
		Liver and Gastric	Clinical Trials	NCT00537121 (2007) + 3 other
		Ovarian	Clinical Trials	NCT00132067 (2005) + 3 other
		Head and neck	Clinical Trials	NCT01267240 (2010) + 1 other
	Belinostat (Beleodaq®)	Peripheral T-cell lymphoma (PTCL)	Approved by FDA (2014)	[224]
		Lymphoma	Clinical Trials	NCT00274651 (2006) + 14 other
		Leukemia	Clinical Trials	NCT00357032(2006) + 5 other
		Lung	Clinical Trials	NCT00926640 (2009) + 3 other
		Ovarian	Clinical Trials	NCT00301756 (2006) + 2 other
		Multiple Myeloma	Clinical Trials	NCT00131261(2005) + 1 other
	Panobinostat (Farydak®)	Multiple Myeloma	Approved by FDA (2015)	[226]
		Lymphoma	Clinical Trials	NCT00425555 (2007) + 28 other
		Leukemia	Clinical Trials	NCT00451035 (2007) + 21 other
		Breast	Clinical Trials	NCT00567879 (2007) + 8 other
		Lung	Clinical Trials	NCT00535951 (2007) + 8 other
		Prostate	Clinical Trials	NCT00419536 (2007) + 5 other
		Colorectal	Clinical Trials	NCT00690677 (2008) + 2 other
		Pancreas	Clinical Trials	NCT01056601 (2010)
	Trichostatin A (TSA)	Solid and hematological	Preclinical	[137]
	Abexinostat	Hematological	Clinical Trials	NCT00473577 (2007) + 4 others
		Advanced solid cancers	Clinical Trials	NCT01543763(2012) + 1 other
		Renal	Clinical Trials	NCT03592472 (2018)
		Sarcoma	Clinical Trials	NCT01027910 (2009)
	Pracinostat	Hematological	Clinical Trials	NCT00741234 (2008) + 7 other

		Prostate and advanced solid tumors	Clinical Trials	NCT00504296 (2007) + 2 other
	Resminostat	Hepatocellular	Clinical Trials	NCT00943449 (2009) + 1 other
		Lymphoma	Clinical Trials	NCT01037478 (2009) + 1 other
	Givinostat	Hematological	Clinical Trials	NCT00496431 (2007)+ 6 other
	CUDC-101	Solid tumors	Clinical Trials	NCT00728793 (2008) + 3 other
	Tubacin	Solid and hematological	Preclinical	[23]
	Tubastatin A	Solid and hematological	Preclinical	[23]
	Ricolinostat (ACY-1215)	Multiple Myeloma	Clinical Trials	NCT01323751 (2011)+ 2 other
		Leukemia and Lymphoma	Clinical Trials	NCT02091063 (2014) + 1 other
		Breast and Gynecological cancer	Clinical Trials	NCT02632071 (2015) + 1 other
Cyclic tetrapeptides	**Romidepsin (Istodax®)**	Cutaneous T-cell lymphoma (CTCL)	Approved by FDA (2009)	[239]
		Peripheral T-cell lymphoma (PTCL)	Approved by FDA (2011)	[240]
		Lymphoma	Clinical Trials	NCT00024180 (2003) + 51 other
		Leukemia	Clinical Trials	NCT00042822 (2003) + 9 other
		Multiple Myeloma	Clinical Trials	NCT00066638 (2003) + 6 other
		Breast	Clinical Trials	NCT00098397 (2004) + 4 other
		Lung	Clinical Trials	NCT00086827 (2004) + 4 other
		Colorectal	Clinical Trials	NCT00077337 (2004) + 2 other
		Prostate	Clinical Trials	NCT00106418 (2005) + 2 other
		Ovarian	Clinical Trials	NCT00085527 (2004) + 2 other
		Melanoma	Clinical Trials	NCT00104884 (2005) + 1 other
Benzamides	**Mocetinostat (MGCD-0103)**	Hematological	Clinical Trials	NCT00324129 (2006) + 12 other
		Lung	Clinical Trials	NCT00511576 (2007) + 2 other
		Melanoma	Clinical Trials	NCT03565406 (2018)
	Entinostat (MSC275)	Breast	Clinical Trials	NCT00676663 (2008) + 20 other
		Hematological	Clinical Trials	NCT00101179 (2005) + 11 other
		Lung	Clinical Trials	NCT00387465 (2006) + 8 other
		Renal	Clinical Trials	NCT01038778 (2009) + 4 other
		Colorrectal	Clinical Trials	NCT01105377(2010) + 2 other
Short chain fatty acids	**Valproic acid**	Hematological	Clinical Trials	NCT00075010 (2003) + 26 other
		Brain and Central Nervous System	Clinical Trials	NCT00302159 (2006) + 11 other
		Head and neck	Clinical Trials	NCT00181220 (2005) + 7 other
		Breast	Clinical Trials	NCT00395655 (2006) +4 other
		Lung	Clinical Trials	NCT00084981 (2004) + 3 other
	Sodium phenylbutyrate	Hematological	Clinical Trials	NCT00004871 (2003) + 6 other
		Brain	Clinical Trials	NCT00006450 (2000) + 1 other
		Colorectal	Clinical Trials	NCT00002796 (2003)

4.3. Bromodomain inhibitors

In the last years, a vast number of small-molecules inhibiting bromodomains have been reported as antitumor drugs. BET inhibitors are deeper developed, being most of them in clinical trials. However, discovery of inhibitors for the rest of bromodomain families will help to understand their roles and find new anti-cancer targets (Figure 10).

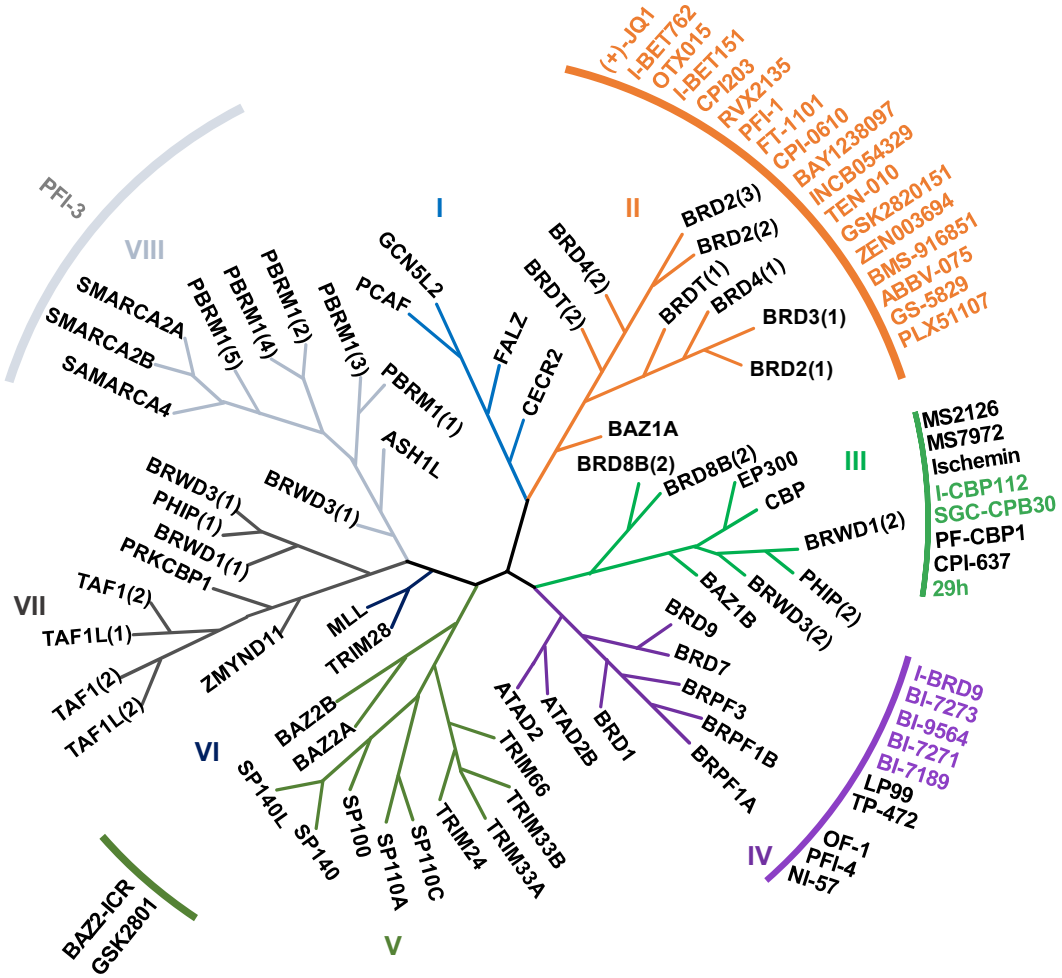

Figure 10: Structure-based phylogeny of the human bromodomains and their inhibitors. *There are 61 bromodomains in 46 bromodomain-containing proteins. Roman numerals indicate the eight major structural classes. Inhibitors reported for each family are indicated. Coloured inhibitors are the ones pointed out in the text. Adapted from Perez-Salvia et al. 2017 [164] and Filippakopoulos at al. 2014 [61].*

BET inhibitors

In 2010, two independent groups reported two small molecules that inhibit BET bromodomains: **JQ1** [17] and **I-BET762** [250]. Both are quite similar in chemical structure and in mechanism. They inhibit BET proteins with higher selectivity over other bromodomains. They act by displacing BET proteins from chromatin by binding to the bromodomain pocket and competing with acetylated lysines.

The first study that reported preclinical efficacy of JQ1 was in NUT midline carcinoma (NMC). In this rare cancer, BRD4 forms a fusion protein with NUT gene (BRD4-NUT) which act as an aberrant transcription factor regulator with oncogenic properties. The treatment with JQ1 displaces the fusion oncoprotein from chromatin and induces squamous differentiation and growth arrest *in vitro* and *in vivo* in NMC [17]. After this study, a high volume of other reports about these inhibitors were published, first in hematological malignancies but then also in solid tumors. There is also an extended number of clinical trials with BET inhibitors [164].

In hematological malignancies including AML, B-cell acute lymphoblastic leukemia, multiple myeloma, Burkitt's lymphoma and diffuse large B cell lymphoma, BET inhibition with JQ1 downregulates *MYC* transcription and MYC target genes involved in tumorigenesis leading to cell cycle arrest and cellular senescence. *MYC* downregulation is the main and most common effect of BET bromodomain inhibition, however there are other genes or mechanisms altered. It is efficient in repressing aberrant oncogenic transcription caused by genetic alterations such as *(Nucleophosmin 1) (NPM1)* mutations and *MLL* translocations in AML. Also, in lymphomas it decreases NF-kB mediated transcription [251].

In solid tumors, there is a large number of studies and clinical trials. In most cases, JQ1 also induces an antiproliferative phenotype by inhibiting MYC and consequently MYC driven transcription. However, there are several effects beyond MYC reported. In castration-resistant prostate cancer (CRPC), JQ1 reduces Androgen receptor (AR) target genes transcription induced by BRD4 [252]. In NSCLC, JQ1 was described to suppress the oncogenic transcription factor *FOS Like 1, AP-1 Transcription Factor Subunit (FOSL1)* and its targets [253], and SCLC cell lines are especially sensitive to JQ1 growth inhibition due

to the downregulation of the lineage specific transcription factor *achaetescute homolog-1 (ASCL1),* which seems to be overexpressed in more than 50% of SCLC patients samples [254]. BRD4 is overexpressed in hepatocellular carcinoma (HCC), being JQ1 treatment effective causing, together with the repression of MYC expression, the upregulation of the pro-apoptotic gene *BCL2 Like 11 (BCL2L11,* commonly named *BIM)* and *p27* [255]. In colon cancer, JQ1 exerts an antiproliferative phenotype especially in CpG island methylator phenotype (CIMP) tumors, due to a CIMP associated super-enhancer from which a long noncoding RNA *colon cancer associated transcript 1 (CCAT1)* is transcribed that is particularly sensitive to JQ1. This super-enhancer regulates *c-MYC* transcription which correlates with the presence of CCAT1, meaning that CCAT1 could be a biomarker for patients likely to respond to BET inhibitors [256]. In pancreatic ductal adenocarcinoma (PDAC), tumor progression was inhibited in patient-derived xenograft models treated with JQ1, by decreasing cell division Cycle 25B (CDC25B) expression, a regulator of cell cycle progression [257].

In breast cancer, JQ1 has been broadly tested and shown to be effective in most subtypes of this tumor [258]. JQ1 mechanism of action sometimes differs between breast cancer subtypes. However, it is common in most of them cell cycle arrest in G1 phase and downregulation of MYC produced by BET inhibition [259]. In Triple Negative Breast Cancer (TNBC) BET inhibition halts cell proliferation without consistently downregulating MYC. However, a disruption of mitosis is observed potentially due to downregulation of Aurora Kinases A and B [260] and the critical mitosis regulator LIN9 [261]. Super-enhancers modulation by JQ1 of several breast cancer oncogenes is also observed in major part of breast cancers. Moreover, prevention of transcription of estrogen receptor (ER)-target genes has been reported in ER+ breast cancers [171]. There have been also several studies of JQ1 in combination with other drugs in standard-therapy resistant breast cancer models. For instance, JQ1 showed synergy with fulvestrant, an ER degrader, in tamoxifen-resistant breast cancer [262]. JQ1 also synergizes with everolimus and resensitizes resistant cells to this drug by depletion of MYC, which is upregulated by BRD4 in everolimus resistant ER+ breast cancers [263].

Since JQ1 was discovered, it has been the archetype molecule of this type of inhibitors and have been used broadly for preclinical studies of BET inhibition due to its open source character for researchers. However, due to its pharmacological properties it has not reach clinical trials.

I-BET762 (GSK525762A/Molibresib) that appeared simultaneously with JQ1, also causes inhibition of growth in NMC, being in clinical trials for this type of cancer and other hematological and solid tumors (Table 3).

Since JQ1 and I-BET762 report, other BET-inhibitors (Figure 11) have been used in preclinical studies and clinical trials summarized in Table 3.

OTX015 (MK-8628) is another BET inhibitor that was reported to have greater anti-proliferative effect than JQ1 in glioblastoma multiforme models and synergizes with conventional therapies such as temozolomide [264]. It also shows cell cycle arrest and apoptosis in acute leukemia cells [265] and is in clinical trials for several hematological cancers and solid tumors. **I-BET151 (GSK1210151A)** was reported as a novel BRD3/BRD4 inhibitor which caused apoptosis and cell cycle arrest in mixed lineage leukemia (MLL) linked with a decrease of *BCL-2*, *MYC* and *Cyclin Dependent Kinase 6 (CDK6)* genes [266]. There are also preclinical studies in myeloma [267], AML with Nucleophosmin 1 mutations (NPM1c) [268], glioblastoma [269], melanoma [270] and ovarian cancer [271] where this compound exerts anti-tumoral activity, however it has not reach clinical trials yet. **CPI203** has been mainly tested in combination with other drugs in cases of resistance. For example, it overcomes resistance to venetoclax in MYC+/BCL2+ double-hit lymphoma [272], and synergizes with lenalidomide in multiple myeloma [273]. **RVX2135** inhibits proliferation in Myc-overexpressing murine lymphoma partly by inducing HDAC-silenced genes, suggesting a synergic combination with HDACi [274]. **PFI-1** was reported to be anti-proliferative in leukemic cell lines. Important to highlight is that different from other BET inhibitors, it also produces a decrease in Aurora B kinase, suggesting that this inhibitor could target this two potent oncogenes simultaneously [275]. It has recently been reported to be an efficient inhibitor in prostate cancer cells by diminishing AR/AR-V7 signalling, being AR-V7 the most prevalent androgen receptor splice variant [276].

Other BET inhibitors are **FT-1101** and **CPI-0610**, in clinical trials for hematological malignancies. **BAY 1238097** and **INCB054329** and **TEN-010** are in clinical trials also for hematological cancers and several solid tumors. **GSK2820151** is being tested in patients with advanced or recurrent solid tumors and **ZEN003694** in Metastasic Castration-Resistant Prostate Cancer. **BMS-986158**, **ABBV-075**, **GS-5829** and **PLX51107** are other BET inhibitors in clinical trials for diverse solid tumors and hematological malignancies (Table 3). From them, GS-5829 has recently been observed to increase apoptosis in uterine serous carcinoma overexpressing C-MYC [277].

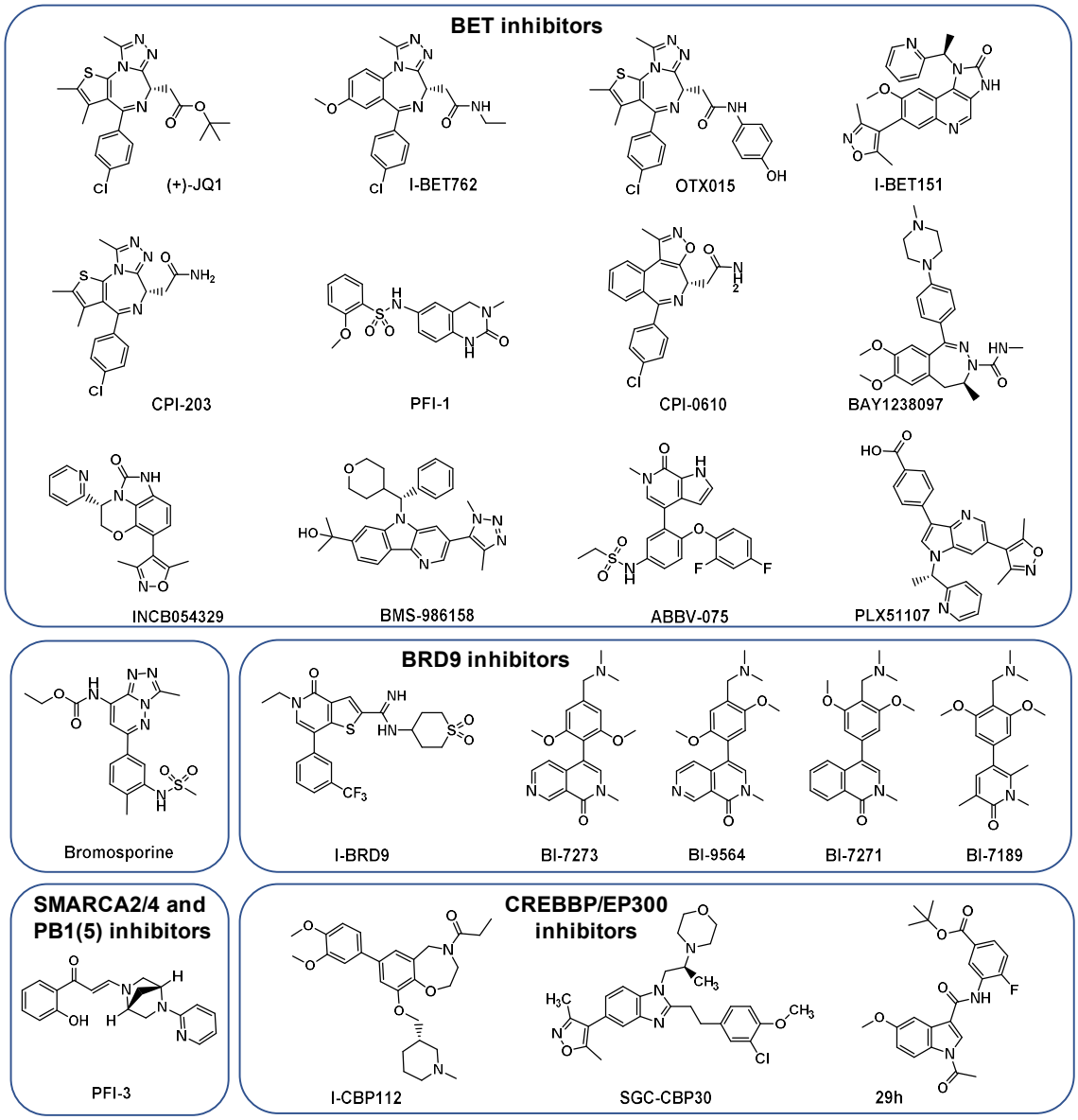

Figure 11: Bromodomain inhibitors chemical structures. *Structures available from BET bromodomain inhibitors and non-BET inhibitors detailed in the text.*

Non BET inhibitors

Non BET bromodomain inhibitors have been less studied. However, discovery of this type of inhibitors would be useful for unveiling its role in multidomain proteins where they belong, that are in many cases epigenetic regulators. This will also be useful to find new druggable proteins for cancer treatment. There are several non BET inhibitors reported that have not been even tested in cancer yet. We will point out only the ones that have been tested in cancer, however none of them is in clinical trials and all need further investigation.

In this sense, **Bromosporine** was made available by the Structural Genomic Consortium (SGC) as a multi-bromodomain inhibitor that targets promiscuously BET and non-BET bromodomains. However, it has been tested in leukemia and it only showed effects of BET bromodomain family inhibition [278].

Inhibitors of BRD9 such as **I-BRD9** has been reported to be selective over the BET family and the highly homologous BRD7 [279]. It has been tested in leukemia and in rhabdoid tumors [280]. Different BRD9 inhibitors **(BI-7273, BI-9564, BI-7271** and **BI-7189)** were also tested in AML and rhabdoid tumors [180, 280, 281].

The SGC reported **PFI-3** as inhibitor of SMARCA2/4 and PB1(5). However, one study with PFI-3 described that inhibition of the bromodomain of SMARCA2/4 did not caused any antiproliferative phenotype. This determined that the ATPase domain, and not the bromodomain, is here the relevant druggable target [282].

CREBBP and p300 bromodomain inhibitors have been probably the most studied, apart from BET inhibitors. **I-CPB112** was reported to inhibit these bromodomains with good selectivity and to exert anti-proliferative effect in leukemia [283]. Moreover, it acts as an activator of HAT activity of CREBBP/p300 on nucleosomes enhancing its antiproliferative effect in cancer [284]. **SGC-CBP30** is another selective CBP/p300 bromodomain inhibitors reported together with I-CBP112 to decrease viability of multiple myeloma cells by directly causing the transcriptional suppression of *Interferon Regulatory Factor 4 (IRF4),* essential for myeloma cells survival, and its target gene *C-MYC* [285]. Recently another CBP/p300 inhibitor named **29h** was reported and tested in castration-resistant prostate cancer [286].

Table 3: Bromodomain inhibitors. *Clinical trials from https://clinicaltrials.gov/ (accessed 2018, November 9).*

CLASS	COMPOUND	TUMOR TYPE	STATUS	REFERENCES/ CLINICAL TRIAL IDENTIFIER
BET inhibitors	**(+)-JQ1**	Hematological, prostate, lung, hepatocellular, colon, pancreatic, breast, glioblastoma, medulloblastoma	Preclinical	[251-258]
	I-BET762 (GSK525762A, Molibresib)	Hematological	Clinical trials	NCT01943851 (2013)
		Lung, colorectal, neuroblastoma, MYCN driven solid tumors, Ras-mutated solid tumors.	Clinical trials	NCT01587703 (2012) NCT03266159 (2017)
		NUT midline carcinoma (NMC)	Clinical trials	NCT01587703 (2012) NCT03702036 (2018)
		Breast	Clinical trials	NCT01587703 (2012) NCT02964507 (2016)
		Prostate	Clinical trials	NCT01587703 (2012) NCT03150056 (2017)
	OTX015 (MK-8628)	Hematological	Clinical trials	NCT02698189 (2016) NCT01713582 (2012) NCT02303782 (2014)
		NUT Midline Carcinoma, breast, lung, prostate, pancreatic	Clinical trials	NCT02698176 (2016) NCT02259114 (2016)
		Glioblastoma multiforme	Clinical trials	NCT02296476 (2014)
	I-BET151 (GSK1210151A)	Hematological, glioblastoma, melanoma, ovarian	Preclinical	[266-271]
	CPI203	Hematological	Preclinical	[272, 273]
	RVX2135	Myc-induced murine lymphoma	Preclinical	[274]
	PFI-1	Leukemia and prostate	Preclinical	[275, 276]
	FT-1101	Hematological	Clinical trials	NCT02543879 (2015)
	CPI-0610	Hematological	Clinical trials	NCT01949883 (2013) NCT02157636 (2014) NCT02158858 (2014)
	BAY1238097	Hematological, hepatocellular, lung, NUT midline carcinoma and melanoma	Clinical trials	NCT02369029 (2015)
	INCB054329	Hematological and advanced solid tumor	Clinical trials	NCT02431260 (2015)
	TEN-010 (RO6870810)	Hematological	Clinical trials	NCT02308761 (2014) NCT03068351 (2017) NCT03255096 (2017)
		Advanced solid tumors	Clinical trials	NCT01987362 (2013)
		Ovarian and Breast	Clinical trials	NCT03292172 (2017)
	GSK2820151	Solid tumors	Clinical trials	NCT02630251 (2015)
	ZEN003694	Metastatic Castration-Resistant Prostate Cancer	Clinical trials	NCT02705469 (2016) NCT02711956 (2016)
	BMS-986158	Advanced solid tumors and hematological malignancies	Clinical trials	NCT02419417 (2015)
	ABBV-075	Breast, lung, prostate and hematological	Clinical trials	NCT02391480 (2015)
	GS-5829	Metastatic Castration-Resistant Prostate Cancer	Clinical trials	NCT02607228 (2015)
		Advanced solid tumors and Lymphomas	Clinical trials	NCT02392611 (2015)
		Breast	Clinical trials	NCT02983604 (2016)

	PLX51107	Solid Tumors and hematological	Clinical trials	NCT02683395 (2016)
Multi-bromodomain inhibitors	**Bromosporine**	Leukemia	Preclinical	[278]
BRD9 inhibitors	**I-BRD9**	Leukemia and rhabdoid tumors	Preclinical	[280]
	BI-7271/BI-7273/BI-9564/BI-7189	Acute Myeloid Leukemia (AML) and rhabdoid tumors	Preclinical	[180, 280, 281]
SMARCA2/4 and PB1(5) inhibitors	**PFI-3**	Lung cancer, synovial sarcoma, rhabdoid cancer, AML (SWI/SNF-mutant cancers)	Preclinical	[282]
CREBBP/EP300 inhibitors	**I-CBP112**	Leukemia and multiple myeloma	Preclinical	[284, 285]
	SGC-CBP30	Multiple myeloma	Preclinical	[285]
	29h	Castration-resistant prostate cancer	Preclinical	[286]

AIMS

Cancer is considered a genetic and epigenetic disease of high diversity and complexity [30]. Aberrancies in the epigenetic marks in DNA and histone tails together with alterations in epigenetic regulators responsible of catalyzing these marks have been shown to be crucial in tumorigenesis [4].

DNA methylation profiles are already used in cancer clinical stage as biomarker and diagnostic tool [54]. The same is thought to happen in the near future with alterations in histone modifiers and histone marks, since recurrent aberrancies are being described in specific types of tumors [287].

The plasticity of the epigenetic landscape compared to the unchangeable nature of genetic alterations has led to an increasing interest in the last years in finding specific drugs able to modulate and correct the epigenetic aberrancies present in tumors. In fact, six epigenetic drugs are already used in the clinics for the treatment of hematological cancers: two DNMTs inhibitors and four HDAC inhibitors. There is also a vast number of clinical trials ongoing with drugs targeting writers, readers and erasers of the epigenome.

The fact that some HDAC inhibitors are already in clinics makes particularly interesting the study of histone acetylation and its enzymatic regulators. Moreover, the discovery of acetylation regulation by HATs or HDACs in proteins different from histones but also very important in tumorigenesis such as the well-known p53 or Myc [8] opened a new layer of research in the field of modulating acetylation as cancer treatment.

HYPOTHESIS

Taking all these scientific considerations into account, the present Doctoral Thesis has been devoted to study epigenetic regulators involved in acetylation of histones and non-histones substrates, as also its targeting with small-inhibitors in cancer. We hypothesized that a more profound investigation about new alterations and function of these epigenetic regulators in cancer will open new venues for treatment. Moreover, we also want to unveil how its targeting with new available small-inhibitors affect molecular mechanisms or genes in different types

of cancer. This knowledge goes in the direction of finding new biomarkers for a more personalized cancer treatment.

To achieve this, we divided the project in three lines of study, where we will investigate the presence of alterations or the effect of small-inhibitors in writers, readers and erasers of lysine acetylation in cancer. For each one we defined specific aims.

Study I

1. **Investigate the role of histone acetyltransferase KAT6B in Small Cell Lung Cancer (SCLC).**

1.1. Study copy number alterations for *KAT6B* gene in SCLC and consequent changes in protein function.

1.2. Examine the phenotype *in vitro* and *in vivo* caused by KAT6B alteration.

1.3. Outline the molecular mechanisms responsible for the phenotype caused by KAT6B aberrancy.

1.4. Evaluate whether KAT6B-aberrant tumors show increased sensitivity to any epigenetic drug or classic chemotherapy agent.

Study II

2. **Unveil the molecular implications of bromodomain inhibitor JQ1 treatment in breast cancer.**

2.1. Investigate the effect of JQ1 in human luminal breast cancer cell lines.

2.2. Explore JQ1 target genes potentially involved in the effect of the drug.

2.3. Check the efficacy of JQ1 *in vivo* in a luminal breast cancer mice model.

Study III

3. Study a new HDAC6 inhibitor (QTX125) in cancer.

3.1. Study the specificity of the new compound QTX125 to HDAC6 and its target α-Tubulin.

3.2. Trial QTX125 antitumor potency in human cancer cell lines

3.3. Investigate QTX125 effect in apoptosis in Mantle Cell Lymphoma (MCL) cell lines.

3.4. Survey QTX125 efficacy *in vivo* in MCL.

3.5. Evaluate QTX125 effect in blood from healthy donors and primary samples of MCL patients.

RESULTS

DIRECTORS REPORT

To who may concern, we authenticate that the PhD student MONTSERRAT PÉREZ SALVIA will present her PhD thesis by scientific publications. Her contribution for each publication will be next pointed out.

Study I:

"KAT6B is a tumor suppressor histone H3 lysine 23 acetyltransferase undergoing genomic loss in small cell lung cancer"

Laia Simó-Riudalbas, **Montserrat Pérez-Salvia**, Fernando Setien, Alberto Villanueva, Catia Moutinho, Anna Martínez-Cardús, Sebastian Moran, Maria Berdasco, Antonio Gomez, Enrique Vidal, Marta Soler, Holger Heyn, Alejandro Vaquero, Carolina de la Torre, Silvia Barceló-Batllori, August Vidal, Luca Roz, Ugo Pastorino, Katalin Szakszon, Guntram Borck, Conceição S. Moura, Fátima Carneiro, Ilse Zondervan, Suvi Savola, Reika Iwakawa, Takashi Kohno, Jun Yokota, and Manel Esteller

Journal: Cancer Research. 2015 Sep 15;75(18):3936-45. doi: 10.1158/0008-5472.CAN-14-3702. Impact factor: 9.13

Contribution:

Montserrat Pérez Salvia participated in most of the experiments developed in coordination with the first author Laia Simó-Riudalbas and supervised by Dr. Manel Esteller. Briefly she was in charge of perform cell proliferation and drugs IC50 assays, qRT-PCR and Western-Blots. She also contributed in obtaining shRNA-KAT6B cells models and collaborated with the preparation of samples for LC/MS-MS. Besides she helped in the analysis and interpretation of generated data and in the manuscript revision. Important to refer that this publication was presented as part of Laia Simó-Riudalbas PhD thesis; also that Montserrat Pérez Salvia has first author permission to present results from this publication in her PhD thesis.

Study II:

"Bromodomain inhibition shows antitumoral activity in mice and human luminal breast cancer"

Montserrat Pérez-Salvia, Laia Simó-Riudalbas, Pere Llinàs-Arias, Laura Roa, Fernando Setien, Marta Soler, Manuel Castro de Moura, James E Bradner, Eva Gonzalez-Suarez, Catia Moutinho and Manel Esteller

Journal: Oncotarget. 2017 May 29;8(31):51621-51629. doi: 10.18632/oncotarget.18255. Impact Factor: 5.16

Contribution:

Montserrat Pérez Salvia was responsible for the experimental design and execution, supervised by Dr. Esteller and Dr. Moutinho. She also performed data analysis and interpretation, together with the manuscript writing and revision.

Study III

"In vitro and in vivo activity of a new small-molecule inhibitor of HDAC6 in mantle cell lymphoma"

Montserrat Perez-Salvia, Eneko Aldaba, Yosu Vara, Myriam Fabre, Cristina Ferrer, Carme Masdeu, Aizpea Zubia, Eider San Sebastian, Dorleta Otaegui, Pere Llinàs-Arias, Margalida Rosselló-Tortella, Maria Berdasco, Catia Moutinho, Fernando Setien, Alberto Villanueva, Eva González-Barca, Josep Muncunill, José-Tomás Navarro, Miguel A. Piris, Fernando P. Cossio and Manel Esteller.

Journal: Haematologica. 2018 Nov;103(11):e537-e540. doi: 10.3324/haematol.2018.189241. Impact factor: 9.09

Contribution:

Montserrat Pérez Salvia was responsible of performing all the experiments related with the biological activity of QTX125 in lymphoma cell lines. This included IC50 assays, determination of acetylation levels of α-tubulin and apoptosis. Besides, she was responsible of testing the compound in primary samples of MCL and healthy donors blood. She also did the analysis and interpretation of the generated data, together with the manuscript writing and revision. All the experiments were supervised by Dr. Esteller and Dr. Moutinho.

Dr. Manel Esteller, M.D, Ph.D.
Epigenetics of Cancer Group, Leader
Cancer Epigenetics and Biology Program (PEBC), Director
Bellvitge Biomedical Research Institute (IDIBELL)
Avda. Gran Vía 199-203
08908 L'Hospitalet de Llobregat, Barcelona, Spain
+34 92607500 ext.3176
mesteller@idibell.cat

Dr. Cátia Moutinho, Ph.D.
Cancer Epigenetics and Biology Program (PEBC)
Bellvitge Biomedical Research Institute (IDIBELL)
Avda. Gran Vía 199-203
08908 L'Hospitalet de Llobregat, Barcelona, Spain
+34 92607500 ext.3176
cmoutinho@idibell.cat

Study I

"KAT6B is a tumor suppressor histone H3 lysine 23 acetyltransferase undergoing genomic loss in small cell lung cancer"

Laia Simó-Riudalbas[1], **Montserrat Pérez-Salvia[1]**, Fernando Setien[1], Alberto Villanueva[2], Catia Moutinho[1], Anna Martínez-Cardús[1], Sebastian Moran[1], Maria Berdasco[1], Antonio Gomez[1], Enrique Vidal[1], Marta Soler[1], Holger Heyn[1], Alejandro Vaquero[3], Carolina de la Torre[4], Silvia Barceló-Batllori[4], August Vidal[5], Luca Roz[6], Ugo Pastorino[7], Katalin Szakszon[8], Guntram Borck[9], Conceição S. Moura[10], Fátima Carneiro[11], Ilse Zondervan[12], Suvi Savola[12], Reika Iwakawa[13], Takashi Kohno[13], Jun Yokota[13,14] & Manel Esteller[1,15,16]

[1]Cancer Epigenetics Group, Cancer Epigenetics and Biology Program (PEBC), Bellvitge Biomedical Research Institute (IDIBELL), Barcelona, Catalonia, Spain. [2]Translational Research Laboratory, Catalan Institute of Oncology (ICO), IDIBELL, Barcelona, Catalonia, Spain. [3]Chromatin Biology Group and [4]Proteomics Unit at PEBC, IDIBELL, Barcelona, Catalonia, Spain. [5]Department of Pathology, Bellvitge University Hospital, IDIBELL, Barcelona, Catalonia, Spain. [6]Tumor Genomics Unit, Department of Experimental Oncology and Molecular Medicine and [7]Thoracic Surgery Unit, Department of Surgery, at Fondazione IRCCS Istituto Nazionale dei Tumori, Milan, Italy. [8]Institute of Pediatrics, Clinical Genetics Center, University of Debrecen, Debrecen, Hungary. [9]Institute of Human Genetics, University of Ulm, Ulm, Germany. [10]Department of Pathology, Centro Hospitalar de São João, Porto, Portugal. [11]Institute of Molecular Pathology and Immunology of the University of Porto (IPATIMUP) and Medical Faculty of University of Porto, Porto, Portugal. [12]MRC-Holland, Amsterdam, the Netherlands. [13]Division of Genome Biology, National Cancer Center Research Institute, Tokyo, Japan. [14]Genomics and Epigenomics of Cancer Prediction Program, Institute of Predictive and Personalized Medicine of Cancer (IMPPC), Badalona, Catalonia, Spain. [15]Department of Physiological Sciences II, School of Medicine, University of Barcelona, Barcelona, Catalonia, Spain. [16]Institucio Catalana de Recerca i Estudis Avançats (ICREA), Barcelona, Catalonia, Spain.

Cancer Research. 2015 Sep 15;75(18):3936-45. doi: 10.1158/0008-5472.CAN-14-3702

ABSTRACT

Recent efforts to sequence human cancer genomes have highlighted that point mutations in genes involved in the epigenetic setting occur in tumor cells. Small cell lung cancer (SCLC) is an aggressive tumor with poor prognosis, where little is known about the genetic events related to its development. Herein, we have identified the presence of homozygous deletions of the candidate histone acetyltransferase *KAT6B*, and the loss of the corresponding transcript, in SCLC cell lines and primary tumors. Furthermore, we show, *in vitro* and *in vivo*, that the depletion of KAT6B expression enhances cancer growth, while its restoration induces tumor suppressor-like features. Most importantly, we demonstrate that KAT6B exerts its tumor inhibitory role through a newly defined type of histone H3 Lys23 acetyltransferase activity.

INTRODUCTION

Small cell lung cancer (SCLC) accounts for about 15% of all lung cancers and is characterized by accelerated growth, frequent metastases and premature death [1]. Although SCLC patients demonstrate many times a complete initial response to chemotherapy, the tumor almost always returns probably due to the original presence of quiescent cells. If the total cancer volume is irradiated, survival of SCLC patients is improved. Importantly, we have poor second-line therapies especially when the cancer comes back quickly after first-line therapy is completed. In this regard, no new biologically targeted therapeutics have shown activity in this tumor type [2]. Comprehensive genomic analyses have revealed genetically altered therapeutic targets in non-small cell lung carcinoma [3], but little is known about the genetic events involved in SCLC beyond the long-recognized high rate of *TP53* and *RB1* mutations [1]. Molecular studies in SCLC have been hampered because these tumors are rarely resected, resulting in a lack of suitable tumor specimens. However, point mutations in genes encoding histone modifiers in SCLC have recently been described [4]. In this regard, disruption of the histone modification landscape is a common event in cancer cells [5, 6], leading to significant changes in chromatin structure and gene expression affecting oncogenes and tumor suppressor genes [7, 8]. In this context, much effort has been devoted to analyzing the exomes of histone

modifiers in search of small nucleotide changes, but cancer-specific copy-number changes have not been particularly studied in profound detail. To address this issue, we have examined the existence of this type of gross genomic alteration for histone modifiers in SCLC that can functionally contribute to the tumoral phenotype and that are of translational relevance.

MATERIAL AND METHODS

Cell lines and primary tumor samples.

Cell lines were purchased from the ATCC (WI-38, NCI-H1963, NCI-H740, NCI-H2171, NCI-H1048, NCI-N417, DMS-114, NCI- H1672, and NCI-H2029), from the Leibniz Institute DSMZ (Jena, Germany)-German Collection of Microorganisms and Cell Cultures (HCC-33), and from Sigma-Aldrich (DMS-273). All cell lines were characterized by short tandem repeat (STR) analysis profiling (LGS Standards SLU) within 6 months after receipt. DNA samples from primary and metastatic tumors of SCLC patients were obtained at surgery or autopsy from 1985 to 2010 at the National Cancer Center Hospital/National Cancer Center Biobank (Tokyo, Japan), Saitama Medical University (Saitama, Japan), and University of Tsukuba (Ibaraki, Japan). The study was approved by the corresponding Institutional Review Boards.

Genotyping microarrays and MLPA analysis

Illumina HumanOmni5-Quad (v1) genotyping array was processed as previously described [9]. For multiplex ligation-dependent probe amplification (MLPA), genomic DNA was subjected to SALSA probemixes containing probes for the *KAT6B* gene, in addition to 21 reference probes, and the analyses were performed using Coffalyser.net software (MRC-Holland).

FISH analysis

The UCSC genome browser was used to select the 10q22.2 region probe for *KAT6B* detection (RP11-668A2), and the telomeric probe in 10p15.3 (RP11-361E18) was used as a control. Bacterial artificial chromosome (BAC) clones were obtained from the BACPAC Resource at the Children's Hospital Oakland

Research Institute (Oakland, CA). Probes were labeled with Spectrum Green and Red dUTP (Abbott).

Quantitative genomic PCR

The deletion frequency of *KAT6B* (evaluated by SYBR Green) was calculated by the standard curve method using the 7900HT SDS program. Results are reported as the *n*-fold copy number increase relative to the *KAT6B* gene (10q22.3).

Expression analysis

qRT-PCR, immunoblotting, immunohistochemistry, and chromatin immunoprecipitation (ChIP) assays were performed as previously described [9]. For microarray expression array analysis, total RNA from NCI-N417 and HCC-33 cells expressing two different short hairpin RNA (shRNA) sequences against KAT6B and two different scrambled sequences was labeled and hybridized onto a Human Gene Expression G3 v2 60K array following the manufacturer's instructions. qRT-PCR/ChIP primers and antibodies are described in Supplementary Table S1.

KAT6B mutational screening

KAT6B mutations were screened in complementary DNA from 60 SCLC patients and the SCLC lines using direct sequencing (primers in Supplementary Table S1).

Short hairpin interference and ectopic expression assays.

Two hairpin RNA (shRNA) molecules targeting two different gene sequences of KAT6B mRNA (shRNA5 and shRNA8) were designed and transfected into NCI-N417 and HCC-33 cells. The described sequences were mutated in two sites to obtain two shRNA scrambled sequences (Supplementary Table S1). For ectopic expression experiments, cDNA from human KAT6B longest isoform was purchased from BioSource (I.M.A.G.E. predicted full-length cDNA clones IRCBp5005P0112Q). *KAT6B* gene was subcloned from pCR-XL-TOPO bacterial expression vector to pRetroX-Tight-Pur mammalian expression vector, within the

Retro-XTM Tet-On Advanced Inducible Expression System. A FLAG-tag in the carboxy-terminal end of the protein separated by a flexible Gly–Ser–Gly sequence was introduced.

In vitro proliferation assays

Cell proliferation was determined by the 3-(4,5-dimethyl-2- thiazolyl)-2,5-diphenyl-2H-tetrazolium bromide (MTT) and XTT (2,3-Bis-(2-Methoxy-4-Nitro-5-Sulfophenyl)-2H-Tetrazolium-5-Carboxanilide) assays. The soft agar colony formation assay was performed in 6-well culture plates. Cell proliferation was also determined by counting living cells in the Neubauer chamber using the Trypan blue approach. For dose-response assays, 10,000 to 20,000 cells were seeded in 96-well plates.

Mouse xenograft and metastasis models

Athymic nude male mice were subcutaneously injected in each flank with a total of 3.5 x 10^6 scramble NCI-N417 cells (n = 10) and shRNA NCI-N417 cells (n = 10). Tumor growth was monitored every 3 to 4 days by measuring tumor width and length. Pieces (3 mm^3) of subcutaneous mouse tumors were implanted in mouse lungs to generate an orthotopic SCLC mouse model (8 animals for each experiment). For the drug experiments, either irinotecan (24 mg/kg) or vehicle (saline buffer) was injected into the peritoneal cavity once a week for 3 weeks. For the metastasis model, 1.5 x 10^6 cells were injected into the spleen of 24 mice. Hepatic metastases were examined macroscopically and microscopically. Mouse experiments were approved by the IDIBELL Animal Care Committee.

LC/MS-MS, protein sequence database searching, and SRM

Histone extracts were loaded into an 18% acrylamide/bisacrylamide gel and the histone H3 bands were excised and trypsin-digested. Peptide extracts were analyzed by liquid chromatography-tandem mass spectrometry (LC/MS-MS) using an EASY nLC II (Proxeon) coupled to an amaZon ETD Ion Trap. Data were generated with Data Analyst 4.1 software. MS and MS/MS data were analyzed with ProteinScape 3.1.2 software using Mascot 2.4.0 as the search engine and

SwissProt database. Identification was verified using a nanoACQUITY UPLC (Waters) chromatographer coupled to a high-resolution LTQ Orbitrap VelosTM MS. H3K23 acetylation levels were quantified by selected reaction monitoring (SRM) analyzing the precursor and fragment ion masses from acetylated peptides on a hybrid triple quadrupole/ion trap mass spectrometer instrument.

In vitro histone acetylation assays

Histone acetyltransferase assays were performed with GST-Flag–tagged KAT6B HAT domain purified from *Escherichia coli*. One hundred nanograms of HAT domain was incubated in 20 μmol/L [acetyl-1-14C] coenzyme A and 1 μg core histones for 2 hours at 30ºC. Incorporated ^{14}C was detected by fluorography with low-energy intensifying screen and loading was assessed by Coomassie staining. For H3K23ac Western blot analysis, histone acetyltransferase assays using core histones as substrate and unlabeled acetyl coenzyme A as cofactor were performed. Recombinant GST-Histone H3 was purified from *E. coli* and used as substrates (1 μg) in the second radioactive histone acetylation assay.

RESULTS

Presence of *KAT6B* homozygous deletion in SCLC that leads to gene inactivation.

We first screened a collection of 10 human SCLC cell lines for copy-number alterations in histone-modifier genes using the Illumina Infinium HumanOmni5 microarray, which interrogates 4,301,332 SNPs per sample. These included HCC-33, NCI-N417, NCI-H1048, NCI-H1963, NCI-H2029, DMS-114, DMS-273, NCI-H740, NCI-H2171, and NCI-H1672. Primary normal tissues, such as lung epithelium and leukocytes, were used as normal copy-number control samples. Microarray SNP data have been deposited at the Gene Expression Omnibus (GEO) under accession number GSE62775. Using this approach, we confirmed the presence of previously described aberrant copy number changes in a subset of SCLC cell lines of histone modifiers, such as the CBP histone acetyltransferases (homozygous deletion; ref. 10) and the histone methyltransferase SETDB1 (gene amplification; ref. 9). However, and most

interestingly, we found a previously unreported homozygous deletion of the candidate K(lysine) acetyltransferase 6B (*KAT6B*; refs. 11–13), also known as *MYST4* and *MORF*, in two of the 10 (20%) SCLC cell lines: NCI-H1963 (463,888 bp) and NCIH740 (780,137 bp; Fig. 1A). The tumor suppressor *PTEN*, undergoing also homozygous deletion in SCLC [14] and located 12,830,231 bp far away from the *KAT6B* gene, was not included within the described minimal deleted regions. *KAT6B* undergoes genomic translocation in subtypes of acute myeloid leukemia [15, 16] and uterine leiomyomata [17], and *KAT6B* mutations have also been recently associated with the development of genitopatellar syndrome and Say-Barber-Biesecker-Young-Simpson syndrome (SBBYSS or Ohdo syndrome; refs. 18–20). Data mining of the Cancer Cell Line Encyclopedia copy number variation data derived from a lower resolution SNP microarray [21] confirmed the presence of the *KAT6B* homozygous deletion in NCI-H1963 (Supplementary Fig. S1), while NCI-H740 was not included in the described study. Using a quantitative genomic PCR approach (Fig. 1B), MLPA (Fig. 1C) and fluorescence *in situ* hybridization (FISH; Fig. 1D), we confirmed the presence of the *KAT6B* homozygous deletion in NCI-H1963 and NCI-H740. The remaining eight SCLC cell lines did not exhibit any homozygous loss of *KAT6B* (Fig. 1A–D). *KAT6B* 5'-CpG island promoter methylation was not found in any SCLC cell line (Supplementary Fig. S1). Copy number and RNA expression levels for other histone acetyltransferases in the studied SCLC cell lines are shown in Supplementary Fig. S2. The SCLC cell lines underwent mutational screening for the 18 exons of the *KAT6B* gene using direct Sanger sequencing. The only nucleotide change that we detected was, in the NCI-H1048 cell line, a deletion of a GAA triplet coding for a glutamic acid within a stretch of glutamic amino acids in exon 16: it has been described as a polymorphic variant in the COSMIC Sanger database. Splicing defects were not specifically sought and could be another mechanism of gene silencing. Using quantitative reverse-transcription PCR and Western blot analysis, we found that the expression of KAT6B for both mRNA and protein was lost in the SCLC cancer cell lines NCI-H1963 and NCI-H740, which harbor the *KAT6B* homozygous deletion (Fig. 1E and Supplementary Fig. S3).

Figure 1

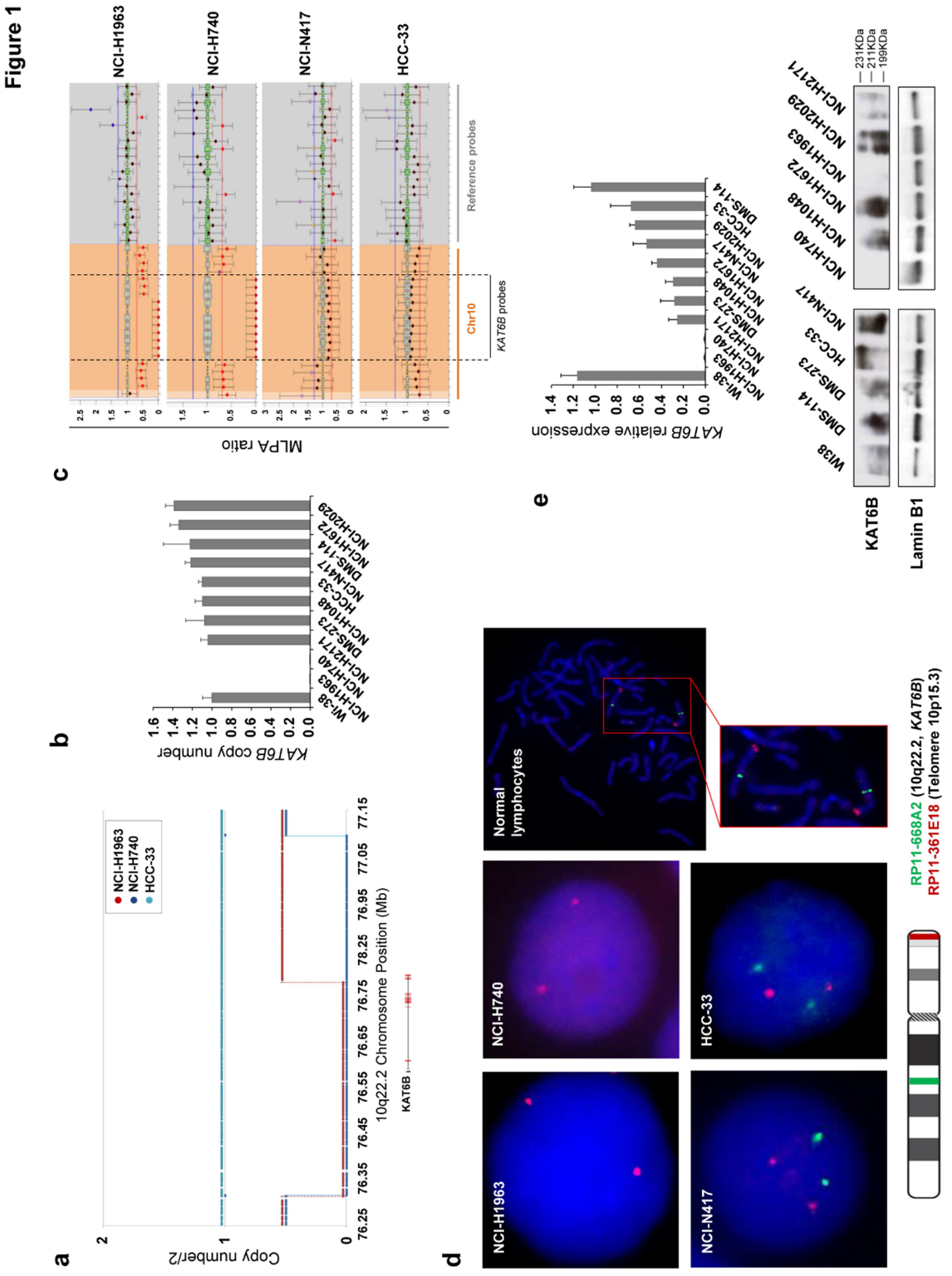
a
Copy number/2
10q22.2 Chromosome Position (Mb)
NCI-H1963
NCI-H740
HCC-33
KAT6B
b
KAT6B copy number
c
MLPA ratio
NCI-H1963
NCI-H740
NCI-N417
HCC-33
Chr10
KAT6B probes
Reference probes
d
Normal lymphocytes
NCI-H740
HCC-33
NCI-H1963
NCI-N417
RP11-668A2 (10q22.2, KAT6B)
RP11-361E18 (Telomere 10p15.3)
e
KAT6B relative expression
KAT6B
Lamin B1
231KDa
211KDa
199KDa

Figure 1. ***Determination of KAT6B gene homozygous deletion and its association with RNA and protein loss in SCLC cell lines***. ***A****, graph depicting the homozygously deleted KAT6B region in 10q22.2, identified with the Illumina Infinium HumanOmni5 microarray. The NCI-H1963 cell line has the smallest deleted region (463,888 bp) that encompasses the KAT6B gene. NCI-H740 has a homozygously deleted region of (780,137 bp). HCC-33 is shown as an example of an SCLC cell line with two KAT6B normal copies.* ***B****, assessment of KAT6B copy number by quantitative genomic PCR. The amplification frequency of KAT6B was calculated by the standard curve method using the 7900HT SDS program. DNA from normal lung fibroblasts (Wi-38) was used as the reference standard.* ***C****, MLPA assay. Two different probe mixes contain one probe for each exon of the KAT6B gene, two probes upstream and one probe for intron 3 (orange). Twenty reference probes are included (grey). MLPA images from one of the two probe mixes are shown. Values of 0 were considered as homozygous loss. NCI-H1963 and NCI-H740 cell lines show the KAT6B homozygous deletion, while HCC-33 and NCI-N417 are shown as examples of KAT6B two copy number cells.* ***D****, FISH of the KAT6B gene. The UCSC Genome Browser was used to select the BAC clone spanning the 10p15.3 region for the KAT6B gene, RP11-361E18. A telomeric BAC clone located in the telomeric 10p15.3 region was used as a control. Probes were verified to give a single signal on normal commercial lymphocyte metaphase slides.* ***E****, quantitative reverse transcription PCR (top) and Western blot analysis (bottom) demonstrate loss of KAT6B mRNA and protein (the three existing isoforms are shown), respectively, in homozygously deleted NCI-H1963 and NCI-H740 cells*

KAT6B has tumor suppressor-like properties in cancer cells

Once we had demonstrated the presence of *KAT6B* genomic loss in the SCLC cell lines, we examined its contribution to the tumorigenic phenotype *in vitro* and *in vivo*. We first analyzed the effect of KAT6B depletion in lung cancer cells retaining both copies of genes such as HCC33 and N417 (Fig. 2A and Supplementary Fig. S3). Supplementary Table S1 illustrates the shRNA sequences used. We observed that the reduction of KAT6B expression in the described cells, compared with the scramble shRNAs, had cancer growth-enhancing features, such as increased viability in the MTT assay (Fig. 2B), and formed more colonies (Fig. 2C). The XTT assay and Trypan blue staining further confirmed the growth-enhancing features of KAT6B-induced depletion (Supplementary Fig. S4). Interestingly, we observed that KAT6B shRNA-depleted cells also showed diminished expression of Brahma (BRM), a known KAT6B target (Supplementary Fig. S4; ref. 22), and the BRM-target E-cadherin (Supplementary Fig. S4; ref. 23), both being proteins that influence cell proliferation and metastasis. shRNA-mediated depletion of KAT6B also induced an increase in Rb phosphorylation (Supplementary Fig. S4). We next tested the ability of KAT6B shRNA-transfected N417 cells to form subcutaneous tumors in nude mice compared with scramble shRNA-transfected cells (Fig. 2D). Cells with shRNA-mediated depletion of KAT6B formed tumors with a greater weight and volume, but N417-scramble shRNA-transfected cells showed much lower tumorigenicity (Fig. 2D). We then performed an orthotopic growth study, implanting equal-sized tumor pieces from the subcutaneous model in the lung. We observed that orthotopic KAT6B shRNA-depleted tumors were significantly bigger and heavier than the scramble shRNA-derived tumors (Fig. 2E). We also proceeded with the converse experiment in which we used a retroviral-inducible expression system to recover by transfection the expression of KAT6B (longest isoform, 231 kDa) in H1963 cells bearing the aforementioned homozygous gene deletion (Fig. 2F). H1963 cells transfected with either the empty or the KAT6B vector were subcutaneously injected into the nude mice. Tumors originated from KAT6B-transfected H1963 cells had a significantly smaller volume than empty vector-transfected-derived tumors after doxycycline activation of gene expression (Fig. 2F). The halt in cellular growth upon restoration of KAT6B expression was

observed for a long period of time (49 days; Supplementary Fig. S4). Finally, the potential distant inhibitory dissemination activity of KAT6B was measured in athymic mice by direct spleen injection and analysis of metastasis formation in the liver (Fig. 2G). Whereas numerous metastatic nodules developed in the liver following injection of KAT6B shRNA-depleted empty N417 cells, less metastasis formation was observed with the scramble shRNA-transfected cells (Fig. 2G). Overall, our findings suggest tumor-suppressor and dissemination-inhibitor roles for KAT6B.

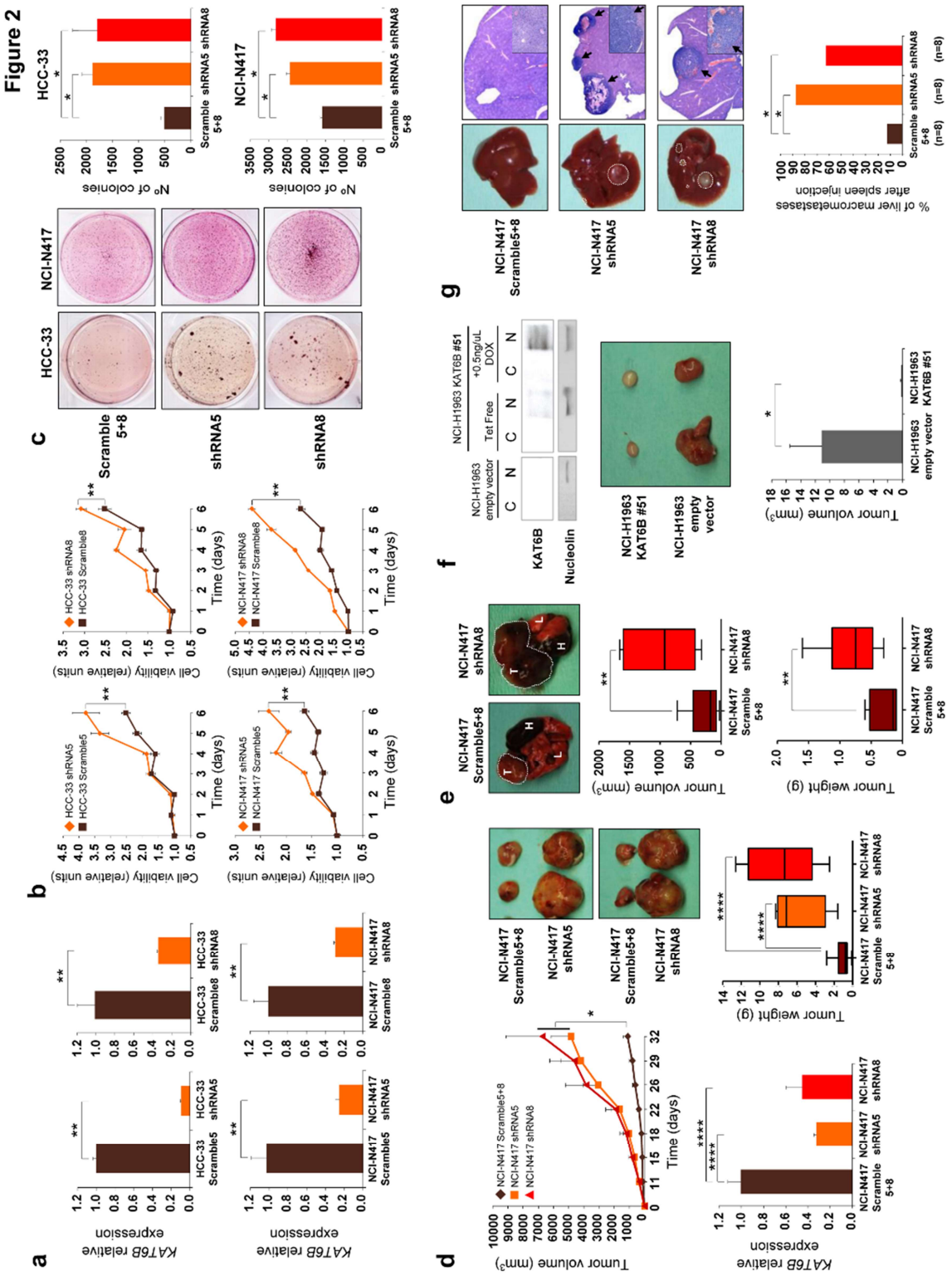

Figure 2

***Figure 2**. **Growth-inhibitory effects of KAT6B in SCLC**. **A**, downregulation of the KAT6B gene by short hairpins using two target sequences (shRNA5 and shRNA8) in NCI-N417 and HCC-33 cells. Significance of permutation tests, **, P < 0.01. **B**, the short hairpin KAT6B-depleted cells were significantly more viable in the MTT assay than in the scrambled shRNA-transfected cells. Significance of ANOVAs, **, P < 0.01. **C**, the colony formation assay showed that NCI-N417 and HCC-33 cells transfected with the shRNA against KAT6B formed significantly more colonies than did scrambled shRNA-transfected cells. Data are mean ± SEM (n = 3). Significance of permutation tests, *, P < 0.05. **D**, effect of KAT6B shRNA-mediated depletion on the growth of subcutaneous tumors in nude mice derived from NCI-N417 cells. There was a significant increase in tumor volume and weight in the KAT6B shRNA-depleted cells. Data are mean ± SEM (n = 10). Low KAT6B mRNA levels in shRNA5 and shRNA8 NCI-N417 tumors confirmed the stability of the transfection after 32 days. ANOVAs, *, P < 0.05; ****, P < 0.0001. **E**, KAT6B shRNA-mediated depletion also significantly increased the volume and weight of orthotopic tumors derived from NCI-N417 cells implanted in the lung of nude mice. Significance of permutation tests, *, P < 0.05. **F**, recovery of KAT6B expression in NCI-H1963 cells (top), using a retroviral transfection Tet-ON system, decreased the volume of subcutaneous tumors implanted in nude mice (bottom). Significance of permutation test, *, P < 0.05. **G**, KAT6B shRNA-depleted NCI-N417 cells show significantly higher dissemination capacity after spleen injection. Illustrative surgery samples and hematoxylin and eosin staining of colonized liver after spleen injection are shown. Fisher exact test, *, P < 0.05.*

Lysine 23 of histone H3 as a target of KAT6B-mediated acetylation

We next wondered about the molecular mechanisms that could mediate the identified tumor-suppressor features of KAT6B. In trying to address this issue, we first encountered the serious obstacle that the histone lysine residues targeted for acetylation by human KAT6B have not been completely characterized *in vivo*. KAT6B is a member of the MYST family of histone acetyltransferases that also includes KAT6A (MYST3/ MOZ), KAT7 (MYST2/HBO1), KAT5 (Tip60), and KAT8 (MYST1/MOF; Fig. 3A). Because of the greater homology of KAT6B with the *bona fide* histone H3 acetyltransferase KAT6A [24–26], which also undergoes genomic translocations in acute myelogenous leukemia [27, 28], and the initially reported *in vitro* specificity of the KAT6A/KAT6B complex for histone H3 but not for histone H4 [29, 30], we focused our interest on this particular histone. To

identify the histone H3 target sites for KAT6B, we compared H1963 cells transduced with an empty vector or with the full-length KAT6B expression vector (Fig. 3B). We used histone acid extracts resolved in an SDS–PAGE gel, followed by digestion of the histone H3 band and LC/MS-MS analysis. We determined from precursor signal intensity of the two acetylated peptides, K.QLATK^{23ac}AAR and R.KQLATK^{23ac}AAR.K, that acetylation of H3-K23 was enriched upon KAT6B transfection in H1963 cells (Fig. 3C). Targeted quantification of acetylation of H3-K23 residue by SRM confirmed the enhancement of this acetylated residue upon transduction-mediated recovery of KAT6B expression in the H1963 cell line (Fig. 3D). Using SRM, we were also able to study a patient with the SBBYS type of Ohdo syndrome, who was carrying truncating mutation of *KAT6B* [31, 32], and who showed a reduced level of both acetylated H3-K23 peptides (Fig. 3D). Western blot analyses also confirmed the LC/MS-MS data by showing that H3-K23 acetylation increased upon KAT6B transfection in H1963 cells (Fig. 3E). The activity of KAT6B for acetyl-K23 H3 was confirmed by Western blot analysis in two additional models: KAT6B shRNA-depleted N417 cells showed a reduction of the described acetylation mark (Fig. 3E), and the aforementioned SBBYS type of Ohdo syndrome patient with the *KAT6B* truncating mutation also had a lower level of acetylated H3-K23 (Fig. 3E). KAT6B specificity for this histone residue was further demonstrated by showing that acetylation of lysine 14 of histone H3 and lysine 16 of histone H4, mediated by the MYST family members KAT6A (MYST3/MOZ; refs. 25, 26, 29) and KAT8 (MYST1/MOF; refs. 33, 34), respectively, were not modified upon KAT6B restoration, depletion, or mutation (Fig. 3E). We also developed *in vitro* histone acetylation assays to further show the activity of KAT6B for H3K23 acetylation. Using purified histone core proteins from HeLa cells and a construct for the KAT6B-specific HAT domain, we confirmed that it acetylated H3-K23 (Supplementary Fig. S5). Importantly, a mutant HAT domain protein for KAT6B in K815, a strictly conserved lysine residue in the MYST family [35], was unable to acetylate H3-K23 (Supplementary Fig. S5). In addition, the *in vitro* activity of KAT6B for H3-K23 was confirmed using a recombinant histone H3 as a substrate: the wild-type cloned KAT6B-HAT domain acetylated the described residue and the K815 mutant was unable to do so (Supplementary Fig. S5). Using shRNA-mediated depletion of four histone deacetylases (HDAC1, HDAC2, HDCA3, and HDAC6) in NCI-N417 cells, we

observed that, upon HDAC1 downregulation, there was an increase in acetylated H3-K23 levels (Supplementary Fig. S5), suggesting that this last HDAC mediates the deacetylation event at this residue.

We next wondered about gene targets whose normal expression could be diminished in cancer cells by the loss of KAT6B-mediated H3-K23 promoter acetylation, a histone mark usually associated with gene activation. To identify KAT6B target genes that might fit this candidate criterion, we used the shRNA approach to deplete KAT6B expression in N417 and HCC33 (both with the normal two copies of the *KAT6B* gene) followed by expression microarray hybridization. The complete list of genes undergoing expression changes is shown in Supplementary Table S2 (only the list of downregulated genes is shown here due to space, a complete list with gene expression data is available at http://cancerres.aacrjournals.org). Microarray expression data are available at GEO under accession number GSE62775. Using this approach, we identified 32 common genes repressed in both KAT6B-shRNA-depleted lung cancer cell lines that were upregulated in scramble shRNA-transfected cells (Supplementary Table S2). We confirmed the expression changes of 25 candidate genes (78%) by quantitative reverse-transcription PCR (Fig. 3F and Supplementary Fig. S5). The shift in H3-K23 acetylation status in their respective promoters for four candidate genes was observed by quantitative ChIP (Fig. 3F).

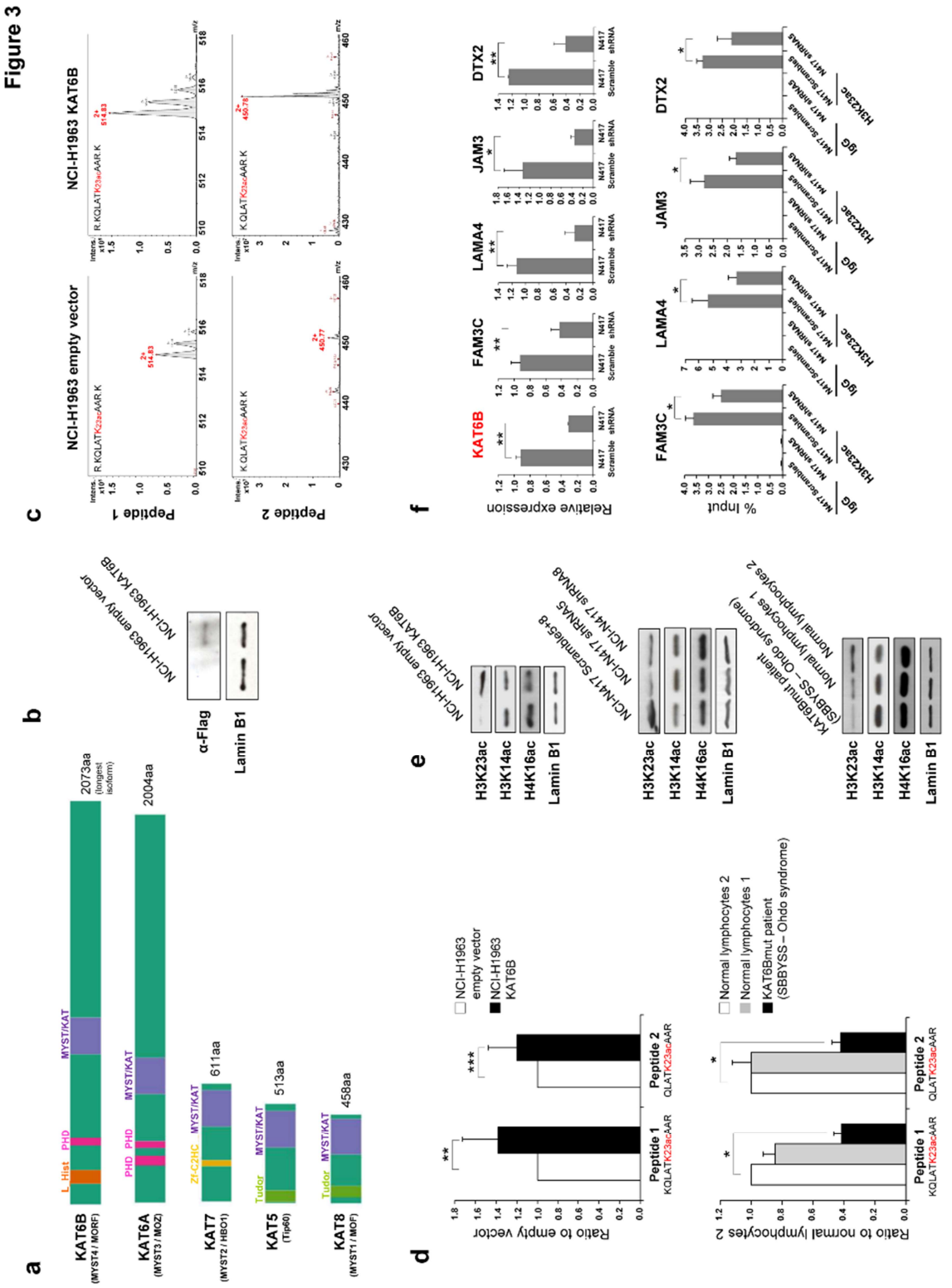
Figure 3
a
KAT6B (MYST4 / MORF)
KAT6A (MYST3 / MOZ)
KAT7 (MYST2 / HBO1)
KAT5 (Tip60)
KAT8 (MYST1 / MOF)
L Hist
PHD
MYST/KAT
Zf-C2HC
Tudor
2073aa (longest isoform)
2004aa
611aa
513aa
458aa
b
NCI-H1963 empty vector
NCI-H1963 KAT6B
α-Flag
Lamin B1
c
NCI-H1963 empty vector
NCI-H1963 KAT6B
Peptide 1
Peptide 2
R.KQLATK23acAAR.K
K.QLATK23acAAR.K
d
NCI-H1963 empty vector
NCI-H1963 KAT6B
Ratio to empty vector
Peptide 1 KQLATK23acAAR
Peptide 2 QLATK23acAAR
Normal lymphocytes 2
Normal lymphocytes 1
KAT6Bmut patient (SBBYSS – Ohdo syndrome)
Ratio to normal lymphocytes 2
e
NCI-H1963 empty vector
NCI-H1963 KAT6B
NCI-N417 Scramble8
NCI-N417 shRNA5
NCI-N417 shRNA8
KAT6Bmut patient (SBBYSS – Ohdo syndrome)
Normal lymphocytes 1
Normal lymphocytes 2
H3K23ac
H3K14ac
H4K16ac
Lamin B1
f
KAT6B
FAM3C
LAMA4
JAM3
DTX2
Relative expression
% Input
N417 Scramble shRNA
N417 shRNA5
N417 shRNA8
IgG
H3K23ac

Figure 3. KAT6B is a histone acetyltransferase targeting lysine 23 of histone H3. ***A****, diagram of the MYST (SAS/MOZ) family with its recognized domains. The domains depicted are: L_Hist, linker histone H1/H5 domain H15; PHD, zinc_finger PHD type; Tudor_knot, RNA binding activity-knot of a chromodomain; Zf-C2HC, zinc finger, C2H2 type; MYST/KAT, MYST-type HAT (histone acetyltransferase) domain.* ***B****, Western blot analysis shows efficient transduction of KAT6B in NCI-H1963 cells in comparison with empty vector–transfected cells.* ***C****, MS spectra of QLATKacAAR and KQLATKacAAR tryptic peptides identified by LC/MS-MS. A representative figure is shown of the precursor intensity based on the integration of the signal from the extracted ion chromatogram. KAT6B NCI-H1963-transfected cells show a sharp increase in H3K23 acetylation intensity in both of the identified peptides compared with the empty vector–transfected cells.* ***D****, SRM quantification of the two H3K23ac peptides. Results were normalized with respect to the transitions of the corresponding heavy synthetic peptide and were related to the empty vector (top) or normal lymphocytes (bottom). Targeted quantification confirms the enhancement of this acetylated residue for the two peptides upon transfection-mediated recovery of KAT6B expression in H1963 cells (top) and its reduction in a patient of SBBYS type of Ohdo syndrome carrying a truncating mutation of KAT6B (bottom). Differences between the transitions were examined with the Student t test. *, P < 0.05; **, P < 0.01; ***, P < 0.001.* ***E****, Western blot analysis confirms the activity of KAT6B for H3K23ac upon transfection in NCI-H1963–deleted cells (top), in KAT6B shRNA-depleted NCI-N417 cells (middle), and in the SBBYSS or Ohdo syndrome patient with the KAT6B-truncating mutation (bottom). H3K14ac and H4K16ac did not change in any condition.* ***F****, qRT-PCR and H3K23ac ChIP analysis shows that, upon KAT6B-shRNA depletion in NCI-N417 cells, the downregulation of the candidate genes is associated with diminished acetylation of H3K23 residue in the promoters. Permutation tests, **, P < 0.05; *, P < 0.01.*

KAT6B genomic loss occurs in SCLC patients and confers sensitivity to irinotecan

Finally, we sought to demonstrate that the presence of *KAT6B* homozygous deletion was not a specific feature of *in vitro*–grown SCLC cell lines and that it also occurred in primary tumors of SCLC patients. Herein, we performed MLPA analyses for the *KAT6B* locus using a collection of 60 tumors from SCLC patients and identified the *KAT6B* homozygous deletion in eight SCLC tumors (13%; Fig. 4A). Codeletion of *PTEN* was not observed in the SCLC tumors with *KAT6B*

genomic loss according to CNV microarray data [36]. Interestingly, screening for nonsense and indels in the *KAT6B* coding sequence in these 60 SLC cases, we identified a deletion of a "C" in the last exon (exon 18; c.3824delC) that later creates a stop codon and renders a 798 amino acids shorter protein, suggesting alternative pathways for the inactivation of the studied gene. Microarray expression data were available for 19 of the SCLC patients studied [36], including four who had the *KAT6B* homozygous deletion, and we observed an association between *KAT6B* genomic loss and lower levels of the transcript (Fig. 4B). Immunohistochemical analyses of 20 SCLC cases showed overall loss of KAT6B expression and acetyl-K23 H3 in the four tumors with *KAT6B* deletion, whereas both protein and histone mark were clearly stained in the remaining 16 samples without *KAT6B* genomic loss (except in one case where other mechanisms might account for an observed lack of staining). Illustrative cases are shown in Supplementary Fig. S6. Interestingly, in those SCLC patients for whom we have clinical information and a long follow-up over different stages (n = 26), the presence of the *KAT6B* homozygous deletion was associated with significantly shorter progression-free survival (log-rank test; P = 0.014; hazard ratio; 4.95; 95% confidence interval, 1.21– 20.28; Fig. 4C).

The observation that the *KAT6B* homozygous deletion also occurred in SCLC patients with even worse prognosis prompted us to examine whether the loss of this HAT was associated with a particular sensitivity to any anticancer drug. Similar scenarios have been described for inhibitors of histone methyltransferases, such as DOT1L [37] and the BET family of acetyl-lysine-recognizing chromatin "adaptor" proteins [38–40] in which hematologic malignancies associated with gene-activating events involving targets of these pathways are more sensitive to these drugs. Using the model of KAT6B shRNA-transfected versus scramble shRNA-transfected N417 cells and the calculation of IC50 values according to the MTT assay, we did not observe any difference between the two types of cells for 28 HDAC inhibitors that target class I, IIA, IIB, and III, in addition to pan-inhibitors (Supplementary Fig. S7). The compounds and their HDAC targets can be found in Supplementary Table S3. In addition, we did not observe any difference in sensitivity for classic SCLC chemotherapy agents such as cisplatin or etoposide (Supplementary Fig. S7). However, we found that

KAT6B-depleted cells were significantly more sensitive to the growth-inhibitory effect mediated by the chemotherapy agent irinotecan, under clinical trials in SCLC, than any of the scramble shRNA clones (Fig. 4D). The same result was observed for HCC-33 cells (Fig. 4D). We also extended the *in vitro* cell viability experiments to the *in vivo* mouse model, thereby confirming that orthotopic SCLC tumors derived from KAT6B shRNA-depleted N417 cells were significantly more responsive to irinotecan than scramble shRNA-derived tumors (Fig. 4E). Within our SCLC clinical cohort, 42% of cases (11 of 26) underwent chemotherapy, but mainly platin-based combinations. Only 4 patients received irinotecan-based chemotherapy and none of them had *KAT6B* homozygous deletion. Thus, it was unfeasible to assess the role of *KAT6B* deletion as a predictive factor of irinotecan-based treatment outcome in this setting. Related to why irinotecan could be particularly effective in *KAT6B*-deleted tumors, it has been reported that the MYST family of HATs facilitates ataxia–telangiectasia mutated (ATM) kinase-mediated DNA-damage response [41] and, thus, it is possible that irinotecan-induced DNA damage cannot be so efficiently repaired in the KAT6B deficient tumors, leading to the enhanced cell death. In this regard, we found that KAT6B shRNA-mediated depletion caused a reduction of ATM expression and, upon irinotecan treatment, a lower phosphorylation of H2AX (Supplementary Fig. S8). Overall, these data suggest the existence of a therapeutic "niche" for the use of irinotecan in the aforementioned subset of SCLC cases harboring the *KAT6B* homozygous deletion.

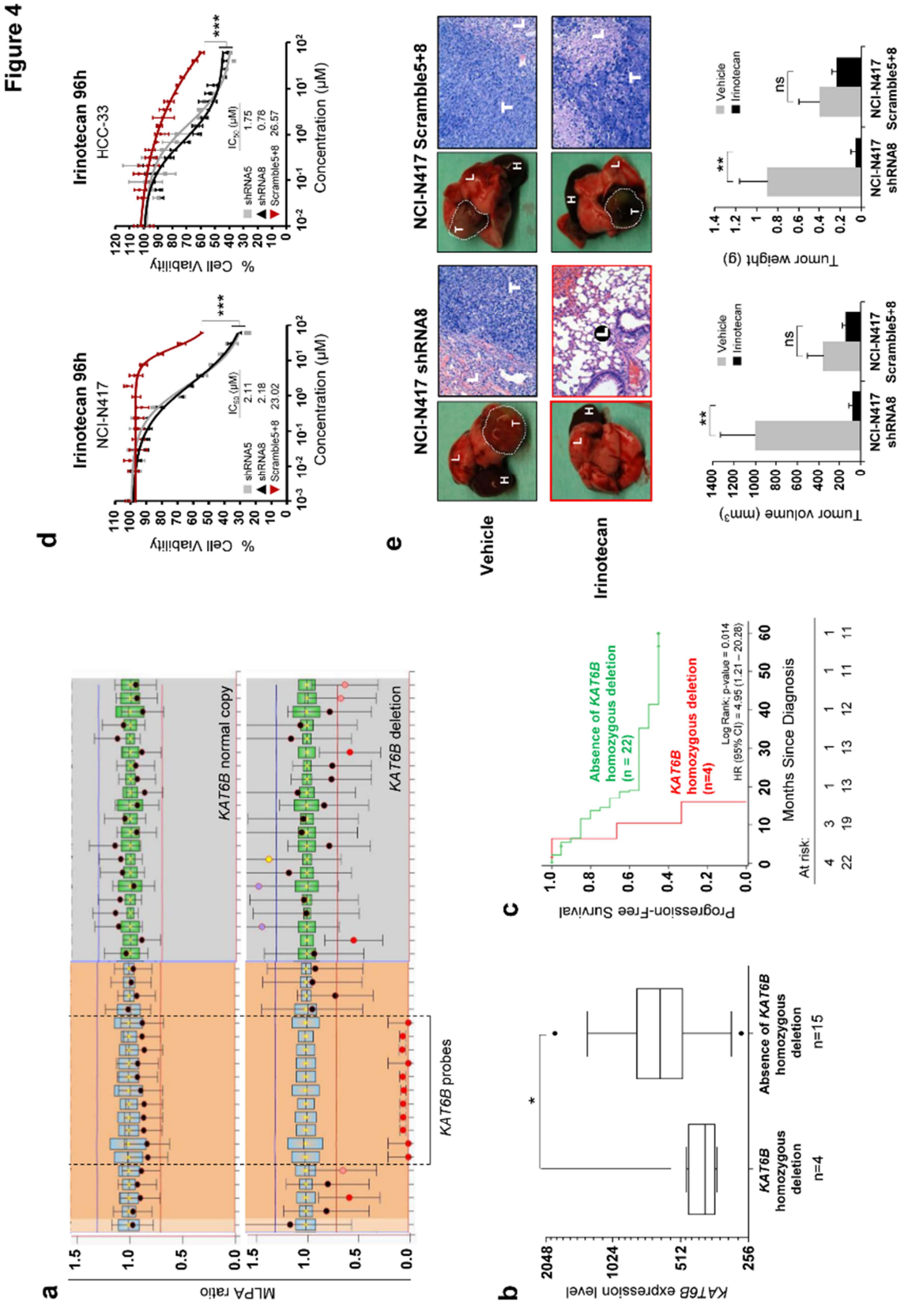
Figure 4
a
MLPA ratio
KAT6B normal copy
KAT6B deletion
KAT6B probes
b
KAT6B expression level
KAT6B homozygous deletion n=4
Absence of KAT6B homozygous deletion n=15
c
Progression-Free Survival
Absence of KAT6B homozygous deletion (n = 22)
KAT6B homozygous deletion (n=4)
Log Rank: p-value = 0.014
HR (95% CI) = 4.95 (1.21 – 20.28)
Months Since Diagnosis
At risk:
d
Irinotecan 96h
NCI-N417
HCC-33
% Cell Viability
Concentration (µM)
shRNA5
shRNA8
Scramble5+8
e
NCI-N417 shRNA8
NCI-N417 Scramble5+8
Vehicle
Irinotecan
Tumor volume (mm³)
Tumor weight (g)
Vehicle
Irinotecan
ns

Figure 4*. Genomic loss of KAT6B in SCLC patients and sensitivity to irinotecan.** ***A*, examples of assessment of KAT6B copy number by MLPA in an SCLC patient without loss (top) and in one with homozygous deletion (bottom).* ***B****, the presence of KAT6B homozygous deletion is significantly associated with loss of expression of the KAT6B transcript in tumors from SCLC patients. The box plots illustrate the distribution of microarray expression values; the central solid line indicates the median; the limits of the box show the upper and lower quartiles. Mann–Whitney test, *, P < 0.05.* ***C****, the Kaplan–Meier analysis of progression-free survival among a cohort of SCLC cases according to KAT6B genomic status. KAT6B homozygous deletion is significantly associated with a shorter progression-free survival (log-rank test; P = 0.014; hazard ratio, 4.95; 95% confidence interval, 1.21–20.28).* ***D****, KAT6B shRNA-depleted NCI-N417 and HCC-33 cells were significantly more sensitive to the antiproliferative effect of irinotecan than were shRNA scramble-transfected cells. ANOVAs, ***, P < 0.001.* ***E****, orthotopic tumors-derived from KAT6B shRNA-depleted NCI-N417 cells were more sensitive to irinotecan than were shRNA scramble-derived tumors according to tumor volume and weight. L, Lung; H, Heart; T, Tumor. Significance of permutation tests, **, P < 0.01.*

DISCUSSION

The initial high response rates to platinum-based chemotherapy regimens for SCLC in the late 1970s and early 1980s caused great expectations for these therapies. However, these hopes were shattered by the recognition of low 5-year survival rates, in most instances only approximately 5% [1, 2, 42]. More recent trials with targeted therapies in SCLC have failed with no new drugs progressing treatments beyond those of cisplatin and etoposide [1, 2, 42]. One of the main reasons for this disappointing scenario is our limited knowledge of the molecular driver events in SCLC. Beyond the high prevalence of *TP53* and *RB1* mutations, which have not proven amenable to pharmacology-based therapies so far, we have a scarce knowledge of the genetic defects underlying the natural history of SCLC. A recent breakthrough in this area has been the identification of mutations in histone modifiers, such as the histone methyltransferase *MLL1* or the histone acetyltransferases *CREBBP (KAT3A)* and *EP300 (KAT3B),* in a subset of SCLCs [4]. In this context, our identification of *KAT6B* homozygous deletions in both SCLC cell lines and primary tumors upgrades the genetic disruption of histone modifier genes as the second most common class of altered genes in SCLC.

Importantly, we define for the first time, an *in vivo* target site for the acetyltransferase activity of KAT6B, lysine 23 of histone H3. This histone posttranslational modification has been previously associated with a more open chromatin state and the transcriptional activation of the underlying DNA sequence [43, 44]. Interestingly, the diminished acetylation of H3-K23 seems to be a hallmark of SCLC tumorigenesis, because the other two frequently mutated histone acetyltransferases (CREBBP and EP300) can also target this particular histone amino acid [43–45].

An interesting issue derived from our studies is the potential exploitation of the KAT6B histone acetyltransferase defect to design more personalized therapies that could improve the dismal outcome of SCLC. Epigenetic drugs are the focus of a growing interest in the cancer arena; however, a critical issue is going to be the selection of those patients that are more likely to respond to these compounds. For example, pediatric brain-stem gliomas harboring a mutation in K27 of histone H3.3 are more sensitive to the pharmacologic inhibition of a K27 demethylase [46]. Herein, we did not observe that KAT6B depletion increases sensitivity to HDAC inhibitors, but other epigenetic inhibitors can be tested in this model. These include bromodomain inhibitors, targeting BET (bromodomain and extra-terminal domain) proteins that "read" the acetylated histone residues [39–41], or inhibitors of histone methyltransferases/demethylases, taking in account the competition between acetylation and methylation that occurs at K23-H3 [47]. In addition, because KAT6B tumor-suppressor properties are, in part, mediated by downstream genes, like *BRM*, then might the restoration of these gene(s) be therapeutic. However, we have already found a drug where the diminished expression of KAT6B increases SCLC sensitivity in cell and animal models: irinotecan. Currently, this compound is a second-line treatment for the extensive stage of SCLC, while a platinum agent and etoposide are first-line therapies [1, 2, 42]. Interestingly, as irinotecan is an effective drug for other tumor types, such as colon cancer, it would be interesting to explore if KAT6B status is associated with sensitivity to this drug beyond SCLC. Herein, our results pinpoint a subgroup of SCLC patients, those carrying the *KAT6B* genomic loss, where prospective clinical trials to assess the efficacy of irinotecan can be further studied.

SUPPLEMENTARY DATA

a

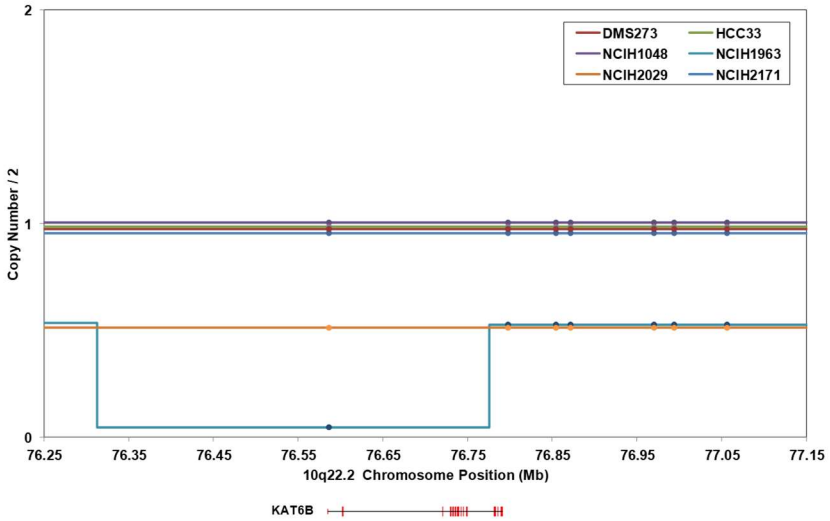

b

TargetID	CHR	MAPINFO	UCSC REFGENE NAME	UCSC REFGENE GROUP	RELATION TO UCSC CPG ISLAND	NCI-H1672	DMS-114	NCI-N417	HCC-33	NCI-H2029	NCI-H2171	NCI-H1048	DMS-273
cg20120430	10	76585161	MYST4	TSS1500	Island	0.004	0.032	0.012	0.019	0.039	0.007	0.026	0.017
cg24671245	10	76585406	MYST4	TSS1500	Island	0.098	0.058	0.068	0.148	0.149	0.108	0.139	0.154
cg04396765	10	76585478	MYST4	TSS1500	Island	0.040	0.051	0.054	0.065	0.067	0.084	0.051	0.085
cg17147776	10	76585791	MYST4	TSS1500	Island	0.004	0.006	0.007	0.008	0.003	0.014	0.017	0.009
cg06972998	10	76585851	MYST4	TSS1500	Island	0.030	0.062	0.065	0.075	0.056	0.058	0.093	0.060
cg18491775	10	76586186	MYST4	TSS200	Island	0.065	0.084	0.086	0.090	0.060	0.066	0.089	0.090
cg10739686	10	76586254	MYST4	TSS200	Island	0.056	0.070	0.103	0.082	0.127	0.083	0.111	0.123
cg26605858	10	76586308	MYST4	TSS200	Island	0.036	0.048	0.045	0.072	0.065	0.070	0.076	0.087
cg10359932	10	76586319	MYST4	TSS200	Island	0.056	0.042	0.034	0.059	0.070	0.029	0.047	0.079
cg11348552	10	76586321	MYST4	TSS200	Island	0.031	0.044	0.047	0.062	0.039	0.036	0.052	0.063
cg11128436	10	76586368	MYST4	TSS200	Island	0.022	0.056	0.044	0.061	0.047	0.040	0.044	0.060
cg15912797	10	76586382	MYST4;MYST4	1stExon;5'UTR	Island	0.041	0.073	0.071	0.084	0.040	0.054	0.073	0.091
cg09631472	10	76586650	MYST4	5'UTR	Island	0.060	0.041	0.052	0.088	0.090	0.077	0.067	0.089
cg18040181	10	76588616	MYST4	5'UTR	S_Shore	0.970	0.419	0.924	0.972	0.919	0.933	0.918	0.898
cg00432328	10	76589109	MYST4	5'UTR	S_Shelf	0.922	0.783	0.771	0.895	0.855	0.863	0.927	0.881
cg20721467	10	76597927	MYST4	5'UTR		0.296	0.800	0.091	0.461	0.835	0.200	0.685	0.630
cg08789630	10	76599281	MYST4	5'UTR		0.934	0.884	0.903	0.927	0.914	0.926	0.904	0.930
cg14111928	10	76602391	MYST4	5'UTR		0.911	0.830	0.865	0.913	0.900	0.905	0.875	0.902
cg24243879	10	76614628	MYST4	Body		0.495	0.891	0.126	0.540	0.912	0.642	0.896	0.097
cg25006851	10	76622627	MYST4	Body		0.945	0.783	0.923	0.918	0.905	0.878	0.880	0.964
cg02135122	10	76642824	MYST4	Body		0.934	0.905	0.868	0.917	0.938	0.925	0.889	0.919
cg16045355	10	76650254	MYST4	Body		0.906	0.885	0.867	0.876	0.892	0.895	0.864	0.863
cg03610439	10	76658262	MYST4	Body		0.848	0.912	0.886	0.903	0.869	0.844	0.889	0.869
cg11849327	10	76682695	MYST4	Body		0.874	0.580	0.888	0.893	0.895	0.891	0.813	0.797
cg07559420	10	76686512	MYST4	Body		0.843	0.498	0.858	0.903	0.921	0.813	0.822	0.882
cg07172755	10	76686668	MYST4	Body		0.953	0.726	0.933	0.924	0.934	0.927	0.859	0.882
cg19368031	10	76688843	MYST4	Body		0.916	0.662	0.867	0.882	0.903	0.909	0.879	0.880
cg25126854	10	76697566	MYST4	Body		0.842	0.722	0.242	0.527	0.338	0.931	0.665	0.842
cg16198468	10	76708051	MYST4	Body		0.047	0.651	0.107	0.065	0.065	0.277	0.069	0.214
cg15863598	10	76708663	MYST4	Body		0.910	0.734	0.801	0.918	0.923	0.924	0.750	0.924
cg15163862	10	76721440	MYST4	Body		0.152	0.804	0.870	0.785	0.887	0.857	0.833	0.861
cg06098530	10	76727919	MYST4	Body		0.066	0.349	0.216	0.162	0.108	0.523	0.081	0.707
cg06752157	10	76728568	MYST4	Body		0.842	0.915	0.709	0.847	0.802	0.893	0.378	0.854
cg13411830	10	76735881	MYST4	Body		0.954	0.895	0.919	0.933	0.953	0.912	0.914	0.953
cg02976898	10	76742856	MYST4	Body		0.947	0.920	0.926	0.966	0.939	0.923	0.914	0.921
cg24520885	10	76747956	MYST4	Body		0.852	0.763	0.737	0.885	0.839	0.847	0.656	0.438
cg07410339	10	76768310	MYST4	Body		0.945	0.760	0.884	0.920	0.950	0.864	0.771	0.939
cg14219256	10	76779305	MYST4	Body		0.369	0.511	0.293	0.439	0.322	0.431	0.299	0.485
cg00366037	10	76781121	MYST4	Body		0.838	0.692	0.838	0.897	0.903	0.696	0.768	0.878
cg05791881	10	76789214	MYST4	Body		0.943	0.872	0.852	0.920	0.915	0.826	0.752	0.922
cg24543574	10	76789311	MYST4	Body		0.805	0.855	0.816	0.830	0.882	0.820	0.775	0.823
cg07672076	10	76789460	MYST4	Body		0.962	0.929	0.925	0.924	0.931	0.890	0.897	0.940
cg11867607	10	76790371	MYST4	Body		0.840	0.829	0.862	0.850	0.870	0.849	0.827	0.830
cg07299586	10	76792579	MYST4	3'UTR		0.899	0.799	0.794	0.861	0.896	0.829	0.645	0.759

Supplementary Figure 1. KAT6B copy number and DNA methylation status in SCLC cell lines. A) *Normalized copy number estimations from the Cancer Cell Line Encyclopedia project, for the q22.2 region of chromosome 10, where KAT6B is located (gene representation at bottom). Lines represent regions with same copy number estimation, while dots are the mean copy number per gene.* ***B)*** *Methylation CpG sites for the KAT6B gene, interrogated by HumanMethylation450 microarray. CpG sites associated information such as chromosome (CHR), position (MAPINFO), gene associated (UCSC REFGENE NAME), relation to the position of the gene (UCSC REFGENE GROUP) and localization in terms of CpG abundance (RELATION TO UCSC CPG ISLAND) is provided, followed by methylation levels (β-values) for each cell line (p-value < 0.01).*

a

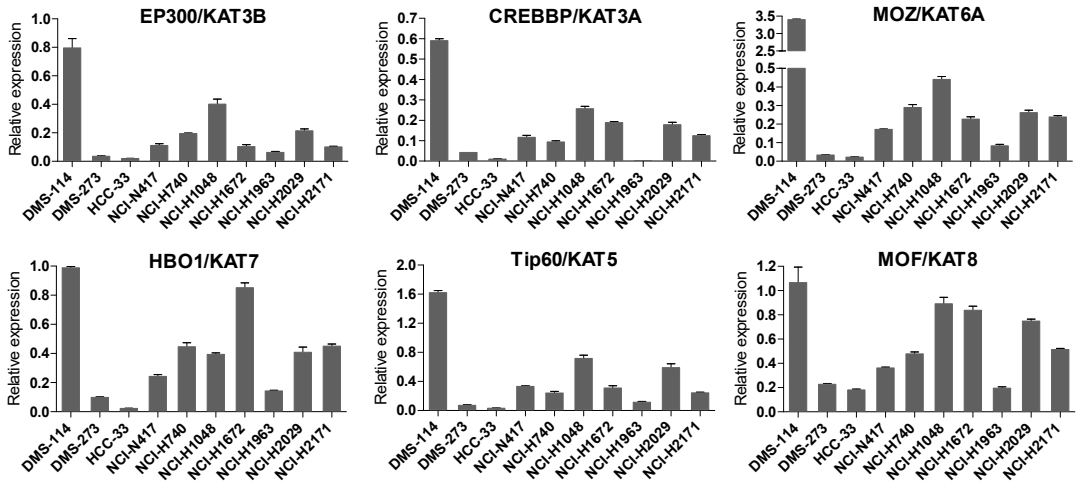

b

	WI38	DMS-114	DMS-273	HCC-33	NCI-N417	NCI-H740	NCI-H1048	NCI-H1672	NCI-H1963	NCI-H2029	NCI-H2171
EP300/KAT3B	2	2	2	2	2	2	2	2	2	2	2
CREBBP/KAT3A	2	3	3	2	2	1	1	2	2 / 0 *	2	2
MOZ/KAT6A	2	3	2	1	2	2	2	1	2	1	2
HBO1/KAT7	2	2	2	2	2	3	2	3	2	2	2
Tip60/KAT5	2	2	2	3	2	2	2	2	2	2	2
MOF/KAT8	2	2	3	2	1	2	2	2	2	2	2

***Supplementary Figure 2**. **Copy number and expression levels of six KATs in SCLC cell lines. A)** Expression levels of six KAT proteins were studied by quantitative reverse-transcription PCR in ten small cell lung cancer cell lines. **B)** Copy number status of these acetyltransferases was analyzed using the Illumina HumanOmni5 genotyping array. Code: 1, one gene copy; 2, two gene copies; 3, three gene copies. *2/0, CNV microarray analysis confirmed a previously reported homozygous deletion for exons 1 to 3 of CREBBP gene in the NCI-H1963 cell line.*

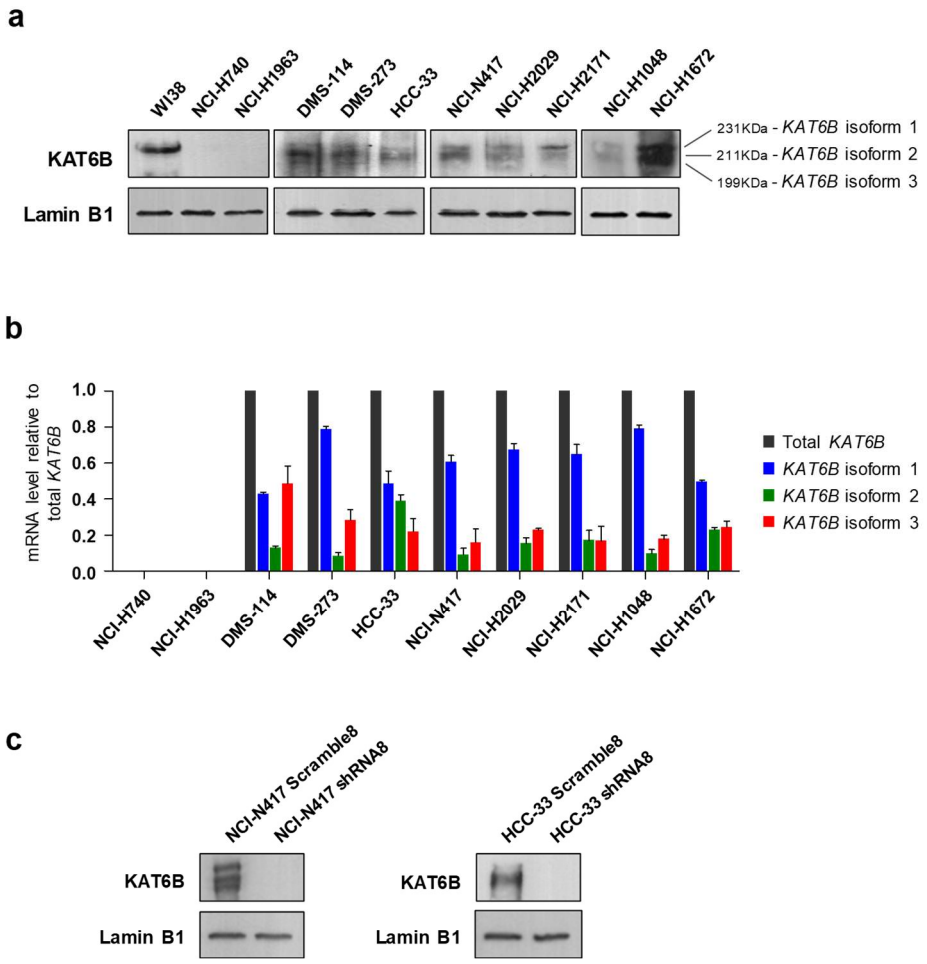

***Supplementary Figure 3**. **A)** Western blot analysis shows deletion of all three isoforms in NCI-H740 and NCI-H1963 cells. **B)** Expression levels of KAT6B isoforms by specific qRT-PCR reported as relative expression to total KAT6B in each cell line. **C)** Effective downregulation of the KAT6B protein by short hairpin RNA in NCI-N417 and HCC-33 cells was analyzed in western blot.*

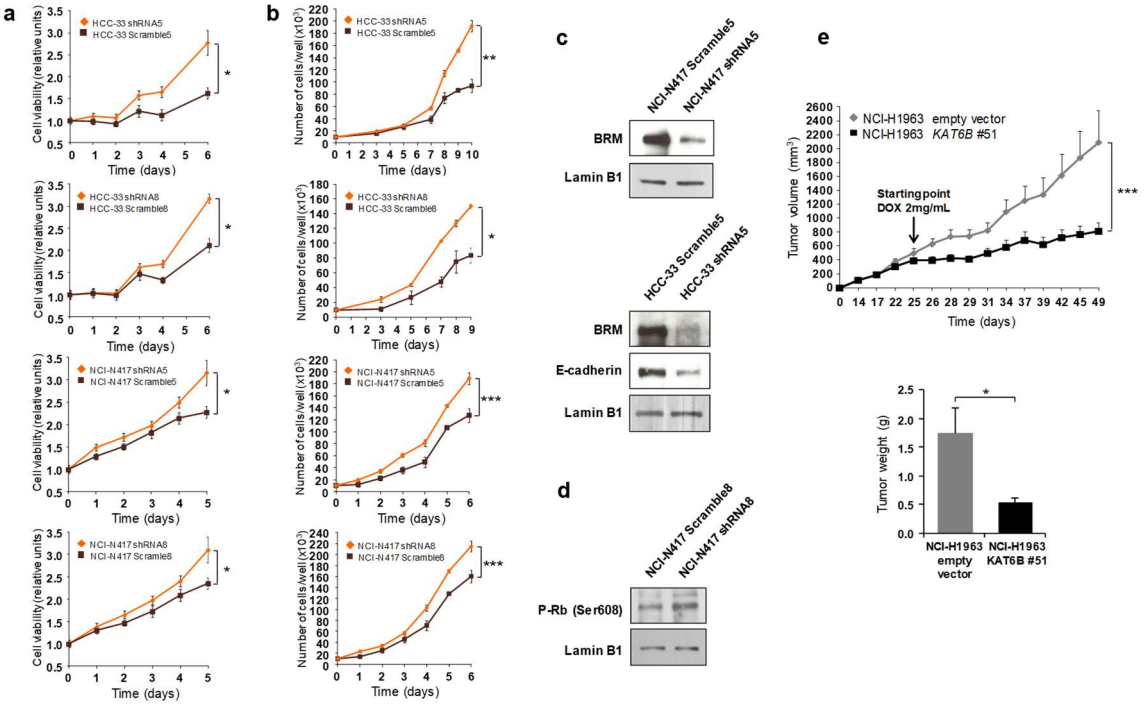

Supplementary Figure 4. *The short hairpin KAT6B-depleted cells presented higher growth rate than the scramble cells in the XTT assay* ***(A)*** *and after cell counting using the trypan blue exclusion method* ***(B)****.* ***C)*** *Western blot analyses of BRM and E-cadherin proteins were performed in KAT6B shRNA-depleted NCI-N417 and HCC-33 cells. BRM and E-cadherin expression decreased upon KAT6B downregulation.* ***D)*** *shRNA-mediated depletion of KAT6B also induced an increase in Rb phosphorylation at serine 608.* ***E)*** *KAT6B expression halt tumor growth for a long period of time (49 days) in the subcutaneous mouse model. Significance of ANOVAs: *, $p < 0.05$; **, $p < 0.01$; *** $p < 0.001$; ****, $p < 0.0001$.*

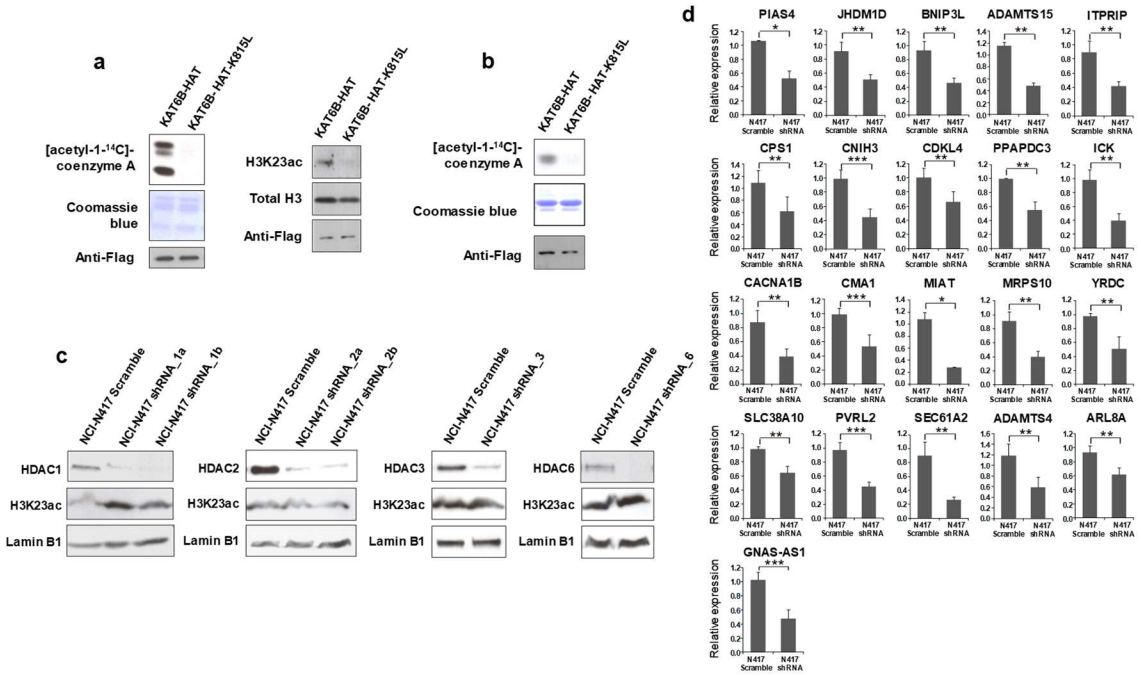

Supplementary Figure 5. Biochemical and cellular assays to determine KAT6B activity. A) *KAT6B especifically acetylates lysine 23 of histone H3 in vitro. Recombinant GST-Flag-tagged KAT6B HAT domains (wild type, and K815L mutant) were assayed for the presence of histone acetyltransferase activity (left-top). Core histones used as substrates were stained with Comassie blue (left-midle). Flag-tagged wild-type and catalytically inactive HAT domains were analyzed in western blot (left-bottom). Recombinant GST-Flag-tagged KAT6B HAT were assayed in western blot for the presence of specific histone H3K23 acetyltransferase activity (right-top). Histone H3 from core histones used as substrates was analyzed in western blot (righ-middle). Flag-tag HAT domains were analyzed in western blot (right-bottom).* ***B)*** *Recombinant GST-Flag-tagged KAT6B HAT domains were assayed for the presence of histone acetyltransferase activity on recombinant histone H3 (top). Recombinant histone H3 was stained with Comassie blue (midle) and GST-Flag-tagged KAT6B HAT domains were analyzed in western blots (bottom).* ***C)*** *The expression of HDAC1, 2, 3 and 6 was diminished using specific shRNAs targeting each protein in NCI-N417 cells. Western blot analysis of each HDAC and the acetylation of H3K23 revealed that HDAC1 is involved in H3K23 deacetylation.* ***D)*** *Quantitative reverse-transcription PCR results confirmed the microarray expression data: twenty-one genes (in addition to the four genes shown in Fig. 3f) presented significantly less expression in KAT6B shRNA-depleted cells than in scramble cells. Significance of permutation tests: *, p <0.05; **, p < 0.01; ***, p <0.001.*

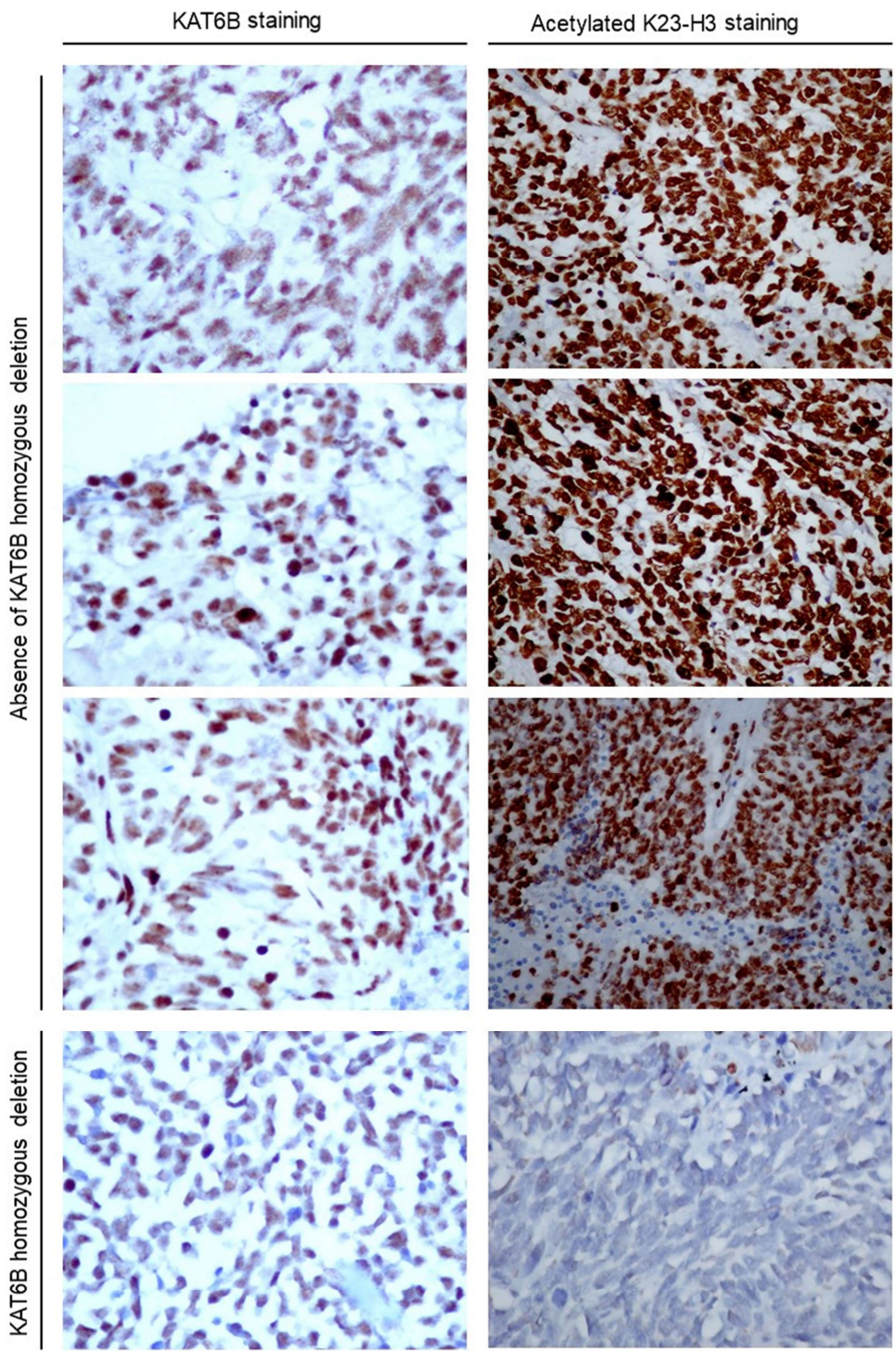

***Supplementary Figure 6**. Immunohistochemistry studies for KAT6B and acetylated K23-H3 staining according to KAT6B deletion status in four illustrative cases of SCLC tumors. Positive staining is shown in brown.*

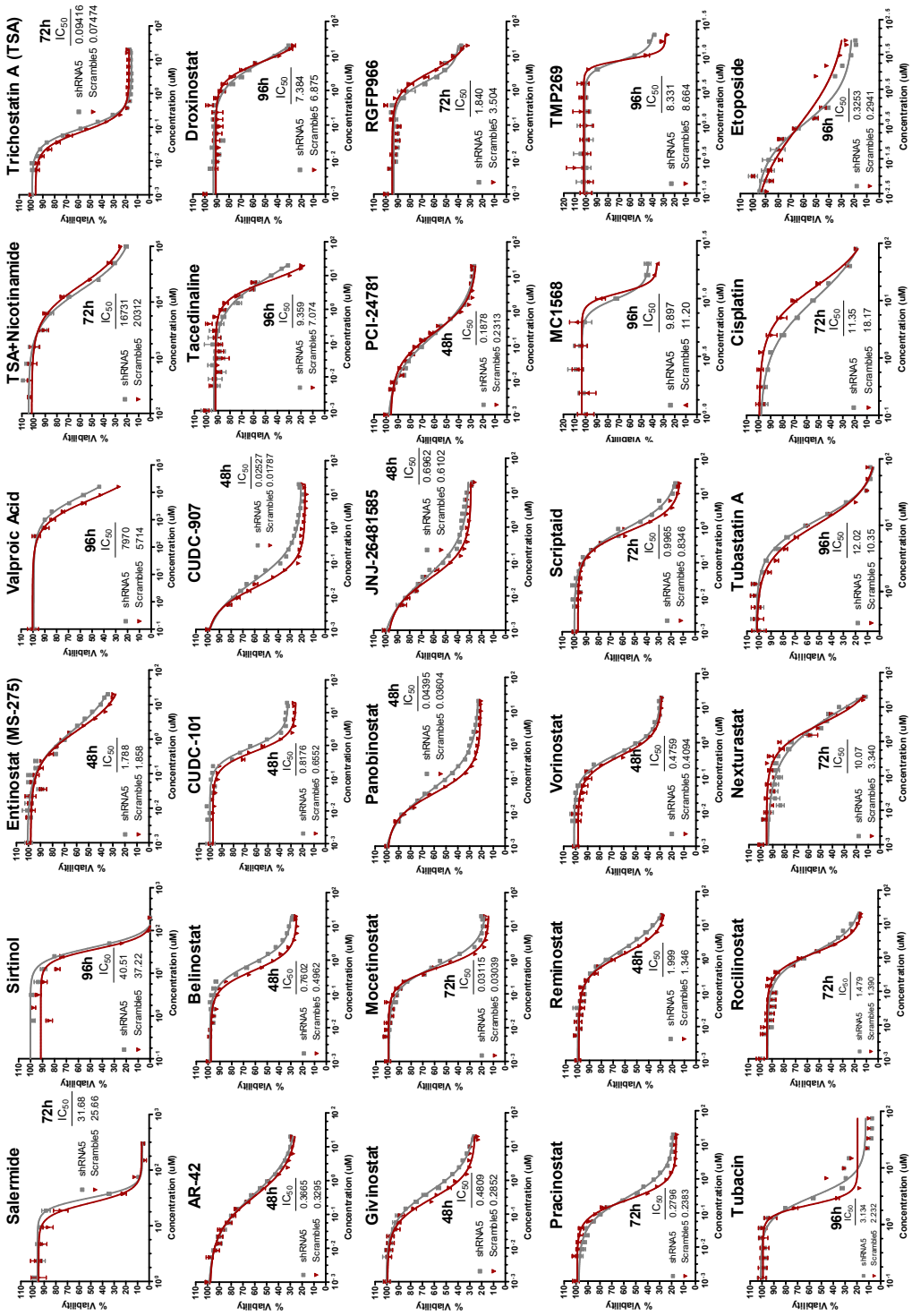

Supplementary Figure 7. *Twenty-eight histone deacetylase inhibitors and two classical drugs in SCLC chemotherapy such as cisplatin and etoposide were employed to determine IC50 values in KAT6B shRNA-transfected vs scramble shRNA-transfected NCI-N417 cells.*

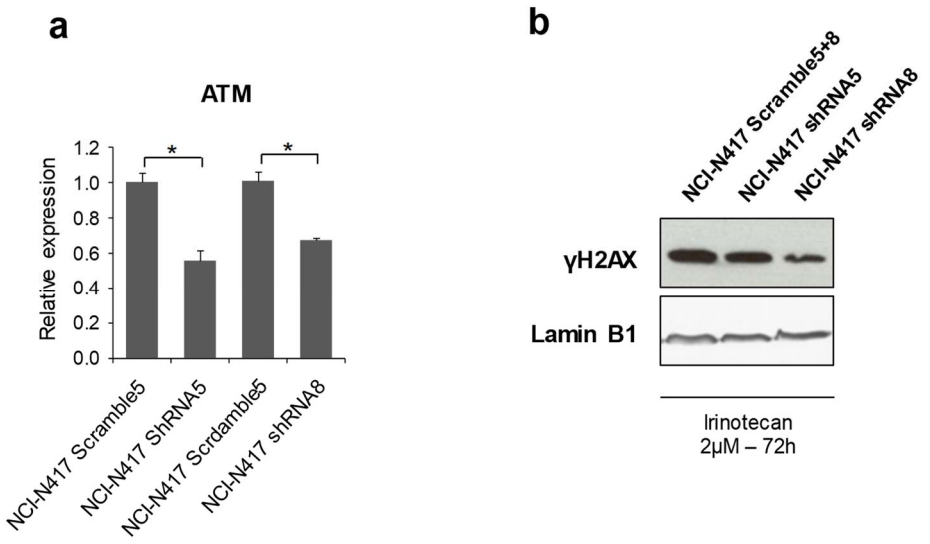

***Supplementary Figure 8**. **Effect of KAT6B shRNA-mediated depletion in ATM expression and H2AX phosphorylation**. KAT6B shRNA-mediated depletion caused a reduction of ATM expression **(A)** and, upon irinotecan treatment, a lower phosphorylation of H2AX than in shRNA-scramble cells **(B)**.*

Supplementary Table 1. *List of antibodies and primer sets used in the study.*

Antibody name	Reference	Company	Application	Dilution
Anti-KAT6B	HPA006104	Sigma	WB/IHC	1:25
Anti-FLAG-HRP	A8592	Sigma	WB	1:1000
H3K23ac	#8848	Cell Signaling	WB	1:50
	sc-34262	Santa Cruz	ChIP	1 µg/ChIP
	ab47813	abcam	IHC	1:500
H3K14ac	06-911	Millipore	WB	1:500
H4K16ac	07-329	Millipore	WB	1:1000
H3	ab1791	Abcam	WB	1:5000
BRM (N-19)	sc-6450	Santa Cruz Biotech	WB	1:50
E-cadherin (24E10)	#3195	Cell Signaling	WB	1:2000
Ph-Rb (Ser608)	#2181	Cell Signaling	WB	1:500
HDAC1	sc-8410X	Santa Cruz Biotech	WB	1:1000
HDAC2	04-229	Millipore	WB	1:5000
HDAC3	ab7030	Abcam	WB	1:500
HDAC6	#7558	Cell Signaling	WB	1:1000
Nucleolin	sc-8031	Santa Cruz	WB	1:1000
Lamin B1	ab16048	Abcam	WB	1:1000

Primers for genomic quantitative PCR	
GqPCR_KAT6B_F	GTCTGTCTGCAGGGCTTTTC
GqPCR_KAT6B_R	CACCACAATGGGTCACAGAG
GqPCR_RPS24_F	ACTTGGGAAATGCTGTGTCC
GqPCR_RPS24_R	AGAGGCTTTGCCAGATTTCA

Primers for qRT-PCR	
qRTPCR_KAT6B_F	GTCAGCCTTCTACCCCATGA
qRTPCR_KAT6B_R	GCCACAATCTGCACAAGAGA
qRTPCR_GAPDH_F	GAAGGTGAAGGTCGGAGTCA
qRTPCR_GAPDH_R	TGGACTCCACGACGTACTCA
qRTPCR_HPRT1_F	TGACACTGGCAAAACAATGCA
qRTPCR_ HPRT1 _R	GGTCCTTTTCACCAGCAAGCT
qRTPCR_FAM3C_F	TACGATGATGGAGCAACCAA
qRTPCR_ FAM3C_R	CCACCACAGAAGACCCAGTT
qRTPCR_LAMA4_F	CATGTGGTTGGACCCCTGAA
qRTPCR_LAMA4_R	GTATGCAGCCTGTGAAGGGT
qRTPCR_JAM3_F	TGCCTGACTTCTTCCTGCTG
qRTPCR_JAM3_R	CGATCCTGGGGTCACTTGTC

qRTPCR_DTX2_F	CTCGCTGGCCCCTTACATTA
qRTPCR_DTX2_R	ACAGACGCTGGCTTCATAGG
qRTPCR_PIAS4_F	GAGAATCTGTTACTCAGACAC
qRTPCR_PIAS4_R	GCTTATTGGAGGGGTAGTAG
qRTPCR_JHDM1D_F	GGAGGAACTGGCACAGACAT
qRTPCR_JHDM1D_R	GTGAAGGGAGCCTGAGTCCTA
qRTPCR_BNIP3L_F	GCTGGAACACGTACCATCCT
qRTPCR_BNIP3L_R	GATCTGCCCATCTTCTTGTGG
qRTPCR_ADAMTS15_F	GCTGCAAGAAGGTGACTGGA
qRTPCR_ADAMTS15_R	GCTGTTCTTCAGAGCCAGGT
qRTPCR_ITPRIP_F	TTAACTCAAGCCACCCCAAG
qRTPCR_ITPRIP_R	TGTGACTCTTGGCTCCCTCT
qRTPCR_CPS1_F	AATTGATTAGAGATGGCAGC
qRTPCR_CPS1_R	AATTAGTGAGGAGAGGGATTC
qRTPCR_CNIH3_F	CGACACTTTGAGTTACTGTC
qRTPCR_CNIH3_R	GCAGTAAAGGTAGTAGAAGAAG
qRTPCR_CDKL4_F	CCAAATCTTGTGAACCTCATC
qRTPCR_CDKL4_R	CTCCATTTGGGTTTCTTTCC
qRTPCR_PPAPDC3_F	TCATGAATCTGCTCCTGG
qRTPCR_PPAPDC3_R	TGAGGAAGAACTTGGACAC
qRTPCR_ICK_F	AGGCACTTCGATATCCTTAC
qRTPCR_ICK_R	TGTGGTTTTTCTGAATCCTG
qRTPCR_CACNA1B_F	TTGACAATATCCTGTTTGCC
qRTPCR_CACNA1B_R	CCGCATCGTTTGTATTATAGAG
qRTPCR_CMA1_F	AAGGTCTATAACAGTCACCC
qRTPCR_CMA1_R	ATCGTGGTGAAGAGTAGAAG
qRTPCR_MIAT_F	TAACCAAGGTCCACAGAAC
qRTPCR_MIAT_R	AAATAGACCCTGGACTGC
qRTPCR_MRPS10_F	GCCATGGAAGTAACAAAGAC
qRTPCR_MRPS10_R	CACTCTCCACTTAAACATACTC
qRTPCR_YRDC_F	CAAGGACCTAAACCCTTTTAC
qRTPCR_YRDC_R	ATAACCAAGGACAACTGAGG
qRTPCR_SLC38A10_F	AGCAGCAGCAAAAAGATG
qRTPCR_SLC38A10_R	CCACAGAGAGGGTAAGTG
qRTPCR_PVRL2_F	ATGATGACAACTGGTACCTC
qRTPCR_PVRL2_R	GAAGGTGGTATTGAACAGAC
qRTPCR_SEC61A2_F	GATACACCGAAAGATAGAGC
qRTPCR_SEC61A2_R	ACTGAATGAGATCAGGAGAC
qRTPCR_ADAMTS4_F	AGAAGAAGTTTGACAAGTGC
qRTPCR_ADAMTS4_R	CACATTGTTGTATCCGTACC

qRTPCR_ARL8A_F	AGATTGAGGCCTCTAAGAAC
qRTPCR_ARL8A_R	TCATTTTCTCAATCAGCTCC
qRTPCR_GNAS-AS1_F	CCTCCTTTTCGACGACTGAT
qRTPCR_GNAS-AS1_R	ACAGCTGCAGAAGGTTCCAG
qRTPCR_KAT3B_F	AAAAATAAGAGCAGCCTGAG
qRTPCR_KAT3B _R	AGACCTCTTTATGCTTCTCC
qRTPCR_KAT3A_F	AACATGTCACTCAGGACC
qRTPCR_KAT3A _R	AATATTCATCCCTGCTGTTG
qRTPCR_KAT6A_F	ACTCCTTAAAGATGGACCTC
qRTPCR_KAT6A_R	GGCTTATCCTTTTCATGTGG
qRTPCR_KAT7_F	AAAGAGACAGGACCTGATTG
qRTPCR_KAT7_R	GCAACAGAGAAATGACAGAC
qRTPCR_KAT5_F	CAAGAGTTATTCCCAGAACC
qRTPCR_KAT5_R	GTAGTCTTCCGTTGATTCTTTC
qRTPCR_KAT8_F	GATTTACTGTCAGAACCTGTG
qRTPCR_KAT8_R	GTCAGGATGTAAAAGACGAAC
qRTPCR_KAT6B isoform1_F	AGCTTGACAGACGGAAGGAT
qRTPCR_ KAT6B isoform1_R	CTTCCACCCCACTCTCACAC
qRTPCR_KAT6B isoform2_F	ACTTCTCATGTGTTGGCTACAGA
qRTPCR_ KAT6B isoform2_R	AAGTTCCTGGGCCTGCTTA
qRTPCR_KAT6B isoform3_F	AGGAAGGGGGTCACCTGA
qRTPCR_ KAT6B isoform3_R	AAGTTCCTGGGCCTGCTTA
qRTPCR_ ATM_F	ACCATTGTAGAGGTCCTTC
qRTPCR_ ATM_R	GTCTCATTAAGACACGTTCAG

Primers for KAT6B sequencing	
Seq_KAT6B_F1	GAAGTCAAAGTGATCTCACAAGC
Seq_KAT6B_F2	GGGATGTGGATTTGCCAAGTCTGC
Seq_KAT6B_F3	CACAAAAGCTAAAACCTCCACC
Seq_KAT6B_F4	TGACAGACGGAAGGATTAAACC
Seq_KAT6B_F5	TGAAAAGGGCTGTCATCTGG
Seq_KAT6B_F6	AGCTGAGAAAGAGGCTGAGCG
Seq_KAT6B_F7	CTGTGAGATTGAAGTGGAGG
Seq_KAT6B_F8	GAGCCTGACGAGCAGGTAAC
Seq_KAT6B_F9	GTCGATACAGAGTTCAAAGAGGG
Seq_KAT6B_F10	TCACAGAACAGCTGCTCCTATAGC
Seq_KAT6B_F11	AAGCACAAGCTACCATGACC
Seq_KAT6B_F12	GGCTATATGAATCAAACGCCC

shRNA and scrambled oligonucleotides	
KAT6B_shRNA5_F	GATCCCCGAAGCTATACAGAAAATAATTCAAGAG ATTATTTTCTGTATAGCTTCTTTTTGGAAA
KAT6B_shRNA5_R	AATTTTTCCAAAAAGAAGCTATACAGAAAATAATC TCTTGAATTATTTTCTGTATAGCTTCGGG
KAT6B_Scramble5_F	GATCCCCGAAGTTATACAGAAGATAATTCAAGAG ATTATCTTCTGTATAACTTCTTTTTGGAAA
KAT6B_Scramble5_R	AATTTTTCCAAAAAGAAGTTATACAGAAGATAATC TCTTGAATTATCTTCTGTATAACTTCGGG
KAT6B_shRNA8_F	GATCCCCGATTGAATTTGGTAAATATTTCAAGAG AATATTTACCAAATTCAATCTTTTTGGAAA
KAT6B_shRNA8_R	AATTTTTCCAAAAAGATTGAATTTGGTAAATATTC TCTTGAAATATTTACCAAATTCAATCGGG
KAT6B_Scramble8_F	GATCCCCGATTGCATTTGGTAAGTATTTCAAGAG AATACTTACCAAATGCAATCTTTTTGGAAA
KAT6B_Scramble8_R	AATTTTTCCAAAAAGATTGCATTTGGTAAGTATTC TCTTGAAATACTTACCAAATGCAATCGGG
HDAC1_shRNA1a_F	GATCCGCCGCAAGAACTCTTCCAACTTCAAGAGA GTTGGAAGAGTTCTTGCGGTTTTTTG
HDAC1_shRNA1a_R	AATTCAAAAAACCGCAAGAACTCTTCCAACTCTCT TGAAGTTGGAAGAGTTCTTGCGGCG
HDAC1_shRNA1b_F	GATCCGCTGCTCAACTATGGTCTCTTCAAGAGAG AGACCATAGTTGAGCAGCTTTTTTG
HDAC1_shRNA1b_R	AATTCAAAAAAGCTGCTCAACTATGGTCTCTCTCT TGAAGAGACCATAGTTGAGCAGCG
HDAC2_shRNA2a_F	GATCCGCAGTCTCACCAATTTCAGATTCAAGAGA TCTGAAATTGGTGAGACTGTTTTTTG
HDAC2_shRNA2a_R	AATTCAAAAAACAGTCTCACCAATTTCAGATCTCT TGAATCTGAAATTGGTGAGACTGCG
HDAC2_shRNA2b_F	GATCCGCCTATTATCTCAAAGGTGTTCAAGAGAC ACCTTTGAGATAATAGGCTTTTTTG
HDAC2_shRNA2b_R	AATTCAAAAAAGCCTATTATCTCAAAGGTGTCTCT TGAACACCTTTGAGATAATAGGCG
HDAC3_shRNA3_F	GATCCGCGGTGTCCTTCCACAAATATTCAAGAGA TATTTGTGGAAGGACACCGTTTTTTG
HDAC3_shRNA3_R	AATTCAAAAAACGGTGTCCTTCCACAAATATCTCT TGAATATTTGTGGAAGGACACCGCG
HDAC6_shRNA6_F	GATCCGCCGGTTTGCTGAAAAGGAATTCAAGAGA TTCCTTTTCAGCAAACCGGTTTTTTG

HDAC6_shRNA6_R	AATTCAAAAAACCGGTTTGCTGAAAAGGAATCTC TTGAATTCCTTTTCAGCAAACCGGCG
HDAC_Scramble_F	GATCCGCGCAGAACAAATTCGTCCATTCAAGAGA TGGACGAATTTGTTCTGCGTTTTTTACGCGTG
HDAC_Scramble_R	AATTCACGCGTAAAAAACGCAGAACAAATTCGTC CATCTCTTGAATGGACGAATTTGTTCTGCGCG

Primers for KAT6B cloning	
KAT6B_SphI_F	TCACCCAGCAGATGTCCAACATCAGCGGGAGCT GCAGCATGC
KAT6B_EcoRI_Flag_R	TTTTTTGAATTCCTACTTATCGTCGTCATCCTTGT AATCTCCTGATCCCCTTCTCATGTAGGAGCCATT GAGAGACTGTTTGGACATGCCTGTGTTCATGTAG
NotI_BssHII_F	GGCCGCGGGAAACG
NotI_BssHII_R	GCGCGCAAAGGGCG

ChIP primers	
ChIP_FAM3C_F	CGGGACCACGGATGATGATT
ChIP_ FAM3C_R	GGATGATGGAAACCGCTCCT
ChIP_LAMA4_F	GGGAGAGAGAGGCTGGAACT
ChIP_ LAMA4_R	ATTTTCCCTCCTCTCCGTGT
ChIP_JAM3_F	CTGGGGATCTGCAGTTCATT
ChIP_ JAM3_R	CGGATAAGAGTCTGCGTGGT
ChIP_DTX2_F	CACATGTATGTACTGGCACCAT
ChIP_ DTX2_R	CACCTGCTCCGGTCTATGTT

Supplementary Table 2. *List of 32 commonly downregulated genes upon depletion of KAT6B gene in NCI-N417 and HCC-33 cell lines. Normalized intensities from the array in each sample and log Fold Changes from the analysis are depicted.*

logFC HCC33	logFC N417	Gene Symbol	GeneName	N417 sh5	N417 sh8	HCC33 sh5	HCC33 sh8	N417 scr5	N417 scr8	HCC33 scr5	HCC33 scr8
-1.382	-0.753	TRPM8	transient receptor potential cation channel, subfamily M, member 8	5.085	4.858	6.224	5.758	5.626	5.306	7.217	7.064
-1.237	-0.772	TPTE2	transmembrane phosphoinositide 3-phosphatase and tensin homolog 2	4.849	4.731	4.778	4.898	5.353	5.127	5.925	5.224
-1.124	-0.623	KAT6B	K(lysine) acetyltransferase 6B	6.858	7.158	7.418	7.875	7.547	7.546	8.705	8.713
-1.026	-1.188	ICK	intestinal cell (MAK-like) kinase	7.772	7.546	7.134	6.758	8.713	8.807	7.831	7.925
-0.943	-1.313	PAN3-AS1	PAN3 antisense RNA 1 (non-protein coding)	6.073	6.044	5.882	5.954	7.277	7.021	6.461	6.901
-0.933	-0.738	ALB	albumin	4.622	4.662	5.028	5.042	5.077	4.951	5.953	5.306
-0.922	-0.769	JAM3	junctional adhesion molecule 3	9.370	8.874	9.333	9.220	9.946	9.798	10.113	10.252
-0.882	-0.876	OR2T6	olfactory receptor, family 2, subfamily T, member 6	5.212	4.731	5.028	5.116	5.464	5.596	5.560	5.690
-0.850	-0.981	NEAT1	nuclear paraspeckle assembly transcript 1 (non-protein coding)	11.462	10.973	5.917	6.299	11.936	12.411	6.582	7.039
-0.811	-0.717	PPAPDC3	phosphatidic acid phosphatase type 2 domain containing 3	9.475	9.414	5.772	5.838	10.405	9.867	6.202	6.684
-0.779	-0.612	CDKL4	cyclin-dependent kinase-like 4	5.031	5.152	4.778	4.855	5.482	5.539	5.212	5.253
-0.754	-0.794	CNIH3	cornichon homolog 3 (Drosophila)	6.695	6.746	5.373	5.069	7.607	7.204	5.778	5.644
-0.743	-0.836	CPS1	carbamoyl-phosphate synthase 1, mitochondrial	4.687	4.637	5.111	5.183	4.943	5.267	5.533	5.709
-0.741	-0.716	BNIP3L	BCL2/adenovirus E1B 19kDa interacting protein 3-like	9.753	9.705	9.633	9.659	10.314	10.506	10.321	10.430
-0.722	-0.944	LAMA4	laminin, alpha 4	5.358	5.833	4.858	5.183	6.375	6.294	5.494	5.392
-0.709	-0.659	CCL28	chemokine (C-C motif) ligand 28	4.367	4.422	4.604	4.855	4.562	4.690	5.055	5.088
-0.696	-1.480	FAM3C	family with sequence similarity 3, member C	8.583	7.615	7.790	7.375	9.252	9.762	8.194	8.272
-0.650	-0.734	CACNA1B	calcium channel, voltage-dependent, N type, alpha 1B subunit	4.622	4.701	4.543	4.690	5.155	4.925	4.855	4.948
-0.643	-1.539	ADAMTS4	ADAM metallopeptidase with thrombospondin type 1 motif, 4	6.498	5.799	4.925	5.116	7.010	7.875	5.302	5.498
-0.601	-1.435	CMA1	chymase 1, mast cell	4.604	4.243	4.460	4.422	4.778	5.306	4.637	4.673
-0.580	-0.746	ITPRIP	inositol 1,4,5-trisphosphate receptor interacting protein	8.775	8.716	9.365	8.982	9.702	9.241	9.799	9.683
-0.576	-1.602	MIAT	myocardial infarction associated transcript (non-protein coding)	6.054	5.409	11.643	11.635	6.820	7.047	12.232	12.182
-0.554	-0.610	ADAMTS15	ADAM metallopeptidase with thrombospondin type 1 motif, 15	4.711	4.731	4.874	4.742	5.055	5.031	5.180	5.003
-0.536	-0.867	GNAS-AS1	GNAS antisense RNA 1 (non-protein coding)	9.515	9.118	7.539	7.700	10.357	9.960	8.060	8.182
-0.535	-0.631	DTX2	deltex homolog 2 (Drosophila)	4.983	4.858	5.085	5.082	5.274	5.364	5.390	5.422
-0.534	-0.884	MRPS10	mitochondrial ribosomal protein S10	11.020	10.480	10.780	10.743	11.652	11.541	11.450	11.133
-0.517	-0.676	JHDM1D	jumonji C domain containing histone demethylase 1 homolog D (S. cerevisiae)	6.997	6.838	6.045	6.017	7.607	7.396	6.451	6.439
-0.514	-0.640	YRDC	yrdC domain containing (E. coli)	12.330	12.105	12.198	12.459	12.768	12.952	12.898	12.784
-0.490	-0.610	SLC38A10	solute carrier family 38, member 10	5.142	5.152	5.692	5.570	5.464	5.692	6.054	5.925
-0.487	-0.961	PVRL2	poliovirus receptor-related 2 (herpesvirus entry mediator B)	8.325	8.185	5.085	5.152	8.992	9.343	5.422	5.407
-0.453	-0.857	SEC61A2	Sec61 alpha 2 subunit (S. cerevisiae)	6.553	6.484	6.274	6.179	7.489	6.998	6.640	6.558
-0.450	-0.611	ARL8A	ADP-ribosylation factor-like 8A	11.492	11.279	11.538	11.554	12.028	11.926	11.942	12.045

Supplementary Table 3. *The thirty-HDAC inhibitors used in the study and their specificity.*

HDACi	HDAC class	Target protein
Salermide	Class III	SIRT1, SIRT2
Sirtinol	Class III	SIRT1, SIRT2
Entinostat (MS-275)	Class I	HDAC1, HDAC3
Valproic Acid	Non specific	-
Nicotinamide	Class III	Sirtuins in general
Trichostatin A (TSA)	Class I - Class II	No sirtuins
AR-42	Pan-HDACi	-
Belinostat	General HDACi	-
CUDC-101	Multitarget HDACi	-
CUDC-907	HDACi - PI3Ki	-
Tacedinaline	Class I	HDAC1, HDAC3
Droxinostat	Class I - Class IIB	HDAC1, 8, 6
Givinostat	Class I - Class II	-
Mocetinostat	Class I	HDAC1, HDAC2
Panobinostat	General HDACi	-
JNJ-26481585	Pan-HDACi	-
PCI-24781	Class I - Class IIB	HDAC1, 6, 8, 10
RGFP966	Class I	HDAC3 (specific)
Pracinostat	Class I, II, IV	General
Resminostat	Class I - Class II	HDAC1, 3, 6
Vorinostat	Class I - Class II	-
Scriptaid	Class I	HDAC 1, 3, 8
MC1568	Class IIA	HDAC4, 5, 7, 9
TMP269	Class IIA	HDAC4, 5, 7, 9
Tubacin	Class IIB	HDAC6 (specific)
Rocilinostat	Class IIB	HDAC6 (specific)
Nexturastat A	Class IIB	HDAC6 (specific)
Tubastatin A	Class IIB	HDAC6 (specific)

REFERENCES

1. van Meerbeeck JP, Fennell DA, De Ruysscher DK. Small-cell lung cancer. Lancet 2011;378:1741–55.
2. Pillai RN, Owonikoko TK. Small cell lung cancer: therapies and targets. Semin Oncol 2014;41:133–42.
3. Buettner R, Wolfm J, Thomas RK. Lessons learned from lung cancer genomics: the emerging concept of individualized diagnostics and treatment. J Clin Oncol 2013;31:1858–65.
4. Peifer M, Fernández-Cuesta L, Sos ML, George J, Seidel D, Kasper LH, et al. Integrative genome analyses identify key somatic driver mutations of small-cell lung cancer. Nat Genet 2012;44:1104–10.
5. Fraga MF, Ballestar E, Villar-Garea A, Boix-Chornet M, Espada J, Schotta G, et al. Loss of acetylation at Lys16 and trimethylation at Lys20 of histone H4 is a common hallmark of human cancer. Nat Genet 2005;37:391–400.
6. Seligson DB, Horvath S, Shi T, Yu H, Tze S, Grunstein M, et al. Global histone modification patterns predict risk of prostate cancer recurrence. Nature 2005;435:1262–6.
7. Berdasco M, Esteller M. Aberrant epigenetic landscape in cancer: how cellular identity goes awry. Dev Cell 2010;19:698–711.
8. Dawson MA, Kouzarides T. Cancer epigenetics: from mechanism to therapy. Cell 2012;150:12–27.
9. Kishimoto M, Kohno T, Okudela K, Otsuka A, Sasaki H, Tanabe C, et al. Mutations and deletions of the CBP gene in human lung cancer. Clin Cancer Res 2005;11:512–9.
10. Rodriguez-Paredes M, Martinez de Paz A, Simó-Riudalbas L, Sayols S, Moutinho C, Moran S, et al. Gene amplification of the histone methyltransferase SETDB1 contributes to human lung tumorigenesis. Oncogene 2014;33:2807–13.
11. Champagne N, Bertos NR, Pelletier N, Wang AH, Vezmar M, Yang Y, et al. Identification of a human histone acetyltransferase related to monocytic leukemia zinc finger protein. J Biol Chem 1999;274:28528–36.
12. Yang XJ, Ullah M. MOZ and MORF, two large MYSTic HATs in normal and cancer stem cells. Oncogene 2007;26:5408–19.
13. Klein BJ, Lalonde ME, Côté J, Yangm X J, Kutateladze TG. Crosstalk between epigenetic readers regulates the MOZ/MORF HAT complexes. Epigenetics 2014;9:186–93.
14. Forgacs E, Biesterveld EJ, Sekido Y, Fong K, Muneer S, Wistuba II, et al. Mutational analysis of the PTEN/MMAC1 gene in lung cancer. Oncogene 1998; 17(12):1557-65.

15. Panagopoulos I, Fioretos T, Isaksson M, Samuelsson U, Billström R, Strömbeck B, et al. Fusion of the MORF and CBP genes in acute myeloid leukemia with the t(10;16)(q22;p13). Hum Mol Genet 2001;10:395–404.

16. Vizmanos JL, Larráyoz MJ, Lahortiga I, Floristán F, Alvarez C, Odero MD, et al. t(10;16)(q22;p13) and MORF-CREBBP fusion is a recurrent event in acute myeloid leukemia. Genes Chromosomes Cancer 2003;36:402–5.

17. Moore SD, Herrick SR, Ince TA, Kleinman MS, Dal Cin P, Morton CC, et al. Uterine leiomyomata with t(10;17) disrupt the histone acetyltransferase MORF. *Cancer Res* 2004;64:5570–7.

18. Clayton-Smith J, O'Sullivan J, Daly S, Bhaskar S, Day R, Anderson B, et al. Whole-exome-sequencing identifies mutations in histone acetyltransferase gene KAT6B in individuals with the Say-Barber-Biesecker variant of Ohdo syndrome. Am J Hum Genet 2011;89:675–81.

19. Campeau PM, Kim JC, Lu JT, Schwartzentruber JA, Abdul-Rahman OA, Schlaubitz S, et al. Mutations in KAT6B, encoding a histone acetyltransferase, cause Genitopatellar syndrome. Am J Hum Genet 2012;90:282–9.

20. Simpson MA, Deshpande C, Dafou D, Vissers LE, Woollard WJ, Holder SE, et al. De novo mutations of the gene encoding the histone acetyltransferase KAT6B cause Genitopatellar syndrome. Am J Hum Genet 2012;90:290–4.

21. Barretina J, Caponigro G, Stransky N, Venkatesan K, Margolin AA, Kim S, et al. The Cancer Cell Line Encyclopedia enables predictive modelling of anticancer drug sensitivity. Nature 2012;483:603–7.

22. Kahali B, Gramling SJ, Marquez SB, Thompson K, Lu L, Reisman D. Identifying targets for the restoration and reactivation of BRM. Oncogene 2014;33(5):653-64.

23. Banine F, Bartlett C, Gunawardena R, Muchardt C, Yaniv M, Knudsen ES, et al. SWI/SNF chromatin-remodeling factors induce changes in DNA methylation to promote transcriptional activation. Cancer Res 2005; 65(9):3542-7.

24. Voss AK, Collin C, Dixon MP, Thomas T. Moz and retinoic acid coordinately regulate H3K9 acetylation, Hox gene expression, and segment identity. Dev Cell 2009;17:674–86.

25. Qiu Y, Liu L, Zhao C, Han C, Li F, Zhang J, et al. Combinatorial readout of unmodified H3R2 and acetylated H3K14 by the tandem PHD finger of MOZ reveals a regulatory mechanism for HOXA9 transcription. Genes Dev 2012;26:1376–91.

26. Dreveny I, Deeves SE, Fulton J, Yue B, Messmer M, Bhattacharya A, *et al*. The double PHD finger domain of MOZ/MYST3 induces α-helical structure of the histone H3 tail to facilitate acetylation and methylation sampling and modification. Nucl Acids Res 2014;42:822–35.

27. Borrow J, Stanton VP Jr, Andresen JM, Becher R, Behm FG, Chaganti RS, et al. The translocation t(8;16)(p11;p13) of acute myeloid leukaemia fuses a putative acetyltransferase to the CREB-binding protein. Nat Genet 1996;14:33–41.

28. Kitabayashi I, Aikawa Y, Yokoyama A, Hosoda F, Nagai M, Kakazu N, et al. Fusion of MOZ and p300 histone acetyltransferases in acute monocytic leukemia with a t(8;22)(p11;q13) chromosome translocation. Leukemia 2001;15:89–94.

29. Doyon Y, Cayrou C, Ullah M, Landry AJ, Côté V, Selleck W, et al. ING tumor suppressor proteins are critical regulators of chromatin acetylation required for genome expression and perpetuation. Mol Cell 2006;21:51–64.

30. Ali M, Yan K, Lalonde ME, Degerny C, Rothbart SB, Strahl BD, et al. Tandem PHD fingers of MORF/MOZ acetyltransferases display selectivity for acetylated histone H3 and are required for the association with chromatin. J Mol Biol 2012;424:328–38.

31. Szakszon K, Berényi E, Jakab A, Bessenyei B, Balogh E, Köbling T, et al. Blepharophimosis mental retardation syndrome Say-Barber/Biesecker/Young-Simpson type - new findings with neuroimaging. Am J Med Genet A 2011;155A:634–7.

32. Szakszon K, Salpietro C, Kakar N, Knegt AC, Oláh É, Dallapiccola B, et al. De novo mutations of the gene encoding the histone acetyltransferase KAT6B in two patients with Say-Barber/Biesecker/Young-Simpson syndrome. Am. J. Med. Genet. A 2013;161A:884–8.

33. Taipale M, Rea S, Richter K, Vilar A, Lichter P, Imhof A, et al. hMOF histone acetyltransferase is required for histone H4 lysine 16 acetylation in mammalian cells. Mol Cell Biol 2005;25:6798-810.

34. Smith ER, Cayrou C, Huang R, Lane WS, Côté J, Lucchesi JC, et al. A human protein complex homologous to the Drosophila MSL complex is responsible for the majority of histone H4 acetylation at lysine 16. Mol Cell Biol 2005;25:9175-88.

35. Yuan H, Rossetto D, Mellert H, Dang W, Srinivasan M, Johnson J, et al. MYST protein acetyltransferase activity requires active site lysine autoacetylation. EMBO J. 2012;31:58-70.

36. Iwakawa R, Takenaka M, Kohno T, Shimada Y, Totoki Y, Shibata T, et al. Genome-wide identification of genes with amplification and/or fusion in small cell lung cancer. Genes Chromosomes Cancer 2013;52:802–16.

37. Daigle SR, Olhava EJ, Therkelsen CA, Majer CR, Sneeringer CJ, Song J, et al. Selective killing of mixed lineage leukemia cells by a potent small-molecule DOT1L inhibitor. Cancer Cell 2011;20:53–65.

38. Zuber J, Shi J, Wang E, Rappaport AR, Herrmann H, Sison EA, et al. RNAi screen identifies Brd4 as a therapeutic target in acute myeloid leukaemia. Nature 2011;478:524–8.

39. Delmore JE, Issa GC, Lemieux ME, Rahl PB, Shi J, Jacobs HM, et al. BET bromodomain inhibition as a therapeutic strategy to target c-Myc. Cell 2011;146:904–17.

40. Dawson MA, Prinjha RK, Dittmann A, Giotopoulos G, Bantscheff M, Chan WI, et al. Inhibition of BET recruitment to chromatin as an effective treatment for MLL-fusion leukaemia. Nature 2011;478:529–33.

41. Vonlaufen N, Naguleswaran A, Coppens I, Sullivan WJ Jr. MYST family lysine acetyltransferase facilitates ataxia telangiectasia mutated (ATM) kinase-mediated DNA damage response in Toxoplasma gondii. J Biol Chem 2010;285(15):11154-61.

42. Jett JR, Schild SE, Kesler KA, Kalemkerian GP. Treatment of small cell lung cancer: Diagnosis and management of lung cancer, 3rd ed: American College of Chest Physicians evidence-based clinical practice guidelines. Chest 2013;143:e400S-19S.

43. Kebede AF, Schneider R, Daujat S. Novel types and sites of histone modifications emerge as players in the transcriptional regulation contest. FEBS J 2015;282(9):1658-74.

44. Rothbart SB, Strahl BD. Interpreting the language of histone and DNA modifications. Biochim Biophys Acta 2014;1839:627-43.

45. Schiltz RL, Mizzen CA, Vassilev A, Cook RG, Allis CD, Nakatani Y, et al. Overlapping but distinct patterns of histone acetylation by the human coactivators p300 and PCAF within nucleosomal substrates. J Biol Chem 1999;274:1189-92.

46. Hashizume R, Andor N, Ihara Y, Lerner R, Gan H, Chen X, et al. Pharmacologic inhibition of histone demethylation as a therapy for pediatric brainstem glioma. Nat Med 2014;20(12):1394-6

47. Papazyan R, Voronina E, Chapman JR, Luperchio TR, Gilbert TM, Meier E, et al. Methylation of histone H3K23 blocks DNA damage in pericentric heterochromatin during meiosis. Elife 2014;3:e02996.

Study II

"Bromodomain inhibition shows antitumoral activity in mice and human luminal breast cancer"

Montserrat Pérez-Salvia[1], Laia Simó-Riudalbas[1], Pere Llinàs-Arias[1], Laura Roa[1], Fernando Setien[1], Marta Soler[1], Manuel Castro de Moura[1], James E. Bradner[2], Eva Gonzalez-Suarez[1], Catia Moutinho[1] and Manel Esteller[1,3,4]

[1]Cancer Epigenetics and Biology Program (PEBC), Bellvitge Biomedical Research Institute (IDIBELL), Barcelona, Catalonia, Spain

[2]Novartis Institutes for Biomedical Research, Cambridge, MA, USA

[3]Physiological Sciences Department, School of Medicine and Health Sciences, University of Barcelona (UB), Barcelona, Catalonia, Spain

[4]Institució Catalana de Recerca i Estudis Avançats (ICREA), Barcelona, Catalonia,Spain

Oncotarget. 2017 May 29;8(31):51621-51629. doi: 10.18632/ oncotarget.18255.

ABSTRACT

BET bromodomain inhibitors, which have an antitumoral effect against various solid cancer tumor types, have not been studied in detail in luminal breast cancer, despite the prevalence of this subtype of mammary malignancy. Here we demonstrate that the BET bromodomain inhibitor JQ1 exerts growth-inhibitory activity in human luminal breast cancer cell lines associated with a depletion of the C-MYC oncogene, but does not alter the expression levels of the BRD4 bromodomain protein. Interestingly, expression microarray analyses indicate that, upon JQ1 administration, the antitumoral phenotype also involves downregulation of relevant breast cancer oncogenes such as the Breast Carcinoma-Amplified Sequence 1 (BCAS1) and the PDZ Domain-Containing 1 (PDZK1). We have also applied these *in vitro* findings in an *in vivo* model by studying a transgenic mouse model representing the luminal B subtype of breast cancer, the MMTV-PyMT, in which the mouse mammary tumor virus promoter is used to drive the expression of the polyoma virus middle T-antigen to the mammary gland. We have observed that the use of the BET bromodomain inhibitor for the treatment of established breast neoplasms developed in the MMTV-PyMT model shows antitumor potential. Most importantly, if JQ1 is given before the expected time of tumor detection in the MMTV-PyMT mice, it retards the onset of the disease and increases the survival of these animals. Thus, our findings indicate that the use of bromodomain inhibitors is of great potential in the treatment of luminal breast cancer and merits further investigation.

INTRODUCTION

Breast cancer is a leading cause of cancer death in women, estimated to account for more than 450,000 deaths worldwide every year [1]. Despite the improved early detection of the disease and the new therapies, the major health concern associated with breast cancer persists probably due to several factors, among them the biological heterogeneity of the pathology. Classical clinical and pathological markers, such as the status of the estrogen and progesterone receptors and *human epidermal growth factor 2 (HER2)* gene amplification, are useful for classifying patients according to prognosis and adequate treatments, but it has been the emergence of genomic technologies, such as global

expression profiling, that has allowed an intrinsic molecular classification [2–4]. In this regard, five distinct intrinsic molecular subtypes are recognized: luminal A, luminal B, HER-2 enriched, basal-like and claudin-low, together with a normal breast-like group [2–4]. These subgroups relate to the clinically used immunohistochemical classification and, for example, luminal A is estrogen receptor- and/ or progesterone receptor-positive but with a low Ki-67 index, whereas luminal B is estrogen receptor- and/ or progesterone receptor-positive and high Ki-67 index. Overall, the majority of breast tumors are positive for the hormone receptors and, thus, amenable to endocrine therapies. However, in the natural history of the disease, progression is associated with the acquisition of resistance to the endocrine treatment, limiting the efficacy of these pharmacological compounds. In addition, the survival curves of luminal B subtype cross those of basal-like disease at ten years [4]. Thus, given the high frequency of luminal breast cancer, the generation of endocrine therapy-associated resistances and the poor outcome of the luminal B subtype, the development of new drugs for these patients is essential.

One interesting avenue to explore is the targeting of the epigenome of breast cancer cells. In this regard, DNA demethylating agents and histone deacetylase inhibitors have been clinically approved for certain subtypes of leukemias and lymphomas [5]. New promising agents are compounds that can block the “reading” of the acetylated histone marks, preventing the active transcription of growth-promoting genes. This is the case of the BET bromodomain inhibitors that remove BET bromodomain proteins from their chromatin targets by competing with acetylated histone residues [6]. The patterns of histone acetylation shifts in human tumors [7] and recent data have shown that the BET bromodomain inhibitor inhibits the growth of triple-negative breast cancer cell lines and xenografts [8–15]. Thus, we sought to determine whether BET bromodomain inhibitors were also effective not only in luminal breast cancer cell lines, but also in a mouse model of luminal B breast cancer (MMTV-PyMT) [16]. Furthermore, we also characterized gene targets involved in the antiproliferative effect mediated by the BET bromodomain inhibitor JQ1 [17].

RESULTS

The bromodomain inhibitor JQ1 decreases cell viability of human luminal breast cancer cell lines in association with downregulation of C-MYC and mammary oncogenic proteins

To study the cellular impact of JQ1 as a candidate growth inhibitor for luminal breast cancer, we chose the initial biological model of two human cancer cell lines with a well characterized luminal phenotype, MCF7 and T47D [18, 19]. Using the 3-(4,5-dimethyl-2- thiazolyl)-2,5-diphenyl-2H-tetrazolium bromide (MTT) assay to measure cell viability in the chosen cancer cell lines, we observed that JQ1 inhibited cancer cell growth dose-dependently (Figure 1A). Interestingly, IC50 sensitivity to this first-in-class BET bromodomain inhibitor compound is in the same range as that of other antitumoral drugs that target histone modifications, such as histone deacetylases [20] and histone kinases [21, 22]. The next step was to show that the growth inhibition-mediated effect of the JQ1 compound occurred in the context of the induced downregulation of C-MYC, as has been described in other models [23, 24]. Western blot and quantitative reverse transcription-polymerase chain reaction (qRT-PCR) demonstrated that JQ1 diminished C-MYC expression levels (Figure 1B) in both luminal breast cancer cell lines. As expected [17, 23, 24], the use of JQ1 did not modify the expression levels of the bromodomain protein BRD4, as also shown by western blot and qRT-PCR (Figure 1B).

Figure 1

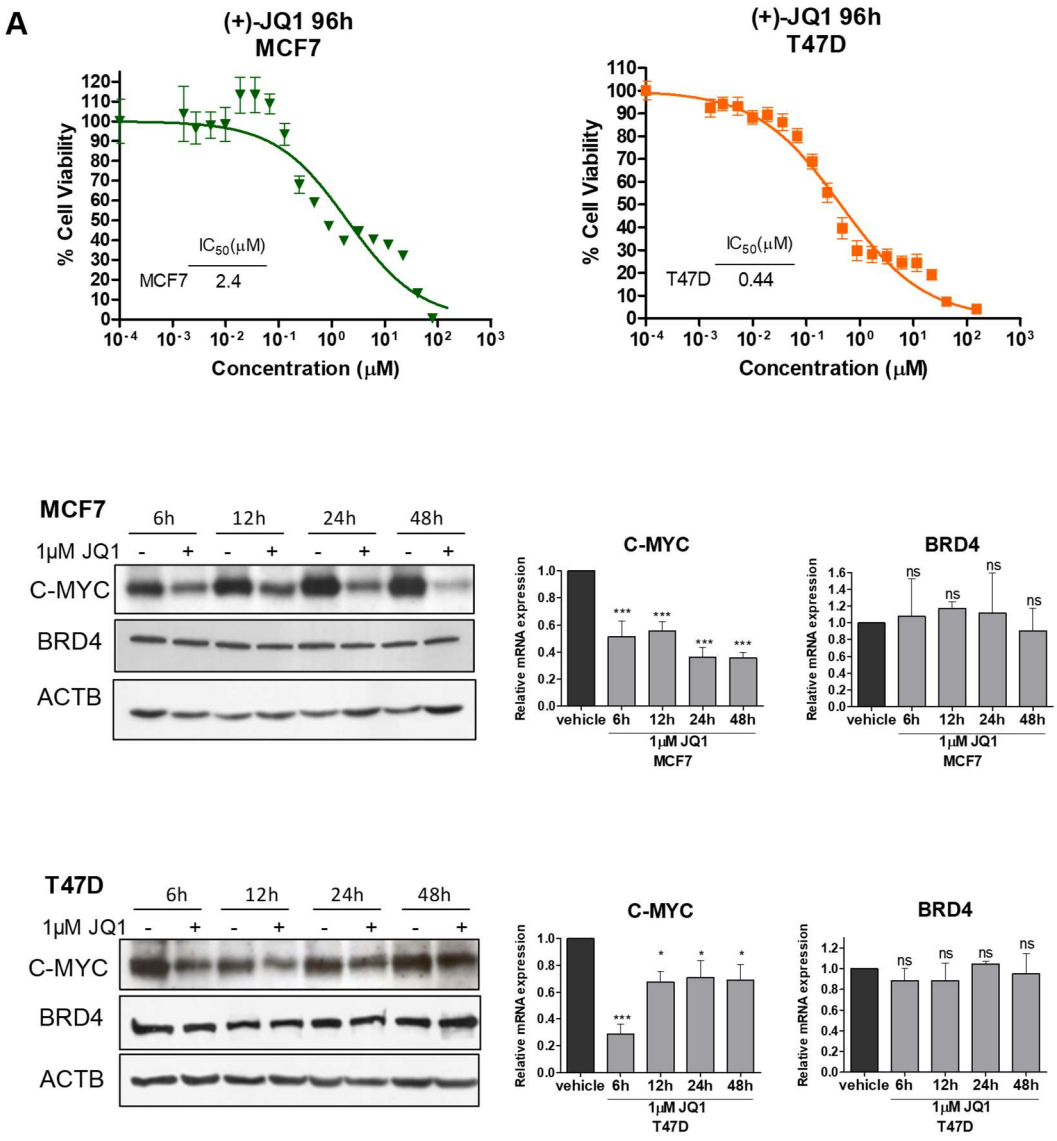

Figure 1: JQ1 treatment of human luminal breast cancer cell lines reduces cell viability and downregulates C-MYC. (A) *Effect of JQ1 on cell viability determined by the MTT assay in MCF7 and T47D cells. The corresponding half-maximal inhibitory concentration (IC50) values are shown for each cell line.* ***(B)*** *Downregulation of C-MYC upon JQ1 treatment (1 μM) at 6, 12, 24 and 48 h in breast cancer cell lines, as determined by Western blot (left) and qRT-PCR (right). BRD4 expression levels do not change. *P<0.05; ***P<0.001; ns: non-significant.*

We next sought to identify other gene targets that, in addition to the well characterized depletion of the C-MYC oncogene, could also explain the observed growth inhibitory effect of the use of the BET bromodomain inhibitor. We performed an expression microarray experiment in MCF7 and T47D cells treated with a vehicle compared with those in which we used the JQ1 compound (Figure 2A). The expression microarray data have been deposited in the Gene Expression Omnibus (GEO) repository under Accession Number GSE95287. Of the set of 36,712 unique genes included in the microarray, 1,149 (3.1%) significantly changed in a shared manner in both cell lines; 420 (36.6%) of them were upregulated and 729 (63.4%) were downregulated. The latter set constitutes the putative direct substrates of JQ1 that act by removing the BET bromodomain proteins from their regulatory regions through competition with acetylated histone residues that are usually associated with active transcription [6]. Gene functional annotation analysis for these transcripts was performed by computing gene overlapping with GSEA KEGG and GO signature collections. Among the 729 genes downregulated upon JQ1 use, we observed an overrepresentation of KEGG pathways and GO biological process terms related with pathways in cancer and regulation of cell proliferation, respectively (False Discovery Rate q-value <0.05) (Supplementary Figure 1 and Supplementary Table 1). Among the top candidate genes commonly downregulated, our attention was particularly drawn by the presence of the transcripts for the *PDZ Domain-Containing 1 (PDZK1)* and the *Breast Carcinoma-Amplified Sequence 1 (BCAS1)* genes, which encode two oncoproteins that have been linked to mammary tumorigenesis [25–28]. PDZK1 promotes estrogen-mediated growth of breast cancer cells [25, 26], whereas *BCAS1* undergoes gene amplification-associated overexpression in breast cancer [27] and has been implicated in breast cancer progression [28]. The downregulation of these transcripts upon JQ1 administration was validated by qRT-PCR in the same RNA extracts as used for microarray hybridization (Figure 2B) and when the experiment was repeated in a new batch of cells treated for different times (Figure 2C). We also assessed to what extent the effects of JQ1 are mediated by its silencing of C-MYC compared to PDZK1 and BCAS1. Upon efficient short hairpin RNA (shRNA) mediated downregulation of MYC, PDZK1 or BCAS1 in MCF7 and T47D (Supplementary Figure 2A), we observed a similar significant decrease in the cell

viability determined by the MTT assay (Supplementary Figure 2B and 2C). These data suggest that all three proteins exert a similar role as growth promoting factors in these luminal breast cancer cell lines. Importantly, the growth inhibition mediated by the use of JQ1 is higher than the one observed for the depletion of each factor (Supplementary Figure 2B and 2C). Thus, the observed growth-inhibitory effects of bromodomain inhibition in the luminal cells studied can be explained not only by the diminished expression of C-MYC, but also by a global reduction in the levels of transforming genes such as those exemplified by the PDZK1 and BCAS1 breast cancer oncogenes.

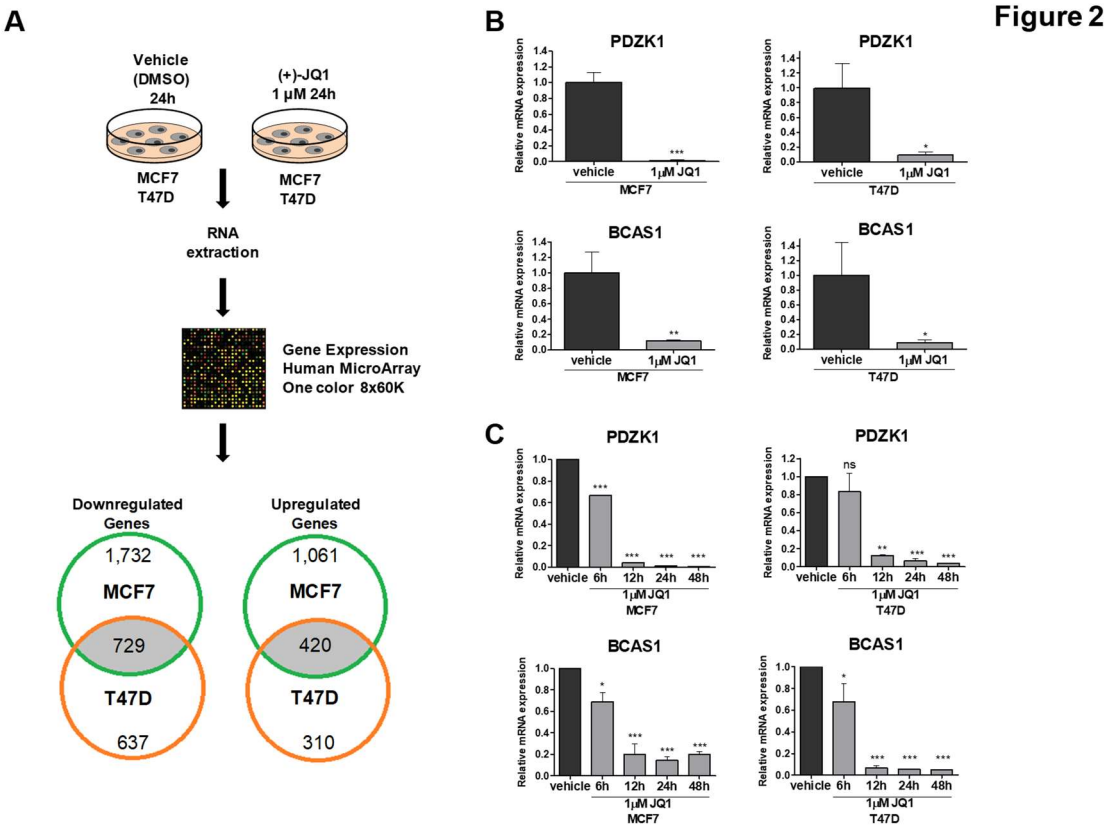

Figure 2: Expression microarray analyses identify PDZK1 and BCAS1 as breast cancer oncoproteins downregulated by JQ1 treatment in human luminal breast cancer cell lines. (A) *Flowchart of the expression microarray experiment.* ***(B)*** *qRT-PCR validation of the microarray results for PDZK1 and BCAS1.* ***(C)*** *Downregulation of PDZK1 and BCAS1, determined by qRT-PCR, upon JQ1 use at different times. *P<0.05; **P<0.01; ***P<0.001.*

Bromodomain inhibition shows antitumoral activity and retards the onset of luminal breast tumors in the MMTV-PyMT luminal breast cancer mouse model

We next transferred our experiments from the *in vitro* and cell line assays described above to the *in vivo* setting in a mouse model of luminal breast cancer. The antitumoral activity of JQ1 was evaluated using MMTV-PyMT transgenic mice that spontaneously develop multifocal luminal B breast tumors [16]. To assess the efficacy of JQ1 at inhibiting the growth of established tumors, we started the treatment when the total tumor volumes of each animal reached ~ 1,000-2,700 mm^3 (Figure 3A). We randomly selected eight MMTV-PyMT mice as the control group treated with vehicle and another eight for JQ1 treatment (25 mg/kg). Tumor volume was monitored every 2-3 days. The lack of toxicity of the drug was found under the described conditions. The use of the BET bromodomain inhibitor was significantly associated with the development of smaller breast tumors than those that occurred in the control group (Figure 3B).

Finally, once we had established the efficacy of JQ1 at inhibiting the growth of established luminal breast tumors, we considered whether the drug not only had a therapeutic, but also a preventive effect. The impact of BET bromodomain inhibition on preventing spontaneous mammary tumors that naturally arise in MMTV-PyMT mice was evaluated as described in Figure 3C. Briefly, the MMTV-PyMT mice were randomly divided into a treatment group (25 mg/kg, n=5) and a vehicle group (n=7). JQ1 was administered when mice were 4 weeks old and when no palpable or visible tumors existed. Tumor volume was monitored every 2-3 days. We observed that those MMTV-PyMT mice receiving the BET bromodomain inhibitor experienced later onset of breast cancer and developed significantly smaller tumors (Figure 3D). Most notably, the treatment with JQ1 increased the overall survival of the MMTV-PyMT mice in comparison to those that received the mock treatment (Figure 3E). These results suggest that bromodomain inhibitors may exert a protective anti-tumorigenic effect against tumorigenesis, and that it would be worthwhile exploring the benefits of using them in the context of individuals with a high-risk of developing breast cancer and other malignancies.

Figure 3

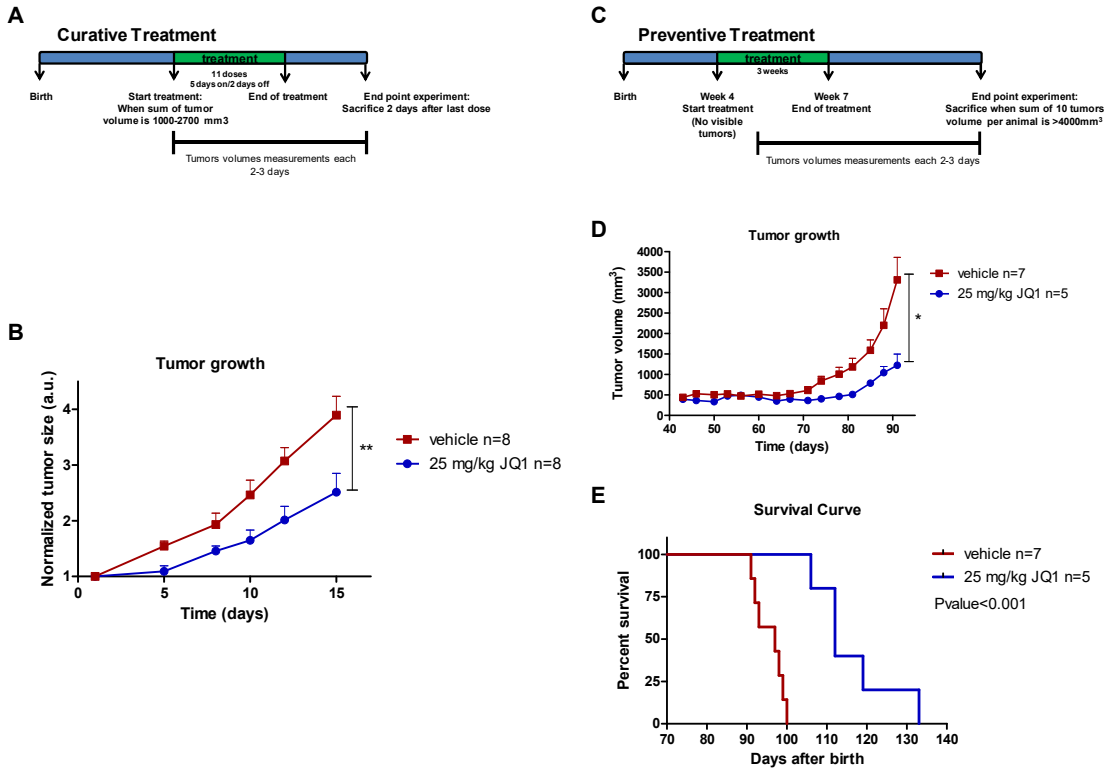

Figure 3: JQ1 treatment inhibits growth and prevents formation of luminal breast tumors in the MMTV-PyMT mouse model. ***(A)*** *Design of the "curative treatment experiment".* ***(B)*** *Tumor volume monitored over time in vehicle- and JQ1-treated MMTV-PyMT mice. **P<0.01.* ***(C)*** *Design of the "prevention treatment experiment".* ***(D)*** *Tumor volume monitored over time in vehicle- and JQ1-treated MMTV-PyMT mice. *P<0.05.* ***(E)*** *Kaplan-Meier survival curves for vehicle- and JQ1-treated MMTV-PyMT mice. Statistical differences tested with Log Rank (Mantel-Cox) test.*

DISCUSSION

Herein, we have analyzed the effect of the BET bromodomain inhibitor JQ1 in the context of luminal breast cancer in mouse models and human cells. Our results highlight how using the epigenetic drug yields remarkable antitumoral effects against luminal breast tumors in association with the downregulation of its known target C-MYC. These findings represent the first demonstration *in vivo* of the antiproliferative characteristics of this small molecule for this particular mammary cancer subtype. Importantly, the impact of JQ1 on the transcriptional landscape of the treated breast cancer cells extends beyond the depletion of C-MYC to

affect hundreds of other genes. Among the candidates that can also mediate the growth inhibitory action of the compound, we have further characterized the JQ1-associated downregulation of two important breast cancer oncogenes, *BCAS1* and *PDZK1*. Our findings suggest that the anticancer effect observed for the BET bromodomain inhibitor involves many cellular and signalling pathways and that the target genes can have tumor-type-specific patterns.

Our study also provides at least another interesting indication of the significant role of bromodomain proteins in tumorigenesis. We show that the use of the BET bromodomain inhibitor JQ1 prevents the development of breast cancer in mice. Our results demonstrate that the administration of JQ1 in the MMTV-PyMT significantly delayed the development of breast tumors and increased overall survival. Notably, the treatment of the mice with the epigenetic drug did not result in any evident adverse developmental consequences in these animals. These results, in addition to identifying a key role for bromodomain proteins in breast carcinogenesis, are encouraging as proof-of-concept that these types of compounds may be useful in cancer chemoprevention strategies. In this regard, it would be worth pre-clinically testing the efficacy of BET bromodomain inhibitors in diminishing the onset of disease in women at high-risk of developing breast cancer, such as those that are carriers of germline mutations in the tumor suppressor and DNA repair genes *BRCA1* and *BRCA2*. Interestingly, recent findings indicate that the presence of *BRCA1* mutations is associated with augmented proliferation of luminal progenitor cells [29–32] and, thus, JQ1 could be used in pre-neoplastic tissue to block these hyperactive cells in their course towards full cancer development.

Finally, it is relevant to mention that although JQ1 was the first-in-class BET bromodomain inhibitor, other drugs have been developed with similar or identical targets [6], such as I-BET151 [33], RVX-208 [34] and OTX015 [15, 35], that can work in the breast cancer models studied and that could be tested. However, all these drugs have common features that interfere with the binding of bromodomain protein to their targets in normal and cancer cells, so far with little specificity. It is in this context that the necessity might emerge for a more personalized cancer treatment using BET bromodomain inhibitors based on the genomic alterations observed in individual patients. In this regard, the presence

of point mutations, gene copy number alterations and translocations involving histone acetyltransferases, histone deacetylases and the bromodomain proteins themselves [36–38] could be important biomarkers for predicting the true therapeutic potential of these drugs.

MATERIALS AND METHODS

Cell lines

The human luminal breast cancer cell lines MCF7 and T47D used in this study were purchased from the American Type Culture Collection (ATCC). MCF7 and T47D were cultured in DMEM and RPMI, respectively. Both mediums were supplemented with 10% fetal bovine serum and the cells were grown at 37°C and 5% CO_2.

Dose-response assays

For dose-response assays, 3000 cells were seeded in 96-well plates. The optimal number of cells for each experiment was determined to ensure that each one was in growth phase at the assay endpoint. After overnight incubation, experimental medium containing increasing concentrations of JQ1 was added into each well. Cell viability assay was determined at 96 h after treatment, by the 3-(4,5-dimethyl-2-thiazolyl)-2,5-diphenyl-2H-tetrazolium bromide (MTT) assay. Briefly, MTT reagent was added and incubated for 3 h, after which the cells were lysed for 16 h with MTT lysis buffer (50% N-N dimethylformamide, 20% sodium dodecyl sulfate, 2.5% glacial acetic acid, 2.1% 1N HCl, at pH 4.7). Plates were measured at 560 nm using a spectrophotometer.

RNA isolation and quantitative PCR

Total RNA was extracted using a Maxwell® RSC simply RNA Cell Kit (Promega). Real-time PCR reactions were performed following the methods for use of SYBR Green (Applied Biosystems). GAPDH was used as an endogenous control to enable normalization. Specific primers are detailed in Supplementary Table 2.

Immunoblotting assays

Total protein from cells was extracted with Laemmli sample buffer (62.5 mM Tris-HCl pH 6.8, 25% glycerol, 2% SDS, 0.01% bromophenol blue, 5% β-mercaptoethanol). Specific antibodies against target proteins are detailed in Supplementary Table 2.

Gene expression microarray analysis

For expression array analysis, twelve RNA samples were extracted using a Maxwell® RSC simply RNA Cell Kit (Promega) and sent to the CRG Genomics Unit (Barcelona). RNA was extracted from three independent biological replicates treated with JQ1 (1 μM 24h) and three independent biological replicates treated with vehicle (DMSO). Expression data from the Agilent Gene Expression one-color chip human 8x60K microarrays were analyzed with the Bioconductor limma library v3.28 in the R v3.3.0 statistical environment. Briefly, the extracted intensities were background-corrected by applying the normexp calculation. The background-corrected $\log_2$-transformed values were quantile-normalized to make data from all arrays comparable. After filtering out control and low-level expression probes, we applied empirical Bayes statistics within the limma package for two class comparisons in order to calculate the difference in expression between conditions. Transcripts with significant differences (absolute logFC > 1 and adjusted $p < 0.05$) were considered for further analysis. The gene functional annotation analysis was performed by computing gene overlapping with GSEA KEGG and GO signature collections. We used a hypergeometric test to assess the overrepresentation of specific functions in the gene set tested. The associated hypergeometric p-value was corrected for multiple hypotheses testing according to Benjamini and Hochberg. Finally, we selected the 10 most significant over-represented terms with a False Discovery Rate q-value below 0.05.

Short hairpin interference

Two different sequence gene specific hairpin RNA molecules (shRNAs) for C-MYC, PDZK1, or BCAS1 mRNA were designed and transduced into MCF7 and T47D breast cancer cell lines. shRNA against the MSS2 yeast protein (not

present in mammals) was used as scrambled (control). shRNAs and scramble sequences can be found in Supplementary Table 2. All shRNA molecules were ligated into pLVX-shRNA2-ZsGreen plasmid from Clontech, using BamHI and EcoRI restriction enzymes. Each shRNA-encoding plasmid (10 µg) was mixed with 7.5 µg of ps-PAX2 and 2.5 µg of PMD2.G plasmid in 1 ml JetPRIME buffer and 50 µl of JetPRIME. Upon 10 min of RT incubation, the transfection mix was added dropwise on a 10 cm culture plate containing HEK293-TLV lentiviral packaging cells at 80% confluence. After 72 h, medium with high-titer lentiviral particles was 0.45 µm filtered. MCF7 and T47D target cells were cultured in virus containing medium for 24 h. As transduction efficiencies were higher than 95%, and in order to avoid the cloning bias-effect, we chose working with a pool of cells with high expression of shRNA constructs. Cell proliferation was determined by the MTT assay. A total of 1000 cells of MCF7 or 2000 cells of T47D were plated onto 96-well plates in the corresponding medium with vehicle or with 1µM JQ1. MTT was added on 8 consecutive days at a final concentration of 5 mg/mL and further procedure was done as described previously.

Mouse model

MMTV-PyMT$^+$ male mice (FVB/Nj strain) were kindly provided by Dr. Gonzalez-Suarez (IDIBELL, Barcelona, Spain). Transgenic females were obtained by breeding FVB/Nj females with PyMT$^+$ transgenic males. All mouse experiments were approved by the IDIBELL Animal Care and Use Committee and performed in accordance with the guidelines of The International Guiding Principles for Biomedical Research Involving Animals, developed by the Council for International Organizations of Medical Sciences (CIOMS).

Curative *in vivo* treatment

When the total tumor volume of each animal reached ~ 1,000-2,700 mm^3, PyMT$^+$ female mice were randomized into a JQ1 treatment group (25 mg/kg, n=8) and a vehicle (control) group (n=8). JQ1 or vehicle (1:10 DMSO:10% hydroxypropyl β cyclodextrin) was administered daily intraperitoneally for 11 doses on a 5-days-on/2-days-off dosing schedule. Tumor growth was monitored every 2-3 days by measuring tumor width (*W*) and length (*L*). Tumor volume, *V*, was then estimated

from the formula $V=\pi/6x(L \times W^2)$ and reported as the sum of all the tumor volumes for each animal and the mean and SEM of each mouse group. Two days after completion of the treatment, mice were euthanized.

Preventive *in vivo* treatment

PyMT$^+$female mice were randomly divided into a JQ1 treatment group (25 mg/kg, n=5) and a vehicle (control) group (n=7). When mice were 4 weeks old and no palpable or visible tumors were present, JQ1 or vehicle (1:10 DMSO:10% hydroxypropyl β cyclodextrin) were administered intraperitoneally daily for 3 weeks on a 5-days-on/2-days-off dosing schedule. Tumor growth was monitored every 2-3 days by measuring tumor width (*W*) and length (*L*). Tumor volume, *V*, was then estimated from the formula $V=\pi/6x(L \times W^2)$. Mice were euthanized when the total 10 tumor volume per animal was greater than 4,000 mm^3.

Statistical analysis

Real Time Quantitative PCR results were statistically analyzed with a Two samples T test, in the case where JQ1 treated and not treated samples were compared and in the case of shRNA depletion; with a Tukey Multiple comparisons of mean test, in time course experiments cases. Concerning tumor and cell growth experiments we used an AUC Vardi test with 1000 permutations. Kaplan-Meier survival curves statistical differences were tested with Log Rank (Mantel-Cox) test. P values less than 0.05 were considered significant (*P>0.05; **P>0.005; ***P>0.001; n.s = no significance).

ACKNOWLEDGMENTS

We thank the staff of the Animal Core Facility of IDIBELL for mouse care and maintenance.

SUPPLEMENTARY DATA

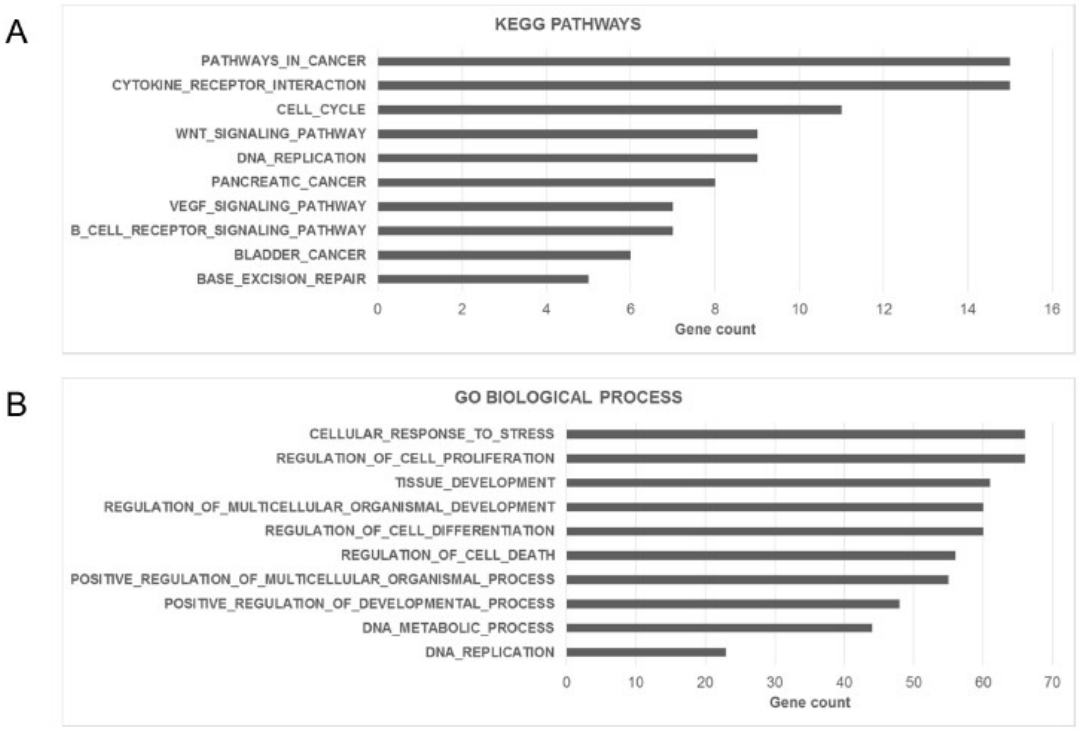

Supplementary Figure 1: Gene functional annotation analyses in both MCF7 and T47D breast cancer cell lines for the downregulated gene set upon JQ1 use. (A) *Overrepresented KEGG pathways,* ***(B)*** *GO biological process terms.*

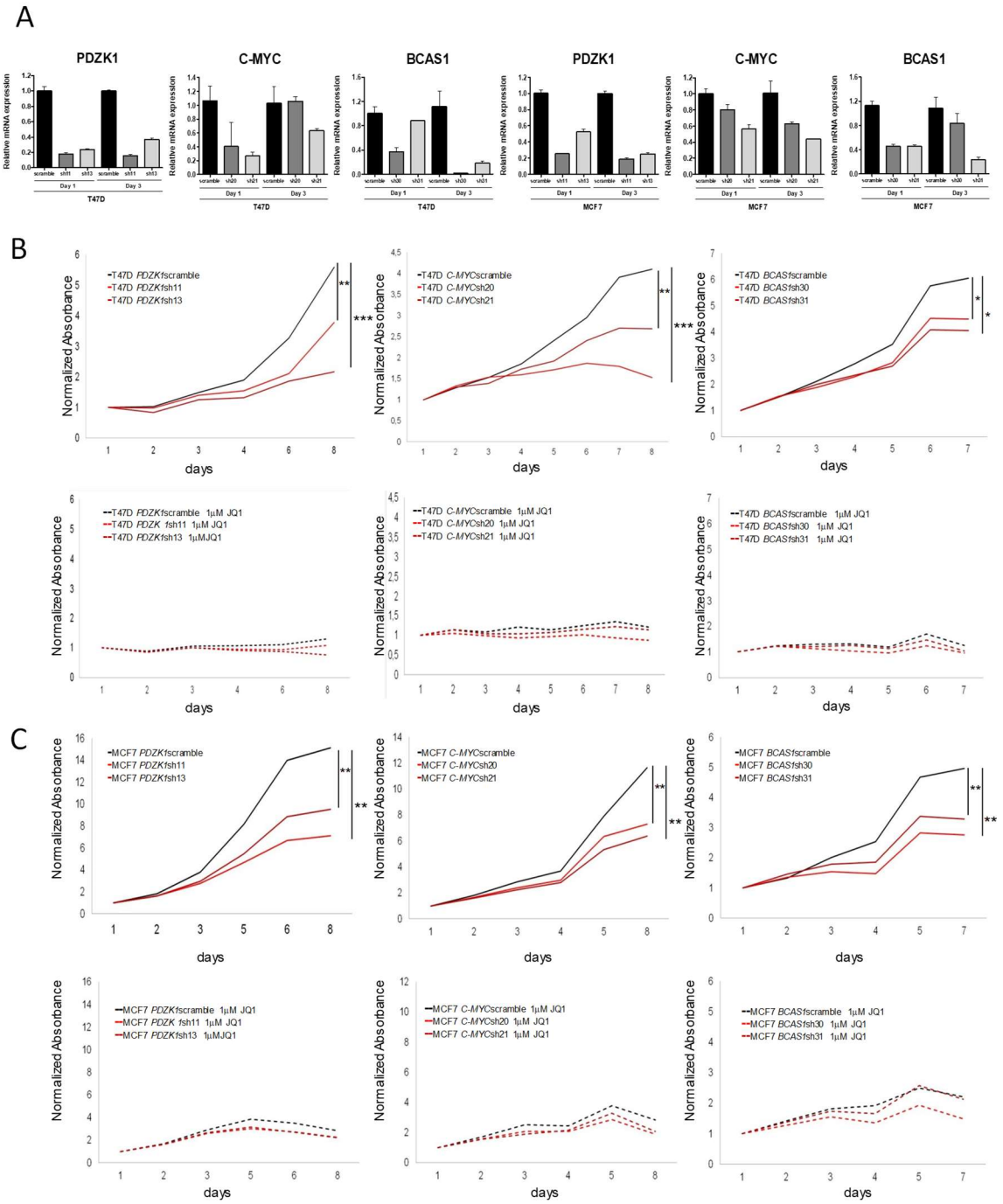

Supplementary Figure 2: Short hairpin RNA (shRNA) mediated downregulation of C-MYC, PDZK1 or BCAS1 in luminal breast cancer cell lines. (A) *Quantitative RT-PCR analyses to show the efficient depletion of the target genes upon shRNA use. Effect on cell growth determined by the MTT assay of the shRNA-mediated depletion of C-MYC, PDZK1 or BCAS1 in T47D* ***(B)*** *and MCF7* ***(C)*** *cells. Scramble shRNA and two target specific shRNAs for each gene are shown. The use of JQ1 treatment in these shRNAs transduced cells is also represented. *P<0.05; **P<0.01; ***P<0.001.*

Supplementary Table 1: *KEGG and GO analyses*

Gene set name	# Genes in gene set (K)	# Genes in overlap (k)	k/K	p-value	FDR q-value
KEGG_DNA_REPLICATION	36	9	0.25	3.13E-10	5.82E-08
KEGG_CELL_CYCLE	128	11	0.0859	4.19E-07	3.90E-05
KEGG_CYTOKINE_RECEPTOR_INTERACTION	267	15	0.0562	9.09E-07	5.63E-05
KEGG_PANCREATIC_CANCER	70	8	0.1143	1.87E-06	8.68E-05
KEGG_BLADDER_CANCER	42	6	0.1429	9.98E-06	3.44E-04
KEGG_PATHWAYS_IN_CANCER	328	15	0.0457	1.11E-05	3.44E-04
KEGG_B_CELL_RECEPTOR_SIGNALING_ PATHWAY	75	7	0.0933	3.18E-05	8.05E-04
KEGG_VEGF_SIGNALING_PATHWAY	76	7	0.0921	3.46E-05	8.05E-04
KEGG_BASE_EXCISION_REPAIR	35	5	0.1429	5.62E-05	1.16E-03
KEGG_WNT_SIGNALING_PATHWAY	151	9	0.0596	8.77E-05	1.62E-03
GO_REGULATION_OF_CELL_PROLIFERATION	1496	66	0.0441	6.90E-20	3.06E-16
GO_CELLULAR_RESPONSE_TO_STRESS	1565	66	0.0422	6.93E-19	1.54E-15
GO_DNA_METABOLIC_PROCESS	758	44	0.058	8.05E-18	1.19E-14
GO_TISSUE_DEVELOPMENT	1518	61	0.0402	1.55E-16	1.72E-13
GO_REGULATION_OF_CELL_DIFFERENTIATION	1492	60	0.0402	2.71E-16	2.40E-13
GO_DNA_REPLICATION	208	23	0.1106	9.84E-16	7.27E-13
GO_POSITIVE_REGULATION_OF_ MULTICELLULAR_ORGANISMAL_PROCESS	1395	55	0.0394	1.17E-14	7.43E-12
GO_REGULATION_OF_CELL_DEATH	1472	56	0.038	2.90E-14	1.61E-11
GO_REGULATION_OF_MULTICELLULAR_ ORGANISMAL_DEVELOPMENT	1672	60	0.0359	4.13E-14	2.04E-11
GO_POSITIVE_REGULATION_OF_ DEVELOPMENTAL_PROCESS	1142	48	0.042	6.27E-14	2.78E-11

Top, Overrepresented KEGG pathways corresponding to the significant downregulated genes in MCF7 and T47D cell lines. The table shows the genes overlapping each gene set and the associated hypergeometric test's p-value. *Below*, Overrepresented GO biological process terms corresponding to the significant downregulated genes in MCF7 and T47D cell lines. The table shows the genes overlapping each gene set and the associated hypergeometric test's p-value.

Supplementary Table 2. *Primers for qRT-PCR, antibodies used in the western blot and shRNAs sequences.*

Primers for qRT-PCR				
BRD4_Hs_qPCR_F	CAACAAGCCTGGAGATGACA			
BRD4_Hs_qPCR_R	GGAGGAGTCGATGCTTGAGT			
MYC_Hs_qPCR_F	CCGCTTCTCTGAAAGGCTCT			
MYC_Hs_qPCR_R	AAGCTAACGTTGAGGGGCAT			
PDZK1_Hs_qPCR_F	AAACTCTGCAGGCTGGCTAA			
PDZK1_Hs_qPCR_R	TCCACCACCTTCTCATAGGG			
BCAS1_Hs_qPCR_F	CCAGAAGGACTGGAGACTGC			
BCAS1_Hs_qPCR_R	CTTGGGTCTCCTGGGATGTA			
GAPDH_Hs_qPCR_F	GAAGGTGAAGGTCGGAGTCA			
GAPDH_Hs_qPCR_R	TGGACTTCACGACGTACTCA			
Antibodies Name	**Reference**	**Company**	**Application**	**Dilution**
Anti-BRD4	ab128874	Abcam	WB	1:1000
C-MYC (D84C12)	5605	Cell signaling	WB	1:1000
Actin-beta HRP	A3854	Sigma	WB	1:20000
Lentiviral shRNAs				
Scramble_F	gatccGCGCAGAACAAATTCGTCCATTCAAGAGATGGACGAATTT GTTCTGCGTTTTTTACGCGTg			
Scramble_R	aattcACGCGTAAAAAACGCAGAACAAATTCGTCCATCTCTTGAAT GGACGAATTTGTTCTGCGCg			
PDZK1_sh11_F	gatccGCCTTCAAGATGGAGACAGATTCAAGAGATCTGTCTCCAT CTTGAAGGTTTTTTACGCGTg			
PDZK1_sh11_R	aattcACGCGTAAAAAACCTTCAAGATGGAGACAGATCTCTTGAAT CTGTCTCCATCTTGAAGGCg			
PDZK1_sh13_F	gatccGGTGGACTTGAAAGAGTTGTTCAAGAGACAACTCTTTCAA GTCCACCTTTTTTACGCGTg			
PDZK1_sh13_R	aattcACGCGTAAAAAAGGTGGACTTGAAAGAGTTGTCTCTTGAAC AACTCTTTCAAGTCCACCg			
MYC_sh20_F	gatccGCACGAAACTTTGCCCATAGTTCAAGAGACTATGGGCAAA GTTTCGTGTTTTTTACGCGTg			
MYC_sh20_R	aattcACGCGTAAAAAACACGAAACTTTGCCCATAGTCTCTTGAAC TATGGGCAAAGTTTCGTGCg			
MYC_sh21_F	gatccGCTTCACCAACAGGAACTATTCAAGAGATAGTTCCTGTTG GTGAAGCTTTTTTACGCGTg			
MYC_sh21_R	aattcACGCGTAAAAAAGCTTCACCAACAGGAACTATCTCTTGAAT AGTTCCTGTTGGTGAAGCg			
BCAS1_sh30_F	gatccACCAGAAGCAGAGACTTACTTCAAGAGAGTAAGTCTCTGC TTCTGGTTTTTTTACGCGTg			
BCAS1_sh30_R	aattcACGCGTAAAAAAACCAGAAGCAGAGACTTACTCTCTTGAAG TAAGTCTCTGCTTCTGGTg			
BCAS1_sh31_F	gatccGCACACAGTTCAGCACTTAGTTCAAGAGACTAAGTGCTGA ACTGTGTGTTTTTTACGCGTg			
BCAS1_sh31_R	aattcACGCGTAAAAAACACACAGTTCAGCACTTAGTCTCTTGAAC TAAGTGCTGAACTGTGTGCg			

REFERENCES

1. La Vecchia C, Bosetti C, Lucchini F, Bertuccio P, Negri E, Boyle P, Levi F. Cancer mortality in Europe, 2000-2004, and an overview of trends since 1975. Ann Oncol. 2010; 21:1323-1360.

2. Perou CM, Sørlie T, Eisen MB, van de Rijn M, Jeffrey SS, Rees CA, Pollack JR, Ross DT, Johnsen H, Akslen LA, Fluge O, Pergamenschikov A, Williams C, et al. Molecular portraits of human breast tumours. Nature. 2000; 406:747-752.

3. Cancer Genome Atlas Network. Comprehensive molecular portraits of human breast tumours. Nature 2012; 490:61-70.

4. Prat A, Pineda E, Adamo B, Galván P, Fernández A, Gaba L, Díez M, Viladot M, Arance A, Muñoz M. Clinical implications of the intrinsic molecular subtypes of breast cancer. Breast. 2015; 24:S26-S35.

5. Simó-Riudalbas L, Esteller M. Targeting the histone orthography of cancer: drugs for writers, erasers and readers. Br J Pharmacol. 2015; 172:2716-2732.

6. Pérez-Salvia M, Esteller M. Bromodomain inhibitors and cancer therapy: from structures to applications. Epigenetics. 2017; 12:323-339.

7. Fraga MF, Ballestar E, Villar-Garea A, Boix-Chornet M, Espada J, Schotta G, Bonaldi T, Haydon C, Ropero S, Petrie K, Iyer NG, Pérez-Rosado A, Calvo E, et al. Loss of acetylation at Lys16 and trimethylation at Lys20 of histone H4 is a common hallmark of human cancer. Nat Genet. 2005; 37:391-400.

8. Shi J, Wang Y, Zeng L, Wu Y, Deng J, Zhang Q, Lin Y, Li J, Kang T, Tao M, Rusinova E, Zhang G, Wang C, et al. Disrupting the interaction of BRD4 with diacetylated Twist suppresses tumorigenesis in basal-like breast cancer. Cancer Cell. 2014; 25:210-225.

9. Borbely G, Haldosen LA, Dahlman-Wright K, Zhao C. Induction of USP17 by combining BET and HDAC inhibitors in breast cancer cells. Oncotarget. 2015; 6:33623- 33635. doi: 10.18632/oncotarget.5601.

10. Shu S, Lin CY, He HH, Witwicki RM, Tabassum DP, Roberts JM, Janiszewska M, Huh SJ, Liang Y, Ryan J, Doherty E, Mohammed H, Guo H, et al. Response and resistance to BET bromodomain inhibitors in triple-negative breast cancer. Nature. 2016; 529:413-417.

11. da Motta LL, Ledaki I, Purshouse K, Haider S, De Bastiani MA, Baban D, Morotti M, Steers G, Wigfield S, Bridges E, Li JL, Knapp S, Ebner D, et al. The BET inhibitor JQ1 selectively impairs tumour response to hypoxia and downregulates CA9 and angiogenesis in triple negative breast cancer. Oncogene. 2017; 36:122-132.

12. Pérez-Peña J, Serrano-Heras G, Montero JC, Corrales- Sánchez V, Pandiella A, Ocaña A. In silico analysis guides selection of BET inhibitors for triple-negative breast cancer treatment. Mol Cancer Ther. 2016; 15:1823-1833.

13. Andrieu G, Tran AH, Strissel KJ, Denis GV. BRD4 regulates breast cancer dissemination through Jagged1/ Notch1 signaling. Cancer Res. 2016; 76:6555-6567.

14. Sahni JM, Gayle SS, Bonk KL, Vite LC, Yori JL, Webb B, Ramos EK, Seachrist DD, Landis MD, Chang JC, Bradner JE, Keri RA. Bromodomain and extraterminal protein inhibition blocks growth of triple-negative breast cancers through the suppression of aurora kinases. J Biol Chem. 2016; 291:23756-23768.

15. Vázquez R, Riveiro ME, Astorgues-Xerri L, Odore E, Rezai K, Erba E, Panini N, Rinaldi A, Kwee I, Beltrame L, Bekradda M, Cvitkovic E, Bertoni F, et al. The bromodomain inhibitor OTX015 (MK-8628) exerts anti-tumor activity in triple-negative breast cancer models as single agent and in combination with everolimus. Oncotarget. 2017; 8:7598-7613. doi: 10.18632/ oncotarget.13814.

16. Guy CT, Cardiff RD, Muller WJ. Induction of mammary tumors by expression of polyomavirus middle T oncogene: a transgenic mouse model for metastatic disease. Mol Cell Biol. 1992; 12:954-961.

17. Filippakopoulos P, Qi J, Picaud S, Shen Y, Smith WB, Fedorov O, Morse EM, Keates T, Hickman TT, Felletar I, Philpott M, Munro S, McKeown MR, et al. Selective inhibition of BET bromodomains. Nature. 2010; 468:1067-1073.

18. Kabos P, Haughian JM, Wang X, Dye WW, Finlayson C, Elias A, Horwitz KB, Sartorius CA. Cytokeratin 5 positive cells represent a steroid receptor negative and therapy resistant subpopulation in luminal breast cancers. Breast Cancer Res Treat. 2011; 128:45-55.

19. Iwanaga R, Wang CA, Micalizzi DS, Harrell JC, Jedlicka P, Sartorius CA, Kabos P, Farabaugh SM, Bradford AP, Ford HL. Expression of Six1 in luminal breast cancers predicts poor prognosis and promotes increases in tumor initiating cells by activation of extracellular signal-regulated kinase and transforming growth factor-beta signaling pathways. Breast Cancer Res. 2012; 14:R100.

20. Zubia A, Ropero S, Otaegui D, Ballestar E, Fraga MF, Boix-Chornet M, Berdasco M, Martinez A, Coll-Mulet L, Gil J, Cossío FP, Esteller M. Identification of (1H)-pyrroles as histone deacetylase inhibitors with antitumoral activity. Oncogene. 2009; 28:1477-1484.

21. Carpinelli P, Moll J. Aurora kinases and their inhibitors: more than one target and one drug. Adv Exp Med Biol. 2008; 610:54-73.

22. Huertas D, Soler M, Moreto J, Villanueva A, Martinez A, Vidal A, Charlton M, Moffat D, Patel S, McDermott J, Owen J, Brotherton D, Krige D, et al. Antitumor activity of a small-molecule inhibitor of the histone kinase Haspin. Oncogene. 2012; 31:1408-1418.

23. Delmore JE, Issa GC, Lemieux ME, Rahl PB, Shi J, Jacobs HM, Kastritis E, Gilpatrick T, Paranal RM, Qi J, Chesi M, Schinzel AC, McKeown MR, et

al. BET bromodomain inhibition as a therapeutic strategy to target c-Myc. Cell. 2011; 146:904-917.

24. Mertz JA, Conery AR, Bryant BM, Sandy P, Balasubramanian S, Mele DA, Bergeron L, Sims RJ 3rd. Targeting MYC dependence in cancer by inhibiting BET bromodomains. Proc Natl Acad Sci U S A. 2011; 108:16669-16674.

25. Dunbier AK, Anderson H, Ghazoui Z, Folkerd EJ, A'hern R, Crowder RJ, Hoog J, Smith IE, Osin P, Nerurkar A, Parker JS, Perou CM, Ellis MJ, et al. Relationship between plasma estradiol levels and estrogen-responsive gene expression in estrogen receptor-positive breast cancer in postmenopausal women. J Clin Oncol. 2010; 28:1161-1167.

26. Kim H, Abd Elmageed ZY, Ju J, Naura AS, Abdel-Mageed AB, Varughese S, Paul D, Alahari S, Catling A, Kim JG, Boulares AH. PDZK1 is a novel factor in breast cancer that is indirectly regulated by estrogen through IGF-1R and promotes estrogen-mediated growth. Mol Med. 2013; 19:253-262.

27. Collins C, Rommens JM, Kowbel D, Godfrey T, Tanner M, Hwang SI, Polikoff D, Nonet G, Cochran J, Myambo K, Jay KE, Froula J, Cloutier T, et al. Positional cloning of ZNF217 and NABC1: genes amplified at 20q13.2 and overexpressed in breast carcinoma. Proc Natl Acad Sci U S A. 1998; 95:8703-8708.

28. Fenne IS, Helland T, Flågeng MH, Dankel SN, Mellgren G, Sagen JV. Downregulation of steroid receptor coactivator-2 modulates estrogen-responsive genes and stimulates proliferation of mcf-7 breast cancer cells. PLoS One. 2013; 8:e70096.

29. Lim E, Vaillant F, Wu D, Forrest NC, Pal B, Hart AH, Asselin-Labat ML, Gyorki DE, Ward T, Partanen A, Feleppa F, Huschtscha LI, Thorne HJ, et al. Aberrant luminal progenitors as the candidate target population for basal tumor development in BRCA1 mutation carriers. Nat Med. 2009; 15:907-913.

30. Molyneux G, Geyer FC, Magnay FA, McCarthy A, Kendrick H, Natrajan R, Mackay A, Grigoriadis A, Tutt A, Ashworth A, Reis-Filho JS, Smalley MJ. BRCA1 basal-like breast cancers originate from luminal epithelial progenitors and not from basal stem cells. Cell Stem Cell. 2010; 7:403-417.

31. Proia TA, Keller PJ, Gupta PB, Klebba I, Jones AD, Sedic M, Gilmore H, Tung N, Naber SP, Schnitt S, Lander ES, Kuperwasser C. Genetic predisposition directs breast cancer phenotype by dictating progenitor cell fate. Cell Stem Cell. 2011; 8:149-163.

32. Nolan E, Lindeman GJ, Visvader JE. Out-RANKing BRCA1 in mutation carriers. Cancer Res. 2017; 77:595-600.

33. Dawson MA, Prinjha RK, Dittmann A, Giotopoulos G, Bantscheff M, Chan WI, Robson SC, Chung CW, Hopf C, Savitski MM, Huthmacher C, Gudgin E, Lugo D, et al. Inhibition of BET recruitment to chromatin as an effective treatment for MLL-fusion leukaemia. Nature. 2011; 478:529-533.

34. Picaud S, Wells C, Felletar I, Brotherton D, Martin S, Savitsky P, Diez-Dacal B, Philpott M, Bountra C, Lingard H, Fedorov O, Müller S, Brennan PE, et al. RVX-208, an inhibitor of BET transcriptional regulators with selectivity for the second bromodomain. Proc Natl Acad Sci U S A. 2013; 110:19754-19759.

35. Boi M, Gaudio E, Bonetti P, Kwee I, Bernasconi E, Tarantelli C, Rinaldi A, Testoni M, Cascione L, Ponzoni M, Mensah AA, Stathis A, Stussi G, et al. The BET bromodomain inhibitor OTX015 affects pathogenetic pathways in preclinical B-cell tumor models and synergizes with targeted drugs. Clin Cancer Res. 2015; 21:1628-1638.

36. Simó-Riudalbas L, Esteller M. Cancer genomics identifies disrupted epigenetic genes. Hum Genet. 2014; 133:713-725.

37. Haery L, Thompson RC, Gilmore TD. Histone acetyltransferases and histone deacetylases in B- and T-cell development, physiology and malignancy. GenesCancer. 2015; 6:184-213. doi: 10.18632/genesandcancer.65.

38. Simó-Riudalbas L, Pérez-Salvia M, Setien F, Villanueva A, Moutinho C, Martínez-Cardús A, Moran S, Berdasco M, Gomez A, Vidal E, Soler M, Heyn H, Vaquero A, et al. KAT6B is a tumor suppressor histone H3 lysine 23 acetyltransferase undergoing genomic loss in small cell lung cancer. Cancer Res. 2015; 75:3936-3945.

Study III

"In vitro and in vivo activity of a new small-molecule inhibitor of HDAC6 in mantle cell lymphoma"

Montserrat Perez-Salvia[1], Eneko Aldaba[2], Yosu Vara[2], Myriam Fabre[3], Cristina Ferrer[3], Carme Masdeu[4], Aizpea Zubia[5], Eider San Sebastian[5], Dorleta Otaegui[6], Pere Llinàs-Arias[1], Margalida Rosselló-Tortella[1], Maria Berdasco[1], Catia Moutinho[1], Fernando Setien[1], Alberto Villanueva[7], Eva González-Barca[8], Josep Muncunill[9], José-Tomás Navarro[9], Miguel A. Piris[10], Fernando P. Cossio[5] and Manel Esteller[1,11,12,13]

[1]Cancer Epigenetics and Biology Program (PEBC), Bellvitge Biomedical Research Institute (IDIBELL) L'Hospitalet, Barcelona, Catalonia; [2]Quimatryx, San Sebastian; [3]Oncomatryx, Arteaga Auzoa, 43, Derio; [4]Department of Organic Chemistry I, Universidad del País Vasco/Euskal Herriko Unibertsitatea (UPV/EHU), San Sebastián; [5]Department of Organic Chemistry I, Centro de Innovación en Química Avanzada (ORFEO-CINQA), Universidad del País Vasco/Euskal Herriko Unibertsitatea (UPV/EHU), Donostia International Physics Center (DIPC), San Sebastián; [6]Mass Spectrometry Platform, CIC biomaGUNE, San Sebastian; [7]Laboratory of Translational Research, Catalan Institute of Oncology (ICO), IDIBELL L'Hospitalet, Barcelona, Catalonia; [8]Department of Hematology, ICO-Hospital Duran i Reynals, IDIBELL, University of Barcelona, L'Hospitalet, Barcelona, Catalonia; [9]Department of Hematology, ICO-Hospital Universitari Germans Trias i Pujol, Josep Carreras Leukaemia Research Institute, Universitat Autònoma de Barcelona, Badalona, Catalonia; [10]Pathology Service, Fundación Jiménez Díaz, Madrid; [11]Centro de Investigacion Biomedica en Red Cancer (CIBERONC), Madrid; [12]Physiological Sciences Department, School of Medicine and Health Sciences, University of Barcelona (UB), L'Hospitalet, Catalonia and [13]Institucio Catalana de Recerca i Estudis Avançats (ICREA), Barcelona, Catalonia, Spain

Journal: Haematologica. 2018 Nov;103(11):e537-e540.
doi: 10.3324/haematol.2018.189241.

INTRODUCTION

Cancer origin and development is associated not only with genetic alterations, but also with the disturbance of epigenetic profiles [1]. In this regard, the tumoral epigenome is characterized by both specific and general shifts in the DNA methylation and histone-modification landscapes [1]. However, in contrast to genetic disruption, the effect of epigenetic modifications or marks may potentially be reversed by the use of drugs that target enzymes involved in adding, removing or signaling DNA methylation and histone modifications [1]. This basic knowledge has been adopted into clinical practice, and inhibitors of histone deacetylases and DNA demethylating agents have been approved for use in the therapy of hematologic malignancies, such as cutaneous T-cell lymphoma and myelodysplastic syndrome, respectively [2]. Other promising epigenetic drugs include inhibitors of histone methyltransferases [2], histone demethylases [2], histone kinases [3], and bromodomain proteins that interfere with the 'reading'of acetylated histone residues [4,5].

Histone deacetylase 6 (HDAC6) is a protein modifier that is an increasingly attractive pharmacological target. It is a member of class IIb of the histone deacetylase family, together with HDAC10 [6]. Unlike most HDACs, HDAC6 is expressed primarily in the cytoplasm and its deacetylase activity involves mainly non-histone substrates, such as the cytoskeletal protein α-tubulin and the heat shock protein Hsp90. In this way, it plays an important role in microtubule dynamics and chaperone signalling [6]. HDAC6 is involved in various human diseases, and in cancer promotes tumor initiation, development, and metastasis, having been shown to be over-expressed in various tumor types. Interestingly, the observation that the HDAC6 knock-out mouse is not lethal [7] in contrast to those undergoing complete loss of class I, II and III HDACs, suggests that specific HDAC6 inhibitors may be better tolerated than pan-HDAC inhibitors or drugs that target the other HDAC classes. In this regard, the compounds tubacin, its derivative tubastatin A and ACY-1215 (Ricolinostat) are selective HDAC6 inhibitors [8]. The latter agent is undergoing clinical trials as a single agent or in combination for the treatment of multiple myeloma and other tumors *(clinicaltrials.gov identifiers: 01997840, 01323751, 02189343, 01583283).* Given the interest in HDAC6 inhibition, we decided to design, synthesize, and test the

activity of new small-molecule inhibitors of HDAC6 that could have a potential antitumor impact.

RESULTS AND DISCUSION

Almost all HDAC inhibitors, including those of HDAC6, share a typical structure comprising three primary regions: i) a zinc-chelating group that binds the zinc ion present at the active site, preventing activation of the enzyme (typically, a hydroxamic acid in HDAC6 inhibitors); ii) a hydrophobic linker region that mimics the 1,4-butylene alkyl chain of the lysine residue present in the natural substrates of HDACs; and iii) a filling-cap group, usually an aromatic or heteroaromatic ring, that binds to the substrate-binding region of the enzyme and fills the entrance to the hydrophobic channel. Variations in one or more of these regions may result in greater selectivity to one isoform than the others. Thus, the HDAC6 hydrophobic channel appears wider than that of other HDAC subtypes, suggesting that replacement of the traditional alkyl chain linker with bulkier and shorter aromatic moieties might enhance HDAC6 selectivity. Taking into account these HDAC6 inhibitor structures, the structural differences between HDAC6 and other HDAC isoforms (and also the structural information of our previously developed HDAC inhibitors [9]), a new potential HDAC6 selective inhibitor was designed and synthesized: QTX125 [3-(3-furyl)-N-{4-[(hydroxyamino)carbonyl] benzyl-5-(4-hydroxyphenyl)-1H-pyrrole-2-carboxamide] (Figure 1A). QTX125 was synthesized by means of a 7-step synthetic procedure, starting with an aldol condensation reaction of 4-hydroxyacetophenone with 3-furaldehyde to obtain the corresponding α,β-unsaturated ketone. This ketone was then treated with ethyl nitroacetate and triethylamine, the mixture obtained being oxidized by means of the Nef reaction with sodium ethoxide to yield the corresponding γ-ketoester. Through a cyclization reaction of this ester in the presence of ammonium salts [10], good yields of the ethyl 3-(furan-3-yl)-5-(4-hydroxyphenyl)-1H-pyrrole-2-carboxylate were obtained. Deprotection of the methyl ester group of the pyrrole, and coupling with the methyl 4-(aminomethyl)benzoate yielded the corresponding amide. Further elaboration produced the final hydroxamic acid. It is noteworthy that, as designed, the synthesis is well-suited to kilogram-scale production.

The selectivity of QTX125 for inhibiting HDAC6 function in comparison with all the other HDACs was measured by determining the *in vitro* enzymatic activity of 50 μM of each acetylated AMC-labeled peptide substrate enzyme (HDAC1, HDAC2, HDAC3, HDAC4, HDAC5, HDAC6, HDAC7, HDAC8, HDAC9, HDAC10 and HDAC11) *(Online Supplementary Appendix).* QTX125 demonstrated an exceptional specificity for inhibiting HDAC6 enzymatic activity (Figure 1A). To test the capacity of QTX125 as an antitumor agent, we first determined the 72-hour IC50 values using the MTS [3-(4,5-dimethylthiazol-2-yl)-5-(3-carboxymethoxyphenyl)-2-(4- sulfophenyl)-2H-tetrazolium] assay in a panel of 48 human cancer cell lines, including solid tumors (breast, prostate, kidney, colorectal, lung, pancreas, liver, osteosarcoma, glioblastoma, fibrosarcoma, melanoma, and ovarian cancer), and hematologic malignancies [chronic myelogenous leukemia, multiple myeloma, Hodgkin lymphoma, Burkitt cell lymphoma, follicular lymphoma, and mantle cell lymphoma (MCL)] *(Online Supplementary Appendix).* We observed that QTX125 had the strongest growth-inhibitory effect in Burkitt cell lymphoma, follicular lymphoma, and MCL (Figure 1B).

Mantle cell lymphoma therapy constitutes an unmet medical need because there is no single accepted treatment approach for the disease [11]. R-CHOP (rituximab, cyclophosphamide, doxorubicin, vincristine, prednisone) is a common first-line therapeutic approach, but is of limited duration [12]. Due to the antitumoral effect of QTX125 in MCL cell lines and its specificity in blocking HDAC6 activity that we observed here, we decided to characterize in detail QTX125 in MCL, further encouraged by the finding that HDAC6 activity is essential for MCL growth [13]. The growth-inhibitory effect of QTX125 at nanomolar levels in the aforementioned MCL cell lines was confirmed by the 3-(4,5-dimethylthiazol-2-yl)-2,5- diphenyltetrazolium bromide (MTT) assay, and the cell count of alive cells by trypan blue staining and by flow cytometry of AnnexinV/PI *(Online Supplementary Figure S1).*

A further analysis of the MCL cell lines MINO, REC-1, IRM-2 and HBL-2 also showed that the use of QTX125 induced dose-dependent hyperacetylation of α-tubulin (Figure 1C), the best known target of HDAC6, thus providing further validation that the drug targets this particular enzyme. Trichostatin A was used

as a general inhibitor for HDAC classes I, IIA, IIB (including HDAC6) and IV, whereas sodium butyrate was used as an HDAC inhibitor that does not affect HDAC6 (Figure 1C) [14]. The three available HDAC6 inhibitors (tubastatin A, tubacin, and ACY1215) were also used as specific positive controls for HDAC6-inhibition mediated hyperacetylation of α-tubulin (Figure 1C). Importantly, QTX125 was able to induce α-tubulin acetylation even at 10 nM concentration whereas the other HDAC6 inhibitors did not (Figure 1C). In our MCL cell lines, and with QTX125, we did not observe any increase in CD20 expression as occurs with other HDAC6 inhibitors in Burkitt and diffuse large B-cell lymphoma cell lines [15]*(Online Supplementary Figure S2).* Strikingly, QTX125 was the most powerful inhibitor of growth in the MCL cell lines compared with the other three HDAC6 inhibitors reported (Figure 1C).

Figure 1

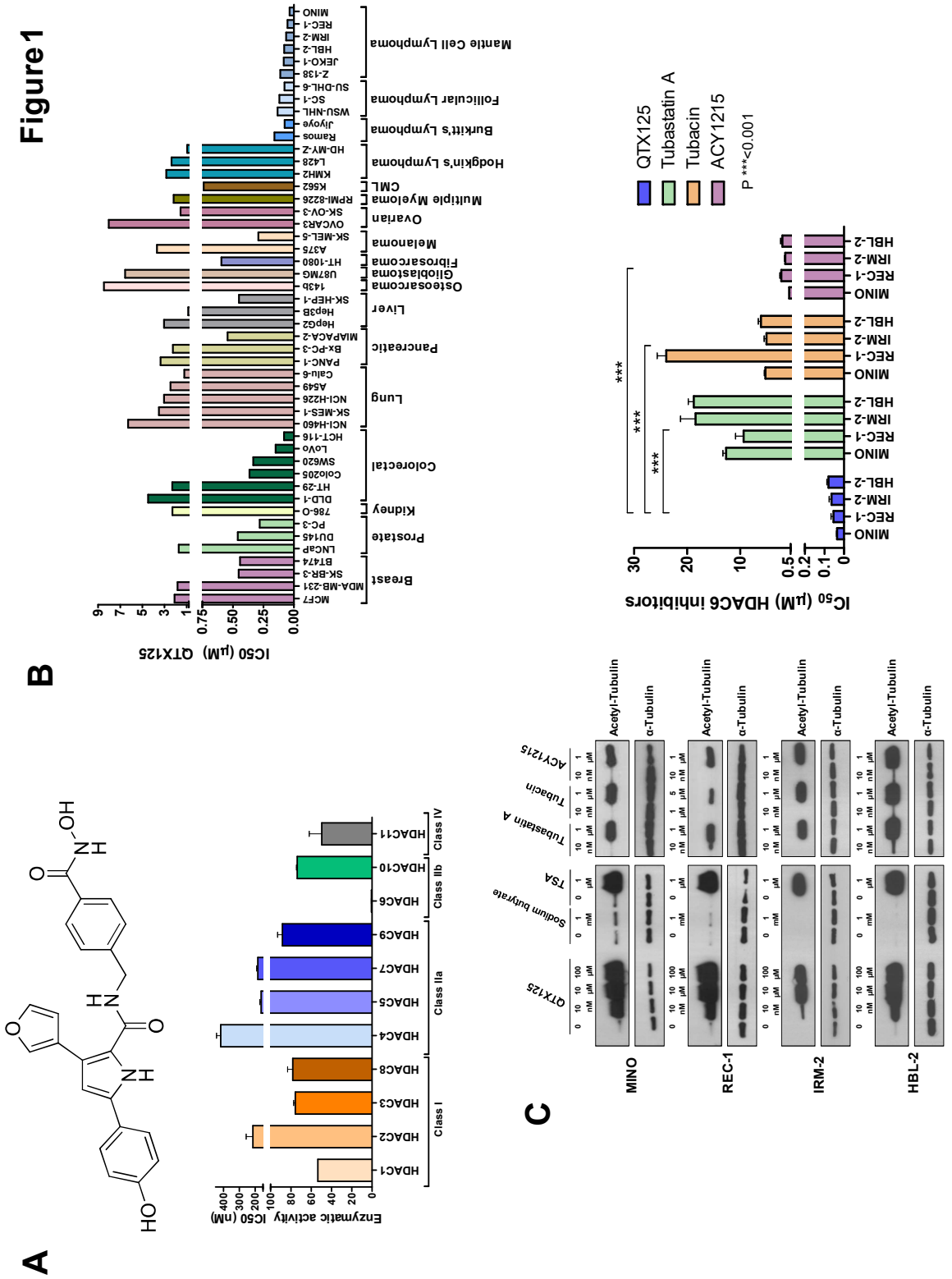
A
B
C
QTX125
Tubastatin A
Tubacin
ACY1215
P ***<0.001
IC50 (μM) HDAC6 inhibitors
Enzymatic activity IC50 (nM)
Class I
Class IIa
Class IIb
Class IV
Acetyl-Tubulin
α-Tubulin
MINO
REC-1
IRM-2
HBL-2
Sodium butyrate
TSA

Figure 1. Chemical structure and HDAC specificity of QTX125 and its effect on α-tubulin acetylation and cell growth. (A) *(Top) Chemical structure of QTX125. (Below) In vitro enzymatic activity of 11 HDACs upon QTX125 use.* ***(B)*** *Growth-inhibitory effect of QTX125 in cancer cell lines determined by the MTS assay.* ***(C)*** *(Left) Western-blot assays in MINO, REC-1, IRM-2 and HBL-2 cells show the induction of α-tubulin hyperacetylation upon QTX125 administration. Sodium butyrate is shown as an HDAC inhibitor that does not affect HDAC6 (negative control). TSA is shown as an HDAC inhibitor that affects all HDAC classes, including HDAC6 (positive control). The effect of the three available specific HDAC6 inhibitors (tubastatin A, tubacin, and ACY1215) is also shown. Total α-tubulin is used as a loading control. (Right) Growth-inhibitory effect of QTX125 in the mantle cell lymphoma cell lines determined by the MTS assay in comparison to the other, previously described HDAC6 inhibitors. CML: chronic myelogenous leukemia.*

We also showed that the observed inhibition of cell proliferation upon QTX125 administration was associated with the induction of subsequent apoptosis demonstrated by annexin V/propidium iodide double staining (Figure 2A) and the cleavage of caspase-9, caspase-8, caspase-3, and PARP (Figure 2B) *(Online Supplementary Appendix)*. Finally, we translated our experiments from the *in vitro* assays described above to the *in vivo* setting of a mouse model. The antitumor activity of QTX125 was evaluated using REC-1 cells xenografted in nude mice *(Online Supplementary Appendix)*. We randomly selected 8 mice as the control group treated with vehicle and another 8 for QTX125 treatments (intraperitoneal administration of 60 mg/kg in two different regimens). Tumor volume was monitored every two days. The use of the HDAC6 inhibitor QTX125 was significantly associated with the inhibition of lymphoma growth in comparison to the control group (Figure 2C). The extent of blockage of tumor growth was similar to that observed in xenografted lymphomas treated with cyclophosphamide, a DNA alkylating drug commonly used in MCL therapy [11,12]. Use of QTX125 was also associated with the growth inhibition of a second xenografted MCL cell line, MINO (Figure 2C).

Figure 2

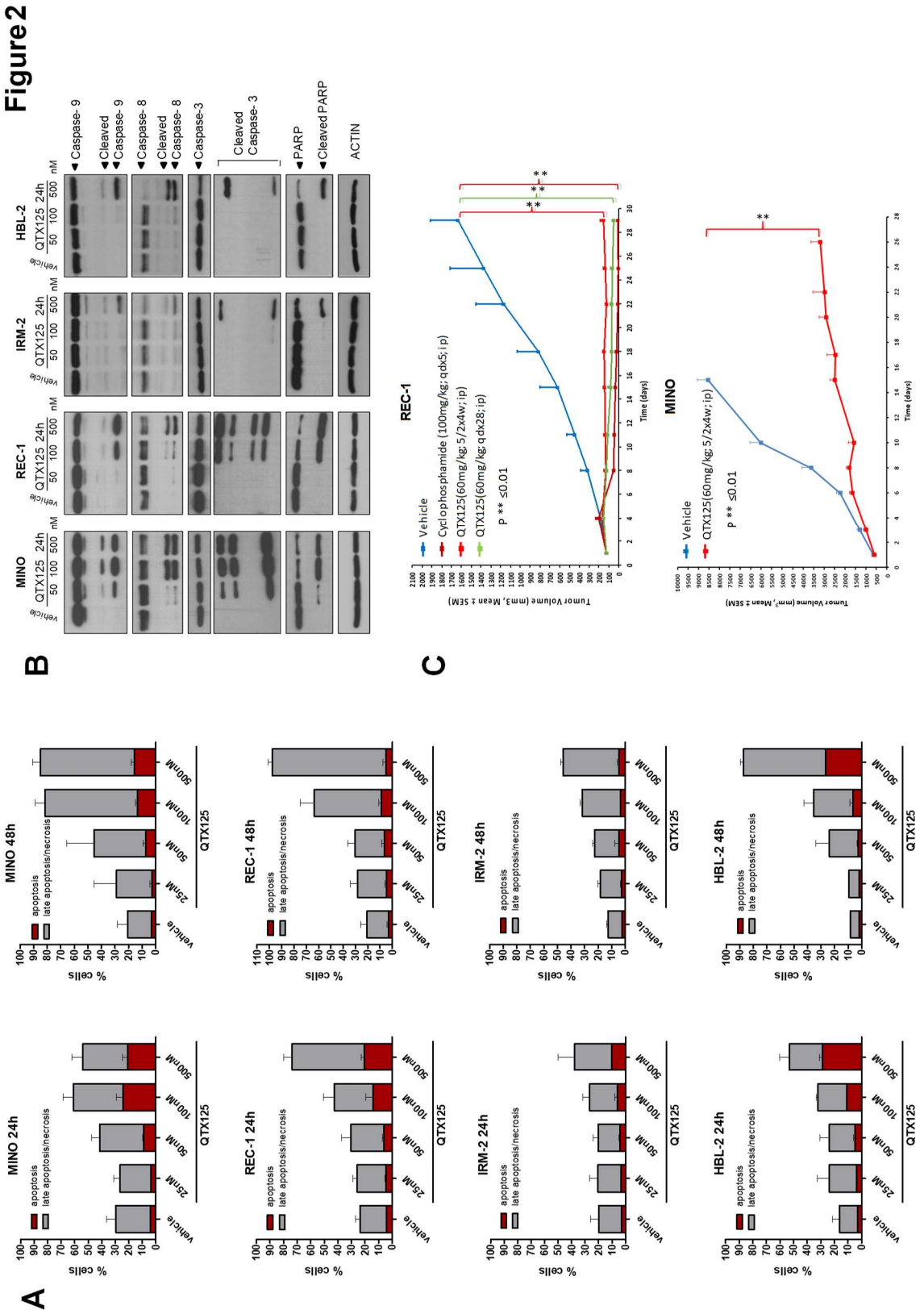
A
MINO 24h
REC-1 24h
IRM-2 24h
HBL-2 24h
MINO 48h
REC-1 48h
IRM-2 48h
HBL-2 48h
apoptosis
late apoptosis/necrosis
% cells
vehicle
25nM
50nM
100nM
500nM
QTX125
B
MINO
REC-1
IRM-2
HBL-2
vehicle
QTX125 50
100
500
24h
nM
Caspase- 9
Cleaved Caspase- 9
Caspase- 8
Cleaved Caspase- 8
Caspase-3
Cleaved Caspase- 3
PARP
Cleaved PARP
ACTIN
C
REC-1
Vehicle
Cyclophosphamide (100mg/kg; qdx5; i.p)
QTX125(60mg/kg; 5/2x4w; i.p)
QTX125(60mg/kg; qdx28; i.p)
P ** ≤0.01
Tumor Volume (mm3, Mean ± SEM)
Time (days)
MINO
Vehicle
QTX125(60mg/kg; 5/2x4w; i.p)
P ** ≤0.01
Tumor Volume (mm3, Mean ± SEM)
Time (days)

Figure 2. QTX125 use in mantle cell lymphoma (MCL) induces cell death by apoptosis and inhibits lymphoma growth in xenografted mice. (A) *Quantification of the flow cytometry values of annexin V/PI incorporation (Alexa Fluor® 488 Annexin V/Dead Cell Apoptosis Kit, Invitrogen) to show the proapoptotic effect of QTX125 on the MCL cell lines MINO, REC-1, IRM-2 and HBL-2.* ***(B)*** *Induction of programmed cell death upon QTX125 administration shown by the cleavage of caspase-9, caspase-8, caspase-3, and PARP in the western blot assay. Actin is used as a loading control.* ***(C)*** *Antitumoral activity of QTX125 in REC-1 and MINO xenografts in nude mice. For REC-1, tumor volume was monitored over time in vehicle and QTX125-treated (two regimens) and cyclophosphamide-treated mice (Mann–Whitney U-test). qdx5: daily dosing for 5 days; 5/2x4w: 5 days of dosing/2 days off for 4 weeks; qdx28: daily dosing for 28 days. For MINO, tumor volume was monitored over time in vehicle and QTX125-treated mice (5/2x4w: 5 days of dosing/2 days off for 4 weeks). The vehicle group arm was stopped at 15 days for ethical reasons.*

The cytotoxicity of QTX125 was also evaluated in 2 primary samples obtained from patients with MCL (see *Online Supplementary Table S1* for details of patients' samples). Incubation with QTX125 strongly reduced cell viability, with IC50 values of 0.120 and 0.182 μM (Figure 3A). Non-malignant lymphocytes, such as peripheral blood mononuclear cells (PBMCs), $CD3^+$ cells (T cells) and $CD19^+$ (B cells) were more resistant to QTX125-mediated growth inhibition (Figure 3B) than MCL cell lines *(Online Supplementary Figure S1)* or MCL primary samples (Figure 3A).

Overall, our results show that the QTX125 compound obtained is a new HDAC6-specific inhibitor that inhibits cell-growth inhibition and causes programmed cell death in association with increased levels of acetylated α-tubulin, its most recognizable target. The antitumoral effect is particularly evident in MCL models, both in culture and *in vivo,* surpassing the efficacy of currently available HDAC6 inhibitors. We demonstrate, therefore, the efficacy of QTX125 in the pre-clinical setting and suggest it warrants further assessment as a novel candidate agent for use in epigenetic lymphoma therapy.

Figure 3

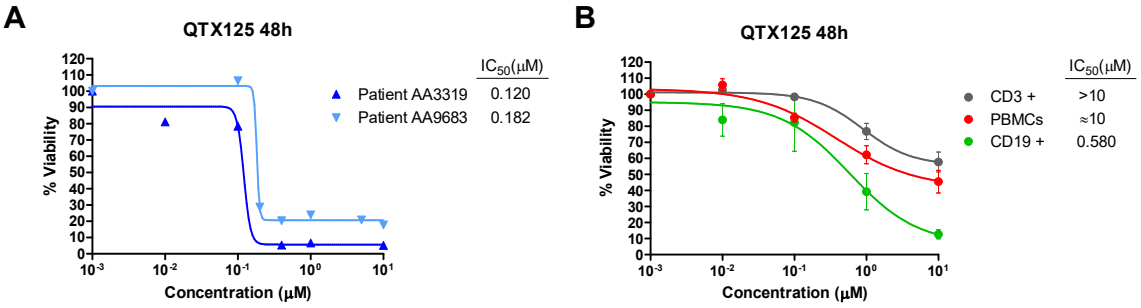

Figure 3. QTX125 use in primary mantle cell lymphoma (MCL) samples and normal blood. ***(A)*** *Effect of QTX125 in cell viability determined by flow cytometry of AnnexinV/7AAD negative cells in primary MCL samples from the patients AA3319 and AA9683. IC50 values are shown for each sample.* ***(B)*** *Effect of QTX125 in cell viability determined by flow cytometry of AnnexinV/7AAD negative cells in peripheral blood mononuclear cells (PBMCs), $CD3^+$ and $CD19^+$ cells obtained from healthy donors (n=4). IC50 values are shown for each sample.*

SUPPLEMENTARY METHODS AND FIGURES

In vitro inhibitory activity of histone deacetylase

50 µM of substrate peptide (see 'substrate peptides' section below) and an optimal concentration of the corresponding enzyme (see 'enzymes' section below) in the assay buffer and 1% final concentration of DMSO were incubated in the presence of gradient concentrations of inhibitors (10-dose IC50 mode with 3-fold serial dilution) at 30°C for 2 h. The reactions were carried out in a 96-well microplate for fluorometry in a 50 µl reaction volume. After the deacetylation reaction, Fluor-de-Lys-Developer (BioMol Cat.# KI-105) was added to each well to digest the deacetylated substrate, thus producing the fluorescent signal. The reaction was allowed to proceed for 45 minutes at 30°C with 5% CO_2; then the fluorescent signal was measured with an excitation wavelength at 360 nm and an emission wavelength at 460 nm in a microplate-reading fluorometer (GeminiXS; Molecular Devices, Sunnyvale, CA). A curve of Deacetylated Standard (Biomol, Cat. # KI-142; made from 100 µM with 1:2 dilution and 10-doses, 6 µl) allowed the conversion of fluorescent signal into micromoles of deacetylated product. All experiments were performed in triplicate. IC50 was calculated by fitting the experimental data to a dose-response curve. DMSO was used as negative control;

Substrate peptides: All HDAC assays were performed using acetylated AMC-labeled peptide substrate:

- Substrate for isoforms HDAC1, 2, 3, 4, 5, 6, 7, 9, 10 and 11 assays: Acetylated fluorogenic peptide from p53 residues 379-382 (RHKKAc) (BioMol Cat. # KI-104).

- Substrate for HDAC8 assays: Acetylated fluorogenic peptide from p53 residues 379-382 (RHKAcKAc) (BioMol Cat. # KI-178).

Assay buffer: 50 mM Tris-HCl, pH 8.0, 137 mM NaCl, 2.7 mM KCl, 1 mM $MgCl_2$ (supplement with 1 mg/ml BSA for dilution) (BioMol Cat. # KI-143).

Enzymes:

-HDAC1 assay: 75 nM Human HDAC1 (GenBank Accession No. NM_004964): Full length with C-terminal GST tag, MW= 79.9 kDa, expressed by baculovirus expression system in Sf9 cells (BioMol Cat. # SE-456).

-HDAC2 assay: 5 nM Human HDAC2 (GenBank Accession No. Q92769): Full length with C-terminal His tag, MW= 60 kDa, expressed by baculovirus expression system in Sf9 cells (BioMol Cat. # SE-500).

-HDAC3 assay: 2.3 nM Human HDAC3/NcoR2 (GenBank Accession No. NM_003883 for HDAC3, GenBank Accession No.NM_006312 for NcoR2): Complex of human HDAC3, full length with C-terminal His tag, MW= 49.7 kDa, and human NCOR2, Nterminal GST tag, MW= 39 kDa, co-expressed in baculovirus expression system (BioMol Cat. # SE-507).

-HDAC4 assay: 266 nM Human HDAC4 (GenBank Accession No. NM_006037): Amino acids 627-1085 with N-terminal GST tag, MW= 75.2 kDa, expressed in baculovirus expression system (BioMol, Hamburg, Germany).

-HDAC5 assay: 588 nM Human HDAC5 (GenBank Accession No. NM_001015053): Full length with Nterminal GST tag, MW= 150 kDa, expressed by baculovirus expression system in Sf9 cells (BioMol, Hamburg, Germany).

-HDAC6 assay: 13 nM Human HDAC6 (GenBank Accession No. BC069243): Full length with N-terminal GST tag, MW= 159 kDa, expressed by baculovirus expression system in Sf9 cells (BioMol Cat. # SE-508).

-HDAC7 assay: 962 nM Human HDAC7 (GenBank Accession No. AY302468): Amino acids 518-end with N-terminal GST tag, MW= 78 kDa, expressed in baculovirus expression system (BioMol, Hamburg, Germany).

-HDAC8 assay: 119 nM Human HDAC8 (GenBank Accession No. NM018486): Full length, MW=42 kDa, expressed in an E. coli expression system (BioMol Cat. # SE-145).

-HDAC9 assay: 986 nM Human HDAC9 (GenBank Accession No. NM178423): Amino acids 604-1066 with C-terminal His tag, MW= 50.7 kDa, expressed in baculovirus expression system (BioMol, Hamburg, Germany).

-HDAC10 assay: 781 nM Human HDAC10 (GenBank Accession No. NM_032019):Amino acids 1-631 with Nterminal GST tag, MW= 96 kDa, expressed by baculovirus expression system in Sf9 cells (BioMol Cat. # SE-559).

-HDAC11 assay: 781 nM Human HDAC11 (GenBank Accession No. NM_BC009676) with N-terminal GST tag, MW= 66 kDa, expressed in baculovirus expression system (BioMol Cat. # SE-560).

Cell lines and primary samples

The following 48 cell lines were used in the study: Breast cancer (BT474, MCF-7, MDA-MB-231, SK-BR-3), Prostate cancer (DU145, LNCaP, PC-3), Colorectal cancer (Colo205, DLD-1, HCT-116, HT-29, LoVo, SW620), Lung cancer (A549, Calu-6, NCIH226,NCI-H460, SK-MES-1), Glioblastoma (U87MG), Fibrosarcoma (HT-1080), Pancreatic cancer (MIAPACA-2, Bx-PC-3, PANC-1), Kidney cancer (786-O), Liver cancer (Hep3B, HepG2, SK-HEP-1), Osteosarcoma (143b), Melanoma (A375, SKMEL5), Ovarian cancer (SK-OV-3, OVCAR3), Chronic Myeloid Leukemia (K562), Orthotopic Multiple Myeloma (RPMI-8226), Hodgkin's lymphoma (KMH2, L428 and HD-MY-Z), Burkitt's lymphoma (Ramos and Jiyoye), Follicular Lymphoma (WSU-NHL, SC-1 and SU-DHL-6) and Mantle Cell Lymphoma (MINO, REC-1, IRM-2, HBL-2, Z-138 and JEKO-1). All cancer cell lines were obtained from the American Type Culture Collection (ATCC) or the Leibniz-Institut DSMZ – German Collection of Microorganisms and Cell Cultures (DSMZ), except IRM-2 and HBL-2 that were provided by Miguel A.Piris (Pathology Department, Fundación Jiménez Díaz, Madrid, Spain). IRM-2 and HBL-2 have been widely used as MCL cell line models [1-6] and a detailed description can be found at Cellosaurus - a knowledge resource on cell lines (https://web.expasy.org/cellosaurus). Cells were cultured at 37ºC with 5% CO_2 in the appropriate growth medium. For primary tissues, we obtained buffy coats from anonymous healthy donors through the Catalan Blood and Tissue Bank (CBTB). The CBTB follows the principles of the World Medical Association (WMA) Declaration of Helsinki. Before providing the first blood sample, all donors received detailed oral and written information and signed consent form at the CBTB. Peripheral blood mononuclear cells (PBMCs) were isolated using Ficoll-Paque gradient (Amersham, Buckinghamshire, UK) centrifugation. Lymphatic node cells from two MCL patients were obtained following informed consent and approval of the Institutional Review Boards of the Josep Carreras Institute and the Catalan Institute of Oncology. Cells were cultured in RPMI Medium 1640

supplemented with 10% heat-inactivated fetal bovine serum, 100 U/mL penicillin and 100 µg/mL streptomycin at 37ºC with 5% CO2.

Dose-response assays

For dose-response assays, cell lines were seeded at a density of 5000 to 20000 cells/well in 96-well plates. The optimal number of cells for each experiment was determined to ensure that each one was in growth phase at the assay endpoint. After overnight incubation, experimental culture medium containing increasing concentrations of QTX125, Tubastatin A, Tubacin or ACY1215 was added into each well. Cell viability was determined by MTS or MTT assays at 72h or 96 h after treatment, respectively. MTS assay was performed following the manufacturer's protocol CellTiter 96® Aqueous Non-Radioactive Cell Proliferation Assay MTS (Promega). Briefly, a mixture of MTS [3-(4,5-dimethylthiazol-2-yl)-5-(3-carboxymethoxyphenyl)-2-(4-sulfophenyl)-2H tetrazolium, inner salt; MTS] and an electron coupling reagent (phenazine methosulfate) PMS was freshly prepared in solution, added to each well and incubated for 4 hours at 37ºC in a humidified, 5% CO_2 atmosphere. Absorbance was read at 490 nm using a spectrophotometer. Alternatively, MTT (3-(4,5-dimethyl-2-thiazolyl)-2,5-diphenyl-2H-tetrazolium bromide) reagent was added and incubated for 3 h, after which the cells were lysed for 16 h with MTT lysis buffer (50% N-N dimethylformamide, 20% sodium dodecyl sulfate, 2.5% glacial acetic acid, 2.1% 1N HCl, at pH 4.7). Plates were measured at 560 nm using a spectrophotometer. Cell viability was also determined by cell counting with the Trypan Blue exclusion method.

Immunoblotting assays

Total protein from cells was extracted with Laemmli sample buffer (62.5 mM Tris-HCl pH 6.8, 25% glicerol, 2% SDS, 0.01% Bromophenol Blue, 5% β-mercaptoethanol).Specific antibodies against target proteins were used: α-Tubulin (ab52866, Abcam), Acetylated Tubulin (T6793, Sigma Aldrich), Caspase-9 (133109, Santa Cruz), Caspase-8 (9746, Cell Signaling), Caspase-3 (9668, Cell Signaling), Cleaved Caspase-3 (9661, Cell Signaling), PARP (556362, BD

Pharmingen™), CD20 (ab78237, Abcam), and β-Actin-HRP (A3854, Sigma Aldrich).

Detection of Apoptosis by Flow Cytometry

Cells were treated with QTX125 at 25nM, 50nM, 100nM and 500 nM or with vehicle for 24 and 48h hours. Annexin V-Alexa Fluor® 488/PI staining was used for the quantification of early and late apoptotic cells following manufacturer's instructions (Alexa Fluor® 488 annexin V/Dead Cell Apoptosis Kit with Alexa® Fluor 488 annexin V and PI for Flow Cytometry, V13245 Invitrogen). Briefly, cells were stained with Alexa Fluor® 488 Annexin V and PI for 15 min and were examined by flow cytometry (FACS Canto, BD Biosciences) using 488 nM excitation with 530/30 and 575/26 bandpass filters. A minimum of 10,000 cells was analysed per sample. Quantification and illustration as dot plot was done using FACSDiva Software. Experiments were performed in triplicate. PBMCs from healthy donors (n=4) or cells from MCL patients (n=2) were treated for 48h with increasing concentrations of QTX125. Cells were then washed with PBS. PBMCs from healthy donors were incubated with (APC)-conjugated anti-CD19, and APC-eFluor® 780- conjugated anti-CD3 for 20 min in the dark and then incubated with Annexin V-Alexa Fluor® 488 and 7-amino-actinomicina D (7AAD) in annexin-binding buffer for 15 minutes. Cells from MCL patients were incubated with Annexin V-Alexa Fluor® 488 and 7-amino-actinomicina D (7AAD) in annexin-binding buffer for 15 minutes. Cells were then examined by flow cytometry (FACS Canto II, BD Biosciences). Quantification was done using FACSDiva Software. The results of viability presented correspond to the AnnexinV/7AAD negative cells.

Mouse xenografts

REC-1 and MINO cells were harvested during exponential growth and re-suspended in cold phosphate buffered saline (PBS) at a concentration of 1 x 10^8 cells/mL. Female CB.17 SCID mice (CRL: NU(NCr)-Foxn1nu, Charles River) were used for the study. All mouse experiments were approved and performed in accordance with the guidelines of the Institutional Animal Care Committee of the Bellvitge Biomedical Research Institute. Xenografts were initiated by

subcutaneously implanting a 0.1 mL suspension of 1 x 10^7 REC-1 or MINO tumor cells in 50% MatrigelTM (BD Biosciences) into the right flank of each test animal and tumors were monitored as their volumes approached the target range of 100 to 500 mm^3. Tumors were measured in two dimensions using calipers, and volume was calculated using the formula: V (mm^3)=(L × W^2)/2. After tumor implantation (Day 1 of study) the animals were sorted into the different groups (n=8 for REC-1 and n=10 for MINO) according to the treatment plan summarized below. QTX125 was dissolved at a final concentration of 7.5 mg/mL in a 10%DMSO:35% PEG400 in DI water vehicle. This dosing solution provided a 60 mg/kg dose in an 8 mL/kg dosing volume. The used in vivo dose of QTX125 (60 mg/Kg) for MCL xenografts is similar to the one used in the initial studies of ACY-1215 (50 mg/Kg) for multiple myeloma xenografts [7], the HDAC6 inhibitor that it is undergoing clinical trials in multiple myeloma patients. Cyclophosphamide was dissolved in saline to a final stock concentration of 20 mg/mL, and further diluted to a dosing solution of 10 mg/mL which provided a 100 mg/kg dose in a dosing volume of 10mL/kg. All treatments were administered intraperitoneally (i.p.) at the dosing volumes above and scaled to the body weight of the animal.

Treatment plan for REC-1

Group 1 received vehicle daily for 28 days (qd x 28) and served as the control.

Group 2 received cyclophosphamide at 100 mg/kg daily dosing for 5 days (qd x 5).

Group 3 received QXT125 at 60 mg/kg on a schedule of five days on/two days off for four weeks (5/2 x 4).

Group 4 received QXT125 at 60 mg/kg daily dosing for 28 days (qd x 28).

Tumors were measured using calipers twice per week.

Treatment plan for MINO

Group 1 received vehicle daily until we stopped for ethical reasons because tumor burden was no longer justifiable (15 days).

Group 2 received QXT125 at 60 mg/kg on a schedule of five days on/two days off for four weeks (5/2 x 4).

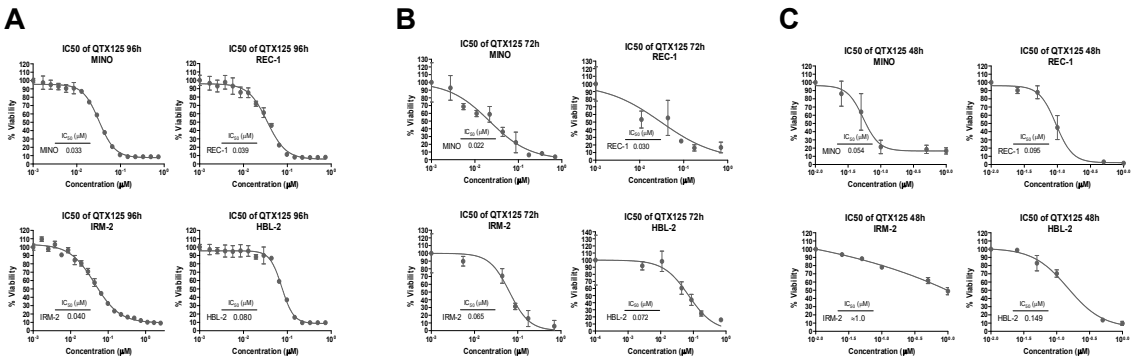

Supplementary Figure S1. *Effect of QTX125 in cell viability in the MCL cell lines MINO, REC-1, IRM-2 and HBL-2 determined by the MTT assay* ***(A)****, cell counting with the Trypan Blue exclusion method* ***(B)****, and flow cytometry where cell viability is expressed as the percentage of AnnexinV/PI negative cells* ***(C)****. IC50 values are shown for each cell line.*

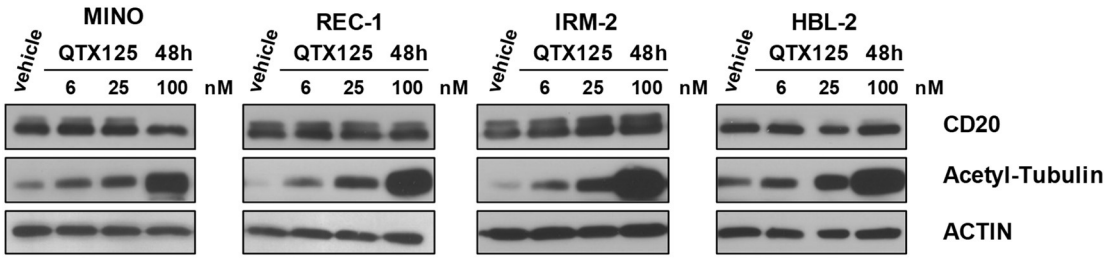

Supplementary Figure S2. *Western-blot for CD20 expression in the MCL cell lines MINO, REC-1, IRM-2 and HBL-2 upon the use of QTX125. Acetylated-Tubulin is shown as a marker of HDAC6 inhibition upon QTX125 use. Actin is shown as a loading control.*

Supplementary Table S1. *Immunophenotype performed by flow cytometry of the two mantle cell lymphoma cases.*

	AA3319	**AA9683**
CD3	8%	6%
CD4	4%	4%
CD8	3%	3%
CD19	92%	95%
CD45	99%	100%
Chains Kappa	0%	0%
Chains Lambda	92%	94%
CD5	94%	98%
CD19/CD5	92%	95%
CD10	1%	1%
CD19/CD10	0%	0%
CD11c	1%	1%
CD19/CD11c	0%	0%
CD20	93%	94%
CD22	91%	91%
CD23	10%	2%
CD38	87%	53%
CD19/CD38	80%	50%
CD43	90%	94%
CD19/CD43	83%	90%
CD79b	91%	88%
CD103	0%	2%
CD200	2%	1%
FMC7	79%	34%
bcl2	Positive	-
Ki67	20	-
Myc	Negative	-
bcl6	Negative	-

REFERENCES

1. Rodríguez-Paredes M, Esteller M. Cancer epigenetics reaches mainstream oncology. Nat Med. 2011;17(3):330-339.
2. Jones PA, Issa JP, Baylin S. Targeting the cancer epigenome for therapy. Nat Rev Genet. 2016;17(10):630-641.
3. Huertas D, Soler M, Moreto J, et al. Antitumor activity of a smallmolecule inhibitor of the histone kinase Haspin. Oncogene. 2012; 318(11):1408-1418.
4. Filippakopoulos P, Knapp S. Targeting bromodomains: epigenetic readers of lysine acetylation. Nat Rev Drug Discov. 2014;13(5):337-356.
5. Pérez-Salvia M, Simó-Riudalbas L, Llinàs-Arias P, et al. Bromodomain inhibition shows antitumoral activity in mice and human luminal breast cancer. Oncotarget. 2017;8(31):51621-51629.
6. Seidel C, Schnekenburger M, Dicato M, Diederich M. Histone deacetylase 6 in health and disease. Epigenomics. 2015;7(1):103-118.
7. Govindarajan N, Rao P, Burkhardt S, et al. Reducing HDAC6 ameliorates cognitive deficits in a mouse model for Alzheimer's disease. EMBO Mol Med. 2013;5(1):52-63.
8. Lernoux M, Schnekenburger M, Dicato M, Diederich M. Anti-cancer effects of naturally derived compounds targeting histone deacetylase 6-related pathways. Pharmacol Res. 2018;129:337-356
9. Zubia A, Ropero S, Otaegui D, et al. Identification of (1H)-pyrroles as histone deacetylase inhibitors with antitumoral activity. Oncogene 2009;28(11):1477-1484.
10. Aginagalde M, Bello T, Masdeu C, Vara Y, Arrieta A, Cossío FP. Formation of □−oxoacids and 1H-pyrrol-2(5H)-ones from α,β−unsaturated ketones and ethyl nitroacetate. J Org Chem. 2010; 75(21):7435-7438.
11. Spurgeon SE, Till BG, Martin P, et al. Recommendations for clinical trial development in mantle cell lymphoma. J Natl Cancer Inst. 2016; 109(1):djw263.
12. Howard OM, Gribben JG, Neuberg DS, et al. Rituximab and CHOP induction therapy for newly diagnosed mantle-cell lymphoma: molecular complete responses are not predictive of progression-free survival. J Clin Oncol. 2002;20(5):1288-1294.
13. Lwin T, Zhao X, Cheng F, et al. A microenvironment-mediated c- Myc/miR-548m/HDAC6 amplification loop in non-Hodgkin B cell lymphomas. J Clin Invest. 2013;123(11):4612-4626.
14. Zhang Y, Li N, Caron C, et al. HDAC-6 interacts with and deacetylates tubulin and microtubules in vivo. EMBO J. 2003;22(5):1168-1179.

15. Bobrowicz M, Dwojak M, Pyrzynska B, et al. HDAC6 inhibition upregulates CD20 levels and increases the efficacy of anti-CD20 monoclonal antibodies. Blood. 2017;130(14):1628-1638.

REFERENCE LIST (SUPPLEMENTARY METHODS)

1. Abe M, Nozawa Y, Wakasa H, Ohno H, Fukuhara S. Characterization and comparison of two newly established Epstein-Barr virus-negative lymphoma Bcell lines. Surface markers, growth characteristics, cytogenetics, and transplantability. Cancer. 1988;61(3):483-490.

2. Mestre-Escorihuela C, Rubio-Moscardo F, Richter JA, et al,. Homozygous deletions localize novel tumor suppressor genes in B-cell lymphomas. Blood. 2007;109(1):271-280.

3. Baran-Marszak F, Boukhiar M, Harel S, et al. Constitutive and B-cell receptorinduced activation of STAT3 are important signaling pathways targeted by bortezomib in leukemic mantle cell lymphoma. Haematologica. 2010;95(11):1865-1872.

4. Pérez-Galán P, Mora-Jensen H, Weniger MA, et al. Bortezomib resistance in mantle cell lymphoma is associated with plasmacytic differentiation. Blood. 2011;117(2):542-552.

5. Beltran E, Fresquet V, Martinez-Useros J, et al. A cyclin-D1 interaction with BAX underlies its oncogenic role and potential as a therapeutic target in mantle cell lymphoma. Proc Natl Acad Sci USA. 2011;108(30):12461-6.

6. Bhatt S, Matthews J, Parvin S, et al. Direct and immune-mediated cytotoxicity of interleukin-21 contributes to antitumor effects in mantle cell lymphoma. Blood. 2015;126(13):1555–1564.

7. Santo L, Hideshima T, Kung AL, et al. Preclinical activity, pharmacodynamic, and pharmacokinetic properties of a selective HDAC6 inhibitor, ACY-1215, in combination with bortezomib in multiple myeloma. Blood. 2012;119(11):2579-89.

RESULTS SUMMARY

STUDY I: *"KAT6B is a tumor suppressor Histone H3 Lysine 23 acetyltransferase undergoing genomic loss in Small Cell Lung Cancer"*

KAT6B is homozygously deleted in SCLC and leads to gene inactivation.

We described a previously unknown homozygous deletion of *KAT6B* in two out of ten (20%) human SCLC cell lines (NCI-H1963 and NCI-H740), after the screening for copy-number alterations in histone-modifier genes using the Illumina Infinium HumanOmni5 microarray. These results were confirmed by quantitative genomic PCR, MLPA and FISH. We then found that the expression of KAT6B was lost at both mRNA (qPCR) and protein level (Western Blot) in both cell lines harboring the homozygous deletion.

KAT6B has tumor suppressor–like properties in cancer cells.

At this point, we studied the role of KAT6B in cancer phenotype *in vitro* and *in vivo*. First, we downregulated KAT6B by short-hairpinRNAs (shRNAs) in two SCLC cell lines retaining both copies of the gene (HCC-33 and N417). We observed that the downregulation of KAT6B had oncogenic properties, such as increased viability in the MTT assay and the formation of more colonies compared to the shRNA-scramble (control) cells. We then moved our hypothesis into *in vivo* experiments. We observed that KAT6B shRNA-downregulated cells injected subcutaneously in nude mice developed bigger tumors than shRNA-scramble cells, as also happened in an orthotopic mouse model. We then investigated the potential inhibitory dissemination activity of KAT6B by direct spleen injection and posterior analysis of metastasis formation in the liver. Mice injected with N417 cells with downregulated KAT6B developed numerous metastatic nodules in the liver whereas less metastasis were observed in the shRNA-scramble cells.

Lysine 23 of histone H3 as a target of KAT6B-mediated acetylation.

Our previous results made us to investigate about the molecular mechanism underlying the tumor-suppressor features that we observed for KAT6B. We focused our attention in histone H3 because of its greater homology with KAT6A and its previously described preference for this histone [288]. Important to refer that the specific residues acetylated by KAT6B were not described. To identify

them we performed LC/MS-MS analysis comparing histone H3 from H1963 cell line transduced with a full-length KAT6B expression vector or with an empty one. We determined qualitatively that acetylation of lysine 23 in H3 was enhanced in KAT6B-trasduced cells according to the precursor signal intensity of the two acetylated peptides K.QLATK^{23ac}AAR and R.KQLATK^{23ac}AAR.K. Then, targeted quantification of H3K23 residue acetylation by SRM confirmed the enrichment of this acetylation mark upon recovery of KAT6B in H1963 cells. We checked this result by Western Blot in the H1963 transduced with KAT6B and in the KAT6B shRNA-downregulated cells models. Moreover, using SRM and Western-Blot we were able to detect a decrease of H3K23 acetylation in a KAT6B truncated by mutation sample from a patient with the SBBYS type of Ohdo syndrome [289] compared to normal lymphocytes. Next, we looked for genes which expression could be regulated by acetylation of KAT6B. For that we performed an Expression Array comparing shRNA-KAT6B downregulated and shRNA-scramble cells in N417 and HCC-33 cell lines. As acetylation is a mark normally related with transcription activation, we focus on the 32 genes found commonly downregulated in both cell lines upon KAT6B silencing. We validated by qRT-PCR the downregulation of 25 of these genes. Additionally, we checked by quantitative ChIP that H3K23Ac was diminished in the promoter of four of these genes.

KAT6B genomic loss occurs in SCLC patients and confers sensitivity to Irinotecan.

In order to find if *KAT6B* deletion also occurred in primary tumors of SCLC patients, we performed MLPA analysis for the *KAT6B* locus using a collection of 60 tumors. We identified the *KAT6B* homozygous deletion in eight SCLC tumors (13%). For the patients we had clinical data (n=26), *KAT6B* homozygous depletion correlated with shorter progression free survival. We also performed immunohistochemistry in 20 SCLC cases. The 4 cases harboring *KAT6B* homozygous deletion showed an overall loss of staining for KAT6B and H3K23Ac.

Our next question was to investigate if the loss of KAT6B conferred sensitivity to any anticancer drug. We tested 28 HDAC inhibitors and the classic SCLC

chemotherapy agents such as cisplatin or etoposide in KAT6B shRNA-downregulated cells vs shRNA-scramble cells by determining the IC50 values through MTT assay. For these drugs we did not observe any difference between the two types of cells. However, we found that KAT6B shRNA-downregulated cells were significantly more sensitive to the chemotherapy agent irinotecan than the shRNA-scramble cells. We also tested irinotecan sensitivity in our orthotopic mice model, where we observed the same. KAT6B downregulated tumors were also significantly more sensitive to irinotecan than shRNA-scramble derived ones. We wondered about the putative mechanism of irinotecan increased sensibility. It has been reported that MYST family of HATs is implicated in ATM-induced DNA damage response. Thus, KAT6B depleted tumors could be less capable of repair irinotecan induced DNA damage. Based on this, we checked that ATM expression was reduced in shRNA-KAT6B downregulated cells. Besides, phosphorylation of H2AX was lower upon irinotecan treatment in these downregulated cells.

STUDY II: *"Bromodomain inhibition shows antitumoral activity in mice and human luminal breast cancer"*

The bromodomain inhibitor JQ1 decreases cell viability of human luminal breast cancer cell lines in association with downregulation of C-MYC.

The study was initiated with the exploration of JQ1 as a potential growth inhibitory compound in luminal breast cancer. For that we selected MCF7 and T47D cell lines, well characterized in literature as luminal phenotype [290, 291]. We obtained the IC50 concentration of JQ1 with MTT assay (micromolar range) and observed that JQ1 inhibited cancer cell growth dose-dependently in both cell lines. Then we checked that this growth inhibition occurred coupled with a downregulation of C-MYC at transcriptional (RT-PCR) and protein levels (Western Blot), but contrarily, BRD4 levels were not altered, as previously described in other models [17, 18, 292]

JQ1 downregulates PDZK1 and BCAS1, two important genes in breast cancer tumorigenesis

Next, we looked for other genes that were in addition of C-MYC potentially involved in the growth inhibition observed upon treatment with the drug. We performed an Expression Array of MCF7 and T47D cell lines treated with 1 μM of JQ1 vs. vehicle (DMSO) for 24h. Of the set of 36,712 unique genes included in the microarray, 1,149 (3.1%) significantly changed in a shared manner in both cell lines; 420 (36.6%) of them were upregulated and 729 (63.4%) were downregulated. The genes in this latter group are the putative targets of JQ1. Between the top candidate genes commonly downregulated in both cell lines, we focused our interest in the *PDZ Domain Containing 1 (PDZK1)* and the *Breast Carcinoma-Amplified Sequence 1 (BCAS1) genes.* Both encode two onco-proteins that have been linked to breast cancer [20, 293]. Their downregulation upon JQ1 administration was validated by qRT-PCR in the same RNA extracts used for the microarray hybridization and again in the same cell lines treated with JQ1 at different times.

We then checked that PDZK1 and BCAS1 were acting as oncogenes in our cell lines, as it did C-MYC. For that, we downregulated these three genes separately using shRNAs in MCF7 and T47D. We observed a similar significant decrease of cell viability by MTT assay for the three genes. Then, we assessed cell proliferation by MTT assay upon treatment with JQ1 in both shRNA-downregulated cells and shRNA-scramble cells for each of the three genes. We observed that JQ1 inhibited cell growth in high level in both conditions and it was not observed any differences in sensitivity to JQ1 between them. Moreover, JQ1 caused higher growth inhibition than the independent downregulation of each of the three genes.

Bromodomain inhibition shows antitumoral activity and retards the onset of luminal breast tumors in the MMTV-PyMT luminal breast cancer mouse model.

After our *in vitro* results, we moved to an *in vivo* model of luminal breast cancer, MMTV-PyMT transgenic mice, which develop spontaneously breast tumors [294]. We decided to test JQ1 in this model using two different approaches: 1) a curative

approach and 2) a preventive one. To test the efficacy of JQ1 as a curative agent *in vivo*, we started treating the animals when the total tumor volumes of each animal was between 1,000-2,700 mm^3. We randomly divided the animals in two groups, eight were treated with JQ1 (25mg/kg) and eight were treated with vehicle. The animals received 11 doses of drug and tumors volumes were monitored every 2-3 days until the end of the experiment (two days after the last dose). The treatment did not show any kind of toxicity in the animals. The treatment with JQ1 led to the development of smaller tumors than the treatment with vehicle.

Then we moved to the preventive approach. For that we started treating the animals at week 4, when no palpable or visible tumors had arisen. Tumors volumes were monitored every 2-3 days. As in the explained experiment above, the animals were randomly divided into a treatment group with JQ1 (25 mg/kg n=5) and a control group (vehicle n=7). Mice were treated for three weeks on a 5 days on/2 days off regime and their tumors were monitored until the sum of tumors volume per animal was over 4000mm^3. We observed that the animals pre-treated with JQ1 developed smaller tumors. The preventive treatment with JQ1 also increased the overall survival in comparison to the mice of the control group.

STUDY III*: "In vitro and in vivo activity of a new small-molecule inhibitor of HDAC6 in mantle cell lymphoma"*

QTX125 is a highly specific HDAC6 inhibitor and exerts growth inhibitory effect in MCL cell lines.

The selectivity of QTX125 for inhibiting HDAC6 function in comparison with all the other HDACs was assessed by *in vitro* enzymatic assay. Then, we tested the antitumoral capacity of QTX125 determining its IC50 at 72h by MTS Assay in 48 human cancer cell lines including solid tumors and hematological malignancies. We observed that QTX125 exert the strongest growth-inhibitory effect in Burkitt's Lymphoma, follicular lymphoma and mantle cell lymphoma (MCL). So, we focus our attention in MCL, and selected MINO, REC-1, IRM-2 and HBL-2 cell lines for

further characterization. With these 4 MCL cell lines, we performed α-tubulin Western-Blot and observed that QTX125 induced dose-dependent hyperacetylation of this best-known target of HDAC6. Trichostatin A was used as positive control, as a general inhibitor for HDAC classes I, IIa, IIb (including HDAC6) and IV, whereas sodium butyrate was used as a negative control as an HDAC inhibitor that does not affect HDAC6 [295]. The three commercially available HDAC6 inhibitors (Tubastatin A, Tubacin, and ACY1215) were also used as specific positive controls. We also checked MCL cell lines sensitivity to these three HDAC6 inhibitors by determining its IC50, being QTX125 the most powerful in these cell lines.

QTX125 inhibits cell growth in association with the induction of apoptosis in MCL.

To test if the observed inhibition of cell proliferation upon QTX125 treatment was associated with the induction of apoptosis, we performed Annexin V/propidium iodide double staining in the four MCL previously selected cell lines treated with QTX125 at different doses (25, 50, 100, 500 nM) at 24 and 48 hours and measured them by Flow Cytometry. An increased level of apoptosis was detected upon treatment. The same was observed by Western-Blot through the cleavage of Caspase-9, Caspase-8, Caspase-3, and PARP.

QTX125 shows antitumoral effect *in vivo* in MCL xenograft mice.

We then translated our experiments to an *in vivo* setting. The antitumor activity of QTX125 was evaluated in mice xenografts models using REC-1 and MINO cells. When the mice had individual tumors ranging from 100 to 500 mm^3 we randomly divided them in the following treatment groups. In REC-1 xenografts, there were 4 groups of treatment (n=8): 1) the control group treated with vehicle, 2,3) two groups of QTX125 treatments (intraperitoneal administration of 60 mg/kg in two different regimens, 5 days of dosing/2 days off for 4 weeks and daily dosing for 28 days) and 4) one group treated with cyclophosphamide (100 mg/kg daily dosing for 5 days). In MINO xenografts, there were two groups of treatment (n=10): 1) the control group treated with vehicle and 2) the group treated with QTX125 (60mg/kg, 5 days on/2 days off). Tumor volume was monitored every

2-3 days. Mice treated with the HDAC6 inhibitor QTX125 experienced an inhibition of lymphoma growth in comparison with the mice treated with vehicle. The decrease in tumor growth was similar to that observed in the group treated with cyclophosphamide, a DNA alkylating drug commonly used in MCL therapy [296, 297].

MCL primary samples show more sensitivity to QTX125 than blood from healthy donors.

At this point, we tested QTX125 in cells from the lymphatic node of two MCL patients, which according to the initial immunophenotype were over 92% CD19/CD5 positive. Incubation with QTX125 strongly reduced cell viability, measured by flow cytometry (AnnexinV/7AAD negative cells). We then evaluated the effect of the compound in non-malignant PBMCs obtained from 4 buffy coats from anonymous healthy donors isolated using Ficoll-Paque gradient centrifugation. After 48h incubation with QTX125, we examined cell viability by flow cytometry (AnnexinV/7AAD negative cells) in PBMCs, CD19+ (B-cells) and CD3+ (T-cells), observing that all of them were more resistant to QTX125 than MCL cell lines and primary samples tested.

GENERAL DISCUSSION

STUDY I: ***"KAT6B is a tumor suppressor Histone H3 Lysine 23 acetyltransferase undergoing genomic loss in Small Cell Lung Cancer"***

Small cell lung cancer is a highly malignant type of cancer that represents approximately 15% of total lung cancer cases diagnosed worldwide. It is characterized for being highly aggressive and by an early occurrence of metastasis. Although it is initially sensitive to chemotherapy, in the vast majority of cases tumors recur, being the mortality very high. For the past 30 years there was no important advances in research or clinics concerning this type of tumor, mainly because of a lack of patient samples to study due to the rarely resection of these tumors. Few years ago, interest and funding for this research line come up in part thanks to engineered mouse models and patient derived xenografts of this disease [10, 298].

It is well known that one hallmark of SCLC is the inactivation of the tumor suppressor genes *TP53* and *RB1* in up to 90% and 65% of cases respectively [10]. In the last years, other genetic and epigenetic alterations were described. They include mutations in histone modifiers *CREBBP, EP300* and *MLL* genes [11]. Interestingly, BET inhibitors showed preclinical growth inhibition and are now in early clinical trials [254]. However, there are no targeted therapies approved yet for SCLC. Thus, new advances on treatments for these patients are needed. Identifying new epigenetic players that could be affected would be interesting, especially if this alteration is druggable or could be used as predictive biomarker of treatment response.

Having this in mind, we looked for copy number alterations in histone modifiers genes in SCLC cell lines. Histone modifiers play an important role in cancer by altering normal histone patterns and mutations in some of them had been reported for this type of lung cancer [11]. We found *KAT6B* homozygous deletion in two out of ten (20%) SCLC cell lines and we checked that it was linked to a lack of expression of KAT6B.

Alterations in KAT6B gene have been described in breast cancer [130] and castration-resistant prostate cancer [131] being also found amplified in a pan-Cancer study [132]. Other modification described for this gene is the fusion to CPB in translocation t(10;16)(q22;p13) related with AML. Based on the very few

studies focused on KAT6B function in cancer, a dual role as oncogene and tumor suppressor depending on the cancer type seems to be a putative characteristic of this gene. Important to refer that this dual role is a common event in some histone modifier enzymes, such as Tip60 or CPB/P300 [87].

In order to unveil which role was playing this unknown deletion of KAT6B in SCLC, we evaluated its effect in tumorigenesis *in vitro* and *in vivo*. Downregulation of KAT6B by shRNA led to an increment in cell growth and to a higher colony formation rate *in vitro.* Moreover, KAT6B-downregulated tumors in xenograft mice and later in orthotopic models were significantly bigger compared to tumors not harbouring the deletion. We also observed an inhibitory dissemination effect of KAT6B with reduced metastasis to the liver *in vivo*. All these experiments showed that KAT6B is a tumor suppressor gene in SCLC. Besides, supporting this phenotype, we observed that expression of Brahma (BRM) was diminished in KAT6B-downregulated cells together with the BRM-target E-cadherin. Both genes are well-known tumor suppressor genes. In fact, BRM had been previously described as a target induced by KAT6B [299].

KAT6B (MYST4/MORF) is a HAT protein, member of MYST family. All the members of this family have been described as writers of specific acetylation marks on lysines, except KAT6B that had not any described acetylation mark. For example, KAT7 is the main source of H4 acetylation by acetylating H4K5, H4K8 and H4K12 residues [119], KAT5 and KAT8 acetylates H4K16 [300], KAT6A catalyzes H4K16 [301], H3K9 and H3K14 [12] and was described after our study that it also acetylates H3K23Ac [133].

Given the unknown target residues of KAT6B, we investigated which acetylation mark could be regulating KAT6B in our system. We focused on H3 due to its similarity with KAT6A and previous evidence of the preference for H3 by MOZ/MORF complexes [288]. We identified lysine 23 in H3 as a putative target residue for KAT6B acetylation. Interestingly, during the review process of our study a paper was published reporting that the *Drosophila* KAT6 Enok was responsible of H3K23 acetylation [13]. KAT6 Enok in *Droshophila* is highly similar to human KAT6A and KAT6B in the MYST domain and N-terminal part [129]. Furthermore, after our publication, a study in 2017 about KAT6A in glioblastoma demonstrated that this protein also acetylates H3K23 [133]. These studies

support our newly described KAT6B mediated H3K23 acetylation. Importantly, this mark is also catalysed by EP300 and CBP, which have also been described mutated in SCLC. This suggests that H3K23 acetylation could be playing an important role in this type of lung cancer, what encourages further investigation [14].

Besides cancer, KAT6B alterations can also be found in rare genetic disorders like Blepharophimosis-ptosis-epicanthus inversus syndrome (BPES) [302], Noonan syndrome [303], Say-Barber-Biesecker-Young-Simpson syndrome (SBBYSS) [289] and genitopatellar syndrome (GPS) [304]. We had the great opportunity to work with a precious sample. It was blood from a 5-years-old patient suffering SBBYSS. This sample was kindly provided by Dr. Guntram Borck (Institute of Human Genetics, University of Ulm, Ulm, Germany) and had *KAT6B* mutated. In immortalized B-lymphocytes from this patient we observed less H3K23 acetylation compared with immortalized B-lymphocytes from healthy donors, confirming our finding that KAT6B mediates acetylation of H3K23.

Our next step was to examine if *KAT6B* genomic deletion was also present in SCLC tumors. Here we found *KAT6B* homozygous deletion in 13% of the SCLC tumors. In the patients we had data, this deletion correlated with shorter progression-free survival. These findings support our reported role of KAT6B as a tumor suppressor gene in SCLC. Moreover, they show up a possibility of clinical translation, what prompted us to investigate if KAT6B deletion could be used as a predictive biomarker of treatment response. Thus, we started the search for any drug which could present increased sensitivity in these patients. Having also in mind that in our model KAT6B has a clear tumor suppressor role, from the point of view of treatment we wanted to find a drug that could benefit SCLC patients with this deletion. Thinking on epigenetic drugs that directly modulate acetylation levels we tried HDAC inhibitors in our system. We hypothesized that HDACs inhibition could compensate the loss of acetylation caused by KAT6B deletion, that might potentially be one of the causes of the oncogenic features observed when this alteration occurs. Despite we tried multiple HDAC inhibitors, including pan-HDAC and class-specific, none of them induced a differential effect between KAT6B-downregulated cells and KAT6B-not downregulated cells. It would have been worth to try bromodomain inhibitors, another class of epigenetic drugs that

could potentially be directing any cellular response based on acetylation marks regulated by KAT6B.

Important to comment that KAT6B has been described as an oncogene in some types of cancer and that KAT6A has also been described to play a role in inhibiting senescence [305]. Based on this, a recent study reported two new KAT6A/B inhibitors. They induce cell cycle exit and senescence, preventing lymphoma progression *in vitro* and *in vivo* [306]. These two compounds inhibit both KAT6B and KAT6A, however the study is only based in this last protein. Probably this dual inhibition is due to the high homology between these two proteins [305].

Targeted therapy against a specific genetic alteration have not been found yet for SCLC. In one hand, this is because genetic defects are poorly described. In the other, because it is easier to find a drug directed against an oncogene aberrantly expressed, than when a tumor suppressor gene like *KAT6B* is absent or in other cases inactivated. For example in Non-Small cell lung cancer (NSCLC), EGFR inhibitors are approved because activating mutations of this protein are a common event in up to 60% cases of lung adenocarcinoma [15]. In the case of SCLC the most common genetic alterations are the inactivation of the two tumor suppressor genes *p53* and *Rb*, for which there is no pharmacological treatment. This means that maybe restoring functional KAT6B would be more beneficial, however it is a difficult approach to achieve in clinics.

In Western countries, the actual first line therapy for SCLC is etoposide-platinum based chemotherapy. In some cases, it can also be combined with radiotherapy. In Eastern countries, irinotecan plus cisplatin are administered now as first-line therapy after clinical studies demonstrated few years ago that this combination increased overall survival over etoposide/cisplatin in Japanese population. However, these results were not achieved in Western population, probably due to pharmacogenomic differences related with the metabolism of irinotecan between Western and Easter population. In second-line therapy there is no consensus on which the best therapeutic regime is. However, topotecan was approved by the FDA as a single-agent in these patients. Actually, there are multiple clinical trials for second-line therapies in SCLC which include also irinotecan [307].

In our *in vitro* system we also tried etoposide and cisplatin, classic SCLC chemotherapeutic agents, but we did not observe differences of sensitivity for them. However, interestingly we found that KAT6B-downregulated cells *in vitro* and *in vivo* were more sensitive to irinotecan. Our hypothesis about the putative mechanism that could be underlying the increased sensitivity to irinotecan by KAT6B-downregulation is related with the reported role of MYST family overexpression in inducing ATM expression and consequently increasing phosphorylation of H2AX, mark of DNA damage [16]. When we checked mRNA levels of ATM, they were lower in KAT6B-downregulated cells. Upon irinotecan treatment levels of γH2AX were also lower than in scramble-cells. Thus, KAT6B-downregulation could increase irinotecan sensitivity because the ATM decreased levels confer to the cells less capability to repair DNA-damage induced by this chemotherapeutic agent.

Considering that irinotecan is actually approved for colon cancer treatment and that is being used in several clinical trials for second-line therapy in SCLC, our results point out that patients harbouring *KAT6B* deletion could benefit of irinotecan as first treatment, due to its higher sensibility. However, further studies are needed to evaluate its higher efficacy as a first-line therapy or a possible combination with the actual platinum-based therapy in this group of patients.

STUDY II: *"Bromodomain inhibition shows antitumoral activity in mice and human luminal breast cancer"*

Breast cancer is the most common cancer in women, with over 2.1 million new cases each year. Classically breast cancer has been characterized based on the status of estrogen-/progesterone-receptors (ER/PR) and amplification of HER2 for prognosis and choice of treatment. Later, a new intrinsic molecular classification arises thanks to new gene expression profiling techniques. According to this latter classification, there are five subtypes: 1) luminal A, 2) luminal B, 3) Her-2 enriched, 4) basal-like and 5) claudin-low, together with a normal-like tumors group [308]. Luminal subtype is ER positive and/or PR positive with low Ki-67 index in luminal A or high Ki-67 in luminal B. Approximately 90-95% of breast tumors are luminal and generally respond to endocrine therapies

that blocks the effect of hormones or decrease its levels such as tamoxifen or aromatase inhibitors. However, resistance to hormone therapies is common [309].

Research on BET inhibitors as novel cancer treatment has been growing quickly and during the development of this project several studies in breast cancer were published. As it was already described in the introduction section, BET inhibition shows efficacy in most subtypes of breast cancer [259]. In luminal breast cancer, it decreases tumor growth, reduces estrogen-dependent transcription [171] and shows increased sensitivity in a tamoxifen-resistant cell line compared to the non-resistant cells [262].

JQ1 is a BET bromodomain inhibitor that since its first publication in 2010, has been used in a large and diverse number of cancer studies. Briefly, it inhibits mainly BET bromodomain BRD4, reader of acetyl lysines in histones and regulator of transcription, that leads to downregulation of important genes in tumorigenesis.

Luminal subtype of breast cancer is the most common and resistance to endocrine therapies creates the need of new therapies. For that, we tested JQ1 in luminal breast cancer and tried to unveil new genes involved in its sensitivity that could be used as predictive biomarkers towards a more personalized therapy. Although some studies report that BRD4 alterations could be related with tumorigenesis in breast cancer and other tumors [310], in our work, we did not focus on any previously existing genetic or epigenetic modifications. This is because there is no correlation in expression of BET proteins with a specific subtype of breast cancer and it seems to vary across human cancer cell lines. Besides, levels of expression of BET proteins or MYC showed no clear correlation with JQ1 sensitivity in breast cancer [311].

In our studied human luminal cancer cell lines JQ1 caused a downregulation of C-MYC at mRNA and protein level without variation of BRD4 expression levels, as previously published [17, 18]. This BRD4 stability could be due to the fact that JQ1 binds to the acetyl lysine binding pocket of BET bromodomain and displaces BRD4 from chromatin in a competitive manner [17].

In order to see what other genes could be involved in luminal breast cancer response to this drug, we performed an Expression Array comparing MCF7 and T47D cell lines treated with JQ1 or vehicle. We detected 3.1% (1149 out of 36712) of genes that changed significantly in both cell lines: 36.6% (420 out of 1149) of which were upregulated whereas 63.4% (729 out of 1149) were downregulated. The higher percentage of downregulated genes was expected since JQ1 causes a decrease in transcription by BRD4 inhibition [312]. From the downregulated top candidate genes potentially affected by JQ1 treatment we focused our interest in *PDZ domain containing 1 (PDZK1)* and *breast carcinoma amplified sequence-1 (BCAS1)* since their stated oncogenic role in breast cancer.

PDZK1 has been correlated with breast malignancy and was weakly detected in normal tissue. It has been described as an estrogen-responsive protein which seems to be not directly regulated by ER-α, but through insulin-like growth factor 1 receptor (IGF-1R) [20]. PDZK1 enhances cellular growth in breast cancer possibly through the stabilization of serine/threonine kinase AKT by increased levels of cochaperone cell division cycle 37 (CDC37) [313]. BCAS1 was initially described to be one of the genes present in the known 20q13.2 amplified region in breast cancer and other tumors, fact that confers bad prognosis and contributes to tumorigenesis [19, 293]. However, its function has not been yet deeply studied, being functional studies needed to unveil its specific role in breast cancer.

Consequently, after identifying and validating PDZK1 and BCAS1 as important targets of JQ1 in luminal cancer cell lines, we interrogated if they were playing an important role in cell proliferation according to their oncogenic reported role. After downregulating these two genes for separated in two luminal breast cancer cell lines we observed a significant decrease in cell proliferation. Moreover, this decrease was in a similar magnitude as the one produced by downregulation of C-MYC.

At this point, we wondered if *PDZK1* and *BCAS1* transcription could be dependent on C-MYC. If this was the case, their downregulation observed upon treatment would be a consequence of C-MYC downregulation by JQ1. We saw that this hypothesis was not right since when we downregulated C-MYC using shRNA, *PDZK1* and *BCAS1* mRNA levels were not reduced in these cells (data

non-published). In fact, some studies suggest that PDZK1 could be involved in MYC upregulation [20].

We have reported *PDZK1* and *BCAS1* as new targets of JQ1 treatment and confirmed their oncogenic role in breast cancer. However, more experiments are required to elucidate if they are direct targets of BRD4. This would clarify if their downregulation upon JQ1 treatment is really due to a direct effect of BRD4 over transcription of these genes. Or contrarily, their transcription or even their function could be indirectly regulated by other genes, different from MYC, which expression could be affected by BRD4 and JQ1 inhibition.

Another important issue that we investigated was if *PDZK1, BCAS1* or *C-MYC* genes involved in JQ1 response could be used as predictive biomarkers of treatment response. For that, we checked if the decreased expression of any of these genes conferred a differential sensitivity to JQ1. We compared cell proliferation upon treatment between scrambleRNA control cells and shRNA-downregulated cells for PDZK1, BCAS1 and C-MYC separately. Our hypothesis considered two possible scenarios: 1) Genes-downregulated cells could be more sensitive to JQ1 than control cells. This could be because this deficiency could act synergistically with other genes differentially affected by the drug in these cells than in control cells; 2) Control cells could be more sensitive than shRNA-downregulated cells. This would mean that any of these genes acts as a driver of luminal breast tumorigenesis. They may be inducing other molecular responses that JQ1 is able to halt, whereas downregulated cells continue growing by an alternative mechanism that JQ1 do not affect. However, in this latter scenario, it would have been interesting to check if the same response is achieved when these genes are overexpressed compared to normal expression. Also, going deeper to find which mechanistic response is induced in both conditions would be needed. Then patients harbouring amplification of any of these genes would specially benefit of treatment with JQ1.

However, we observed a third scenario, where there was a decrease in cell proliferation for both control cells and genes-downregulated cells with no differences in sensitivity. Important to refer that, this decrease in cell growth caused by JQ1 was higher than the one caused by only the silencing of these oncogenes. These results suggest that JQ1 exerts its function inhibiting

transcription in a very wide manner. It potentially affects numerous molecular pathways involved in cancer, some of them already described and others not yet linked to BET inhibition effect. Moreover, these results show that although these genes are potential oncogenic in our system, they do not confer any difference in JQ1 sensitivity. It seems difficult to find a gene which alteration has an important influence in JQ1 response in breast cancer even if it is C-MYC, an important oncogene that modulates several other genes in cancer. In fact, studies of BET inhibition in breast cancer show no correlation between levels of MYC expression and JQ1 sensitivity [311]. These observations have a negative side since it will be difficult to find biomarkers in breast cancer that could allow response prediction to this drug and patients treatment stratification. The positive aspect is if we consider that BET inhibition could be applicable to a broad number of patients independently of their genetic alterations.

At this point, we tested JQ1 in a breast cancer mice model MMTV-PyMT. This *in vivo* model is characterized as luminal subtype and shares expression profiles with the human disease, being widely used. Transgenic female mice develop spontaneously breast tumors up to four weeks from birth [294]. In this model we tested JQ1 in two different methodologies: 1) a curative treatment, common in drug testing studies and 2) a preventive approach. In our curative approach we showed that JQ1 treatment decreased tumor growth, without showing toxicity. In the preventive treatment, we observed that administering the drug before the tumors arise managed to increase mice overall survival. This is quite a new approach, not frequent in research, but really exciting for opening the door to further research in preventive treatments. For example, it could be especially applicable in types of cancers such as breast tumors where BRCA1 or BRCA2 mutations are frequent markers of high risk of developing cancer. Thus, it would be interesting to test JQ1 as a preventing agent in mice harbouring any of these mutations, with the future idea that they could be administered to this high risk population.

BRCA1 plays an important role in preventing MYC-induced breast transformation and MYC-amplification contributes to BRCA1-mutant aggressiveness in tumors [314]. In fact, there is a very recent study reporting that BRCA1 deficiency sensitizes breast cancer cells to BET inhibition, stablishing a synthetic lethality

between BRCA1 and BET bromodomains. BET inhibition alters transcription of genes that increase cell oxidative stress and DNA damage that leads to BRCA1-deficient cells to die [21].

PARP inhibitors (PARPi) are approved by the FDA for the treatment of BRCA1/2 mutated breast and ovarian cancers. There are also recent studies that report synergy between BET inhibitors and PARP inhibitors [310, 315]. This synthetic lethality is based in the induction of homologous recombination (HR) deficiency by BET inhibition that enhances PARPi induced DNA damage in cancer cells [22]. This combination would be especially beneficial to prevent and overcome resistance to PARPi, such as in BRCA-mutant cancers that become resistant to PARPi by recovering BRCA function, and also extends the utility of PARPi to HR-proficient cancers. BRD4 inhibition also induces downregulation of key genes involved in DNA damage repair and cell-cycle checkpoint regulation, which absence causes cell death by mitotic catastrophe [315]. Moreover, BRD4 inhibition also seems to repress *BRCA1* transcription by avoiding its interaction with the promoter and its putative super-enhancer resensitizing cells to PARP inhibition [310].

Overall, these results support the idea that JQ1 is a powerful drug for cancer treatment because of its wide mechanism of action. Further research will help to completely characterize its mechanism in the different cancer types, opening spots for new drugs combinations or for the selection of patients that could benefit from BET inhibition. Furthermore, JQ1 have been broadly tested *in vivo* in preclinical studies with good results of efficacy and low toxicity. This low toxicity reinforces the idea that BET inhibition seems to be quite specific for tumor cells with low effect on normal cells, a really important characteristic in new drugs willing to reach clinics.

STUDY III: ***"In vitro and in vivo activity of a new small-molecule inhibitor of HDAC6 in mantle cell lymphoma"***

HDAC6, unlike other HDACs, is mainly in the cytoplasm and deacetylates non-histone proteins [316]. Its best-known targets are α-Tubulin, Cortactin and Hsp90. HDAC6 plays an important role in cancer regulating cytoskeleton dynamics, mobility, migration and protein degradation by aggresome formation [23]. For that, HDAC6 inhibition is an interesting anticancer therapy to investigate. Important to highlight is that HDAC6 knock-out mice are not lethal whereas most of other HDACs knock-out models die shortly after birth or present serious defects [317]. This means that although there are several pan-HDAC inhibitors available, it is worthy to find specific HDAC6 inhibitors. It will be also a way to avoid undesired toxicity, that has already been observed in the clinics with approved pan-HDAC inhibitors [318].

For this reason, our collaborators from Quimatryx and the University of Basque Country synthesized a new compound (QTX125) that showed high selectivity for HDAC6 over the other HDACs. All the 48 human cancer cell lines from different solid and hematological tumors treated with QTX125 presented a decrease in proliferation upon treatment. However, Burkkit's lymphoma, follicular lymphoma and Mantle Cell Lymphoma (MCL) were the more sensitive cell lines. The rest of hematological cancer cell lines tested, Hodgkin's lymphoma, chronic myelogenous leukemia (CML) and multiple myeloma, were more resistant to QTX125. Maybe because we only have the result from one cell line in the case of CML and multiple myeloma cancers. Thus, it would be necessary to extend it to more cell lines to draw a conclusion. Concerning Hodgkin's lymphoma, this is a differentiated class of lymphoma that have specific characteristics and treatment response. Further research would be encouraged to evaluate the effect of this new compound in more types of leukemia and myeloma. Important to refer that in general, approved HDAC inhibitors were seen to be first more effective in hematological tumors. This is thought to be because of the easier diffusion of the drug in circulating cells compared to the difficulty in solid tumors due to for example the poor formed blood vascular system [319] combined with the poor pharmacokinetics of current HDACi [320]. This can also explain the better sensitivity from these cancers to QTX125. Thus, according to our results,

QTX125 is a drug with high sensitivity in three types of mature B-cell non-Hodgkin lymphomas, and specially in MCL, cancer on which we decided to focus the study for the reasons next pointed.

Mantle Cell Lymphoma is a type of B-cell non-Hodgkin lymphoma generally very aggressive and fast growing. The current first-line treatment is a combination chemotherapy R-CHOP (Rituximab, cyclophosphamide, doxorubicin, vincristine, and prednisone) or R-Bendamustine. In the last years, at the time of relapse, patients are being treated with bortezomib (proteasome inhibitor), lenalidomide (anti-angiogenic) and Ibrutinib (Bruton's tyrosine kinase (BTK) inhibitor) with good results. However, clinical trials with novel agents are always considered for patients with relapsed MCL because they do not achieve a complete cure with the actual treatment. The current standard-treatment gives short remission durations and a median overall survival of 4-5 years [321].

New treatments for MCL are needed and HDAC6 seems to play a role in MCL growth [322]. Moreover, an HDAC6 specific inhibitor would potentially avoid side effects over pan-HDACi. For all these reasons, the search for new specific HDAC6 inhibitors for MCL is an interesting therapeutic option to be explored.

We confirmed that QTX125 was effectively inhibiting HDAC6 in our selected MCL cell lines when we found hyperacetylation of α-Tubulin (main target of HDAC6) upon treatment. We also tested in our model other HDAC6 specific inhibitors available, like Tubacin, Tubastatin A and Ricolinostat (ACY-1215). This confirmed that our new drug response was in the same direction of these other already characterized drugs. In addition, we also found that QTX125 was more potent that the other three inhibitors, inducing hyperacetylation at lower doses and being cells more sensitive to it (lower IC50). This make it a promising agent to treat MCL considering that Ricolinostat is actually in clinical trials.

Once we knew that QTX125 has a potent antitumor activity specially in MCL by inhibiting HDAC6, we decided to unveil if that was due to an induction of apoptosis. We decided to start checking apoptosis before other death mechanisms based on our observations at the microscope and on literature about other pan-HDACi and HDAC6 inhibitors where it seems to be the preferred route of cell death induced by these kind of inhibitors [24, 27, 147]. By flow cytometry

we observed that apoptosis was induced upon treatment of QTX125 in a dose-dependent manner at 24 and 48h. By Western-Blot we were able to interrogate if there was a preferred apoptotic pathway for this new drug. We observed cleavage of Caspase-8 and Caspase-9 initiator caspases of the extrinsic and intrinsic pathways respectively, with consequent cleavage of the effector Caspase-3 and PARP, meaning that both apoptotic pathways are induced upon treatment with QTX125.

Our hypothesis about the possible mechanism of action of this new HDAC6 inhibitor in MCL is related with already existing evidences in literature about HDAC6 inhibition in multiple myeloma and other lymphomas [24, 27]. HDAC6 inhibition with QTX125 may be impairing protein degradation by inhibition of aggresome formation. This would cause a toxic cellular stress by accumulation of misfolded proteins that would end with the induction of an apoptotic response and consequent caspases cascade cleavage. This proposed mechanism would be in concordance with our observations of induction of apoptosis by both intrinsic and extrinsic pathways upon QTX125 treatment. Important to highlight that pharmacological inhibition of cellular mechanisms for protein degradation, which are mainly proteasome and aggresome, is an emerging approach for the treatment of lymphomas and multiple myeloma. This is due to lymphocytes increased protein synthesis. It is necessary for the production of high levels of antibodies required for immune response and makes lymphocytes physiologically upregulate the Unfolded Protein Response (UPR) pathway to maintain proteostasis [25]. In fact, there is evidence of upregulation of key regulatory factors of UPR such as Binding immunoglobulin protein (BiP) or X-box binding protein 1 (XBP-1) in several types of lymphomas. This suggests that lymphoid malignancies are even more dependent on an increased UPR response [24]. Similarly, multiple myeloma is also characterized by an abnormal synthesis and excretion of immunoglobulins. Reason why proteasome inhibitors show good response and have been recently approved for this disease [26]. As the final fate of a protein not correctly folded is its degradation, inhibition of protein degradation pathways which will ultimately end with apoptosis induction is a promising anticancer approach.

What gives more strength for the future clinical application of this new compound is that we had the great opportunity to test it in primary samples extracted from the lymphatic node of two patients diagnosed with MCL. These valuable samples were sensitive to QTX125 at nanomolar doses, similar to the results observed in cell lines. We also tested its toxicity in PBMCs from healthy donors. Interestingly, we observed that they were more resistant to the drug than primary cells from patients or cell lines. This suggests that this compound would potentially cause low toxicity in normal cells in humans.

The results of this study encourage further investigation with QTX125 in order to reach clinical trials for MCL treatment in a near future and possibly make it extensive to other hematological malignancies. Likewise, it would be interesting to test QTX125 in combination with other drugs.

Ricolinostat is the only specific HDAC6 inhibitor in clinical trials now in multiple myeloma, lymphoid malignancies and other cancers such as ovarian and breast mainly in combination with other drugs. In MCL, there are only very few preclinical studies published with Ricolinostat treatment in combination with other drugs [24, 323]. Interestingly, there is currently a clinical trial ongoing of Ricolinostat as a single agent in relapsed Hodgkin or non-Hodgkin lymphoma malignancies which includes a cohort of MCL patients (NCT02091063). It has no results yet and is estimated to finish at the end of 2019.

However, in relapsed MCL there are good results in clinical trials with bortezomib and other proteasome inhibitors such as Ixazobim, alone or in combination with other drugs. This suggests that treatment with HDAC6 inhibitors could also be a good treatment option as it also targets a protein degradation pathway.

Combination of both, QTX125 and bortezomib would be also an interesting possibility to explore in MCL. This combination have been tested with other HDAC6 inhibitors in multiple myeloma preclinically [27] and also in clinical trials [238]. This synergy is potentially explained by the simultaneous inhibition of the proteasome and the aggresome pathways. Consequently, an accumulation of misfolded proteins occurs leading to induction of apoptosis. Also, resistance to proteasome inhibitors arise because cells use then the aggresome pathway as an alternative route for protein degradation. Thus, simultaneous inhibition of both

should be a good approach also to avoid resistance. QTX125 seems to be effective at low nanomolar doses in MCL, meaning that it could have enough potency as a single agent. However, combination treatment with bortezomib could be interesting to prevent or overcome resistance. It has not yet been described, but probably with time resistance mechanisms to HDAC6 inhibition would arise too.

CONCLUSIONS

Based on the results of this PhD thesis we can conclude:

Study I:

- Histone acetyltransferase *KAT6B* undergoes homozygous deletion in Small Cell Lung Cancer (SCLC).
- In SCLC, KAT6B exerts a tumor suppressor role *in vitro* and *in vivo.*
- KAT6B acts as a histone acetyltransferase for lysine 23 of histone H3, the first acetylation site described for this protein.
- KAT6B impairment predicts an increased sensitivity to Irinotecan in SCLC *in vitro* and *in vivo*.

Study II:

- JQ1 inhibits cancer cell growth in luminal breast cancer *in vitro* and *in vivo*.
- JQ1 exerts its antitumoral effect downregulating C-MYC, PDZK1 and BCAS1 expression in breast cancer cell lines.
- JQ1 has stronger growth inhibitory effect than the independent downregulation of C-MYC, PDZK1 or BCAS1.
- JQ1 used as curative treatment leads to the appearance of smaller tumors in a luminal breast cancer mice model.
- As preventive treatment JQ1 increases overall survival and delays the offset of the tumors in a luminal breast cancer mice model.

Study III:

- QTX125 shows high specificity for HDAC6 over the other HDACs (HDAC1-11).
- QTX125 is a new HDAC6 inhibitor.
- QTX125 increases acetylation levels of α-tubulin in a dose-dependent manner.
- QTX125 has antitumoral effect in 48 human cancer cell lines.

- Mantle Cell Lymphoma (MCL) cell lines are highly sensitive to QTX125.
- QTX125 induces apoptosis by cleavage of Caspase-9,8,3 and PARP in MCL cell lines.
- QTX125 exerts antitumoral effect in MCL xenografts.
- MCL primary cells from patients are more sensitive to QTX125 than PBMCs, CD3+ and CD19+ cells from healthy donors.

REFERENCES

1. Alberts, B., *Molecular Biology of the Cell.* Garland Science, 2014.

2. Waddington, C.H., *Preliminary Notes on the Development of the Wings in Normal and Mutant Strains of Drosophila.* Proceedings of the National Academy of Sciences of the United States of America, 1939. 25(7): p. 299-307.

3. Holliday, R., *The inheritance of epigenetic defects.* Science, 1987. 238(4824): p. 163-70.

4. Esteller, M., *Epigenetics in Cancer.* New England Journal of Medicine, 2008. 358(11): p. 1148-1159.

5. Portela, A. and M. Esteller, *Epigenetic modifications and human disease.* Nature Biotechnology, 2010. 28: p. 1057.

6. Li, J., et al., *Role of several histone lysine methyltransferases in tumor development.* Biomedical Reports, 2016. 4(3): p. 293-299.

7. Khan, S.A., D. Reddy, and S. Gupta, *Global histone post-translational modifications and cancer: Biomarkers for diagnosis, prognosis and treatment?* World Journal of Biological Chemistry, 2015. 6(4): p. 333-345.

8. Singh, B.N., et al., *Nonhistone protein acetylation as cancer therapy targets.* Expert review of anticancer therapy, 2010. 10(6): p. 935-954.

9. Simo-Riudalbas, L. and M. Esteller, *Targeting the histone orthography of cancer: drugs for writers, erasers and readers.* Br J Pharmacol, 2015. 172(11): p. 2716-32.

10. George, J., et al., *Comprehensive genomic profiles of small cell lung cancer.* Nature, 2015. 524(7563): p. 47-53.

11. Peifer, M., et al., *Integrative genome analyses identify key somatic driver mutations of small-cell lung cancer.* Nat Genet, 2012. 44(10): p. 1104-10.

12. Huang, F., S.M. Abmayr, and J.L. Workman, *Regulation of KAT6 Acetyltransferases and Their Roles in Cell Cycle Progression, Stem Cell Maintenance, and Human Disease.* Mol Cell Biol, 2016. 36(14): p. 1900-7.

13. Huang, F., et al., *Histone acetyltransferase Enok regulates oocyte polarization by promoting expression of the actin nucleation factor spire.* Genes & development, 2014. 28(24): p. 2750-2763.

14. Henry, R.A., Y.M. Kuo, and A.J. Andrews, *Differences in specificity and selectivity between CBP and p300 acetylation of histone H3 and H3/H4.* Biochemistry, 2013. 52(34): p. 5746-59.

15. da Cunha Santos, G., F.A. Shepherd, and M.S. Tsao, *EGFR mutations and lung cancer.* Annu Rev Pathol, 2011. 6: p. 49-69.

16. Vonlaufen, N., et al., *MYST family lysine acetyltransferase facilitates ataxia telangiectasia mutated (ATM) kinase-mediated DNA damage response in Toxoplasma gondii.* J Biol Chem, 2010. 285(15): p. 11154-61.

17. Filippakopoulos, P., et al., *Selective inhibition of BET bromodomains.* Nature, 2010. 468(7327): p. 1067-73.

18. Delmore, J.E., et al., *BET bromodomain inhibition as a therapeutic strategy to target c-Myc.* Cell, 2011. 146(6): p. 904-17.

19. Beardsley, D.I., et al., *Characterization of the novel amplified in breast cancer-1 (NABC1) gene product.* Experimental Cell Research, 2003. 290(2): p. 402-413.

20. Kim, H., et al., *PDZK1 Is a Novel Factor in Breast Cancer That Is Indirectly Regulated by Estrogen through IGF-1R and Promotes Estrogen-Mediated Growth.* Molecular Medicine, 2013. 19(1): p. 253-262.

21. Zhang, B., et al., *BRCA1 deficiency sensitizes breast cancer cells to bromodomain and extra-terminal domain (BET) inhibition.* Oncogene, 2018. 37(49): p. 6341-6356.

22. Sun, C., et al., *BRD4 Inhibition Is Synthetic Lethal with PARP Inhibitors through the Induction of Homologous Recombination Deficiency.* Cancer Cell, 2018. 33(3): p. 401-416.e8.

23. Li, T., et al., *Histone deacetylase 6 in cancer.* Journal of Hematology & Oncology, 2018. 11(1): p. 111.

24. Amengual, J.E., et al., *Dual targeting of protein degradation pathways with the selective HDAC6 inhibitor, ACY-1215, and bortezomib is synergistic in lymphoma.* Clinical cancer research : an official journal of the American Association for Cancer Research, 2015. 21(20): p. 4663-4675.

25. Gass, J.N., N.M. Gifford, and J.W. Brewer, *Activation of an Unfolded Protein Response during Differentiation of Antibody-secreting B Cells.* Journal of Biological Chemistry, 2002. 277(50): p. 49047-49054.

26. Gandolfi, S., et al., *The proteasome and proteasome inhibitors in multiple myeloma.* Cancer and Metastasis Reviews, 2017. 36(4): p. 561-584.

27. Santo, L., et al., *Preclinical activity, pharmacodynamic, and pharmacokinetic properties of a selective HDAC6 inhibitor, ACY-1215, in combination with bortezomib in multiple myeloma.* Blood, 2012. 119(11): p. 2579-2589.

28. (NCI), N.C.I. *www.cancer.gov/about-cancer/understanding/what-is-cancer: Understanding cancer, what is cancer*. [accessed November 2018].

29. Hanahan, D. and R.A. Weinberg, *The hallmarks of cancer.* Cell, 2000. 100(1): p. 57-70.

30. Hanahan, D. and R.A. Weinberg, *Hallmarks of cancer: the next generation.* Cell, 2011. 144(5): p. 646-74.

31. Esteller, M., *Cancer epigenomics: DNA methylomes and histone-modification maps.* Nat Rev Genet, 2007. 8(4): p. 286-98.

32. Pages, F., et al., *Immune infiltration in human tumors: a prognostic factor that should not be ignored.* Oncogene, 2010. 29(8): p. 1093-102.

33. Grivennikov, S.I., F.R. Greten, and M. Karin, *Immunity, inflammation, and cancer.* Cell, 2010. 140(6): p. 883-99.

34. Llinas-Arias, P. and M. Esteller, *Epigenetic inactivation of tumour suppressor coding and non-coding genes in human cancer: an update.* 2017. 7(9).

35. Ferreira, H.J. and M. Esteller, *Non-coding RNAs, epigenetics, and cancer: tying it all together.* Cancer and Metastasis Reviews, 2018. 37(1): p. 55-73.

36. Esteller, M. and P.P. Pandolfi, *The Epitranscriptome of Noncoding RNAs in Cancer.* Cancer Discovery, 2017.

37. Weber, M., et al., *Distribution, silencing potential and evolutionary impact of promoter DNA methylation in the human genome.* Nat Genet, 2007. 39(4): p. 457-66.

38. Bird, A., *DNA methylation patterns and epigenetic memory.* Genes Dev, 2002. 16(1): p. 6-21.

39. Reik, W. and A. Lewis, *Co-evolution of X-chromosome inactivation and imprinting in mammals.* Nat Rev Genet, 2005. 6(5): p. 403-10.

40. Kacem, S. and R. Feil, *Chromatin mechanisms in genomic imprinting.* Mamm Genome, 2009. 20(9-10): p. 544-56.

41. Doi, A., et al., *Differential methylation of tissue- and cancer-specific CpG island shores distinguishes human induced pluripotent stem cells, embryonic stem cells and fibroblasts.* Nat Genet, 2009. 41(12): p. 1350-3.

42. Zhang, W. and J. Xu, *DNA methyltransferases and their roles in tumorigenesis.* Biomarker Research, 2017. 5: p. 1.

43. Feng, S., S.E. Jacobsen, and W. Reik, *Epigenetic reprogramming in plant and animal development.* Science, 2010. 330(6004): p. 622-7.

44. Wu, H. and Y. Zhang, *Reversing DNA methylation: mechanisms, genomics, and biological functions.* Cell, 2014. 156(1-2): p. 45-68.

45. Rasmussen, K.D. and K. Helin, *Role of TET enzymes in DNA methylation, development, and cancer.* Genes & Development, 2016. 30(7): p. 733-750.

46. Feinberg, A.P. and B. Vogelstein, *Hypomethylation distinguishes genes of some human cancers from their normal counterparts.* Nature, 1983. 301: p. 89.

47. Eden, A., et al., *Chromosomal Instability and Tumors Promoted by DNA Hypomethylation.* Science, 2003. 300(5618): p. 455-455.

48. Greger, V., et al., *Epigenetic changes may contribute to the formation and spontaneous regression of retinoblastoma.* Human Genetics, 1989. 83(2): p. 155-158.

49. Herman, J.G., et al., *Silencing of the VHL tumor-suppressor gene by DNA methylation in renal carcinoma.* Proceedings of the National Academy of Sciences, 1994. 91(21): p. 9700-9704.

50. Gonzalez-Zulueta, M., et al., *Methylation of the 5' CpG Island of the p16/CDKN2 Tumor Suppressor Gene in Normal and Transformed Human Tissues Correlates with Gene Silencing.* Cancer Research, 1995. 55(20): p. 4531-4535.

51. Esteller, M., et al., *Promoter Hypermethylation and BRCA1 Inactivation in Sporadic Breast and Ovarian Tumors.* JNCI: Journal of the National Cancer Institute, 2000. 92(7): p. 564-569.

52. Herman, J.G. and S.B. Baylin, *Gene Silencing in Cancer in Association with Promoter Hypermethylation.* New England Journal of Medicine, 2003. 349(21): p. 2042-2054.

53. Esteller, M., et al., *A Gene Hypermethylation Profile of Human Cancer.* Cancer Research, 2001. 61(8): p. 3225-3229.

54. Moran, S., et al., *Epigenetic profiling to classify cancer of unknown primary: a multicentre, retrospective analysis.* Lancet Oncol, 2016. 17(10): p. 1386-1395.

55. Dawson, Mark A. and T. Kouzarides, *Cancer Epigenetics: From Mechanism to Therapy.* Cell, 2012. 150(1): p. 12-27.

56. Audia, J.E. and R.M. Campbell, *Histone Modifications and Cancer.* Cold Spring Harbor Perspectives in Biology, 2016. 8(4).

57. Kouzarides, T., *Chromatin Modifications and Their Function.* Cell, 2007. 128(4): p. 693-705.

58. Greer, E.L. and Y. Shi, *Histone methylation: a dynamic mark in health, disease and inheritance.* Nature Reviews Genetics, 2012. 13: p. 343.

59. Fraga, M.F., et al., *Loss of acetylation at Lys16 and trimethylation at Lys20 of histone H4 is a common hallmark of human cancer.* Nature Genetics, 2005. 37: p. 391.

60. Lee, J.-S., E. Smith, and A. Shilatifard, *The Language of Histone Crosstalk.* Cell, 2010. 142(5): p. 682-685.

61. Filippakopoulos, P. and S. Knapp, *Targeting bromodomains: epigenetic readers of lysine acetylation.* Nat Rev Drug Discov, 2014. 13(5): p. 337-56.

62. Allfrey, V.G., R. Faulkner, and A.E. Mirsky, *Acetylation and Methylation of histones and their possible role in the regulation of RNA synthesis* Proc Natl Acad Sci U S A, 1964. 51: p. 786-94.

63. Di Martile, M., D. Del Bufalo, and D. Trisciuoglio, *The multifaceted role of lysine acetylation in cancer: prognostic biomarker and therapeutic target.* Oncotarget, 2016. 7(34): p. 55789-55810.

64. Jenuwein, T. and C.D. Allis, *Translating the Histone Code.* Science, 2001. 293(5532): p. 1074-1080.

65. Cohen, I., et al., *Histone Modifiers in Cancer: Friends or Foes?* Genes Cancer, 2011. 2(6): p. 631-47.

66. Bannister, A.J. and T. Kouzarides, *Regulation of chromatin by histone modifications.* Cell Res, 2011. 21(3): p. 381-95.

67. Parthun, M.R., *Hat1: the emerging cellular roles of a type B histone acetyltransferase.* Oncogene, 2007. 26: p. 5319.

68. Yang, X., et al., *HAT4, a Golgi Apparatus-Anchored B-Type Histone Acetyltransferase, Acetylates Free Histone H4 and Facilitates Chromatin Assembly.* Molecular Cell, 2011. 44(1): p. 39-50.

69. Brownell, J.E., et al., *Tetrahymena histone acetyltransferase A: a homolog to yeast Gcn5p linking histone acetylation to gene activation.* Cell, 1996. 84(6): p. 843-51.

70. Hardy, S., et al., *TATA-binding Protein-free TAF-containing Complex (TFTC) and p300 Are Both Required for Efficient Transcriptional Activation.* Journal of Biological Chemistry, 2002. 277(36): p. 32875-32882.

71. Martinez, E., et al., *Human STAGA complex is a chromatin-acetylating transcription coactivator that interacts with pre-mRNA splicing and DNA damage-binding factors in vivo.* Mol Cell Biol, 2001. 21(20): p. 6782-95.

72. Wang, L. and S.Y.R. Dent, *Functions of SAGA in development and disease.* Epigenomics, 2014. 6(3): p. 329-39.

73. Tjeertes, J.V., K.M. Miller, and S.P. Jackson, *Screen for DNA-damage-responsive histone modifications identifies H3K9Ac and H3K56Ac in human cells.* Embo j, 2009. 28(13): p. 1878-89.

74. Guo, R., et al., *GCN5 and E2F1 stimulate nucleotide excision repair by promoting H3K9 acetylation at sites of damage.* Nucleic Acids Res, 2011. 39(4): p. 1390-7.

75. Zheng, X., et al., *Histone acetyltransferase PCAF up-regulated cell apoptosis in hepatocellular carcinoma via acetylating histone H4 and inactivating AKT signaling.* Molecular cancer, 2013. 12(1): p. 96-96.

76. Barlev, N.A., et al., *Acetylation of p53 Activates Transcription through Recruitment of Coactivators/Histone Acetyltransferases.* Molecular Cell, 2001. 8(6): p. 1243-1254.

77. Patel, J.H., et al., *The c-MYC oncoprotein is a substrate of the acetyltransferases hGCN5/PCAF and TIP60.* Mol Cell Biol, 2004. 24(24): p. 10826-34.

78. Frank, S.R., et al., *Binding of c-Myc to chromatin mediates mitogen-induced acetylation of histone H4 and gene activation.* Genes Dev, 2001. 15(16): p. 2069-82.

79. Chen, L., et al., *Lysine acetyltransferase GCN5 potentiates the growth of non-small cell lung cancer via promotion of E2F1, cyclin D1, and cyclin E1 expression.* J Biol Chem, 2013. 288(20): p. 14510-21.

80. Yin, Y.W., et al., *The Histone Acetyltransferase GCN5 Expression Is Elevated and Regulated by c-Myc and E2F1 Transcription Factors in Human Colon Cancer.* Gene Expr, 2015. 16(4): p. 187-96.

81. Fei, H.J., et al., *PCAF acts as a gastric cancer suppressor through a novel PCAF-p16-CDK4 axis.* Am J Cancer Res, 2016. 6(12): p. 2772-2786.

82. Jia, Y.-L., et al., *P300/CBP-associated factor (PCAF) inhibits the growth of hepatocellular carcinoma by promoting cell autophagy.* Cell Death &Amp; Disease, 2016. 7: p. e2400.

83. Gai, X., et al., *Histone acetyltransferase PCAF accelerates apoptosis by repressing a GLI1/BCL2/BAX axis in hepatocellular carcinoma.* Cell Death &Amp; Disease, 2015. 6: p. e1712.

84. Li, Q., et al., *PCAF inhibits hepatocellular carcinoma metastasis by inhibition of epithelial-mesenchymal transition by targeting Gli-1.* Cancer Letters, 2016. 375(1): p. 190-198.

85. Ogryzko, V.V., et al., *The transcriptional coactivators p300 and CBP are histone acetyltransferases.* Cell, 1996. 87(5): p. 953-9.

86. Bannister, A.J., et al., *Stimulation of c-Jun activity by CBP: c-Jun residues Ser63/73 are required for CBP induced stimulation in vivo and CBP binding in vitro.* Oncogene, 1995. 11(12): p. 2509-14.

87. Attar, N. and S.K. Kurdistani, *Exploitation of EP300 and CREBBP Lysine Acetyltransferases by Cancer.* Cold Spring Harb Perspect Med, 2017. 7(3).

88. Iyer, N.G., H. Özdag, and C. Caldas, *p300/CBP and cancer.* Oncogene, 2004. 23: p. 4225.

89. Gu, W. and R.G. Roeder, *Activation of p53 sequence-specific DNA binding by acetylation of the p53 C-terminal domain.* Cell, 1997. 90(4): p. 595-606.

90. Costanzo, A., et al., *DNA damage-dependent acetylation of p73 dictates the selective activation of apoptotic target genes.* Mol Cell, 2002. 9(1): p. 175-86.

91. Chan, H.M., et al., *Acetylation control of the retinoblastoma tumour-suppressor protein.* Nat Cell Biol, 2001. 3(7): p. 667-74.

92. Marzio, G., et al., *E2F family members are differentially regulated by reversible acetylation.* J Biol Chem, 2000. 275(15): p. 10887-92.

93. Martinez-Balbas, M.A., et al., *Regulation of E2F1 activity by acetylation.* Embo j, 2000. 19(4): p. 662-71.

94. Munshi, N., et al., *Acetylation of HMG I(Y) by CBP turns off IFN beta expression by disrupting the enhanceosome.* Mol Cell, 1998. 2(4): p. 457-67.

95. Munshi, N., et al., *Coordination of a transcriptional switch by HMGI(Y) acetylation.* Science, 2001. 293(5532): p. 1133-6.

96. Kalkhoven, E., *CBP and p300: HATs for different occasions.* Biochemical Pharmacology, 2004. 68(6): p. 1145-1155.

97. Nicholson, T.B., N. Veland, and T. Chen, *Chapter 3 - Writers, Readers, and Erasers of Epigenetic Marks*, in *Epigenetic Cancer Therapy*, S.G. Gray, Editor. 2015, Academic Press: Boston. p. 31-66.

98. Avvakumov, N. and J. Côté, *The MYST family of histone acetyltransferases and their intimate links to cancer.* Oncogene, 2007. 26: p. 5395.

99. Ikura, T., et al., *Involvement of the TIP60 Histone Acetylase Complex in DNA Repair and Apoptosis.* Cell, 2000. 102(4): p. 463-473.

100. Sun, Y., et al., *A role for the Tip60 histone acetyltransferase in the acetylation and activation of ATM.* Proceedings of the National Academy of Sciences of the United States of America, 2005. 102(37): p. 13182-13187.

101. Tang, Y., et al., *Tip60-Dependent Acetylation of p53 Modulates the Decision between Cell-Cycle Arrest and Apoptosis.* Molecular Cell, 2006. 24(6): p. 827-839.

102. Sykes, S.M., et al., *Acetylation of the p53 DNA-Binding Domain Regulates Apoptosis Induction.* Molecular Cell, 2006. 24(6): p. 841-851.

103. ME, L.L., et al., *New p53 related genes in human tumors: significant downregulation in colon and lung carcinomas.* Oncol Rep, 2006. 16(3): p. 603-8.

104. Halkidou, K., et al., *Expression of Tip60, an androgen receptor coactivator, and its role in prostate cancer development.* Oncogene, 2003. 22: p. 2466.

105. Chen, G., et al., *Role of Tip60 in human melanoma cell migration, metastasis, and patient survival.* J Invest Dermatol, 2012. 132(11): p. 2632-41.

106. Zhao, H., S. Jin, and A.M. Gewirtz, *The Histone Acetyltransferase TIP60 Interacts with c-Myb and Inactivates Its Transcriptional Activity in Human Leukemia.* J Biol Chem, 2012. 287(2): p. 925-34.

107. Frank, S.R., et al., *MYC recruits the TIP60 histone acetyltransferase complex to chromatin.* EMBO Rep, 2003. 4(6): p. 575-80.

108. Awasthi, S., et al., *A Human T-Cell Lymphotropic Virus Type 1 Enhancer of Myc Transforming Potential Stabilizes Myc-TIP60 Transcriptional Interactions.* Molecular and Cellular Biology, 2005. 25(14): p. 6178-6198.

109. Taubert, S., et al., *E2F-dependent histone acetylation and recruitment of the Tip60 acetyltransferase complex to chromatin in late G1.* Mol Cell Biol, 2004. 24(10): p. 4546-56.

110. Hilfiker, A., et al., *mof, a putative acetyl transferase gene related to the Tip60 and MOZ human genes and to the SAS genes of yeast, is required for dosage compensation in Drosophila.* The EMBO Journal, 1997. 16(8): p. 2054-2060.

111. Cai, Y., et al., *Subunit Composition and Substrate Specificity of a MOF-containing Histone Acetyltransferase Distinct from the Male-specific Lethal (MSL) Complex.* Journal of Biological Chemistry, 2010. 285(7): p. 4268-4272.

112. Zhou, Y., et al., *Reversible acetylation of the chromatin remodelling complex NoRC is required for non-coding RNA-dependent silencing.* Nat Cell Biol, 2009. 11(8): p. 1010-6.

113. Li, X., et al., *Two Mammalian MOF Complexes Regulate Transcription Activation by Distinct Mechanisms.* Molecular Cell, 2009. 36(2): p. 290-301.

114. Gupta, A., et al., *Involvement of Human MOF in ATM Function.* Mol Cell Biol, 2005. 25(12): p. 5292-305.

115. Cao, L., et al., *Correlation of low expression of hMOF with clinicopathological features of colorectal carcinoma, gastric cancer and renal cell carcinoma.* Int J Oncol, 2014. 44(4): p. 1207-14.

116. Stefan, P., et al., *The histone acetyltransferase hMOF is frequently downregulated in primary breast carcinoma and medulloblastoma and constitutes a biomarker for clinical outcome in medulloblastoma.* International Journal of Cancer, 2008. 122(6): p. 1207-1213.

117. Liu, N., et al., *A potential diagnostic marker for ovarian cancer: Involvement of the histone acetyltransferase, human males absent on the first.* Oncol Lett, 2013. 6(2): p. 393-400.

118. Iizuka, M. and B. Stillman, *Histone acetyltransferase HBO1 interacts with the ORC1 subunit of the human initiator protein.* J Biol Chem, 1999. 274(33): p. 23027-34.

119. Doyon, Y., et al., *ING Tumor Suppressor Proteins Are Critical Regulators of Chromatin Acetylation Required for Genome Expression and Perpetuation.* Molecular Cell, 2006. 21(1): p. 51-64.

120. Hung, T., et al., *ING4 Mediates Crosstalk between Histone H3 K4 Trimethylation and H3 Acetylation to Attenuate Cellular Transformation.* Molecular Cell, 2009. 33(2): p. 248-256.

121. Iizuka, M., et al., *Hbo1 Links p53-Dependent Stress Signaling to DNA Replication Licensing.* Molecular and Cellular Biology, 2008. 28(1): p. 140-153.

122. Iizuka, M., et al., *Histone acetyltransferase Hbo1: Catalytic activity, cellular abundance, and links to primary cancers.* Gene, 2009. 436(1): p. 108-114.

123. Borrow, J., et al., *The translocation t(8;16)(p11;p13) of acute myeloid leukaemia fuses a putative acetyltransferase to the CREB–binding protein.* Nature Genetics, 1996. 14: p. 33.

124. Champagne, N., et al., *Identification of a human histone acetyltransferase related to monocytic leukemia zinc finger protein.* J Biol Chem, 1999. 274(40): p. 28528-36.

125. Max, C., et al., *MOZ is fused to p300 in an acute monocytic leukemia with t(8;22).* Genes, Chromosomes and Cancer, 2000. 28(2): p. 138-144.

126. Carapeti, M., et al., *A novel fusion between MOZ and the nuclear receptor coactivator TIF2 in acute myeloid leukemia.* Blood, 1998. 91(9): p. 3127-33.

127. Yoshiaki, C., et al., *The leucine twenty homeobox (LEUTX) gene, which lacks a histone acetyltransferase domain, is fused to KAT6A in therapy-related acute myeloid leukemia with t(8;19)(p11;q13).* Genes, Chromosomes and Cancer, 2014. 53(4): p. 299-308.

128. Kensuke, K., et al., *A novel fusion variant of the MORF and CBP genes detected in therapy-related myelodysplastic syndrome with t(10;16)(q22;p13).* British Journal of Haematology, 2003. 120(2): p. 271-273.

129. Yang, X.-J., *MOZ and MORF acetyltransferases: Molecular interaction, animal development and human disease.* Biochimica et Biophysica Acta (BBA) - Molecular Cell Research, 2015. 1853(8): p. 1818-1826.

130. Lynch, H., et al., *Can unknown predisposition in familial breast cancer be family-specific?* Breast J, 2013. 19(5): p. 520-8.

131. Grasso, C.S., et al., *The mutational landscape of lethal castration-resistant prostate cancer.* Nature, 2012. 487: p. 239.

132. Zack, T.I., et al., *Pan-cancer patterns of somatic copy-number alteration.* Nat Genet, 2013. 45(10): p. 1134-40.

133. Lv, D., et al., *Histone Acetyltransferase KAT6A Upregulates PI3K/AKT Signaling through TRIM24 Binding.* Cancer Research, 2017. 77(22): p. 6190-6201.

134. Taunton, J., C.A. Hassig, and S.L. Schreiber, *A mammalian histone deacetylase related to the yeast transcriptional regulator Rpd3p.* Science, 1996. 272(5260): p. 408-11.

135. Yang, W.M., et al., *Transcriptional repression by YY1 is mediated by interaction with a mammalian homolog of the yeast global regulator RPD3.* Proc Natl Acad Sci U S A, 1996. 93(23): p. 12845-50.

136. Sauve, A.A., *Sirtuin chemical mechanisms.* Biochim Biophys Acta, 2010. 1804(8): p. 1591-603.

137. Li, Y. and E. Seto, *HDACs and HDAC Inhibitors in Cancer Development and Therapy.* Cold Spring Harb Perspect Med, 2016. 6(10).

138. Yamaguchi, T., et al., *Histone deacetylases 1 and 2 act in concert to promote the G1-to-S progression.* Genes & Development, 2010. 24(5): p. 455-469.

139. Lagger, G., et al., *The tumor suppressor p53 and histone deacetylase 1 are antagonistic regulators of the cyclin-dependent kinase inhibitor p21/WAF1/CIP1 gene.* Mol Cell Biol, 2003. 23(8): p. 2669-79.

140. Lin, Y.C., et al., *Statins increase p21 through inhibition of histone deacetylase activity and release of promoter-associated HDAC1/2.* Cancer Res, 2008. 68(7): p. 2375-83.

141. Wilson, A.J., et al., *Histone deacetylase 3 (HDAC3) and other class I HDACs regulate colon cell maturation and p21 expression and are deregulated in human colon cancer.* J Biol Chem, 2006. 281(19): p. 13548-58.

142. Mottet, D., et al., *HDAC4 represses p21(WAF1/Cip1) expression in human cancer cells through a Sp1-dependent, p53-independent mechanism.* Oncogene, 2009. 28(2): p. 243-56.

143. Senese, S., et al., *Role for histone deacetylase 1 in human tumor cell proliferation.* Mol Cell Biol, 2007. 27(13): p. 4784-95.

144. Fan, J., et al., *Down-regulation of HDAC5 inhibits growth of human hepatocellular carcinoma by induction of apoptosis and cell cycle arrest.* Tumour Biol, 2014. 35(11): p. 11523-32.

145. Li, Y., L. Peng, and E. Seto, *HDAC10 Regulates Cell Cycle G2/M Phase Transition via a Novel Let-7-HMGA2-Cyclin A2 Pathway.* Molecular and Cellular Biology, 2015.

146. Archer, S.Y., et al., *The histone deacetylase inhibitor butyrate downregulates cyclin B1 gene expression via a p21/WAF-1-dependent mechanism in human colon cancer cells.* Am J Physiol Gastrointest Liver Physiol, 2005. 289(4): p. G696-703.

147. Zhang, J. and Q. Zhong, *Histone deacetylase inhibitors and cell death.* Cell Mol Life Sci, 2014. 71(20): p. 3885-901.

148. Riley, J.S., et al., *Prognostic and therapeutic relevance of FLIP and procaspase-8 overexpression in non-small cell lung cancer.* Cell Death & Disease, 2013. 4(12): p. e951.

149. Inoue, S., et al., *Inhibition of histone deacetylase class I but not class II is critical for the sensitization of leukemic cells to tumor necrosis factor-related apoptosis-inducing ligand-induced apoptosis.* Cancer Res, 2006. 66(13): p. 6785-92.

150. Feng, L., et al., *Histone deacetylase 3 inhibits expression of PUMA in gastric cancer cells.* J Mol Med (Berl), 2013. 91(1): p. 49-58.

151. Jung, K.H., et al., *HDAC2 overexpression confers oncogenic potential to human lung cancer cells by deregulating expression of apoptosis and cell cycle proteins.* J Cell Biochem, 2012. 113(6): p. 2167-77.

152. Peinado, H., et al., *Snail mediates E-cadherin repression by the recruitment of the Sin3A/histone deacetylase 1 (HDAC1)/HDAC2 complex.* Mol Cell Biol, 2004. 24(1): p. 306-19.

153. Aghdassi, A., et al., *Recruitment of histone deacetylases HDAC1 and HDAC2 by the transcriptional repressor ZEB1 downregulates E-cadherin expression in pancreatic cancer.* Gut, 2012. 61(3): p. 439-48.

154. Hubbert, C., et al., *HDAC6 is a microtubule-associated deacetylase.* Nature, 2002. 417(6887): p. 455-8.

155. Li, Y., D. Shin, and S.H. Kwon, *Histone deacetylase 6 plays a role as a distinct regulator of diverse cellular processes.* The FEBS Journal, 2013. 280(3): p. 775-793.

156. Seidel, C., et al., *Histone deacetylase 6 in health and disease.* Epigenomics, 2015. 7(1): p. 103-118.

157. Geng, H., et al., *HDAC4 protein regulates HIF1alpha protein lysine acetylation and cancer cell response to hypoxia.* J Biol Chem, 2011. 286(44): p. 38095-102.

158. Yoo, Y.G., G. Kong, and M.O. Lee, *Metastasis-associated protein 1 enhances stability of hypoxia-inducible factor-1alpha protein by recruiting histone deacetylase 1.* Embo j, 2006. 25(6): p. 1231-41.

159. Kong, X., et al., *Histone Deacetylase Inhibitors Induce VHL and Ubiquitin-Independent Proteasomal Degradation of Hypoxia-Inducible Factor 1α.* Molecular and Cellular Biology, 2006. 26(6): p. 2019-2028.

160. Seo, H.W., et al., *Transcriptional activation of hypoxia-inducible factor-1alpha by HDAC4 and HDAC5 involves differential recruitment of p300 and FIH-1.* FEBS Lett, 2009. 583(1): p. 55-60.

161. Kato, H., S. Tamamizu-Kato, and F. Shibasaki, *Histone deacetylase 7 associates with hypoxia-inducible factor 1alpha and increases transcriptional activity.* J Biol Chem, 2004. 279(40): p. 41966-74.

162. Caslini, C., et al., *Histone modifications silence the GATA transcription factor genes in ovarian cancer.* Oncogene, 2006. 25(39): p. 5446-61.

163. Lemercier, C., et al., *Class II histone deacetylases are directly recruited by BCL6 transcriptional repressor.* J Biol Chem, 2002. 277(24): p. 22045-52.

164. Perez-Salvia, M. and M. Esteller, *Bromodomain inhibitors and cancer therapy: From structures to applications.* Epigenetics, 2017. 12(5): p. 323-339.

165. Yang, Z., et al., *Recruitment of P-TEFb for stimulation of transcriptional elongation by the bromodomain protein Brd4.* Mol Cell, 2005. 19(4): p. 535-45.

166. Belkina, A.C. and G.V. Denis, *BET domain co-regulators in obesity, inflammation and cancer.* Nature reviews. Cancer, 2012. 12(7): p. 465-477.

167. Yang, Z., N. He, and Q. Zhou, *Brd4 recruits P-TEFb to chromosomes at late mitosis to promote G1 gene expression and cell cycle progression.* Mol Cell Biol, 2008. 28(3): p. 967-76.

168. Denis, G.V., et al., *Identification of transcription complexes that contain the double bromodomain protein Brd2 and chromatin remodeling machines.* J Proteome Res, 2006. 5(3): p. 502-11.

169. Sinha, A., D.V. Faller, and G.V. Denis, *Bromodomain analysis of Brd2-dependent transcriptional activation of cyclin A.* Biochem J, 2005. 387(Pt 1): p. 257-69.

170. Zou, Z., et al., *Brd4 maintains constitutively active NF-κB in cancer cells by binding to acetylated RelA.* Oncogene, 2014. 33(18): p. 2395-2404.

171. Sengupta, S., et al., *Inhibition of BET proteins impair estrogen mediated growth and transcription in breast cancers by pausing RNA polymerase advancement.* Breast cancer research and treatment, 2015. 150(2): p. 265-278.

172. Loven, J., et al., *Selective inhibition of tumor oncogenes by disruption of super-enhancers.* Cell, 2013. 153(2): p. 320-34.

173. Pennacchio, L.A., et al., *Enhancers: five essential questions.* Nature Reviews Genetics, 2013. 14: p. 288.

174. Hnisz, D., et al., *Super-enhancers in the control of cell identity and disease.* Cell, 2013. 155(4): p. 934-47.

175. Filippakopoulos, P. and S. Knapp, *The bromodomain interaction module.* FEBS Letters, 2012. 586(17): p. 2692-2704.

176. Mujtaba, S., et al., *Structural Mechanism of the Bromodomain of the Coactivator CBP in p53 Transcriptional Activation.* Molecular Cell, 2004. 13(2): p. 251-263.

177. Wang, Q., et al., *Small organic molecules targeting PCAF bromodomain as potent inhibitors of HIV-1 replication.* MedChemComm, 2013. 4(4): p. 737-740.

178. Cieniewicz, A.M., et al., *The Bromodomain of Gcn5 Regulates Site Specificity of Lysine Acetylation on Histone H3.* Molecular & Cellular Proteomics : MCP, 2014. 13(11): p. 2896-2910.

179. Shen, W., et al., *Solution structure of human Brg1 bromodomain and its specific binding to acetylated histone tails.* Biochemistry, 2007. 46(8): p. 2100-10.

180. Hohmann, A.F., et al., *Sensitivity and engineered resistance of myeloid leukemia cells to BRD9 inhibition.* Nature Chemical Biology, 2016. 12: p. 672.

181. Yu, X., Z. Li, and J. Shen, *BRD7: a novel tumor suppressor gene in different cancers.* American Journal of Translational Research, 2016. 8(2): p. 742-748.

182. Burrows, A.E., A. Smogorzewska, and S.J. Elledge, *Polybromo-associated BRG1-associated factor components BRD7 and BAF180 are critical regulators of p53 required for induction of replicative senescence.* Proceedings of the National Academy of Sciences of the United States of America, 2010. 107(32): p. 14280-14285.

183. Lau, O.D., et al., *HATs off: selective synthetic inhibitors of the histone acetyltransferases p300 and PCAF.* Mol Cell, 2000. 5(3): p. 589-95.

184. Wu, J., et al., *Bisubstrate Inhibitors of the MYST HATs Esa1 and Tip60.* Bioorganic & Medicinal Chemistry, 2009. 17(3): p. 1381-1386.

185. Bandyopadhyay, K., *Spermidinyl-CoA-based HAT inhibitors block DNA repair and provide cancer-specific chemo- and radiosensitization.* 2009. 8(17): p. 2779-88.

186. Fiorentino, F., A. Mai, and D. Rotili, *Lysine acetyltransferase inhibitors: structure–activity relationships and potential therapeutic implications.* Future Medicinal Chemistry, 2018. 10(9): p. 1067-1091.

187. Hemshekhar, M., et al., *Emerging roles of anacardic acid and its derivatives: a pharmacological overview.* Basic Clin Pharmacol Toxicol, 2012. 110(2): p. 122-32.

188. Kiernan, R., et al., *Post-activation Turn-off of NF-κB-dependent Transcription Is Regulated by Acetylation of p65.* Journal of Biological Chemistry, 2003. 278(4): p. 2758-2766.

189. Tan, J., et al., *Anacardic acid (6-pentadecylsalicylic acid) induces apoptosis of prostate cancer cells through inhibition of androgen receptor and activation of p53 signaling.* Chinese Journal of Cancer Research, 2012. 24(4): p. 275-283.

190. Balasubramanyam, K., et al., *Small Molecule Modulators of Histone Acetyltransferase p300.* Journal of Biological Chemistry, 2003. 278(21): p. 19134-19140.

191. Balasubramanyam, K., et al., *Curcumin, a novel p300/CREB-binding protein-specific inhibitor of acetyltransferase, represses the acetylation of histone/nonhistone proteins and histone acetyltransferase-dependent chromatin transcription.* J Biol Chem, 2004. 279(49): p. 51163-71.

192. Shishodia, S., T. Singh, and M.M. Chaturvedi, *MODULATION OF TRANSCRIPTION FACTORS BY CURCUMIN*, in *The Molecular Targets and Therapeutic Uses of Curcumin in Health and Disease*, B.B. Aggarwal, Y.-J. Surh, and S. Shishodia, Editors. 2007, Springer US: Boston, MA. p. 127-148.

193. Nelson, K.M., et al., *The Essential Medicinal Chemistry of Curcumin.* Journal of Medicinal Chemistry, 2017. 60(5): p. 1620-1637.

194. Balasubramanyam, K., et al., *Polyisoprenylated Benzophenone, Garcinol, a Natural Histone Acetyltransferase Inhibitor, Represses Chromatin Transcription and Alters Global Gene Expression.* Journal of Biological Chemistry, 2004. 279(32): p. 33716-33726.

195. Saadat, N. and S.V. Gupta, *Potential Role of Garcinol as an Anticancer Agent.* Journal of Oncology, 2012. 2012: p. 8.

196. Mantelingu, K., et al., *Specific Inhibition of p300-HAT Alters Global Gene Expression and Represses HIV Replication.* Chemistry & Biology, 2007. 14(6): p. 645-657.

197. Ravindra, K.C., et al., *Inhibition of Lysine Acetyltransferase KAT3B/p300 Activity by a Naturally Occurring Hydroxynaphthoquinone, Plumbagin.* Journal of Biological Chemistry, 2009. 284(36): p. 24453-24464.

198. Subhash, P., et al., *Perspectives on medicinal properties of plumbagin and its analogs.* Medicinal Research Reviews, 2012. 32(6): p. 1131-1158.

199. Liu, Y., et al., *Anticancer Properties and Pharmaceutical Applications of Plumbagin: A Review.* Am J Chin Med, 2017. 45(3): p. 423-441.

200. Choi, K.-C., et al., *Epigallocatechin-3-Gallate, a Histone Acetyltransferase Inhibitor, Inhibits EBV-Induced B Lymphocyte Transformation via Suppression of RelA Acetylation.* Cancer Research, 2009. 69(2): p. 583-592.

201. Seong, A.-R., et al., *Delphinidin, a specific inhibitor of histone acetyltransferase, suppresses inflammatory signaling via prevention of NF-κB acetylation in fibroblast-like synoviocyte MH7A cells.* Biochemical and Biophysical Research Communications, 2011. 410(3): p. 581-586.

202. Patel, K., A. Jain, and D.K. Patel, *Medicinal significance, pharmacological activities, and analytical aspects of anthocyanidins 'delphinidin': A concise report.* Journal of Acute Disease, 2013. 2(3): p. 169-178.

203. Choi, K.-C., et al., *Gallic Acid Suppresses Lipopolysaccharide-Induced Nuclear Factor-κB Signaling by Preventing RelA Acetylation in A549 Lung Cancer Cells.* Molecular Cancer Research, 2009. 7(12): p. 2011-2021.

204. Verma, S., A. Singh, and A. Mishra, *Gallic acid: Molecular rival of cancer.* Environmental Toxicology and Pharmacology, 2013. 35(3): p. 473-485.

205. Selvi B, R., et al., *Sanguinarine Interacts with Chromatin, Modulates Epigenetic Modifications, and Transcription in the Context of Chromatin.* Chemistry & Biology, 2009. 16(2): p. 203-216.

206. Achkar, I.W., et al., *Anticancer potential of sanguinarine for various human malignancies.* Future Med Chem, 2017. 9(9): p. 933-950.

207. Choi, K.-C., et al., *Procyanidin B3, an inhibitor of histone acetyltransferase, enhances the action of antagonist for prostate cancer cells via inhibition of p300-dependent acetylation of androgen receptor.* Biochemical Journal, 2011. 433(1): p. 235-244.

208. Markus, B., et al., *Design, Synthesis, and Biological Evaluation of a Small-Molecule Inhibitor of the Histone Acetyltransferase Gcn5.* Angewandte Chemie International Edition, 2004. 43(30): p. 3974-3976.

209. Holmlund, T., et al., *GCN5 acetylates and regulates the stability of the oncoprotein E2A-PBX1 in acute lymphoblastic leukemia.* Leukemia, 2013. 27(3): p. 578-85.

210. Coffey, K., et al., *Characterisation of a Tip60 Specific Inhibitor, NU9056, in Prostate Cancer.* PLOS ONE, 2012. 7(10): p. e45539.

211. Gao, C., et al., *Rational design and validation of a Tip60 histone acetyltransferase inhibitor.* Sci Rep, 2014. 4: p. 5372.

212. Yang, H., et al., *Small-molecule inhibitors of acetyltransferase p300 identified by high-throughput screening are potent anticancer agents.* Mol Cancer Ther, 2013. 12(5): p. 610-20.

213. Bowers, E.M., et al., *Virtual Ligand Screening of the p300/CBP Histone Acetyltransferase: Identification of a Selective Small Molecule Inhibitor.* Chemistry & Biology, 2010. 17(5): p. 471-482.

214. Gao, X.-n., et al., *A Histone Acetyltransferase p300 Inhibitor C646 Induces Cell Cycle Arrest and Apoptosis Selectively in AML1-ETO-Positive AML Cells.* PLOS ONE, 2013. 8(2): p. e55481.

215. Wang, Y.M., et al., *Histone acetyltransferase p300/CBP inhibitor C646 blocks the survival and invasion pathways of gastric cancer cell lines.* Int J Oncol, 2017. 51(6): p. 1860-1868.

216. Ono, H., M.D. Basson, and H. Ito, *P300 inhibition enhances gemcitabine-induced apoptosis of pancreatic cancer.* Oncotarget, 2016. 7(32): p. 51301-51310.

217. He, H., et al., *Selective p300 inhibitor C646 inhibited HPV E6-E7 genes, altered glucose metabolism and induced apoptosis in cervical cancer cells.* Eur J Pharmacol, 2017. 812: p. 206-215.

218. Lasko, L.M., et al., *Discovery of a selective catalytic p300/CBP inhibitor that targets lineage-specific tumours.* Nature, 2017. 550(7674): p. 128-132.

219. Lim, W. and G. Song, *Inhibitory effects of delphinidin on the proliferation of ovarian cancer cells via PI3K/AKT and ERK 1/2 MAPK signal transduction.* Oncology letters, 2017. 14(1): p. 810-818.

220. Mann, B.S., et al., *FDA approval summary: vorinostat for treatment of advanced primary cutaneous T-cell lymphoma.* Oncologist, 2007. 12(10): p. 1247-52.

221. Bubna, A.K., *Vorinostat—An Overview.* Indian Journal of Dermatology, 2015. 60(4): p. 419-419.

222. Richon, V.M., et al., *Histone deacetylase inhibitor selectively induces p21WAF1 expression and gene-associated histone acetylation.* Proc Natl Acad Sci U S A, 2000. 97(18): p. 10014-9.

223. Tiffon, C., et al., *The histone deacetylase inhibitors vorinostat and romidepsin downmodulate IL-10 expression in cutaneous T-cell lymphoma cells.* Br J Pharmacol, 2011. 162(7): p. 1590-602.

224. Poole, R.M., *Belinostat: first global approval.* Drugs, 2014. 74(13): p. 1543-54.

225. Chowdhury, S., et al., *Histone deacetylase inhibitor belinostat represses survivin expression through reactivation of transforming growth factor beta (TGFbeta) receptor II leading to cancer cell death.* J Biol Chem, 2011. 286(35): p. 30937-48.

226. Garnock-Jones, K.P., *Panobinostat: first global approval.* Drugs, 2015. 75(6): p. 695-704.

227. Sivaraj, D., M.M. Green, and C. Gasparetto, *Panobinostat for the management of multiple myeloma.* Future Oncol, 2017. 13(6): p. 477-488.

228. Yoshida, M., et al., *Potent and specific inhibition of mammalian histone deacetylase both in vivo and in vitro by trichostatin A.* J Biol Chem, 1990. 265(28): p. 17174-9.

229. Karagiannis, T.C., et al., *Trichostatin A accentuates doxorubicin-induced hypertrophy in cardiac myocytes.* Aging (Albany NY), 2010. 2(10): p. 659-668.

230. Sholler, G.S., et al., *PCI-24781 (abexinostat), a novel histone deacetylase inhibitor, induces reactive oxygen species-dependent apoptosis and is synergistic with bortezomib in neuroblastoma.* J Cancer Ther Res, 2013. 2: p. 21.

231. Lopez, G., et al., *Combining PCI-24781, a novel histone deacetylase inhibitor, with chemotherapy for the treatment of soft tissue sarcoma.* Clin Cancer Res, 2009. 15(10): p. 3472-83.

232. Novotny-Diermayr, V., et al., *The oral HDAC inhibitor pracinostat (SB939) is efficacious and synergistic with the JAK2 inhibitor pacritinib (SB1518) in preclinical models of AML.* Blood Cancer J, 2012. 2(5): p. e69.

233. Zhao, J., et al., *The therapeutic properties of resminostat for hepatocellular carcinoma.* Oncoscience, 2018. 5(5-6): p. 196-208.

234. Savino, A.M., et al., *The histone deacetylase inhibitor givinostat (ITF2357) exhibits potent anti-tumor activity against CRLF2-rearranged BCP-ALL.* 2017. 31(11): p. 2365-2375.

235. Ganai, S.A., *Histone deacetylase inhibitor givinostat: the small-molecule with promising activity against therapeutically challenging haematological malignancies.* J Chemother, 2016. 28(4): p. 247-54.

236. Lai, C.J., et al., *CUDC-101, a multitargeted inhibitor of histone deacetylase, epidermal growth factor receptor, and human epidermal growth factor receptor 2, exerts potent anticancer activity.* Cancer Res, 2010. 70(9): p. 3647-56.

237. Galloway, T.J., et al., *A Phase I Study of CUDC-101, a Multitarget Inhibitor of HDACs, EGFR, and HER2, in Combination with Chemoradiation in Patients with Head and Neck Squamous Cell Carcinoma.* Clin Cancer Res, 2015. 21(7): p. 1566-73.

238. Vogl, D.T., et al., *Ricolinostat, the First Selective Histone Deacetylase 6 Inhibitor, in Combination with Bortezomib and Dexamethasone for Relapsed or Refractory Multiple Myeloma.* Clin Cancer Res, 2017. 23(13): p. 3307-3315.

239. Whittaker, S.J., et al., *Final results from a multicenter, international, pivotal study of romidepsin in refractory cutaneous T-cell lymphoma.* J Clin Oncol, 2010. 28(29): p. 4485-91.

240. Coiffier, B., et al., *Results from a pivotal, open-label, phase II study of romidepsin in relapsed or refractory peripheral T-cell lymphoma after prior systemic therapy.* J Clin Oncol, 2012. 30(6): p. 631-6.

241. Ueda, H., et al., *FR901228, a novel antitumor bicyclic depsipeptide produced by Chromobacterium violaceum No. 968. I. Taxonomy, fermentation, isolation, physico-chemical and biological properties, and antitumor activity.* J Antibiot (Tokyo), 1994. 47(3): p. 301-10.

242. Kwon, H.J., et al., *Histone deacetylase inhibitor FK228 inhibits tumor angiogenesis.* Int J Cancer, 2002. 97(3): p. 290-6.

243. Sandor, V., et al., *P21-dependent g(1)arrest with downregulation of cyclin D1 and upregulation of cyclin E by the histone deacetylase inhibitor FR901228.* Br J Cancer, 2000. 83(6): p. 817-25.

244. Fournel, M., et al., *MGCD0103, a novel isotype-selective histone deacetylase inhibitor, has broad spectrum antitumor activity in vitro and in vivo.* Mol Cancer Ther, 2008. 7(4): p. 759-68.

245. Saito, A., et al., *A synthetic inhibitor of histone deacetylase, MS-27-275, with marked in vivo antitumor activity against human tumors.* Proceedings of the National Academy of Sciences, 1999. 96(8): p. 4592-4597.

246. Chateauvieux, S., et al., *Molecular and Therapeutic Potential and Toxicity of Valproic Acid.* Journal of Biomedicine and Biotechnology, 2010. 2010.

247. Su, J.M., et al., *Phase 1 study of valproic acid in pediatric patients with refractory solid or CNS tumors: a children's oncology group report.* Clin Cancer Res, 2011. 17(3): p. 589-97.

248. Kusaczuk, M., et al., *Phenylbutyrate—a pan-HDAC inhibitor—suppresses proliferation of glioblastoma LN-229 cell line.* Tumour Biology, 2016. 37(1): p. 931-942.

249. Nakagawa, H., S. Sasagawa, and K. Itoh, *Sodium butyrate induces senescence and inhibits the invasiveness of glioblastoma cells.* Oncology Letters, 2018. 15(2): p. 1495-1502.

250. Nicodeme, E., et al., *Suppression of inflammation by a synthetic histone mimic.* Nature, 2010. 468(7327): p. 1119-23.

251. Abedin, S.M., C.S. Boddy, and H.G. Munshi, *BET inhibitors in the treatment of hematologic malignancies: current insights and future prospects.* OncoTargets and therapy, 2016. 9: p. 5943-5953.

252. Asangani, I.A., et al., *Therapeutic targeting of BET bromodomain proteins in castration-resistant prostate cancer.* Nature, 2014. 510(7504): p. 278-82.

253. Lockwood, W.W., et al., *Sensitivity of human lung adenocarcinoma cell lines to targeted inhibition of BET epigenetic signaling proteins.* Proc Natl Acad Sci U S A, 2012. 109(47): p. 19408-13.

254. Lenhart, R., et al., *Sensitivity of Small Cell Lung Cancer to BET Inhibition Is Mediated by Regulation of ASCL1 Gene Expression.* Mol Cancer Ther, 2015. 14(10): p. 2167-74.

255. Li, G.Q., et al., *Suppression of BRD4 inhibits human hepatocellular carcinoma by repressing MYC and enhancing BIM expression.* Oncotarget, 2016. 7(3): p. 2462-74.

256. McCleland, M.L., et al., *CCAT1 is an enhancer-templated RNA that predicts BET sensitivity in colorectal cancer.* J Clin Invest, 2016. 126(2): p. 639-52.

257. Garcia, P.L., et al., *The BET bromodomain inhibitor JQ1 suppresses growth of pancreatic ductal adenocarcinoma in patient-derived xenograft models.* Oncogene, 2016. 35(7): p. 833-45.

258. Ocaña, A., C. Nieto-Jiménez, and A. Pandiella, *BET inhibitors as novel therapeutic agents in breast cancer.* Oncotarget, 2017. 8(41): p. 71285-71291.

259. Sahni, J.M. and R.A. Keri, *Targeting bromodomain and extraterminal proteins in breast cancer.* Pharmacological Research, 2018. 129: p. 156-176.

260. Sahni, J.M., et al., *Bromodomain and Extraterminal Protein Inhibition Blocks Growth of Triple-negative Breast Cancers through the Suppression of Aurora Kinases.* The Journal of biological chemistry, 2016. 291(45): p. 23756-23768.

261. Sahni, J.M., et al., *Mitotic Vulnerability in Triple-Negative Breast Cancer Associated with LIN9 Is Targetable with BET Inhibitors.* Cancer research, 2017. 77(19): p. 5395-5408.

262. Feng, Q., et al., *An epigenomic approach to therapy for tamoxifen-resistant breast cancer.* Cell Res, 2014. 24(7): p. 809-19.

263. Bihani, T., et al., *Resistance to everolimus driven by epigenetic regulation of MYC in ER+ breast cancers.* Oncotarget, 2015. 6(4): p. 2407-20.

264. Berenguer-Daize, C., et al., *OTX015 (MK-8628), a novel BET inhibitor, displays in vitro and in vivo antitumor effects alone and in combination with conventional therapies in glioblastoma models.* Int J Cancer, 2016. 139(9): p. 2047-55.

265. Coude, M.M., et al., *BET inhibitor OTX015 targets BRD2 and BRD4 and decreases c-MYC in acute leukemia cells.* Oncotarget, 2015. 6(19): p. 17698-712.

266. Dawson, M.A., et al., *Inhibition of BET recruitment to chromatin as an effective treatment for MLL-fusion leukaemia.* Nature, 2011. 478(7370): p. 529-33.

267. Chaidos, A., et al., *Potent antimyeloma activity of the novel bromodomain inhibitors I-BET151 and I-BET762.* Blood, 2014. 123(5): p. 697-705.

268. Dawson, M.A., et al., *Recurrent mutations, including NPM1c, activate a BRD4-dependent core transcriptional program in acute myeloid leukemia.* Leukemia, 2014. 28(2): p. 311-20.

269. Pastori, C., et al., *BET bromodomain proteins are required for glioblastoma cell proliferation.* Epigenetics, 2014. 9(4): p. 611-20.

270. Gallagher, S.J., et al., *The epigenetic regulator I-BET151 induces BIM-dependent apoptosis and cell cycle arrest of human melanoma cells.* J Invest Dermatol, 2014. 134(11): p. 2795-2805.

271. Liu, A., D. Fan, and Y. Wang, *The BET bromodomain inhibitor i-BET151 impairs ovarian cancer metastasis and improves antitumor immunity.* Cell Tissue Res, 2018.

272. Esteve-Arenys, A., et al., *The BET bromodomain inhibitor CPI203 overcomes resistance to ABT-199 (venetoclax) by downregulation of BFL-1/A1 in in vitro and in vivo models of MYC+/BCL2+ double hit lymphoma.* 2018. 37(14): p. 1830-1844.

273. Diaz, T., et al., *The BET bromodomain inhibitor CPI203 improves lenalidomide and dexamethasone activity in in vitro and in vivo models of multiple myeloma by blockade of Ikaros and MYC signaling.* Haematologica, 2017. 102(10): p. 1776-1784.

274. Bhadury, J., et al., *BET and HDAC inhibitors induce similar genes and biological effects and synergize to kill in Myc-induced murine lymphoma.* Proc Natl Acad Sci U S A, 2014. 111(26): p. E2721-30.

275. Picaud, S., et al., *PFI-1, a highly selective protein interaction inhibitor, targeting BET Bromodomains.* Cancer Res, 2013. 73(11): p. 3336-46.

276. Hupe, M.C., et al., *The BET-inhibitor PFI-1 diminishes AR/AR-V7 signaling in prostate cancer cells.* World J Urol, 2018.

277. Bonazzoli, E., et al., *Inhibition of BET Bromodomain Proteins with GS-5829 and GS-626510 in Uterine Serous Carcinoma, a Biologically Aggressive Variant of Endometrial Cancer.* 2018. 24(19): p. 4845-4853.

278. Picaud, S., et al., *Promiscuous targeting of bromodomains by bromosporine identifies BET proteins as master regulators of primary transcription response in leukemia.* 2016. 2(10): p. e1600760.

279. Theodoulou, N.H., et al., *Discovery of I-BRD9, a Selective Cell Active Chemical Probe for Bromodomain Containing Protein 9 Inhibition.* J Med Chem, 2016. 59(4): p. 1425-39.

280. Kramer, K.F., et al., *BRD9 Inhibition, Alone or in Combination with Cytostatic Compounds as a Therapeutic Approach in Rhabdoid Tumors.* Int J Mol Sci, 2017. 18(7).

281. Martin, L.J., et al., *Structure-Based Design of an in Vivo Active Selective BRD9 Inhibitor.* J Med Chem, 2016. 59(10): p. 4462-75.

282. Vangamudi, B., et al., *The SMARCA2/4 ATPase Domain Surpasses the Bromodomain as a Drug Target in SWI/SNF-Mutant Cancers: Insights*

from cDNA Rescue and PFI-3 Inhibitor Studies. Cancer Res, 2015. 75(18): p. 3865-3878.

283. Picaud, S., et al., *Generation of a Selective Small Molecule Inhibitor of the CBP/p300 Bromodomain for Leukemia Therapy.* Cancer Res, 2015. 75(23): p. 5106-5119.

284. Zucconi, B.E., et al., *Modulation of p300/CBP Acetylation of Nucleosomes by Bromodomain Ligand I-CBP112.* Biochemistry, 2016. 55(27): p. 3727-3734.

285. Conery, A.R., et al., *Bromodomain inhibition of the transcriptional coactivators CBP/EP300 as a therapeutic strategy to target the IRF4 network in multiple myeloma.* eLife, 2016. 5: p. e10483.

286. Xiang, Q., et al., *Discovery and optimization of 1-(1H-indol-1-yl)ethanone derivatives as CBP/EP300 bromodomain inhibitors for the treatment of castration-resistant prostate cancer.* Eur J Med Chem, 2018. 147: p. 238-252.

287. Chervona, Y. and M. Costa, *Histone modifications and cancer: biomarkers of prognosis?* American Journal of Cancer Research, 2012. 2(5): p. 589-597.

288. Ali, M., et al., *Tandem PHD fingers of MORF/MOZ acetyltransferases display selectivity for acetylated histone H3 and are required for the association with chromatin.* Journal of molecular biology, 2012. 424(5): p. 328-338.

289. Katalin, S., et al., *De novo mutations of the gene encoding the histone acetyltransferase KAT6B in two patients with Say-Barber/Biesecker/Young-Simpson syndrome.* American Journal of Medical Genetics Part A, 2013. 161(4): p. 884-888.

290. Kabos, P., et al., *Cytokeratin 5 positive cells represent a steroid receptor negative and therapy resistant subpopulation in luminal breast cancers.* Breast Cancer Res Treat, 2011. 128(1): p. 45-55.

291. Iwanaga, R., et al., *Expression of Six1 in luminal breast cancers predicts poor prognosis and promotes increases in tumor initiating cells by activation of extracellular signal-regulated kinase and transforming growth factor-beta signaling pathways.* Breast Cancer Res, 2012. 14(4): p. R100.

292. Mertz, J.A., et al., *Targeting MYC dependence in cancer by inhibiting BET bromodomains.* Proc Natl Acad Sci U S A, 2011. 108(40): p. 16669-74.

293. Collins, C., et al., *Positional cloning of ZNF217 and NABC1: Genes amplified at 20q13.2 and overexpressed in breast carcinoma.* Proceedings of the National Academy of Sciences of the United States of America, 1998. 95(15): p. 8703-8708.

294. Guy, C.T., R.D. Cardiff, and W.J. Muller, *Induction of mammary tumors by expression of polyomavirus middle T oncogene: a transgenic mouse model for metastatic disease.* Molecular and cellular biology, 1992. 12(3): p. 954-961.

295. Zhang, Y., et al., *HDAC-6 interacts with and deacetylates tubulin and microtubules in vivo.* Embo j, 2003. 22(5): p. 1168-79.

296. Spurgeon, S.E., et al., *Recommendations for Clinical Trial Development in Mantle Cell Lymphoma.* J Natl Cancer Inst, 2017. 109(1).

297. Howard, O.M., et al., *Rituximab and CHOP induction therapy for newly diagnosed mantle-cell lymphoma: molecular complete responses are not predictive of progression-free survival.* J Clin Oncol, 2002. 20(5): p. 1288-94.

298. Gazdar, A.F., P.A. Bunn, and J.D. Minna, *Small-cell lung cancer: what we know, what we need to know and the path forward.* Nature Reviews Cancer, 2017. 17: p. 725.

299. Kahali, B., et al., *Identifying targets for the restoration and reactivation of BRM.* Oncogene, 2013. 33: p. 653.

300. Chen, Q.Y., M. Costa, and H. Sun, *Structure and function of histone acetyltransferase MOF.* AIMS biophysics, 2015. 2(4): p. 555-569.

301. Taipale, M., et al., *hMOF histone acetyltransferase is required for histone H4 lysine 16 acetylation in mammalian cells.* Mol Cell Biol, 2005. 25(15): p. 6798-810.

302. Yu, H.C., et al., *An individual with blepharophimosis-ptosis-epicanthus inversus syndrome (BPES) and additional features expands the phenotype associated with mutations in KAT6B.* Am J Med Genet A, 2014. 164a(4): p. 950-7.

303. Kraft, M., et al., *Disruption of the histone acetyltransferase MYST4 leads to a Noonan syndrome-like phenotype and hyperactivated MAPK signaling in humans and mice.* J Clin Invest, 2011. 121(9): p. 3479-91.

304. Simpson, M.A., et al., *De novo mutations of the gene encoding the histone acetyltransferase KAT6B cause Genitopatellar syndrome.* Am J Hum Genet, 2012. 90(2): p. 290-4.

305. Sheikh, B.N., et al., *MOZ (MYST3, KAT6A) inhibits senescence via the INK4A-ARF pathway.* Oncogene, 2015. 34: p. 5807.

306. Baell, J.B., et al., *Inhibitors of histone acetyltransferases KAT6A/B induce senescence and arrest tumour growth.* Nature, 2018. 560(7717): p. 253-257.

307. Alvarado-Luna, G. and D. Morales-Espinosa, *Treatment for small cell lung cancer, where are we now?-a review.* Translational lung cancer research, 2016. 5(1): p. 26-38.

308. Prat, A., et al., *Clinical implications of the intrinsic molecular subtypes of breast cancer.* Breast, 2015. 24 Suppl 2: p. S26-35.

309. Tong, C.W.S., et al., *Recent Advances in the Treatment of Breast Cancer.* Frontiers in Oncology, 2018. 8: p. 227.

310. Yang, L., et al., *Repression of BET activity sensitizes homologous recombination–proficient cancers to PARP inhibition.* Science translational medicine, 2017. 9(400): p. eaal1645.

311. Shu, S., et al., *Response and resistance to BET bromodomain inhibitors in triple-negative breast cancer.* Nature, 2016. 529: p. 413.

312. Doroshow, D.B., J.P. Eder, and P.M. LoRusso, *BET inhibitors: a novel epigenetic approach.* Annals of Oncology, 2017. 28(8): p. 1776-1787.

313. Kim, H., et al., *Correlation between PDZK1, Cdc37, Akt and Breast Cancer Malignancy: The Role of PDZK1 in Cell Growth through Akt Stabilization by Increasing and Interacting with Cdc37.* Molecular Medicine, 2014. 20(1): p. 270-279.

314. Grushko, T.A., et al., *MYC is amplified in BRCA1-associated breast cancers.* Clin Cancer Res, 2004. 10(2): p. 499-507.

315. Karakashev, S., et al., *BET bromodomain inhibition synergizes with PARP inhibitor in epithelial ovarian cancer.* Cell reports, 2017. 21(12): p. 3398-3405.

316. Chen, P.B., et al., *Hdac6 regulates Tip60-p400 function in stem cells.* Elife, 2013. 2: p. e01557.

317. Haberland, M., R.L. Montgomery, and E.N. Olson, *The many roles of histone deacetylases in development and physiology: implications for disease and therapy.* Nature reviews. Genetics, 2009. 10(1): p. 32-42.

318. Gryder, B.E., Q.H. Sodji, and A.K. Oyelere, *Targeted cancer therapy: giving histone deacetylase inhibitors all they need to succeed.* Future Med Chem, 2012. 4(4): p. 505-24.

319. Tannock, I.F., et al., *Limited Penetration of Anticancer Drugs through Tumor Tissue.* A Potential Cause of Resistance of Solid Tumors to Chemotherapy, 2002. 8(3): p. 878-884.

320. McClure, J.J., X. Li, and C.J. Chou, *Advances and Challenges of HDAC Inhibitors in Cancer Therapeutics.* Adv Cancer Res, 2018. 138: p. 183-211.

321. Vose, J.M., *Mantle cell lymphoma: 2017 update on diagnosis, risk-stratification, and clinical management.* American Journal of Hematology, 2017. 92(8): p. 806-813.

322. Lwin, T., et al., *A microenvironment-mediated c-Myc/miR-548m/HDAC6 amplification loop in non-Hodgkin B cell lymphomas.* The Journal of Clinical Investigation, 2013. 123(11): p. 4612-4626.

323. Cosenza, M., et al., *Ricolinostat, a selective HDAC6 inhibitor, shows anti-lymphoma cell activity alone and in combination with bendamustine.* Apoptosis, 2017. 22(6): p. 827-840.

ANNEXES

Published OnlineFirst July 24, 2015; DOI: 10.1158/0008-5472.CAN-14-3702

Tumor and Stem Cell Biology

Cancer Research

KAT6B Is a Tumor Suppressor Histone H3 Lysine 23 Acetyltransferase Undergoing Genomic Loss in Small Cell Lung Cancer

Laia Simó-Riudalbas[1], Montserrat Pérez-Salvia[1], Fernando Setien[1], Alberto Villanueva[2], Catia Moutinho[1], Anna Martínez-Cardús[1], Sebastian Moran[1], Maria Berdasco[1], Antonio Gomez[1], Enrique Vidal[1], Marta Soler[1], Holger Heyn[1], Alejandro Vaquero[3], Carolina de la Torre[4], Silvia Barceló-Batllori[4], August Vidal[5], Luca Roz[6], Ugo Pastorino[7], Katalin Szakszon[8], Guntram Borck[9], Conceição S. Moura[10], Fátima Carneiro[11], Ilse Zondervan[12], Suvi Savola[12], Reika Iwakawa[13], Takashi Kohno[13], Jun Yokota[13,14], and Manel Esteller[1,15,16]

Abstract

Recent efforts to sequence human cancer genomes have highlighted that point mutations in genes involved in the epigenetic setting occur in tumor cells. Small cell lung cancer (SCLC) is an aggressive tumor with poor prognosis, where little is known about the genetic events related to its development. Herein, we have identified the presence of homozygous deletions of the candidate histone acetyltransferase *KAT6B*, and the loss of the corresponding transcript, in SCLC cell lines and primary tumors. Furthermore, we show, *in vitro* and *in vivo*, that the depletion of KAT6B expression enhances cancer growth, while its restoration induces tumor suppressor–like features. Most importantly, we demonstrate that KAT6B exerts its tumor-inhibitory role through a newly defined type of histone H3 Lys23 acetyltransferase activity. *Cancer Res; 75(18); 3936–45. ©2015 AACR.*

Introduction

Small cell lung cancer (SCLC) accounts for about 15% of all lung cancers and is characterized by accelerated growth, frequent metastases, and premature death (1). Although SCLC patients demonstrate many times a complete initial response to chemotherapy, the tumor almost always returns probably due to the original presence of quiescent cells. If the total cancer volume is irradiated, survival of SCLC patients is improved. Importantly, we have poor second-line therapies especially when the cancer comes back quickly after first-line therapy is completed. In this regard, no new biologically targeted therapeutics have shown activity in this tumor type (2). Comprehensive genomic analyses have revealed genetically altered therapeutic targets in non–small cell lung carcinoma (3), but little is known about the genetic events involved in SCLC beyond the long-recognized high rate of *TP53* and *RB1* mutations (1). Molecular studies in SCLC have been hampered because these tumors are rarely resected, resulting in a lack of suitable tumor specimens. However, point mutations in genes encoding histone modifiers in SCLC have recently been described (4). In this regard, disruption of the histone modification landscape is a common event in cancer cells (5, 6), leading to significant changes in chromatin structure and gene expression affecting oncogenes and tumor suppressor genes (7, 8). In this context, much effort has been devoted to analyzing the exomes of histone modifiers in search of small nucleotide changes, but cancer-specific copy-number changes have not been particularly studied in profound detail. To address this issue, we have examined the existence of this type of gross genomic alteration for histone modifiers in SCLC that can functionally contribute to the tumoral phenotype and that are of translational relevance.

Materials and Methods

Cell lines and primary tumor samples

Cell lines were purchased from the ATCC (WI-38, NCI-H1963, NCI-H740, NCI-H2171, NCI-H1048, NCI-N417, DMS-114, NCI-

[1]Cancer Epigenetics Group, Cancer Epigenetics and Biology Program (PEBC), Bellvitge Biomedical Research Institute (IDIBELL), Barcelona, Catalonia, Spain. [2]Translational Research Laboratory, Catalan Institute of Oncology (ICO), IDIBELL, Barcelona, Catalonia, Spain. [3]Chromatin Biology Group, IDIBELL, Barcelona, Catalonia, Spain. [4]Proteomics Unit at PEBC, IDIBELL, Barcelona, Catalonia, Spain. [5]Department of Pathology, Bellvitge University Hospital, IDIBELL, Barcelona, Catalonia, Spain. [6]Tumor Genomics Unit, Department of Experimental Oncology and Molecular Medicine, Fondazione IRCCS Istituto Nazionale dei Tumori, Milan, Italy. [7]Thoracic Surgery Unit, Department of Surgery, Fondazione IRCCS Istituto Nazionale dei Tumori, Milan, Italy. [8]Institute of Pediatrics, Clinical Genetics Center, University of Debrecen, Debrecen, Hungary. [9]Institute of Human Genetics, University of Ulm, Ulm, Germany. [10]Department of Pathology, Centro Hospitalar de São João, Porto, Portugal. [11]Institute of Molecular Pathology and Immunology of the University of Porto (IPATIMUP) and Medical Faculty of University of Porto, Porto, Portugal. [12]MRC-Holland, Amsterdam, the Netherlands. [13]Division of Genome Biology, National Cancer Center Research Institute, Tokyo, Japan. [14]Genomics and Epigenomics of Cancer Prediction Program, Institute of Predictive and Personalized Medicine of Cancer (IMPPC), Badalona, Catalonia, Spain. [15]Department of Physiological Sciences II, School of Medicine, University of Barcelona, Barcelona, Catalonia, Spain. [16]Institucio Catalana de Recerca i Estudis Avançats (ICREA), Barcelona, Catalonia, Spain.

Note: Supplementary data for this article are available at Cancer Research Online (http://cancerres.aacrjournals.org/).

Corresponding Author: Manel Esteller, Cancer Epigenetics and Biology Program (PEBC), 3rd Floor, Hospital Duran i Reynals, Av.Gran Via de L'Hospitalet 199–203, 08908 L'Hospitalet de Llobregat, Barcelona, Catalonia, Spain. Phone: 34-93-2607253; Fax: 34-93-2607219; E-mail: mesteller@idibell.cat

doi: 10.1158/0008-5472.CAN-14-3702

Published OnlineFirst July 24, 2015; DOI: 10.1158/0008-5472.CAN-14-3702

H1672, and NCI-H2029), from the Leibniz Institute DSMZ (Jena, Germany)-German Collection of Microorganisms and Cell Cultures (HCC-33), and from Sigma-Aldrich (DMS-273). All cell lines were characterized by short tandem repeat (STR) analysis profiling (LGS Standards SLU) within 6 months after receipt. DNA samples from primary and metastatic tumors of SCLC patients were obtained at surgery or autopsy from 1985 to 2010 at the National Cancer Center Hospital/National Cancer Center Biobank (Tokyo, Japan), Saitama Medical University (Saitama, Japan), and University of Tsukuba (Ibaraki, Japan). The study was approved by the corresponding Institutional Review Boards.

Genotyping microarrays and MLPA analysis

Illumina HumanOmni5-Quad (v1) genotyping array was processed as previously described (9). For multiplex ligation-dependent probe amplification (MLPA), genomic DNA was subjected to SALSA probemixes containing probes for the *KAT6B* gene, in addition to 21 reference probes, and the analyses were performed using Coffalyser.net software (MRC-Holland).

FISH analysis

The UCSC genome browser was used to select the 10q22.2 region probe for *KAT6B* detection (RP11-668A2), and the telomeric probe in 10p15.3 (RP11-361E18) was used as a control. Bacterial artificial chromosome (BAC) clones were obtained from the BACPAC Resource at the Children's Hospital Oakland Research Institute (Oakland, CA). Probes were labeled with Spectrum Green and Red dUTP (Abbott).

Quantitative genomic PCR

The deletion frequency of *KAT6B* (evaluated by SYBR Green) was calculated by the standard curve method using the 7900HT SDS program. Results are reported as the *n*-fold copy number increase relative to the *KAT6B* gene (10q22.3).

Expression and chromatin immunoprecipitation analysis

qRT-PCR, immunoblotting, immunohistochemistry, and chromatin immunoprecipitation (ChIP) assays were performed as previously described (9). For microarray expression array analysis, total RNA from NCI-N417 and HCC-33 cells expressing two different short hairpin RNA (shRNA) sequences against KAT6B and two different scrambled sequences was labeled and hybridized onto a Human Gene Expression G3 v2 60K array following the manufacturer's instructions. qRT-PCR/ChIP primers and antibodies are described in Supplementary Table S1.

KAT6B mutational screening

KAT6B mutations were screened in complementary DNA from 60 SCLC patients and the SCLC lines using direct sequencing (primers in Supplementary Table S1).

Short hairpin interference and ectopic expression assays

Two hairpin RNA (shRNA) molecules targeting two different gene sequences of KAT6B mRNA (shRNA5 and shRNA8) were designed and transfected into NCI-N417 and HCC-33 cells. The described sequences were mutated in two sites to obtain two shRNA scrambled sequences (Supplementary Table S1). For ectopic expression experiments, cDNA from human KAT6B longest isoform was purchased from BioSource (I.M.A.G.E. predicted full-length cDNA clones IRCBp5005P0112Q). *KAT6B* gene was subcloned from pCR-XL-TOPO bacterial expression vector to pRetroX-Tight-Pur mammalian expression vector, within the Retro-XTM Tet-On Advanced Inducible Expression System. A FLAG-tag in the carboxy-terminal end of the protein separated by a flexible Gly–Ser–Gly sequence was introduced.

In vitro proliferation assays

Cell proliferation was determined by the 3-(4,5-dimethyl-2-thiazolyl)-2,5-diphenyl-2H-tetrazolium bromide (MTT) and XTT (2,3-Bis-(2-Methoxy-4-Nitro-5-Sulfophenyl)-2H-Tetrazolium-5-Carboxanilide) assays. The soft agar colony formation assay was performed in 6-well culture plates. Cell proliferation was also determined by counting living cells in the Neubauer chamber using the Trypan blue approach. For dose–response assays, 10,000 to 20,000 cells were seeded in 96-well plates.

Mouse xenograft and metastasis models

Athymic nude male mice were subcutaneously injected in each flank with a total of 3.5×10^6 scramble NCI-N417 cells ($n = 10$) and shRNA NCI-N417 cells ($n = 10$). Tumor growth was monitored every 3 to 4 days by measuring tumor width and length. Pieces (3 mm^3) of subcutaneous mouse tumors were implanted in mouse lungs to generate an orthotopic SCLC mouse model (8 animals for each experiment). For the drug experiments, either irinotecan (24 mg/kg) or vehicle (saline buffer) was injected into the peritoneal cavity once a week for 3 weeks. For the metastasis model, 1.5×10^6 cells were injected into the spleen of 24 mice. Hepatic metastases were examined macroscopically and microscopically. Mouse experiments were approved by the IDIBELL Animal Care Committee.

LC/MS-MS, protein sequence database searching, and SRM

Histone extracts were loaded into an 18% acrylamide/bisacrylamide gel and the histone H3 bands were excised and trypsin-digested. Peptide extracts were analyzed by liquid chromatography-tandem mass spectrometry (LC/MS-MS) using an EASY nLC II (Proxeon) coupled to an amaZon ETD Ion Trap. Data were generated with Data Analyst 4.1 software. MS and MS/MS data were analyzed with ProteinScape 3.1.2 software using Mascot 2.4.0 as the search engine and SwissProt database. Identification was verified using a nanoACQUITY UPLC (Waters) chromatographer coupled to a high-resolution LTQ Orbitrap VelosTM MS. H3K23 acetylation levels were quantified by selected reaction monitoring (SRM) analyzing the precursor and fragment ion masses from acetylated peptides on a hybrid triple quadrupole/ion trap mass spectrometer instrument.

In vitro histone acetylation assays

Histone acetyltransferase assays were performed with GST-Flag–tagged KAT6B HAT domain purified from *Escherichia coli*. One hundred nanograms of HAT domain was incubated in 20 μmol/L [acetyl-1-14C] coenzyme A and 1 μg core histones for 2 hours at 30°C. Incorporated ^{14}C was detected by fluorography with low-energy intensifying screen and loading was assessed by Coomassie staining. For H3K23ac Western blot analysis, histone acetyltransferase assays using core histones as substrate and unlabeled acetyl coenzyme A as cofactor were performed. Recombinant GST-Histone H3 was purified from *E. coli* and used as substrates (1 μg) in the second radioactive histone acetylation assay.

Published OnlineFirst July 24, 2015; DOI: 10.1158/0008-5472.CAN-14-3702

Results

Presence of *KAT6B* homozygous deletion in SCLC that leads to gene inactivation

We first screened a collection of 10 human SCLC cell lines for copy-number alterations in histone-modifier genes using the Illumina Infinium HumanOmni5 microarray, which interrogates 4,301,332 SNPs per sample. These included HCC-33, NCI-N417, NCI-H1048, NCI-H1963, NCI-H2029, DMS-114, DMS-273, NCI-H740, NCI-H2171, and NCI-H1672. Primary normal tissues, such as lung epithelium and leukocytes, were used as normal copy-number control samples. Microarray SNP data have been deposited at the Gene Expression Omnibus (GEO) under accession number GSE62775. Using this approach, we confirmed the presence of previously described aberrant copy number changes in a subset of SCLC cell lines of histone modifiers, such as the CBP histone acetyltransferases (homozygous deletion; ref. 10) and the histone methyltransferase SETDB1 (gene amplification; ref. 9). However, and most interestingly, we found a previously unreported homozygous deletion of the candidate K(lysine) acetyltransferase 6B (*KAT6B*; refs. 11–13), also known as *MYST4* and *MORF*, in two of the 10 (20%) SCLC cell lines: NCI-H1963 (463,888 bp) and NCI-H740 (780,137 bp; Fig. 1A). The tumor suppressor *PTEN*, undergoing also homozygous deletion in SCLC (14) and located 12,830,231 bp far away from the *KAT6B* gene, was not included within the described minimal deleted regions. *KAT6B* undergoes genomic translocation in subtypes of acute myeloid

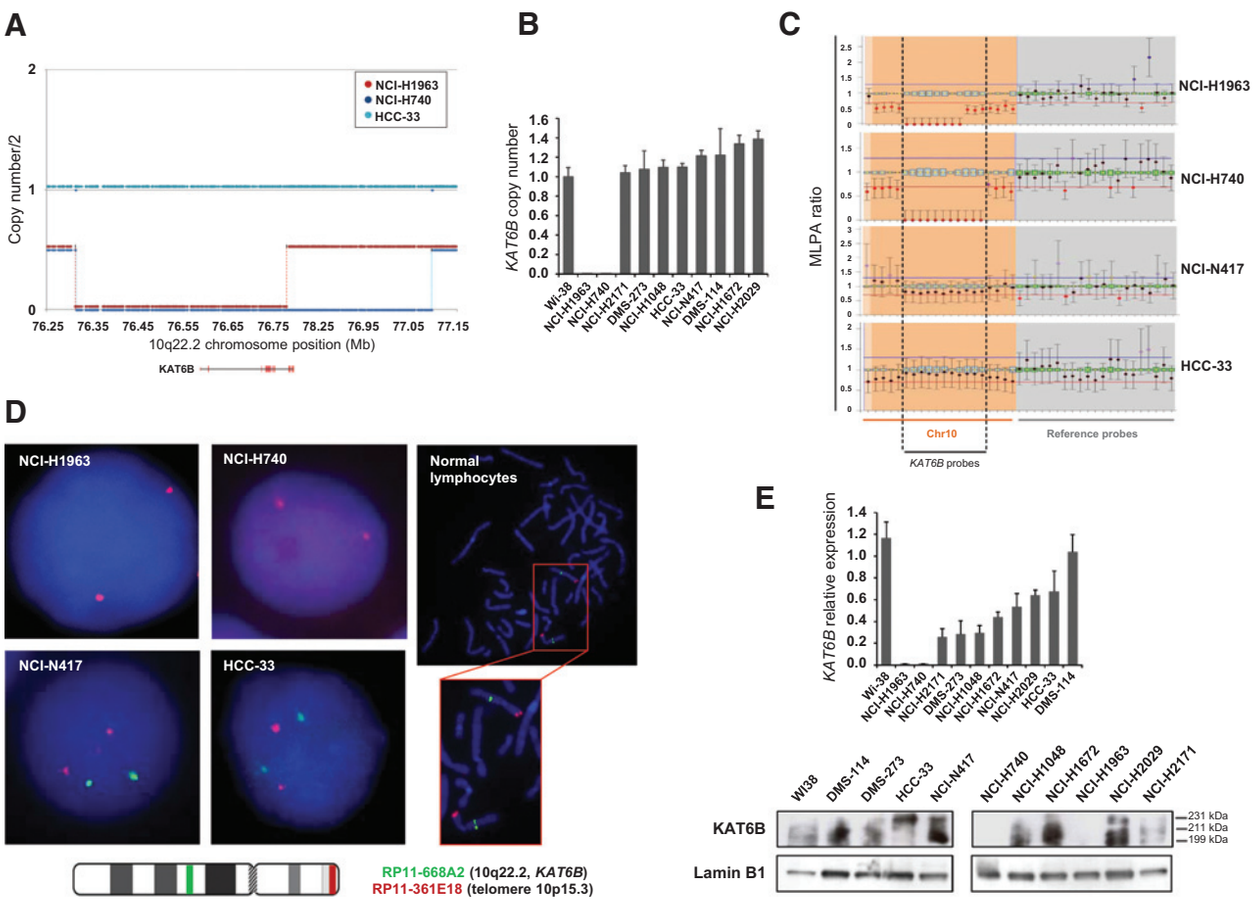

Figure 1.
Determination of *KAT6B* gene homozygous deletion and its association with RNA and protein loss in SCLC cell lines. A, graph depicting the homozygously deleted *KAT6B* region in 10q22.2, identified with the Illumina Infinium HumanOmni5 microarray. The NCI-H1963 cell line has the smallest deleted region (463,888 bp) that encompasses the *KAT6B* gene. NCI-H740 has a homozygously deleted region of (780,137 bp). HCC-33 is shown as an example of an SCLC cell line with two *KAT6B* normal copies. B, assessment of *KAT6B* copy number by quantitative genomic PCR. The amplification frequency of *KAT6B* was calculated by the standard curve method using the 7900HT SDS program. DNA from normal lung fibroblasts (Wi-38) was used as the reference standard. C, MLPA assay. Two different probe mixes contain one probe for each exon of the *KAT6B* gene, two probes upstream and one probe for intron 3 (orange). Twenty reference probes are included (gray). MLPA images from one of the two probe mixes are shown. Values of 0 were considered as homozygous loss. NCI-H1963 and NCI-H740 cell lines show the *KAT6B* homozygous deletion, while HCC-33 and NCI-N417 are shown as examples of *KAT6B* two copy number cells. D, FISH of the *KAT6B* gene. The UCSC Genome Browser was used to select the BAC clone spanning the 10p15.3 region for the *KAT6B* gene, RP11-361E18. A telomeric BAC clone located in the telomeric 10p15.3 region was used as a control. Probes were verified to give a single signal on normal commercial lymphocyte metaphase slides. E, quantitative reverse transcription PCR (top) and Western blot analysis (bottom) demonstrate loss of KAT6B mRNA and protein (the three existing isoforms are shown), respectively, in homozygously deleted NCI-H1963 and NCI-H740 cells.

Published OnlineFirst July 24, 2015; DOI: 10.1158/0008-5472.CAN-14-3702

leukemia (15, 16) and uterine leiomyomata (17), and *KAT6B* mutations have also been recently associated with the development of genitopatellar syndrome and Say-Barber-Biesecker-Young-Simpson syndrome (SBBYSS or Ohdo syndrome; refs. 18–20). Data mining of the Cancer Cell Line Encyclopedia copy-number variation data derived from a lower resolution SNP microarray (21) confirmed the presence of the *KAT6B* homozygous deletion in NCI-H1963 (Supplementary Fig. S1), while NCI-H740 was not included in the described study. Using a quantitative genomic PCR approach (Fig. 1B), MLPA (Fig. 1C) and fluorescence *in situ* hybridization (FISH; Fig. 1D), we confirmed the presence of the *KAT6B* homozygous deletion in NCI-H1963 and NCI-H740. The remaining eight SCLC cell lines did not exhibit any homozygous loss of *KAT6B* (Fig. 1A–D). *KAT6B* 5′-CpG island promoter methylation was not found in any SCLC cell line (Supplementary Fig. S1). Copy number and RNA expression levels for other histone acetyltransferases in the studied SCLC cell lines are shown in Supplementary Fig. S2. The SCLC cell lines underwent mutational screening for the 18 exons of the *KAT6B* gene using direct Sanger sequencing. The only nucleotide change that we detected was, in the NCI-H1048 cell line, a deletion of a GAA triplet coding for a glutamic acid within a stretch of glutamic amino acids in exon 16: it has been described as a polymorphic variant in the COSMIC Sanger database. Splicing defects were not specifically sought and could be another mechanism of gene silencing. Using quantitative reverse-transcription PCR and Western blot analysis, we found that the expression of KAT6B for both mRNA and protein was lost in the SCLC cancer cell lines NCI-H1963 and NCI-H740, which harbor the *KAT6B* homozygous deletion (Fig. 1E and Supplementary Fig. S3).

KAT6B has tumor suppressor–like properties in cancer cells

Once we had demonstrated the presence of *KAT6B* genomic loss in the SCLC cell lines, we examined its contribution to the tumorigenic phenotype *in vitro* and *in vivo*. We first analyzed the effect of KAT6B depletion in lung cancer cells retaining both copies of genes such as HCC33 and N417 (Fig. 2A and Supplementary Fig. S3). Supplementary Table S1 illustrates the shRNA sequences used. We observed that the reduction of KAT6B expression in the described cells, compared with the scramble shRNAs, had cancer growth-enhancing features, such as increased viability in the MTT assay (Fig. 2B), and formed more colonies (Fig. 2C). The XTT assay and Trypan blue staining further confirmed the growth-enhancing features of KAT6B-induced depletion (Supplementary Fig. S4). Interestingly, we observed that KAT6B shRNA-depleted cells also showed diminished expression of Brahma (BRM), a known KAT6B target (Supplementary Fig. S4; ref. 22), and the BRM-target E-cadherin (Supplementary Fig. S4; ref. 23), both being proteins that influence cell proliferation and metastasis. shRNA-mediated depletion of KAT6B also induced an increase in Rb phosphorylation (Supplementary Fig. S4). We next tested the ability of KAT6B shRNA-transfected N417 cells to form subcutaneous tumors in nude mice compared with scramble shRNA-transfected cells (Fig. 2D). Cells with shRNA-mediated depletion of KAT6B formed tumors with a greater weight and volume, but N417-scramble shRNA-transfected cells showed much lower tumorigenicity (Fig. 2D). We then performed an orthotopic growth study, implanting equal-sized tumor pieces from the subcutaneous model in the lung. We observed that orthotopic KAT6B shRNA-depleted tumors were significantly bigger and heavier than the scramble shRNA-derived tumors (Fig. 2E). We also proceeded with the converse experiment in which we used a retroviral-inducible expression system to recover by transfection the expression of KAT6B (longest isoform, 231 kDa) in H1963 cells bearing the aforementioned homozygous gene deletion (Fig. 2F). H1963 cells transfected with either the empty or the KAT6B vector were subcutaneously injected into the nude mice. Tumors originated from KAT6B-transfected H1963 cells had a significantly smaller volume than empty vector–transfected-derived tumors after doxycycline activation of gene expression (Fig. 2F). The halt in cellular growth upon restoration of KAT6B expression was observed for a long period of time (49 days; Supplementary Fig. S4). Finally, the potential distant inhibitory dissemination activity of KAT6B was measured in athymic mice by direct spleen injection and analysis of metastasis formation in the liver (Fig. 2G). Whereas numerous metastatic nodules developed in the liver following injection of KAT6B shRNA-depleted empty N417 cells, less metastasis formation was observed with the scramble shRNA-transfected cells (Fig. 2G). Overall, our findings suggest tumor-suppressor and dissemination-inhibitor roles for KAT6B.

Lysine 23 of histone H3 as a target of KAT6B-mediated acetylation

We next wondered about the molecular mechanisms that could mediate the identified tumor-suppressor features of KAT6B. In trying to address this issue, we first encountered the serious obstacle that the histone lysine residues targeted for acetylation by human KAT6B have not been completely characterized *in vivo*. KAT6B is a member of the MYST family of histone acetyltransferases that also includes KAT6A (MYST3/MOZ), KAT7 (MYST2/HBO1), KAT5 (Tip60), and KAT8 (MYST1/MOF; Fig. 3A). Because of the greater homology of KAT6B with the *bona fide* histone H3 acetyltransferase KAT6A (24–26), which also undergoes genomic translocations in acute myelogenous leukemia (27, 28), and the initially reported *in vitro* specificity of the KAT6A/KAT6B complex for histone H3 but not for histone H4 (29, 30), we focused our interest on this particular histone. To identify the histone H3 target sites for KAT6B, we compared H1963 cells transduced with an empty vector or with the full-length KAT6B expression vector (Fig. 3B). We used histone acid extracts resolved in an SDS–PAGE gel, followed by digestion of the histone H3 band and LC/MS-MS analysis. We determined from precursor signal intensity of the two acetylated peptides, K.QLATK^{23ac}AAR and R.KQLATK^{23ac}AAR.K, that acetylation of H3-K23 was enriched upon KAT6B transfection in H1963 cells (Fig. 3C). Targeted quantification of acetylation of H3-K23 residue by SRM confirmed the enhancement of this acetylated residue upon transduction-mediated recovery of KAT6B expression in the H1963 cell line (Fig. 3D). Using SRM, we were also able to study a patient with the SBBYS type of Ohdo syndrome, who was carrying truncating mutation of KAT6B (31, 32), and who showed a reduced level of both acetylated H3-K23 peptides (Fig. 3D). Western blot analyses also confirmed the LC/MS-MS data by showing that H3-K23 acetylation increased upon KAT6B transfection in H1963 cells (Fig. 3E). The activity of KAT6B for acetyl-K23 H3 was confirmed by Western blot analysis in two additional models: KAT6B shRNA-depleted N417 cells showed a reduction of the described acetylation

Published OnlineFirst July 24, 2015; DOI: 10.1158/0008-5472.CAN-14-3702

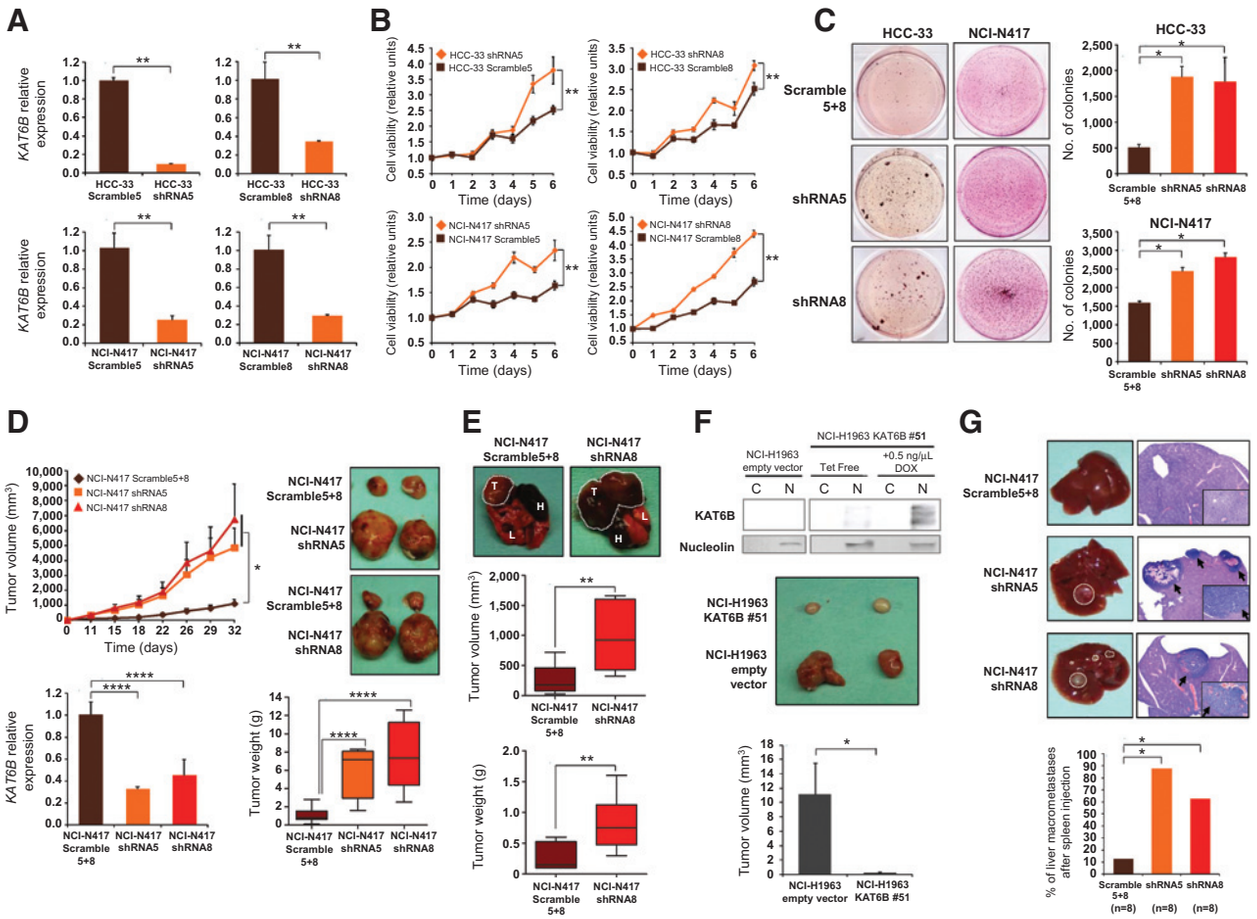

Figure 2.

Growth-inhibitory effects of KAT6B in SCLC. A, downregulation of the *KAT6B* gene by short hairpins using two target sequences (shRNA5 and shRNA8) in NCI-N417 and HCC-33 cells. Significance of permutation tests, **, $P < 0.01$. B, the short hairpin KAT6B-depleted cells were significantly more viable in the MTT assay than in the scrambled shRNA-transfected cells. Significance of ANOVAs, **, $P < 0.01$. C, the colony formation assay showed that NCI-N417 and HCC-33 cells transfected with the shRNA against KAT6B formed significantly more colonies than did scrambled shRNA-transfected cells. Data are mean ± SEM ($n = 3$). Significance of permutation tests, *, $P < 0.05$. D, effect of KAT6B shRNA-mediated depletion on the growth of subcutaneous tumors in nude mice derived from NCI-N417 cells. There was a significant increase in tumor volume and weight in the KAT6B shRNA-depleted cells. Data are mean ± SEM ($n = 10$). Low KAT6B mRNA levels in shRNA5 and shRNA8 NCI-N417 tumors confirmed the stability of the transfection after 32 days. ANOVAs, *, $P < 0.05$; ****, $P < 0.0001$. E, KAT6B shRNA-mediated depletion also significantly increased the volume and weight of orthotopic tumors derived from NCI-N417 cells implanted in the lung of nude mice. Significance of permutation tests, *, $P < 0.05$. F, recovery of KAT6B expression in NCI-H1963 cells (top), using a retroviral transfection Tet-ON system, decreased the volume of subcutaneous tumors implanted in nude mice (bottom). Significance of permutation test, *, $P < 0.05$. G, KAT6B shRNA-depleted NCI-N417 cells show significantly higher dissemination capacity after spleen injection. Illustrative surgery samples and hematoxylin and eosin staining of colonized liver after spleen injection are shown. Fisher exact test, *, $P < 0.05$.

mark (Fig. 3E), and the aforementioned SBBYS type of Ohdo syndrome patient with the *KAT6B* truncating mutation also had a lower level of acetylated H3-K23 (Fig. 3E). KAT6B specificity for this histone residue was further demonstrated by showing that acetylation of lysine 14 of histone H3 and lysine 16 of histone H4, mediated by the MYST family members KAT6A (MYST3/MOZ; refs. 25, 26, 29) and KAT8 (MYST1/MOF; refs. 33, 34), respectively, were not modified upon KAT6B restoration, depletion, or mutation (Fig. 3E). We also developed *in vitro* histone acetylation assays to further show the activity of KAT6B for H3K23 acetylation. Using purified histone core proteins from HeLa cells and a construct for the KAT6B-specific HAT domain, we confirmed that it acetylated H3-K23 (Supplementary Fig. S5). Importantly, a mutant HAT domain protein for KAT6B in K815, a strictly conserved lysine residue in the MYST family (35), was unable to acetylate H3-K23 (Supplementary Fig. S5). In addition, the *in vitro* activity of KAT6B for H3-K23 was confirmed using a recombinant histone H3 as a substrate: the wild-type cloned KAT6B-HAT domain acetylated the described residue and the K815 mutant was unable to do so (Supplementary Fig. S5). Using shRNA-mediated depletion of four histone deacetylases (HDAC1, HDAC2, HDCA3, and HDAC6) in NCI-N417 cells, we observed that, upon HDAC1 downregulation, there was an increase in acetylated H3-K23 levels (Supplementary Fig. S5), suggesting that this last HDAC mediates the deacetylation event at this residue.

We next wondered about gene targets whose normal expression could be diminished in cancer cells by the loss of KAT6B-

Published OnlineFirst July 24, 2015; DOI: 10.1158/0008-5472.CAN-14-3702

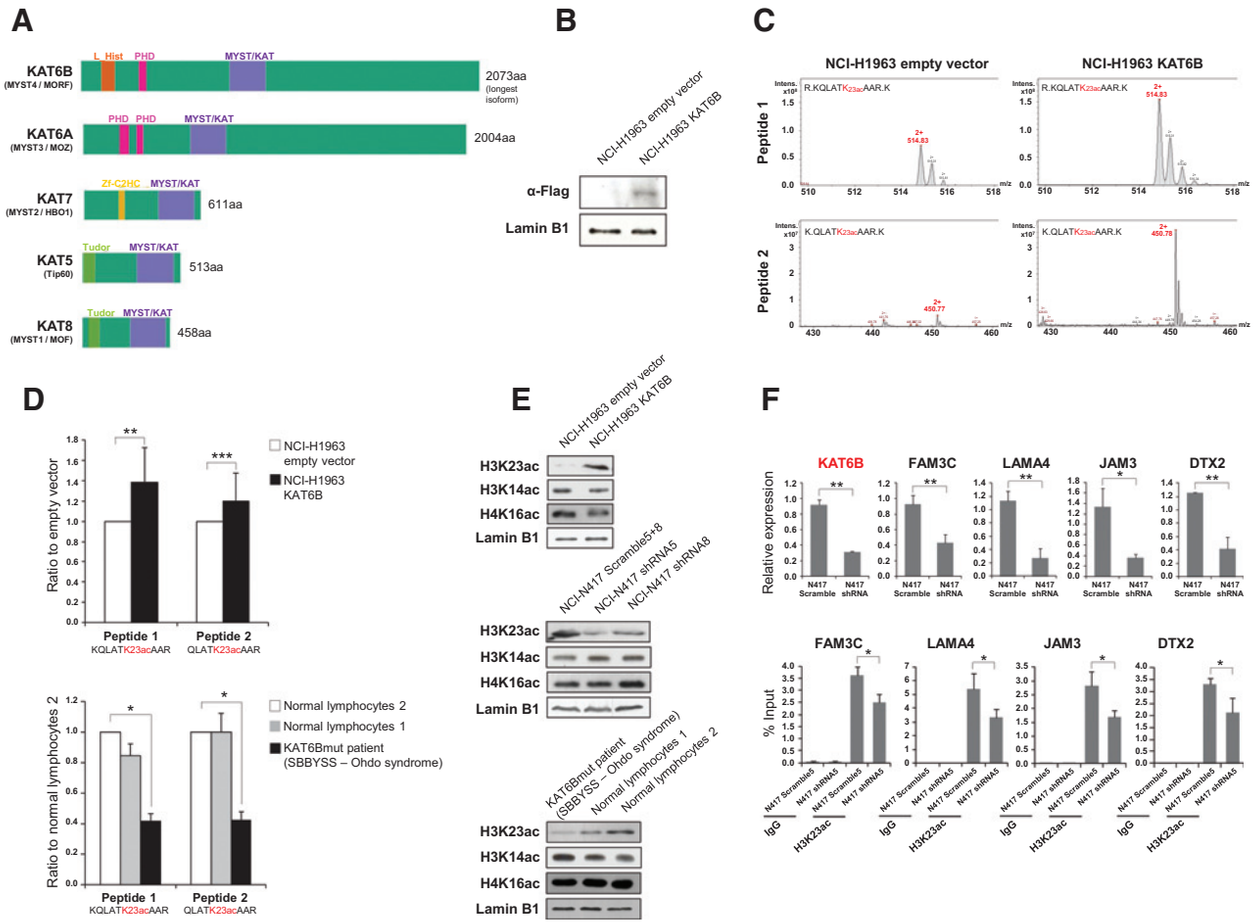

Figure 3.

KAT6B is a histone acetyltransferase targeting lysine 23 of histone H3. A, diagram of the MYST (SAS/MOZ) family with its recognized domains. The domains depicted are: L_Hist, linker histone H1/H5 domain H15; PHD, zinc_finger PHD type; Tudor_knot, RNA binding activity-knot of a chromodomain; Zf-C2HC, zinc finger, C2H2 type; MYST/KAT, MYST-type HAT (histone acetyltransferase) domain. B, Western blot analysis shows efficient transduction of KAT6B in NCI-H1963 cells in comparison with empty vector–transfected cells. C, MS spectra of QLATKacAAR and KQLATKacAAR tryptic peptides identified by LC/MS-MS. A representative figure is shown of the precursor intensity based on the integration of the signal from the extracted ion chromatogram. KAT6B NCI-H1963-transfected cells show a sharp increase in H3K23 acetylation intensity in both of the identified peptides compared with the empty vector–transfected cells. D, SRM quantification of the two H3K23ac peptides. Results were normalized with respect to the transitions of the corresponding heavy synthetic peptide and were related to the empty vector (top) or normal lymphocytes (bottom). Targeted quantification confirms the enhancement of this acetylated residue for the two peptides upon transfection-mediated recovery of KAT6B expression in H1963 cells (top) and its reduction in a patient of SBBYS type of Ohdo syndrome carrying a truncating mutation of *KAT6B* (bottom). Differences between the transitions were examined with the Student *t* test. *, $P < 0.05$; **, $P < 0.01$; ***, $P < 0.001$. E, Western blot analysis confirms the activity of KAT6B for H3K23ac upon transfection in NCI-H1963–deleted cells (top), in KAT6B shRNA-depleted NCI-N417 cells (middle), and in the SBBYSS or Ohdo syndrome patient with the *KAT6B*-truncating mutation (bottom). H3K14ac and H4K16ac did not change in any condition. F, qRT-PCR and H3K23ac ChIP analysis shows that, upon KAT6B-shRNA depletion in NCI-N417 cells, the downregulation of the candidate genes is associated with diminished acetylation of H3K23 residue in the promoters. Permutation tests, **, $P < 0.05$; *, $P < 0.01$.

mediated H3-K23 promoter acetylation, a histone mark usually associated with gene activation. To identify KAT6B target genes that might fit this candidate criterion, we used the shRNA approach to deplete KAT6B expression in N417 and HCC33 (both with the normal two copies of the *KAT6B* gene) followed by expression microarray hybridization. The complete list of genes undergoing expression changes is shown in Supplementary Table S2. Microarray expression data are available at GEO under accession number GSE62775. Using this approach, we identified 32 common genes repressed in both KAT6B-shRNA–depleted lung cancer cell lines that were upregulated in scramble shRNA-transfected cells (Supplementary Table S2). We confirmed the expression changes of 25 candidate genes (78%) by quantitative reverse-transcription PCR (Fig. 3F and Supplementary Fig. S5). The shift in H3-K23 acetylation status in their respective promoters for four candidate genes was observed by quantitative ChIP (Fig. 3F).

KAT6B genomic loss occurs in SCLC patients and confers sensitivity to irinotecan

Finally, we sought to demonstrate that the presence of *KAT6B* homozygous deletion was not a specific feature of *in vitro*–grown SCLC cell lines and that it also occurred in primary tumors of SCLC patients. Herein, we performed MLPA analyses for the

Published OnlineFirst July 24, 2015; DOI: 10.1158/0008-5472.CAN-14-3702

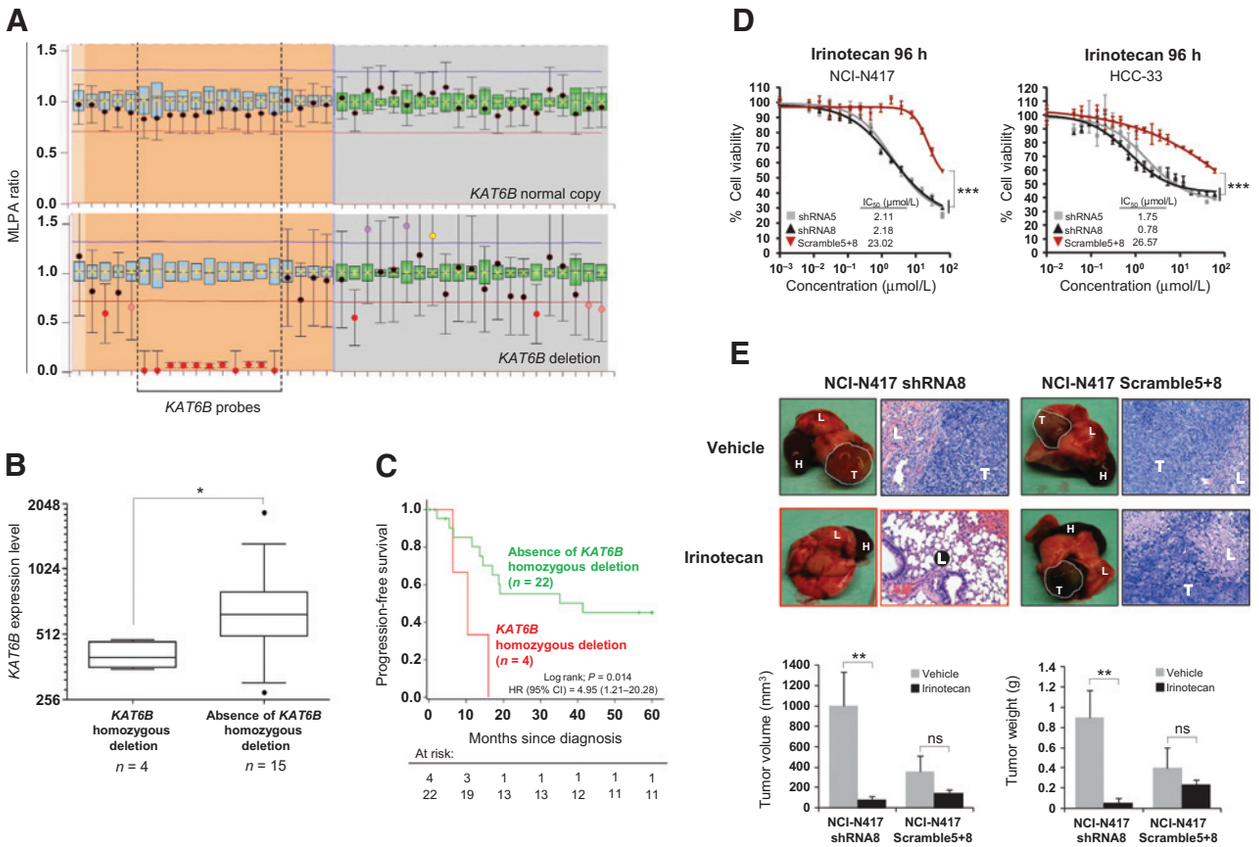

Figure 4.
Genomic loss of *KAT6B* in SCLC patients and sensitivity to irinotecan. A, examples of assessment of *KAT6B* copy number by MLPA in an SCLC patient without loss (top) and in one with homozygous deletion (bottom). B, the presence of *KAT6B* homozygous deletion is significantly associated with loss of expression of the KAT6B transcript in tumors from SCLC patients. The box plots illustrate the distribution of microarray expression values; the central solid line indicates the median; the limits of the box show the upper and lower quartiles. Mann–Whitney test, *, $P < 0.05$. C, the Kaplan–Meier analysis of progression-free survival among a cohort of SCLC cases according to KAT6B genomic status. KAT6B homozygous deletion is significantly associated with a shorter progression-free survival (log-rank test; $P = 0.014$; hazard ratio, 4.95; 95% confidence interval, 1.21–20.28). D, KAT6B shRNA-depleted NCI-N417 and HCC-33 cells were significantly more sensitive to the antiproliferative effect of irinotecan than were shRNA scramble-transfected cells. ANOVAs, ***, $P < 0.001$. E, orthotopic tumors-derived from KAT6B shRNA-depleted NCI-N417 cells were more sensitive to irinotecan than were shRNA scramble-derived tumors according to tumor volume and weight. L, Lung; H, Heart; T, Tumor. Significance of permutation tests, **, $P < 0.01$.

KAT6B locus using a collection of 60 tumors from SCLC patients and identified the *KAT6B* homozygous deletion in eight SCLC tumors (13%; Fig. 4A). Codeletion of *PTEN* was not observed in the SCLC tumors with *KAT6B* genomic loss according to CNV microarray data (36). Interestingly, screening for nonsense and indels in the *KAT6B* coding sequence in these 60 SLC cases, we identified a deletion of a "C" in the last exon (exon 18; c.3824delC) that later creates a stop codon and renders a 798 amino acids shorter protein, suggesting alternative pathways for the inactivation of the studied gene. Microarray expression data were available for 19 of the SCLC patients studied (36), including four who had the *KAT6B* homozygous deletion, and we observed an association between KAT6B genomic loss and lower levels of the transcript (Fig. 4B). Immunohistochemical analyses of 20 SCLC cases showed overall loss of *KAT6B* expression and acetyl-K23 H3 in the four tumors with *KAT6B* deletion, whereas both protein and histone mark were clearly stained in the remaining 16 samples without *KAT6B* genomic loss (except in one case where other mechanisms might account for an observed lack of staining). Illustrative cases are shown in Supplementary Fig. S6. Interestingly, in those SCLC patients for whom we have clinical information and a long follow-up over different stages ($n = 26$), the presence of the *KAT6B* homozygous deletion was associated with significantly shorter progression-free survival (log-rank test; $P = 0.014$; hazard ratio; 4.95; 95% confidence interval, 1.21–20.28; Fig. 4C).

The observation that the *KAT6B* homozygous deletion also occurred in SCLC patients with even worse prognosis prompted us to examine whether the loss of this HAT was associated with a particular sensitivity to any anticancer drug. Similar scenarios have been described for inhibitors of histone methyltransferases, such as DOT1L (37) and the BET family of acetyllysine–recognizing chromatin "adaptor" proteins (38–40) in which hematologic malignancies associated with gene-activating events involving targets of these pathways are more sensitive to these drugs. Using the model of KAT6B shRNA-transfected versus scramble shRNA-transfected N417 cells and the calculation of IC_{50} values according to the MTT assay, we did

Published OnlineFirst July 24, 2015; DOI: 10.1158/0008-5472.CAN-14-3702

not observe any difference between the two types of cells for 28 HDAC inhibitors that target class I, IIA, IIB, and III, in addition to pan-inhibitors (Supplementary Fig. S7). The compounds and their HDAC targets can be found in Supplementary Table S3. In addition, we did not observe any difference in sensitivity for classic SCLC chemotherapy agents such as cisplatin or etoposide (Supplementary Fig. S7). However, we found that KAT6B-depleted cells were significantly more sensitive to the growth-inhibitory effect mediated by the chemotherapy agent irinotecan, under clinical trials in SCLC, than any of the scramble shRNA clones (Fig. 4D). The same result was observed for HCC-33 cells (Fig. 4D). We also extended the *in vitro* cell viability experiments to the *in vivo* mouse model, thereby confirming that orthotopic SCLC tumors derived from KAT6B shRNA-depleted N417 cells were significantly more responsive to irinotecan than scramble shRNA-derived tumors (Fig. 4E). Within our SCLC clinical cohort, 42% of cases (11 of 26) underwent chemotherapy, but mainly platin-based combinations. Only 4 patients received irinotecan-based chemotherapy and none of them had *KAT6B* homozygous deletion. Thus, it was unfeasible to assess the role of *KAT6B* deletion as a predictive factor of irinotecan-based treatment outcome in this setting. Related to why irinotecan could be particularly effective in *KAT6B*-deleted tumors, it has been reported that the MYST family of HATs facilitates ataxia–telangiectasia mutated (ATM) kinase-mediated DNA-damage response (41) and, thus, it is possible that irinotecan-induced DNA damage cannot be so efficiently repaired in the KAT6B deficient tumors, leading to the enhanced cell death. In this regard, we found that KAT6B shRNA-mediated depletion caused a reduction of ATM expression and, upon irinotecan treatment, a lower phosphorylation of H2AX (Supplementary Fig. S8). Overall, these data suggest the existence of a therapeutic "niche" for the use of irinotecan in the aforementioned subset of SCLC cases harboring the *KAT6B* homozygous deletion.

Discussion

The initial high response rates to platinum-based chemotherapy regimens for SCLC in the late 1970s and early 1980s caused great expectations for these therapies. However, these hopes were shattered by the recognition of low 5-year survival rates, in most instances only approximately 5% (1, 2, 42). More recent trials with targeted therapies in SCLC have failed with no new drugs progressing treatments beyond those of cisplatin and etoposide (1, 2, 42). One of the main reasons for this disappointing scenario is our limited knowledge of the molecular driver events in SCLC. Beyond the high prevalence of *TP53* and *RB1* mutations, which have not proven amenable to pharmacology-based therapies so far, we have a scarce knowledge of the genetic defects underlying the natural history of SCLC. A recent breakthrough in this area has been the identification of mutations in histone modifiers, such as the histone methyltransferase *MLL1* or the histone acetyltransferases *CREBBP* (*KAT3A*) and *EP300* (*KAT3B*), in a subset of SCLCs (4). In this context, our identification of *KAT6B* homozygous deletions in both SCLC cell lines and primary tumors upgrades the genetic disruption of histone modifier genes as the second most common class of altered genes in SCLC. Importantly, we define for the first time, an *in vivo* target site for the acetyltransferase activity of KAT6B, lysine 23 of histone H3. This histone posttranslational modification has been previously associated with a more open chromatin state and the transcriptional activation of the underlying DNA sequence (43, 44). Interestingly, the diminished acetylation of H3-K23 seems to be a hallmark of SCLC tumorigenesis, because the other two frequently mutated histone acetyltransferases (CREBBP and EP300) can also target this particular histone amino acid (43–45).

An interesting issue derived from our studies is the potential exploitation of the KAT6B histone acetyltransferase defect to design more personalized therapies that could improve the dismal outcome of SCLC. Epigenetic drugs are the focus of a growing interest in the cancer arena; however, a critical issue is going to be the selection of those patients that are more likely to respond to these compounds. For example, pediatric brainstem gliomas harboring a mutation in K27 of histone H3.3 are more sensitive to the pharmacologic inhibition of a K27 demethylase (46). Herein, we did not observe that KAT6B depletion increases sensitivity to HDAC inhibitors, but other epigenetic inhibitors can be tested in this model. These include bromodomain inhibitors, targeting BET (bromodomain and extra-terminal domain) proteins that "read" the acetylated histone residues (39–41), or inhibitors of histone methyltransferases/demethylases, taking in account the competition between acetylation and methylation that occurs at K23-H3 (47). In addition, because KAT6B tumor-suppressor properties are, in part, mediated by downstream genes, like *BRM*, then might the restoration of these gene(s) be therapeutic. However, we have already found a drug where the diminished expression of KAT6B increases SCLC sensitivity in cell and animal models: irinotecan. Currently, this compound is a second-line treatment for the extensive stage of SCLC, while a platinum agent and etoposide are first-line therapies (1, 2, 42). Interestingly, as irinotecan is an effective drug for other tumor types, such as colon cancer, it would be interesting to explore if KAT6B status is associated with sensitivity to this drug beyond SCLC. Herein, our results pinpoint a subgroup of SCLC patients, those carrying the *KAT6B* genomic loss, where prospective clinical trials to assess the efficacy of irinotecan can be further studied.

Disclosure of Potential Conflicts of Interest

No potential conflicts of interest were disclosed.

Authors' Contributions

Conception and design: A. Villanueva, U. Pastorino, I. Zondervan, M. Esteller
Development of methodology: L. Simó-Riudalbas, M. Pérez-Salvia, F. Setien, A. Villanueva, M. Berdasco, A. Vaquero, C. de la Torre, S. Barceló-Batllori, U. Pastorino, S. Savola
Acquisition of data (provided animals, acquired and managed patients, provided facilities, etc.): A. Villanueva, A. Martínez-Cardús, H. Heyn, A. Vaquero, C. de la Torre, S. Barceló-Batllori, A. Vidal, L. Roz, U. Pastorino, K. Szakszon, G. Borck, I. Zondervan, R. Iwakawa, T. Kohno, J. Yokota, M. Esteller
Analysis and interpretation of data (e.g., statistical analysis, biostatistics, computational analysis): L. Simó-Riudalbas, C. Moutinho, A. Martínez-Cardús, S. Moran, M. Berdasco, A. Gomez, E. Vidal, H. Heyn, A. Vaquero, S. Barceló-Batllori, A. Vidal, C.S. Moura, F. Carneiro, I. Zondervan, S. Savola, M. Esteller
Writing, review, and/or revision of the manuscript: L. Simó-Riudalbas, S. Moran, A. Vidal, L. Roz, G. Borck, C.S. Moura, F. Carneiro, S. Savola, R. Iwakawa, M. Esteller
Administrative, technical, or material support (i.e., reporting or organizing data, constructing databases): C. Moutinho, A. Martínez-Cardús, M. Soler, C. de la Torre, R. Iwakawa, M. Esteller
Study supervision: U. Pastorino, J. Yokota, M. Esteller

Acknowledgments

The authors thank Drs. Masayuki Noguchi, Ryo Nishikawa, Shun-ichi Watanabe, Yoshitaka Narita, and Koji Tsuta for providing SCLC tissues and patients' information.

Grant Support

Supported by the grants FP7/2007-2013 HEALTH-F2-2010-258677–CURELUNG, European Research Council Advanced grants 268626–EPINORC, SAF2011-22803, PIE13/00022-ONCOPROFILE, 13FIS037 and PT13/0001/0033, a Grant-in-Aid from the Ministry of Education, Culture, Sports, Science, and Technology of Japan, a National Cancer Center Research and Development Fund (26-A-1) Cellex Foundation and Catalan Government (2009SGR1315 and 2014SGR633, AGAUR).

The costs of publication of this article were defrayed in part by the payment of page charges. This article must therefore be hereby marked *advertisement* in accordance with 18 U.S.C. Section 1734 solely to indicate this fact.

Received December 22, 2014; revised July 3, 2015; accepted July 19, 2015; published OnlineFirst July 24, 2015.

References

1. van Meerbeeck JP, Fennell DA, De Ruysscher DK. Small-cell lung cancer. Lancet 2011;378:1741–55.
2. Pillai RN, Owonikoko TK. Small cell lung cancer: therapies and targets. Semin Oncol 2014;41:133–42.
3. Buettner R, Wolfm J, Thomas RK. Lessons learned from lung cancer genomics: the emerging concept of individualized diagnostics and treatment. J Clin Oncol 2013;31:1858–65.
4. Peifer M, Fernández-Cuesta L, Sos ML, George J, Seidel D, Kasper LH, et al. Integrative genome analyses identify key somatic driver mutations of small-cell lung cancer. Nat Genet 2012;44:1104–10.
5. Fraga MF, Ballestar E, Villar-Garea A, Boix-Chornet M, Espada J, Schotta G, et al. Loss of acetylation at Lys16 and trimethylation at Lys20 of histone H4 is a common hallmark of human cancer. Nat Genet 2005;37:391–400.
6. Seligson DB, Horvath S, Shi T, Yu H, Tze S, Grunstein M, et al. Global histone modification patterns predict risk of prostate cancer recurrence. Nature 2005;435:1262–6.
7. Berdasco M, Esteller M. Aberrant epigenetic landscape in cancer: how cellular identity goes awry. Dev Cell 2010;19:698–711.
8. Dawson MA, Kouzarides T. Cancer epigenetics: from mechanism to therapy. Cell 2012;150:12–27.
9. Rodriguez-Paredes M, Martinez de Paz A, Simó-Riudalbas L, Sayols S, Moutinho C, Moran S, et al. Gene amplification of the histone methyltransferase SETDB1 contributes to human lung tumorigenesis. Oncogene 2014;33:2807–13.
10. Kishimoto M, Kohno T, Okudela K, Otsuka A, Sasaki H, Tanabe C, et al. Mutations and deletions of the CBP gene in human lung cancer. Clin Cancer Res 2005;11:512–9.
11. Champagne N, Bertos NR, Pelletier N, Wang AH, Vezmar M, Yang Y, et al. Identification of a human histone acetyltransferase related to monocytic leukemia zinc finger protein. J Biol Chem 1999;274:28528–36.
12. Yang XJ, Ullah M. MOZ and MORF, two large MYSTic HATs in normal and cancer stem cells. Oncogene 2007;26:5408–19.
13. Klein BJ, Lalonde ME, Côté J, Yangm X J, Kutateladze TG. Crosstalk between epigenetic readers regulates the MOZ/MORF HAT complexes. Epigenetics 2014;9:186–93.
14. Forgacs E, Biesterveld EJ, Sekido Y, Fong K, Muneer S, Wistuba II, et al. Mutational analysis of the PTEN/MMAC1 gene in lung cancer. Oncogene 1998;17:1557–65.
15. Panagopoulos I, Fioretos T, Isaksson M, Samuelsson U, Billström R, Strömbeck B, et al. Fusion of the MORF and CBP genes in acute myeloid leukemia with the t(10;16)(q22;p13). Hum Mol Genet 2001;10:395–404.
16. Vizmanos JL, Larráyoz MJ, Lahortiga I, Floristán F, Alvarez C, Odero MD, et al. t(10;16)(q22;p13) and MORF-CREBBP fusion is a recurrent event in acute myeloid leukemia. Genes Chromosomes Cancer 2003;36:402–5.
17. Moore SD, Herrick SR, Ince TA, Kleinman MS, Dal Cin P, Morton CC, et al. Uterine leiomyomata with t(10;17) disrupt the histone acetyltransferase MORF. Cancer Res 2004;64:5570–7.
18. Clayton-Smith J, O'Sullivan J, Daly S, Bhaskar S, Day R, Anderson B, et al. Whole-exome-sequencing identifies mutations in histone acetyltransferase gene KAT6B in individuals with the Say-Barber-Biesecker variant of Ohdo syndrome. Am J Hum Genet 2011;89:675–81.
19. Campeau PM, Kim JC, Lu JT, Schwartzentruber JA, Abdul-Rahman OA, Schlaubitz S, et al. Mutations in KAT6B, encoding a histone acetyltransferase, cause Genitopatellar syndrome. Am J Hum Genet 2012;90:282–9.
20. Simpson MA, Deshpande C, Dafou D, Vissers LE, Woollard WJ, Holder SE, et al. *De novo* mutations of the gene encoding the histone acetyltransferase KAT6B cause Genitopatellar syndrome. Am J Hum Genet 2012;90:290–4.
21. Barretina J, Caponigro G, Stransky N, Venkatesan K, Margolin AA, Kim S, et al. The Cancer Cell Line Encyclopedia enables predictive modelling of anticancer drug sensitivity. Nature 2012;483:603–7.
22. Kahali B, Gramling SJ, Marquez SB, Thompson K, Lu L, Reisman D. Identifying targets for the restoration and reactivation of BRM. Oncogene 2014;33:653–64.
23. Banine F, Bartlett C, Gunawardena R, Muchardt C, Yaniv M, Knudsen ES, et al. SWI/SNF chromatin-remodeling factors induce changes in DNA methylation to promote transcriptional activation. Cancer Res 2005;65:3542–7.
24. Voss AK, Collin C, Dixon MP, Thomas T. Moz and retinoic acid coordinately regulate H3K9 acetylation, Hox gene expression, and segment identity. Dev Cell 2009;17:674–86.
25. Qiu Y, Liu L, Zhao C, Han C, Li F, Zhang J, et al. Combinatorial readout of unmodified H3R2 and acetylated H3K14 by the tandem PHD finger of MOZ reveals a regulatory mechanism for HOXA9 transcription. Genes Dev 2012;26:1376–91.
26. Dreveny I, Deeves SE, Fulton J, Yue B, Messmer M, Bhattacharya A, et al. The double PHD finger domain of MOZ/MYST3 induces α-helical structure of the histone H3 tail to facilitate acetylation and methylation sampling and modification. Nucl Acids Res 2014;42:822–35.
27. Borrow J, Stanton VP Jr, Andresen JM, Becher R, Behm FG, Chaganti RS, et al. The translocation t(8;16)(p11;p13) of acute myeloid leukaemia fuses a putative acetyltransferase to the CREB-binding protein. Nat Genet 1996;14:33–41.
28. Kitabayashi I, Aikawa Y, Yokoyama A, Hosoda F, Nagai M, Kakazu N, et al. Fusion of MOZ and p300 histone acetyltransferases in acute monocytic leukemia with a t(8;22)(p11;q13) chromosome translocation. Leukemia 2001;15:89–94.
29. Doyon Y, Cayrou C, Ullah M, Landry AJ, Côté V, Selleck W, et al. ING tumor suppressor proteins are critical regulators of chromatin acetylation required for genome expression and perpetuation. Mol Cell 2006;21:51–64.
30. Ali M, Yan K, Lalonde ME, Degerny C, Rothbart SB, Strahl BD, et al. Tandem PHD fingers of MORF/MOZ acetyltransferases display selectivity for acetylated histone H3 and are required for the association with chromatin. J Mol Biol 2012;424:328–38.
31. Szakszon K, Berényi E, Jakab A, Bessenyei B, Balogh E, Köbling T, et al. Blepharophimosis mental retardation syndrome Say-Barber/Biesecker/Young-Simpson type—new findings with neuroimaging. Am J Med Genet A 2011;155A:634–7.
32. Szakszon K, Salpietro C, Kakar N, Knegt AC, Oláh É, Dallapiccola B, et al. *De novo* mutations of the gene encoding the histone acetyltransferase KAT6B in two patients with Say-Barber/Biesecker/Young-Simpson syndrome. Am J Med Genet A 2013;161A:884–8.
33. Taipale M, Rea S, Richter K, Vilar A, Lichter P, Imhof A, et al. hMOF histone acetyltransferase is required for histone H4 lysine 16 acetylation in mammalian cells. Mol Cell Biol 2005;25:6798–810.
34. Smith ER, Cayrou C, Huang R, Lane WS, Côté J, Lucchesi JC, et al. A human protein complex homologous to the Drosophila MSL complex is responsible for the majority of histone H4 acetylation at lysine 16. Mol Cell Biol 2005;25:9175–88.

35. Yuan H, Rossetto D, Mellert H, Dang W, Srinivasan M, Johnson J, et al. MYST protein acetyltransferase activity requires active site lysine autoacetylation. EMBO J 2012;31:58–70.
36. Iwakawa R, Takenaka M, Kohno T, Shimada Y, Totoki Y, Shibata T, et al. Genome-wide identification of genes with amplification and/or fusion in small cell lung cancer. Genes Chromosomes Cancer 2013;52:802–16.
37. Daigle SR, Olhava EJ, Therkelsen CA, Majer CR, Sneeringer CJ, Song J, et al. Selective killing of mixed lineage leukemia cells by a potent small-molecule DOT1L inhibitor. Cancer Cell 2011;20:53–65.
38. Zuber J, Shi J, Wang E, Rappaport AR, Herrmann H, Sison EA, et al. RNAi screen identifies Brd4 as a therapeutic target in acute myeloid leukaemia. Nature 2011;478:524–8.
39. Delmore JE, Issa GC, Lemieux ME, Rahl PB, Shi J, Jacobs HM, et al. BET bromodomain inhibition as a therapeutic strategy to target c-Myc. Cell 2011;146:904–17.
40. Dawson MA, Prinjha RK, Dittmann A, Giotopoulos G, Bantscheff M, Chan WI, et al. Inhibition of BET recruitment to chromatin as an effective treatment for MLL-fusion leukaemia. Nature 2011;478:529–33.
41. Vonlaufen N, Naguleswaran A, Coppens I, Sullivan WJ Jr. MYST family lysine acetyltransferase facilitates ataxia telangiectasia mutated (ATM) kinase-mediated DNA damage response in Toxoplasma gondii. J Biol Chem 2010;285:11154–61.
42. Jett JR, Schild SE, Kesler KA, Kalemkerian GP. Treatment of small cell lung cancer: Diagnosis and management of lung cancer, 3rd ed: American College of Chest Physicians evidence-based clinical practice guidelines. Chest 2013;143:e400S–19S.
43. Kebede AF, Schneider R, Daujat S. Novel types and sites of histone modifications emerge as players in the transcriptional regulation contest. FEBS J 2015;282:1658–74.
44. Rothbart SB, Strahl BD. Interpreting the language of histone and DNA modifications. Biochim Biophys Acta 2014;1839:627–43.
45. Schiltz RL, Mizzen CA, Vassilev A, Cook RG, Allis CD, Nakatani Y, et al. Overlapping but distinct patterns of histone acetylation by the human coactivators p300 and PCAF within nucleosomal substrates. J Biol Chem 1999;274:1189–92.
46. Hashizume R, Andor N, Ihara Y, Lerner R, Gan H, Chen X, et al. Pharmacologic inhibition of histone demethylation as a therapy for pediatric brainstem glioma. Nat Med 2014;20:1394–6.
47. Papazyan R, Voronina E, Chapman JR, Luperchio TR, Gilbert TM, Meier E, et al. Methylation of histone H3K23 blocks DNA damage in pericentric heterochromatin during meiosis. Elife 2014;3:e02996.

Published OnlineFirst July 24, 2015; DOI: 10.1158/0008-5472.CAN-14-3702

Cancer Research
The Journal of Cancer Research (1916–1930) | The American Journal of Cancer (1931–1940)

AACR American Association for Cancer Research

KAT6B Is a Tumor Suppressor Histone H3 Lysine 23 Acetyltransferase Undergoing Genomic Loss in Small Cell Lung Cancer

Laia Simó-Riudalbas, Montserrat Pérez-Salvia, Fernando Setien, et al.

Cancer Res 2015;75:3936-3945. Published OnlineFirst July 24, 2015.

www.impactjournals.com/oncotarget/ Oncotarget, 2017, Vol. 8, (No. 31), pp: 51621-51629

Research Paper

Bromodomain inhibition shows antitumoral activity in mice and human luminal breast cancer

Montserrat Pérez-Salvia[1], Laia Simó-Riudalbas[1], Pere Llinàs-Arias[1], Laura Roa[1], Fernando Setien[1], Marta Soler[1], Manuel Castro de Moura[1], James E. Bradner[2], Eva Gonzalez-Suarez[1], Catia Moutinho[1] and Manel Esteller[1,3,4]

[1]Cancer Epigenetics and Biology Program (PEBC), Bellvitge Biomedical Research Institute (IDIBELL), Barcelona, Catalonia, Spain

[2]Novartis Institutes for Biomedical Research, Cambridge, MA, USA

[3]Physiological Sciences Department, School of Medicine and Health Sciences, University of Barcelona (UB), Barcelona, Catalonia, Spain

[4]Institució Catalana de Recerca i Estudis Avançats (ICREA), Barcelona, Catalonia, Spain

Correspondence to: *Catia Moutinho,* ***email:*** *cmoutinho@idibell.cat*
Manel Esteller, ***email:*** *mesteller@idibell.cat*

Keywords: *luminal breast cancer, bromodomain inhibitor, C-MYC, JQ1, mice model*

Received: *February 28, 2017* ***Accepted:*** *May 04, 2017* ***Published:*** *May 29, 2017*

ABSTRACT

BET bromodomain inhibitors, which have an antitumoral effect against various solid cancer tumor types, have not been studied in detail in luminal breast cancer, despite the prevalence of this subtype of mammary malignancy. Here we demonstrate that the BET bromodomain inhibitor JQ1 exerts growth-inhibitory activity in human luminal breast cancer cell lines associated with a depletion of the C-MYC oncogene, but does not alter the expression levels of the BRD4 bromodomain protein. Interestingly, expression microarray analyses indicate that, upon JQ1 administration, the antitumoral phenotype also involves downregulation of relevant breast cancer oncogenes such as the Breast Carcinoma-Amplified Sequence 1 (BCAS1) and the PDZ Domain-Containing 1 (PDZK1). We have also applied these *in vitro* findings in an *in vivo* model by studying a transgenic mouse model representing the luminal B subtype of breast cancer, the MMTV-PyMT, in which the mouse mammary tumor virus promoter is used to drive the expression of the polyoma virus middle T-antigen to the mammary gland. We have observed that the use of the BET bromodomain inhibitor for the treatment of established breast neoplasms developed in the MMTV-PyMT model shows antitumor potential. Most importantly, if JQ1 is given before the expected time of tumor detection in the MMTV-PyMT mice, it retards the onset of the disease and increases the survival of these animals. Thus, our findings indicate that the use of bromodomain inhibitors is of great potential in the treatment of luminal breast cancer and merits further investigation.

INTRODUCTION

Breast cancer is a leading cause of cancer death in women, estimated to account for more than 450,000 deaths worldwide every year [1]. Despite the improved early detection of the disease and the new therapies, the major health concern associated with breast cancer persists probably due to several factors, among them the biological heterogeneity of the pathology. Classical clinical and pathological markers, such as the status of the estrogen and progesterone receptors and human epidermal growth factor 2 (HER2) gene amplification, are useful for classifying patients according to prognosis and adequate treatments, but it has been the emergence of genomic technologies, such as global expression profiling, that has allowed an intrinsic molecular classification

[2–4]. In this regard, five distinct intrinsic molecular subtypes are recognized: luminal A, luminal B, HER-2 enriched, basal-like and claudin-low, together with a normal breast-like group [2–4]. These subgroups relate to the clinically used immunohistochemical classification and, for example, luminal A is estrogen receptor- and/or progesterone receptor-positive but with a low Ki-67 index, whereas luminal B is estrogen receptor- and/or progesterone receptor-positive and high Ki-67 index. Overall, the majority of breast tumors are positive for the hormone receptors and, thus, amenable to endocrine therapies. However, in the natural history of the disease, progression is associated with the acquisition of resistance to the endocrine treatment, limiting the efficacy of these pharmacological compounds. In addition, the survival curves of luminal B subtype cross those of basal-like disease at ten years [4]. Thus, given the high frequency of luminal breast cancer, the generation of endocrine therapy-associated resistances and the poor outcome of the luminal B subtype, the development of new drugs for these patients is essential.

One interesting avenue to explore is the targeting of the epigenome of breast cancer cells. In this regard, DNA demethylating agents and histone deacetylase inhibitors have been clinically approved for certain subtypes of leukemias and lymphomas [5]. New promising agents are compounds that can block the "reading" of the acetylated histone marks, preventing the active transcription of growth-promoting genes. This is the case of the BET bromodomain inhibitors that remove BET bromodomain proteins from their chromatin targets by competing with acetylated histone residues [6]. The patterns of histone acetylation shifts in human tumors [7] and recent data have shown that the BET bromodomain inhibitor inhibits the growth of triple-negative breast cancer cell lines and xenografts [8–15]. Thus, we sought to determine whether BET bromodomain inhibitors were also effective not only in luminal breast cancer cell lines, but also in a mouse model of luminal B breast cancer (MMTV-PyMT) [16]. Furthermore, we also characterized gene targets involved in the antiproliferative effect mediated by the BET bromodomain inhibitor JQ1 [17].

RESULTS

The bromodomain inhibitor JQ1 decreases cell viability of human luminal breast cancer cell lines in association with downregulation of C-MYC and mammary oncogenic proteins

To study the cellular impact of JQ1 as a candidate growth inhibitor for luminal breast cancer, we chose the initial biological model of two human cancer cell lines with a well characterized luminal phenotype, MCF7 and T47D [18, 19]. Using the 3-(4,5-dimethyl-2-thiazolyl)-2,5-diphenyl-2H-tetrazolium bromide (MTT) assay to measure cell viability in the chosen cancer cell lines, we observed that JQ1 inhibited cancer cell growth dose-dependently (Figure 1A). Interestingly, IC50 sensitivity to this first-in-class BET bromodomain inhibitor compound is in the same range as that of other antitumoral drugs that target histone modifications, such as histone deacetylases [20] and histone kinases [21, 22]. The next step was to show that the growth inhibition-mediated effect of the JQ1 compound occurred in the context of the induced downregulation of C-MYC, as has been described in other models [23, 24]. Western blot and quantitative reverse transcription-polymerase chain reaction (qRT-PCR) demonstrated that JQ1 diminished C-MYC expression levels (Figure 1B) in both luminal breast cancer cell lines. As expected [17, 23, 24], the use of JQ1 did not modify the expression levels of the bromodomain protein BRD4, as also shown by western blot and qRT-PCR (Figure 1B).

We next sought to identify other gene targets that, in addition to the well characterized depletion of the C-MYC oncogene, could also explain the observed growth inhibitory effect of the use of the BET bromodomain inhibitor. We performed an expression microarray experiment in MCF7 and T47D cells treated with a vehicle compared with those in which we used the JQ1 compound (Figure 2A). The expression microarray data have been deposited in the Gene Expression Omnibus (GEO) repository under Accession Number GSE95287. Of the set of 36,712 unique genes included in the microarray, 1,149 (3.1%) significantly changed in a shared manner in both cell lines; 420 (36.6%) of them were upregulated and 729 (63.4%) were downregulated. The latter set constitutes the putative direct substrates of JQ1 that act by removing the BET bromodomain proteins from their regulatory regions through competition with acetylated histone residues that are usually associated with active transcription [6]. Gene functional annotation analysis for these transcripts was performed by computing gene overlapping with GSEA KEGG and GO signature collections. Among the 729 genes downregulated upon JQ1 use, we observed an overrepresentation of KEGG pathways and GO biological process terms related with pathways in cancer and regulation of cell proliferation, respectively (False Discovery Rate q-value <0.05) (Supplementary Figure 1 and Supplementary Table 1). Among the top candidate genes commonly downregulated, our attention was particularly drawn by the presence of the transcripts for the PDZ Domain-Containing 1 (PDZK1) and the Breast Carcinoma-Amplified Sequence 1 (BCAS1) genes, which encode two oncoproteins that have been linked to mammary tumorigenesis [25–28]. PDZK1 promotes estrogen-mediated growth of breast cancer cells [25, 26], whereas BCAS1 undergoes gene amplification-associated overexpression in breast cancer

[27] and has been implicated in breast cancer progression [28]. The downregulation of these transcripts upon JQ1 administration was validated by qRT-PCR in the same RNA extracts as used for microarray hybridization (Figure 2B) and when the experiment was repeated in a new batch of cells treated for different times (Figure 2C). We also assessed to what extent the effects of JQ1 are mediated by its silencing of C-MYC compared to PDZK1 and BCAS1. Upon efficient short hairpin RNA (shRNA) mediated dowregulation of MYC, PDZK1 or BCAS1 in MCF7 and T47D (Supplementary Figure 2A), we observed a similar significant decrease in the cell viability determined by the MTT assay (Supplementary Figure 2B and 2C). These data suggest that all three proteins exert a similar role as growth promoting factors in these luminal breast cancer cell lines. Importantly, the growth inhibition mediated

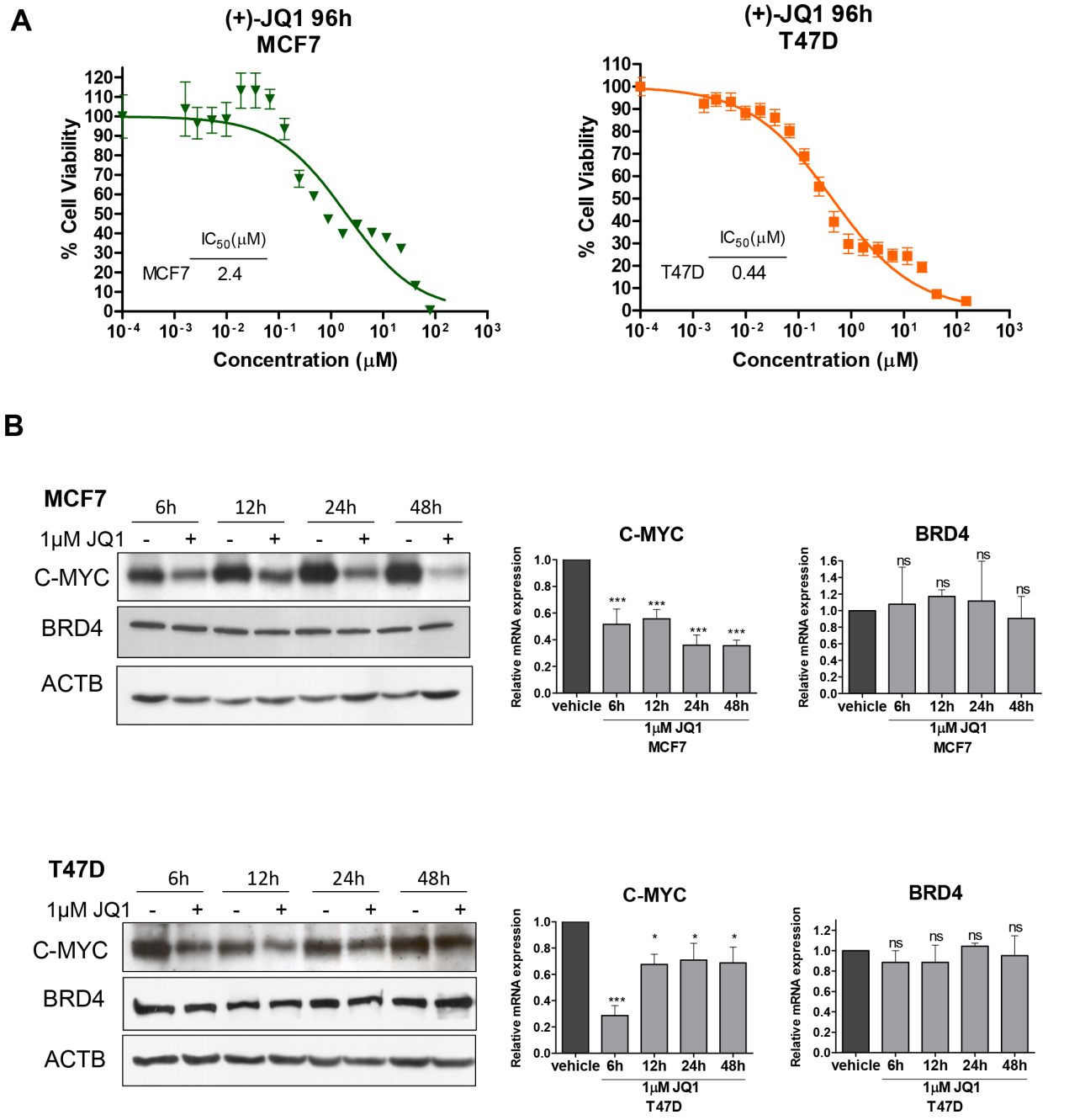

Figure 1: JQ1 treatment of human luminal breast cancer cell lines reduces cell viability and downregulates C-MYC. **(A)** Effect of JQ1 on cell viability determined by the MTT assay in MCF7 and T47D cells. The corresponding half-maximal inhibitory concentration (IC50) values are shown for each cell line. **(B)** Downregulation of C-MYC upon JQ1 treatment (1 μM) at 6, 12, 24 and 48 h in breast cancer cell lines, as determined by Western blot (left) and qRT-PCR (right). BRD4 expression levels do not change. *P<0.05; ***P<0.001; ns: non-significant.

by the use of JQ1 is higher than the one observed for the depletion of each factor (Supplementary Figure 2B and 2C). Thus, the observed growth-inhibitory effects of bromodomain inhibition in the luminal cells studied can be explained not only by the diminished expression of C-MYC, but also by a global reduction in the levels of transforming genes such as those exemplified by the PDZK1 and BCAS1 breast cancer oncogenes.

Bromodomain inhibition shows antitumoral activity and retards the onset of luminal breast tumors in the MMTV-PyMT luminal breast cancer mouse model

We next transferred our experiments from the *in vitro* and cell line assays described above to the *in vivo* setting in a mouse model of luminal breast cancer. The antitumoral activity of JQ1 was evaluated using MMTV-PyMT transgenic mice that spontaneously develop multifocal luminal B breast tumors [16]. To assess the efficacy of JQ1 at inhibiting the growth of established tumors, we started the treatment when the total tumor volumes of each animal reached ~ 1,000-2,700 mm^3 (Figure 3A). We randomly selected eight MMTV-PyMT mice as the control group treated with vehicle and another eight for JQ1 treatment (25 mg/kg). Tumor volume was monitored every 2-3 days. The lack of toxicity of the drug was found under the described conditions. The use of the BET bromodomain inhibitor was significantly associated with the development of smaller breast tumors than those that occurred in the control group (Figure 3B).

Finally, once we had established the efficacy of JQ1 at inhibiting the growth of established luminal breast tumors, we considered whether the drug not only had a

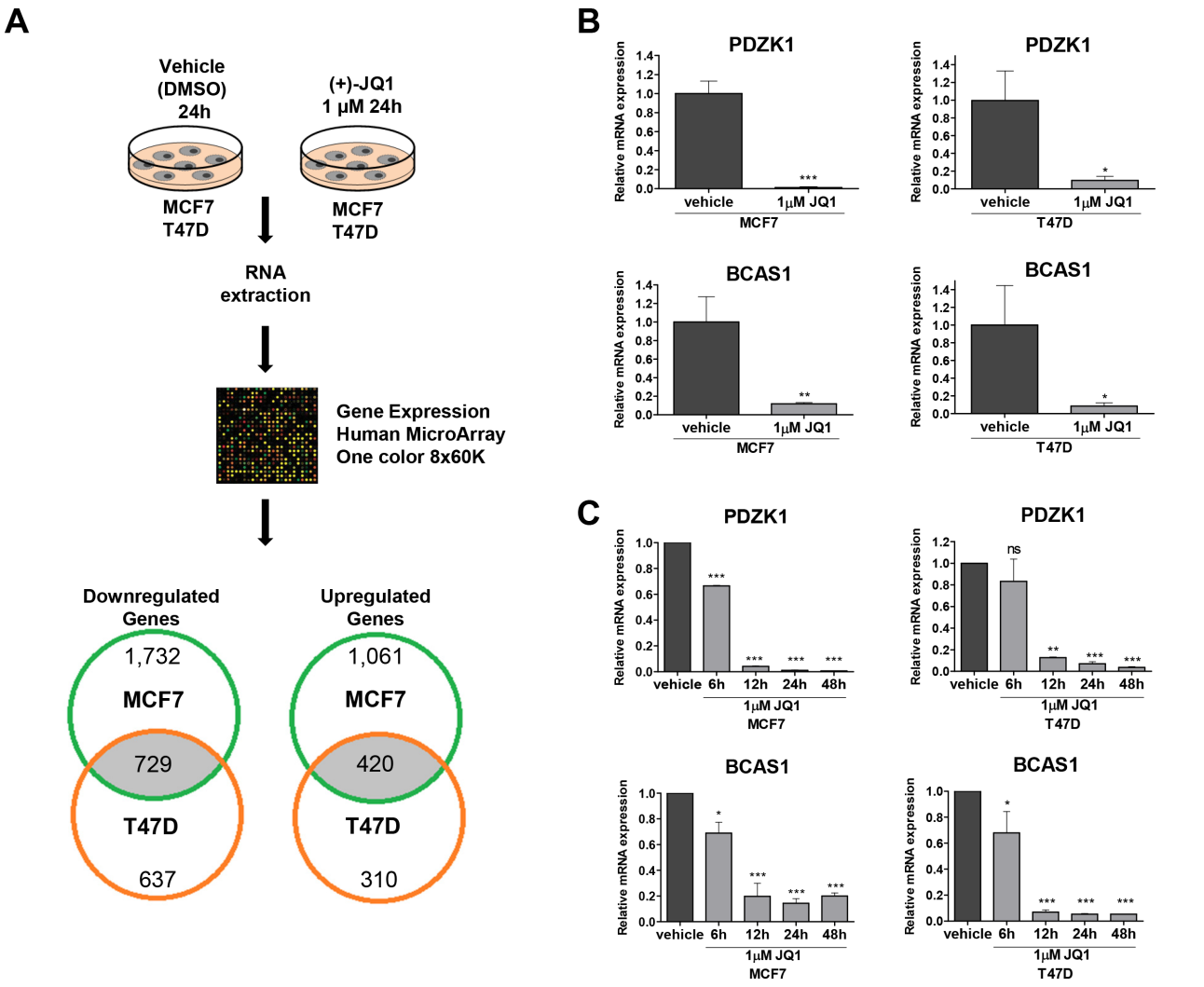

Figure 2: Expression microarray analyses identify PDZK1 and BCAS1 as breast cancer oncoproteins downregulated by JQ1 treatment in human luminal breast cancer cell lines. (A) Flowchart of the expression microarray experiment. **(B)** qRT-PCR validation of the microarray results for PDZK1 and BCAS1. **(C)** Downregulation of PDZK1 and BCAS1, determined by qRT-PCR, upon JQ1 use at different times. *P<0.05; **P<0.01; ***P<0.001.

therapeutic, but also a preventive effect. The impact of BET bromodomain inhibition on preventing spontaneous mammary tumors that naturally arise in MMTV-PyMT mice was evaluated as described in Figure 3C. Briefly, the MMTV-PyMT mice were randomly divided into a treatment group (25 mg/kg, n=5) and a vehicle group (n=7). JQ1 was administered when mice were 4 weeks old and when no palpable or visible tumors existed. Tumor volume was monitored every 2-3 days. We observed that those MMTV-PyMT mice receiving the BET bromodomain inhibitor experienced later onset of breast cancer and developed significantly smaller tumors (Figure 3D). Most notably, the treatment with JQ1 increased the overall survival of the MMTV-PyMT mice in comparison to those that received the mock treatment (Figure 3E). These results suggest that bromodomain inhibitors may exert a protective anti-tumorigenic effect against tumorigenesis, and that it would be worthwhile exploring the benefits of using them in the context of individuals with a high-risk of developing breast cancer and other malignancies.

DISCUSSION

Herein, we have analyzed the effect of the BET bromodomain inhibitor JQ1 in the context of luminal breast cancer in mouse models and human cells. Our results highlight how using the epigenetic drug yields remarkable antitumoral effects against luminal breast tumors in association with the downregulation of its known target C-MYC. These findings represent the first demonstration *in vivo* of the antiproliferative characteristics of this small molecule for this particular mammary cancer subtype. Importantly, the impact of JQ1 on the transcriptional landscape of the treated breast cancer cells extends beyond the depletion of C-MYC to affect hundreds of other genes. Among the candidates that can also mediate the growth inhibitory action of the compound, we have further characterized the JQ1-associated downregulation of two important breast cancer oncogenes, BCAS1 and PDZK1. Our findings suggest that the anticancer effect observed for the BET bromodomain inhibitor involves many cellular and signaling pathways

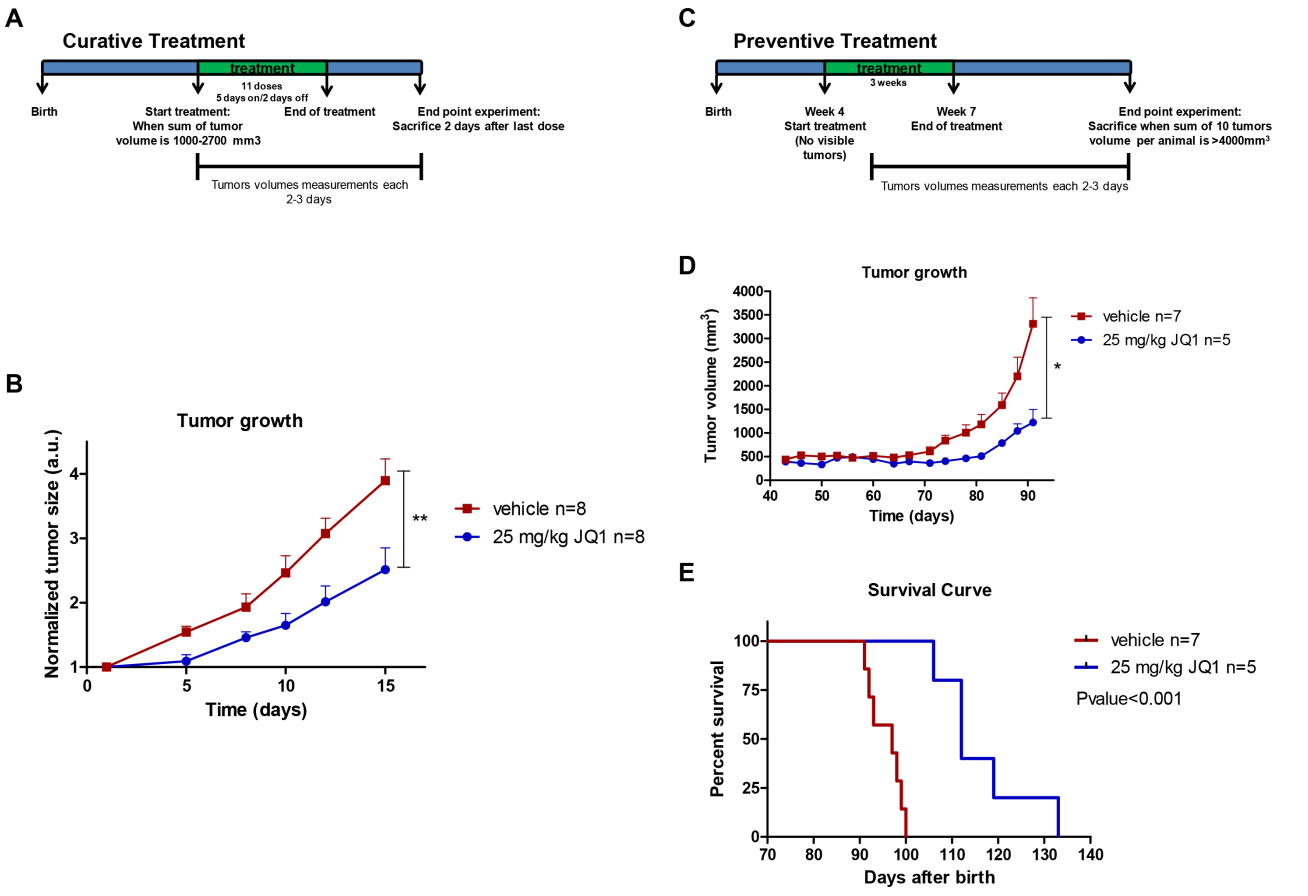

Figure 3: JQ1 treatment inhibits growth and prevents formation of luminal breast tumors in the MMTV-PyMT mouse model. (A) Design of the "curative treatment experiment". **(B)** Tumor volume monitored over time in vehicle- and JQ1-treated MMTV-PyMT mice. **P<0.01. **(C)** Design of the "prevention treatment experiment". **(D)** Tumor volume monitored over time in vehicle- and JQ1-treated MMTV-PyMT mice. *P<0.05. **(E)** Kaplan-Meier survival curves for vehicle- and JQ1-treated MMTV-PyMT mice. Statistical differences tested with Log Rank (Mantel-Cox) test.

and that the target genes can have tumor-type-specific patterns.

Our study also provides at least another interesting indication of the significant role of bromodomain proteins in tumorigenesis. We show that the use of the BET bromodomain inhibitor JQ1 prevents the development of breast cancer in mice. Our results demonstrate that the administration of JQ1 in the MMTV-PyMT significantly delayed the development of breast tumors and increased overall survival. Notably, the treatment of the mice with the epigenetic drug did not result in any evident adverse developmental consequences in these animals. These results, in addition to identifying a key role for bromodomain proteins in breast carcinogenesis, are encouraging as proof-of-concept that these types of compound may be useful in cancer chemoprevention strategies. In this regard, it would be worth pre-clinically testing the efficacy of BET bromodomain inhibitors in diminishing the onset of disease in women at high-risk of developing breast cancer, such as those that are carriers of germline mutations in the tumor suppressor and DNA repair genes BRCA1 and BRCA2. Interestingly, recent findings indicate that the presence of BRCA1 mutations is associated with augmented proliferation of luminal progenitor cells [29–32] and, thus, JQ1 could be used in pre-neoplastic tissue to block these hyperactive cells in their course towards full cancer development.

Finally, it is relevant to mention that although JQ1 was the first-in-class BET bromodomain inhibitor, other drugs have been developed with similar or identical targets [6], such as I-BET151 [33], RVX-208 [34] and OTX015 [15, 35], that can work in the breast cancer models studied and that could be tested. However, all these drugs have common features that interfere with the binding of bromodomain protein to their targets in normal and cancer cells, so far with little specificity. It is in this context that the necessity might emerge for a more personalized cancer treatment using BET bromodomain inhibitors based on the genomic alterations observed in individual patients. In this regard, the presence of point mutations, gene copy number alterations and translocations involving histone acetyltransferases, histone deacetylases and the bromodomain proteins themselves [36–38] could be important biomarkers for predicting the true therapeutic potential of these drugs.

MATERIALS AND METHODS

Cell lines

The human luminal breast cancer cell lines MCF-7 and T47D used in this study were purchased from the American Type Culture Collection (ATCC). MCF-7 and T47D were cultured in DMEM and RPMI, respectively. Both mediums were supplemented with 10% fetal bovine serum and the cells were grown at 37°C and 5% CO_2.

Dose-response assays

For dose-response assays, 3000 cells were seeded in 96-well plates. The optimal number of cells for each experiment was determined to ensure that each one was in growth phase at the assay endpoint. After overnight incubation, experimental medium containing increasing concentrations of JQ1 was added into each well. Cell viability assay was determined at 96 h after treatment, by the 3-(4,5-dimethyl-2-thiazolyl)-2,5-diphenyl-2H-tetrazolium bromide (MTT) assay. Briefly, MTT reagent was added and incubated for 3 h, after which the cells were lysed for 16 h with MTT lysis buffer (50% N-N dimethylformamide, 20% sodium dodecyl sulfate, 2.5% glacial acetic acid, 2.1% 1N HCl, at pH 4.7). Plates were measured at 560 nm using a spectrophotometer.

RNA isolation and quantitative PCR

Total RNA was extracted using a Maxwell® RSC simply RNA Cell Kit (Promega). Real-time PCR reactions were performed following the methods for use of SYBR Green (Applied Biosystems). GAPDH was used as an endogenous control to enable normalization. Specific primers are detailed in Supplementary Table 2.

Immunoblotting assays

Total protein from cells was extracted with Laemmli sample buffer (62.5 mM Tris-HCl pH 6.8, 25% glycerol, 2% SDS, 0.01% bromophenol blue, 5% β-mercaptoethanol). Specific antibodies against target proteins are detailed in Supplementary Table 2.

Gene expression microarray analysis

For expression array analysis, twelve RNA samples were extracted using a Maxwell® RSC simply RNA Cell Kit (Promega) and sent to the CRG Genomics Unit (Barcelona). RNA was extracted from three independent biological replicates treated with JQ1 (1 μM 24h) and three independent biological replicates treated with vehicle (DMSO). Expression data from the Agilent Gene Expression one-color chip human 8x60K microarrays were analyzed with the Bioconductor limma library v3.28 in the R v3.3.0 statistical environment. Briefly, the extracted intensities were background-corrected by applying the normexp calculation. The background-corrected $\log_2$-transformed values were quantile-normalized to make data from all arrays comparable. After filtering out control and low-level expression probes, we applied empirical Bayes statistics within the limma package for two class comparisons in order to calculate the difference in expression between conditions. Transcripts with significant differences (absolute logFC > 1 and adjusted $p < 0.05$) were considered for further analysis. The gene functional annotation analysis was performed

by computing gene overlapping with GSEA KEGG and GO signature collections. We used a hypergeometric test to assess the overrepresentation of specific functions in the gene set tested. The associated hypergeometric p-value was corrected for multiple hypotheses testing according to Benjamini and Hochberg. Finally, we selected the 10 most significant over-represented terms with a False Discovery Rate q-value below 0.05.

Short hairpin interference

Two different sequence gene specific hairpin RNA molecules (shRNAs) for C-MYC, PDZK1, or BCAS1 mRNA were designed and transduced into MCF7 and T47D breast cancer cell lines. shRNA against the MSS2 yeast protein (not present in mammals) was used as scrambled (control). shRNAs and scramble sequences can be found in Supplementary Table 2. All shRNA molecules were ligated into pLVX-shRNA2-ZsGreen plasmid from Clontech, using BamHI and EcoRI restriction enzymes. Each shRNA-encoding plasmid (10 µg) was mixed with 7.5 µg of ps-PAX2 and 2.5 µg of PMD2.G plasmid in 1 ml JetPRIME buffer and 50 µl of JetPRIME. Upon 10 min of RT incubation, the transfection mix was added dropwise on a 10 cm culture plate containing HEK293-TLV lentiviral packaging cells at 80% confluence. After 72 h, medium with high-titer lentiviral particles was 0.45 µm filtered. MCF7 and T47D target cells were cultured in virus containing medium for 24 h. As transduction efficiencies were higher than 95%, and in order to avoid the cloning bias-effect, we chose working with a pool of cells with high expression of shRNA constructs. Cell proliferation was determined by the MTT assay. A total of 1000 cells of MCF7 or 2000 cells of T47D were plated onto 96-well plates in the corresponding medium with vehicle or with 1µM JQ1. MTT was added on 8 consecutive days at a final concentration of 5 mg/mL and further procedure was done as described previously.

Mouse model

MMTV-PyMT$^+$ male mice (FVB/Nj strain) were kindly provided by Dr. Gonzalez-Suarez (IDIBELL, Barcelona, Spain). Transgenic females were obtained by breeding FVB/Nj females with PyMT$^+$ transgenic males. All mouse experiments were approved by the IDIBELL Animal Care and Use Committee and performed in accordance with the guidelines of The International Guiding Principles for Biomedical Research Involving Animals, developed by the Council for International Organizations of Medical Sciences (CIOMS).

Curative *in vivo* treatment

When the total tumor volume of each animal reached ~ 1,000-2,700 mm^3, PyMT$^+$ female mice were randomized into a JQ1 treatment group (25 mg/kg, n=8) and a vehicle (control) group (n=8). JQ1 or vehicle (1:10 DMSO:10% hydroxypropyl β cyclodextrin) was administered daily intraperitoneally for 11 doses on a 5-days-on/2-days-off dosing schedule. Tumor growth was monitored every 2-3 days by measuring tumor width (W) and length (L). Tumor volume, V, was then estimated from the formula $V=\pi/6x(L \times W^2)$ and reported as the sum of all the tumor volumes for each animal and the mean and SEM of each mouse group. Two days after completion of the treatment, mice were euthanized.

Preventive *in vivo* treatment

PyMT$^+$ female mice were randomly divided into a JQ1 treatment group (25 mg/kg, n=5) and a vehicle (control) group (n=7). When mice were 4 weeks old and no palpable or visible tumors were present, JQ1 or vehicle (1:10 DMSO:10% hydroxypropyl β cyclodextrin) were administered intraperitoneally daily for 3 weeks on a 5-days-on/2-days-off dosing schedule. Tumor growth was monitored every 2-3 days by measuring tumor width (W) and length (L). Tumor volume, V, was then estimated from the formula $V=\pi/6x(L \times W^2)$. Mice were euthanized when the total 10 tumor volume per animal was greater than 4,000 mm^3.

Statistical analysis

Real Time Quantitative PCR results were statistically analyzed with a Two samples T test, in the case where JQ1 treated and not treated samples were compared an din the case of shRNA depletion; with a Tukey Multiple comparasions of mean test, in time course experiments cases. Concerning tumor and cell growth experiments we used an AUC Vardi test with 1000 permutations. Kaplan-Meier survival curves statistical differences were tested with Log Rank (Mantel-Cox) test. P values less than 0.05 were considered significant (*P>0.05; **P>0.005; ***P>0.001; n.s = no significance).

ACKNOWLEDGMENTS

We thank the staff of the Animal Core Facility of IDIBELL for mouse care and maintenance.

CONFLICTS OF INTEREST

The authors declare no conflicts of interest.

GRANT SUPPORT

This work was supported by the Instituto de Salud Carlos III (ISCIII), co-financed by the European Development Regional Fund, 'A way to achieve Europe' ERDF, under the TRANSCAN ERA-NET on Translational Cancer Research grant no. AC14/00023 and CANCER13-

FP-011 and the Integrated Project of Excellence no. PIE13/00022 (ONCOPROFILE), the Spanish Cancer Research Network (RTICC) no. RD12/0036/0039, the Cellex Foundation, Obra Social "La Caixa" and the Health and Science Departments of the Catalan Government (Generalitat de Catalunya) AGAUR–project no. 2014SGR633. ME is an ICREA Research Professor.

REFERENCES

1. La Vecchia C, Bosetti C, Lucchini F, Bertuccio P, Negri E, Boyle P, Levi F. Cancer mortality in Europe, 2000-2004, and an overview of trends since 1975. Ann Oncol. 2010; 21:1323-1360.
2. Perou CM, Sørlie T, Eisen MB, van de Rijn M, Jeffrey SS, Rees CA, Pollack JR, Ross DT, Johnsen H, Akslen LA, Fluge O, Pergamenschikov A, Williams C, et al. Molecular portraits of human breast tumours. Nature. 2000; 406:747-752.
3. Cancer Genome Atlas Network. Comprehensive molecular portraits of human breast tumours. Nature 2012; 490:61-70.
4. Prat A, Pineda E, Adamo B, Galván P, Fernández A, Gaba L, Díez M, Viladot M, Arance A, Muñoz M. Clinical implications of the intrinsic molecular subtypes of breast cancer. Breast. 2015; 24:S26-S35.
5. Simó-Riudalbas L, Esteller M. Targeting the histone orthography of cancer: drugs for writers, erasers and readers. Br J Pharmacol. 2015; 172:2716-2732.
6. Pérez-Salvia M, Esteller M. Bromodomain inhibitors and cancer therapy: from structures to applications. Epigenetics. 2017; 12:323-339.
7. Fraga MF, Ballestar E, Villar-Garea A, Boix-Chornet M, Espada J, Schotta G, Bonaldi T, Haydon C, Ropero S, Petrie K, Iyer NG, Pérez-Rosado A, Calvo E, et al. Loss of acetylation at Lys16 and trimethylation at Lys20 of histone H4 is a common hallmark of human cancer. Nat Genet. 2005; 37:391-400.
8. Shi J, Wang Y, Zeng L, Wu Y, Deng J, Zhang Q, Lin Y, Li J, Kang T, Tao M, Rusinova E, Zhang G, Wang C, et al. Disrupting the interaction of BRD4 with diacetylated Twist suppresses tumorigenesis in basal-like breast cancer. Cancer Cell. 2014; 25:210-225.
9. Borbely G, Haldosen LA, Dahlman-Wright K, Zhao C. Induction of USP17 by combining BET and HDAC inhibitors in breast cancer cells. Oncotarget. 2015; 6:33623-33635. doi: 10.18632/oncotarget.5601.
10. Shu S, Lin CY, He HH, Witwicki RM, Tabassum DP, Roberts JM, Janiszewska M, Huh SJ, Liang Y, Ryan J, Doherty E, Mohammed H, Guo H, et al. Response and resistance to BET bromodomain inhibitors in triple-negative breast cancer. Nature. 2016; 529:413-417.
11. da Motta LL, Ledaki I, Purshouse K, Haider S, De Bastiani MA, Baban D, Morotti M, Steers G, Wigfield S, Bridges E, Li JL, Knapp S, Ebner D, et al. The BET inhibitor JQ1 selectively impairs tumour response to hypoxia and downregulates CA9 and angiogenesis in triple negative breast cancer. Oncogene. 2017; 36:122-132.
12. Pérez-Peña J, Serrano-Heras G, Montero JC, Corrales-Sánchez V, Pandiella A, Ocaña A. In silico analysis guides selection of BET inhibitors for triple-negative breast cancer treatment. Mol Cancer Ther. 2016; 15:1823-1833.
13. Andrieu G, Tran AH, Strissel KJ, Denis GV. BRD4 regulates breast cancer dissemination through Jagged1/Notch1 signaling. Cancer Res. 2016; 76:6555-6567.
14. Sahni JM, Gayle SS, Bonk KL, Vite LC, Yori JL, Webb B, Ramos EK, Seachrist DD, Landis MD, Chang JC, Bradner JE, Keri RA. Bromodomain and extraterminal protein inhibition blocks growth of triple-negative breast cancers through the suppression of aurora kinases. J Biol Chem. 2016; 291:23756-23768.
15. Vázquez R, Riveiro ME, Astorgues-Xerri L, Odore E, Rezai K, Erba E, Panini N, Rinaldi A, Kwee I, Beltrame L, Bekradda M, Cvitkovic E, Bertoni F, et al. The bromodomain inhibitor OTX015 (MK-8628) exerts anti-tumor activity in triple-negative breast cancer models as single agent and in combination with everolimus. Oncotarget. 2017; 8:7598-7613. doi: 10.18632/oncotarget.13814.
16. Guy CT, Cardiff RD, Muller WJ. Induction of mammary tumors by expression of polyomavirus middle T oncogene: a transgenic mouse model for metastatic disease. Mol Cell Biol. 1992; 12:954-961.
17. Filippakopoulos P, Qi J, Picaud S, Shen Y, Smith WB, Fedorov O, Morse EM, Keates T, Hickman TT, Felletar I, Philpott M, Munro S, McKeown MR, et al. Selective inhibition of BET bromodomains. Nature. 2010; 468:1067-1073.
18. Kabos P, Haughian JM, Wang X, Dye WW, Finlayson C, Elias A, Horwitz KB, Sartorius CA. Cytokeratin 5 positive cells represent a steroid receptor negative and therapy resistant subpopulation in luminal breast cancers. Breast Cancer Res Treat. 2011; 128:45-55.
19. Iwanaga R, Wang CA, Micalizzi DS, Harrell JC, Jedlicka P, Sartorius CA, Kabos P, Farabaugh SM, Bradford AP, Ford HL. Expression of Six1 in luminal breast cancers predicts poor prognosis and promotes increases in tumor initiating cells by activation of extracellular signal-regulated kinase and transforming growth factor-beta signaling pathways. Breast Cancer Res. 2012; 14:R100.
20. Zubia A, Ropero S, Otaegui D, Ballestar E, Fraga MF, Boix-Chornet M, Berdasco M, Martinez A, Coll-Mulet L, Gil J, Cossío FP, Esteller M. Identification of (1H)-pyrroles as histone deacetylase inhibitors with antitumoral activity. Oncogene. 2009; 28:1477-1484.
21. Carpinelli P, Moll J. Aurora kinases and their inhibitors: more than one target and one drug. Adv Exp Med Biol. 2008; 610:54-73.
22. Huertas D, Soler M, Moreto J, Villanueva A, Martinez A, Vidal A, Charlton M, Moffat D, Patel S, McDermott J, Owen J, Brotherton D, Krige D, et al. Antitumor activity

of a small-molecule inhibitor of the histone kinase Haspin. Oncogene. 2012; 31:1408-1418.

23. Delmore JE, Issa GC, Lemieux ME, Rahl PB, Shi J, Jacobs HM, Kastritis E, Gilpatrick T, Paranal RM, Qi J, Chesi M, Schinzel AC, McKeown MR, et al. BET bromodomain inhibition as a therapeutic strategy to target c-Myc. Cell. 2011; 146:904-917.
24. Mertz JA, Conery AR, Bryant BM, Sandy P, Balasubramanian S, Mele DA, Bergeron L, Sims RJ 3rd. Targeting MYC dependence in cancer by inhibiting BET bromodomains. Proc Natl Acad Sci U S A. 2011; 108:16669-16674.
25. Dunbier AK, Anderson H, Ghazoui Z, Folkerd EJ, A'hern R, Crowder RJ, Hoog J, Smith IE, Osin P, Nerurkar A, Parker JS, Perou CM, Ellis MJ, et al. Relationship between plasma estradiol levels and estrogen-responsive gene expression in estrogen receptor-positive breast cancer in postmenopausal women. J Clin Oncol. 2010; 28:1161-1167.
26. Kim H, Abd Elmageed ZY, Ju J, Naura AS, Abdel-Mageed AB, Varughese S, Paul D, Alahari S, Catling A, Kim JG, Boulares AH. PDZK1 is a novel factor in breast cancer that is indirectly regulated by estrogen through IGF-1R and promotes estrogen-mediated growth. Mol Med. 2013; 19:253-262.
27. Collins C, Rommens JM, Kowbel D, Godfrey T, Tanner M, Hwang SI, Polikoff D, Nonet G, Cochran J, Myambo K, Jay KE, Froula J, Cloutier T, et al. Positional cloning of ZNF217 and NABC1: genes amplified at 20q13.2 and overexpressed in breast carcinoma. Proc Natl Acad Sci U S A. 1998; 95:8703-8708.
28. Fenne IS, Helland T, Flågeng MH, Dankel SN, Mellgren G, Sagen JV. Downregulation of steroid receptor coactivator-2 modulates estrogen-responsive genes and stimulates proliferation of mcf-7 breast cancer cells. PLoS One. 2013; 8:e70096.
29. Lim E, Vaillant F, Wu D, Forrest NC, Pal B, Hart AH, Asselin-Labat ML, Gyorki DE, Ward T, Partanen A, Feleppa F, Huschtscha LI, Thorne HJ, et al. Aberrant luminal progenitors as the candidate target population for basal tumor development in BRCA1 mutation carriers. Nat Med. 2009; 15:907-913.
30. Molyneux G, Geyer FC, Magnay FA, McCarthy A, Kendrick H, Natrajan R, Mackay A, Grigoriadis A, Tutt A, Ashworth A, Reis-Filho JS, Smalley MJ. BRCA1 basal-like breast cancers originate from luminal epithelial progenitors and not from basal stem cells. Cell Stem Cell. 2010; 7:403-417.
31. Proia TA, Keller PJ, Gupta PB, Klebba I, Jones AD, Sedic M, Gilmore H, Tung N, Naber SP, Schnitt S, Lander ES, Kuperwasser C. Genetic predisposition directs breast cancer phenotype by dictating progenitor cell fate. Cell Stem Cell. 2011; 8:149-163.
32. Nolan E, Lindeman GJ, Visvader JE. Out-RANKing BRCA1 in mutation carriers. Cancer Res. 2017; 77:595-600.
33. Dawson MA, Prinjha RK, Dittmann A, Giotopoulos G, Bantscheff M, Chan WI, Robson SC, Chung CW, Hopf C, Savitski MM, Huthmacher C, Gudgin E, Lugo D, et al. Inhibition of BET recruitment to chromatin as an effective treatment for MLL-fusion leukaemia. Nature. 2011; 478:529-533.
34. Picaud S, Wells C, Felletar I, Brotherton D, Martin S, Savitsky P, Diez-Dacal B, Philpott M, Bountra C, Lingard H, Fedorov O, Müller S, Brennan PE, et al. RVX-208, an inhibitor of BET transcriptional regulators with selectivity for the second bromodomain. Proc Natl Acad Sci U S A. 2013; 110:19754-19759.
35. Boi M, Gaudio E, Bonetti P, Kwee I, Bernasconi E, Tarantelli C, Rinaldi A, Testoni M, Cascione L, Ponzoni M, Mensah AA, Stathis A, Stussi G, et al. The BET bromodomain inhibitor OTX015 affects pathogenetic pathways in preclinical B-cell tumor models and synergizes with targeted drugs. Clin Cancer Res. 2015; 21:1628-1638.
36. Simó-Riudalbas L, Esteller M. Cancer genomics identifies disrupted epigenetic genes. Hum Genet. 2014; 133:713-725.
37. Haery L, Thompson RC, Gilmore TD. Histone acetyltransferases and histone deacetylases in B- and T-cell development, physiology and malignancy. GenesCancer. 2015; 6:184-213. doi: 10.18632/genesandcancer.65.
38. Simó-Riudalbas L, Pérez-Salvia M, Setien F, Villanueva A, Moutinho C, Martínez-Cardús A, Moran S, Berdasco M, Gomez A, Vidal E, Soler M, Heyn H, Vaquero A, et al. KAT6B is a tumor suppressor histone H3 lysine 23 acetyltransferase undergoing genomic loss in small cell lung cancer. Cancer Res. 2015; 75:3936-3945.

Bromodomain inhibition shows antitumoral activity in mice and human luminal breast cancer

SUPPLEMENTARY MATERIALS

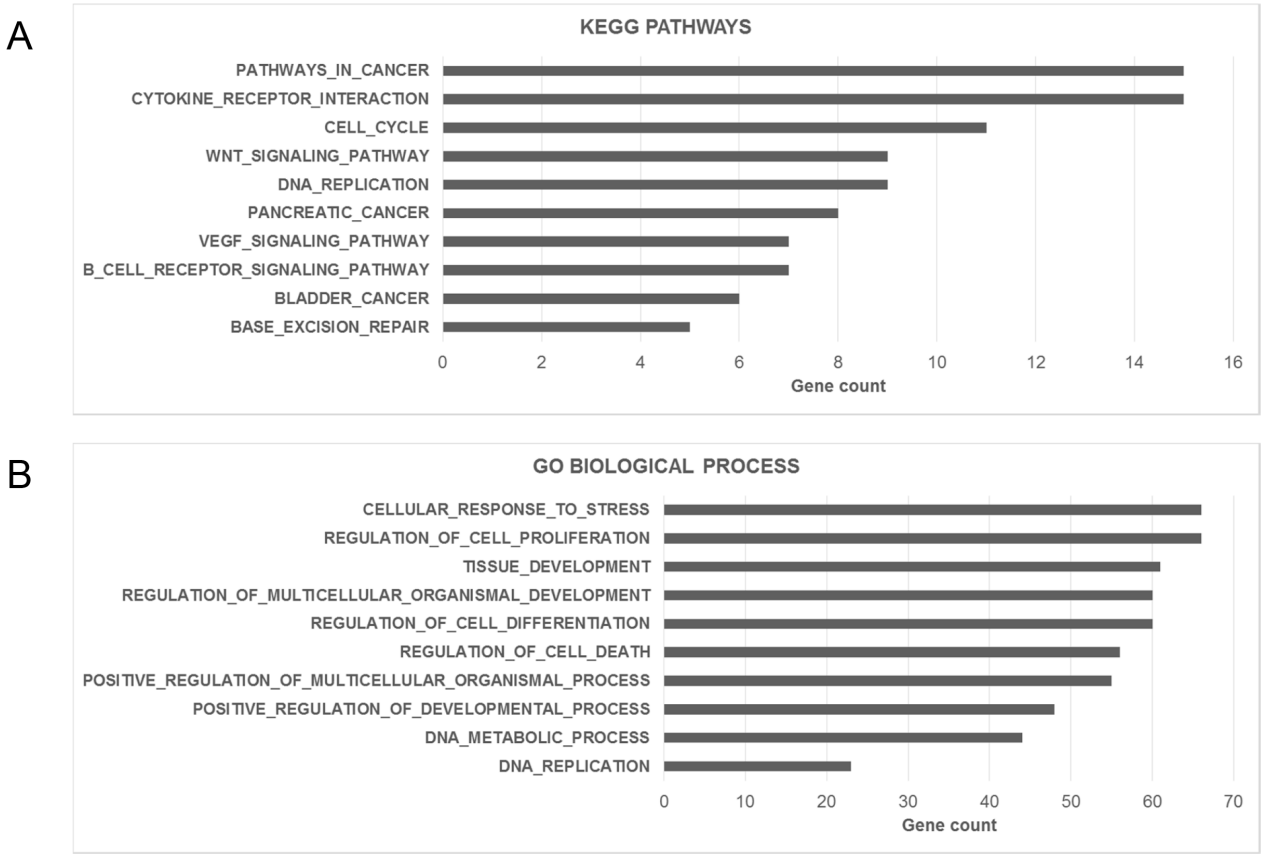

Supplementary Figure 1: Gene functional annotation analyses in both MCF7 and T47D breast cancer cell lines for the downregulated gene set upon JQ1 use. (A) Overrepresented KEGG pathways, **(B)** GO biological process terms.

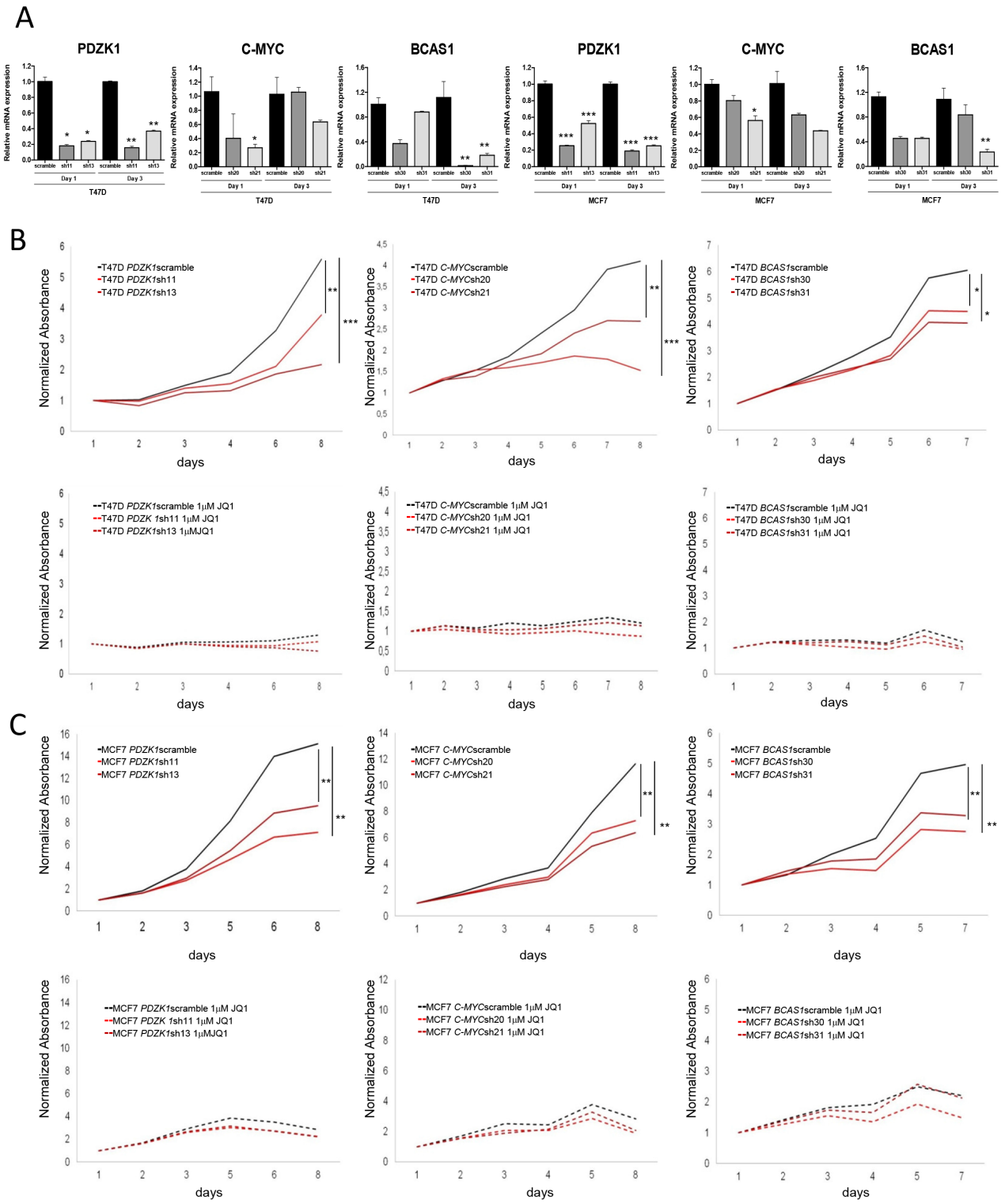

Supplementary Figure 2: Short harpin RNA (shRNA) mediated dowregulation of C-MYC, PDZK1 or BCAS1 in luminal breast cancer cell lines. (A) Quantitative RT-PCR analyses to show the effficient depletion of the target genes upon shRNA use. Effect on cell growth determined by the MTT assay of the shRNA-mediated depletion of C-MYC, PDZK1 or BCAS1 in T47D **(B)** and MCF7 **(C)** cells. Scramble shRNA and two target specific shRNAs for each gene are shown. The use of JQ1 treatment in these shRNAs transduced cells is also represented. *P<0.05; **P<0.01; ***P<0.001.

Supplementary Table 1: KEGG and GO analyses

Gene set name	# Genes in gene set (K)	# Genes in overlap (k)	k/K	p-value	FDR q-value
KEGG_DNA_REPLICATION	36	9	0.25	3.13E-10	5.82E-08
KEGG_CELL_CYCLE	128	11	0.0859	4.19E-07	3.90E-05
KEGG_CYTOKINE_RECEPTOR_INTERACTION	267	15	0.0562	9.09E-07	5.63E-05
KEGG_PANCREATIC_CANCER	70	8	0.1143	1.87E-06	8.68E-05
KEGG_BLADDER_CANCER	42	6	0.1429	9.98E-06	3.44E-04
KEGG_PATHWAYS_IN_CANCER	328	15	0.0457	1.11E-05	3.44E-04
KEGG_B_CELL_RECEPTOR_SIGNALING_ PATHWAY	75	7	0.0933	3.18E-05	8.05E-04
KEGG_VEGF_SIGNALING_PATHWAY	76	7	0.0921	3.46E-05	8.05E-04
KEGG_BASE_EXCISION_REPAIR	35	5	0.1429	5.62E-05	1.16E-03
KEGG_WNT_SIGNALING_PATHWAY	151	9	0.0596	8.77E-05	1.62E-03
GO_REGULATION_OF_CELL_PROLIFERATION	1496	66	0.0441	6.90E-20	3.06E-16
GO_CELLULAR_RESPONSE_TO_STRESS	1565	66	0.0422	6.93E-19	1.54E-15
GO_DNA_METABOLIC_PROCESS	758	44	0.058	8.05E-18	1.19E-14
GO_TISSUE_DEVELOPMENT	1518	61	0.0402	1.55E-16	1.72E-13
GO_REGULATION_OF_CELL_DIFFERENTIATION	1492	60	0.0402	2.71E-16	2.40E-13
GO_DNA_REPLICATION	208	23	0.1106	9.84E-16	7.27E-13
GO_POSITIVE_REGULATION_OF_ MULTICELLULAR_ORGANISMAL_PROCESS	1395	55	0.0394	1.17E-14	7.43E-12
GO_REGULATION_OF_CELL_DEATH	1472	56	0.038	2.90E-14	1.61E-11
GO_REGULATION_OF_MULTICELLULAR_ ORGANISMAL_DEVELOPMENT	1672	60	0.0359	4.13E-14	2.04E-11
GO_POSITIVE_REGULATION_OF_ DEVELOPMENTAL_PROCESS	1142	48	0.042	6.27E-14	2.78E-11

Top, Overrepresented KEGG pathways corresponding to the significant downregulated genes in MCF7 and T47D cell lines. The table shows the genes overlapping each gene set and the associated hypergeometric test's p-value. *Below*, Overrepresented GO biological process terms corresponding to the significant downregulated genes in MCF7 and T47D cell lines. The table shows the genes overlapping each gene set and the associated hypergeometric test's p-value.

Supplementary Table 2: Primers for qRT-PCR, antibodies used in the western blot and shRNAs sequences

Primers for qRT-PCR				
BRD4_Hs_qPCR_F	CAACAAGCCTGGAGATGACA			
BRD4_Hs_qPCR_R	GGAGGAGTCGATGCTTGAGT			
MYC_Hs_qPCR_F	CCGCTTCTCTGAAAGGCTCT			
MYC_Hs_qPCR_R	AAGCTAACGTTGAGGGGCAT			
PDZK1_Hs_qPCR_F	AAACTCTGCAGGCTGGCTAA			
PDZK1_Hs_qPCR_R	TCCACCACCTTCTCATAGGG			
BCAS1_Hs_qPCR_F	CCAGAAGGACTGGAGACTGC			
BCAS1_Hs_qPCR_R	CTTGGGTCTCCTGGGATGTA			
GAPDH_Hs_qPCR_F	GAAGGTGAAGGTCGGAGTCA			
GAPDH_Hs_qPCR_R	TGGACTTCACGACGTACTCA			
Antibodies name	**Reference**	**Company**	**Application**	**Dilution**
Anti-BRD4	ab128874	Abcam	WB	1:1000
C-MYC (D84C12)	5605	Cell signaling	WB	1:1000
Actin-beta HRP	A3854	Sigma	WB	1:20000
Lentiviral shRNAs				
Scramble_F	gatccGCGCAGAACAAATTCGTCCATTCAAGAGATGGACGAATTTGTTCTGCGTTTTTTACGCGTg			
Scramble_R	aattcACGCGTAAAAAACGCAGAACAAATTCGTCCATCTCTTGAATGGACGAATTTGTTCTGCGCg			
PDZK1_sh11_F	gatccGCCTTCAAGATGGAGACAGATTCAAGAGATCTGTCTCCATCTTGAAGGTTTTTTACGCGTg			
PDZK1_sh11_R	aattcACGCGTAAAAAACCTTCAAGATGGAGACAGATCTCTTGAATCTGTCTCCATCTTGAAGGCg			
PDZK1_sh13_F	gatccGGTGGACTTGAAAGAGTTGTTCAAGAGACAACTCTTTCAAGTCCACCTTTTTTACGCGTg			
PDZK1_sh13_R	aattcACGCGTAAAAAAGGTGGACTTGAAAGAGTTGTCTCTTGAACAACTCTTTCAAGTCCACCg			
MYC_sh20_F	gatccGCACGAAACTTTGCCCATAGTTCAAGAGACTATGGGCAAAGTTTCGTGTTTTTTACGCGTg			
MYC_sh20_R	aattcACGCGTAAAAAACACGAAACTTTGCCCATAGTCTCTTGAACTATGGGCAAAGTTTCGTGCg			
MYC_sh21_F	gatccGCTTCACCAACAGGAACTATTCAAGAGATAGTTCCTGTTGGTGAAGCTTTTTTACGCGTg			
MYC_sh21_R	aattcACGCGTAAAAAAGCTTCACCAACAGGAACTATCTCTTGAATAGTTCCTGTTGGTGAAGCg			
BCAS1_sh30_F	gatccACCAGAAGCAGAGACTTACTTCAAGAGAGTAAGTCTCTGCTTCTGGTTTTTTTACGCGTg			
BCAS1_sh30_R	aattcACGCGTAAAAAAACCAGAAGCAGAGACTTACTCTCTTGAAGTAAGTCTCTGCTTCTGGTg			
BCAS1_sh31_F	gatccGCACACAGTTCAGCACTTAGTTCAAGAGACTAAGTGCTGAACTGTGTGTTTTTTACGCGTg			
BCAS1_sh31_R	aattcACGCGTAAAAAACACACAGTTCAGCACTTAGTCTCTTGAACTAAGTGCTGAACTGTGTGCg			

In vitro and *in vivo* activity of a new small-molecule inhibitor of HDAC6 in mantle cell lymphoma

Cancer origin and development is associated not only with genetic alterations, but also with the disturbance of epigenetic profiles.[1] In this regard, the tumoral epigenome is characterized by both specific and general shifts in the DNA methylation and histone-modification landscapes.[1] However, in contrast to genetic disruption, the effect of epigenetic modifications or marks may potentially be reversed by the use of drugs that target enzymes involved in adding, removing or signaling DNA methylation and histone modifications.[1] This basic knowledge has been adopted into clinical practice, and inhibitors of histone deacetylases and DNA demethylating agents have been approved for use in the therapy of hematologic malignancies, such as cutaneous T-cell lymphoma and myelodysplastic syndrome, respectively.[2] Other promising epigenetic drugs include inhibitors of histone methyltransferases,[2] histone demethylases,[2] histone kinases,[3] and bromodomain proteins that interfere with the 'reading' of acetylated histone residues.[4,5]

Histone deacetylase 6 (HDAC6) is a protein modifier that is an increasingly attractive pharmacological target. It is a member of class IIb of the histone deacetylase family, together with HDAC10.[6] Unlike most HDACs, HDAC6 is expressed primarily in the cytoplasm and its deacetylase activity involves mainly non-histone substrates, such as the cytoskeletal protein α-tubulin and the heatshock protein Hsp90. In this way, it plays an important role in microtubule dynamics and chaperone signaling.[6] HDAC6 is involved in various human diseases, and in cancer promotes tumor initiation, development, and metastasis, having been shown to be over-expressed in various tumor types. Interestingly, the observation that the HDAC6 knock-out mouse is not lethal[7] in contrast to those undergoing complete loss of class I, II and III HDACs, suggests that specific HDAC6 inhibitors may be better tolerated than pan-HDAC inhibitors or drugs that target the other HDAC classes. In this regard, the compounds tubacin, its derivative tubastatin A and ACY-1215 (Ricolinostat) are selective HDAC6 inhibitors.[8] The latter agent is undergoing clinical trials as a single agent or in combination for the treatment of multiple myeloma and other tumors (*clinicaltrials.gov identifiers: 01997840, 01323751, 02189343, 01583283*). Given the interest in HDAC6 inhibition, we decided to design, synthesize, and test the activity of new small-molecule inhibitors of HDAC6 that could have a potential antitumor impact.

Almost all HDAC inhibitors, including those of HDAC6, share a typical structure comprising three primary regions: i) a zinc-chelating group that binds the zinc

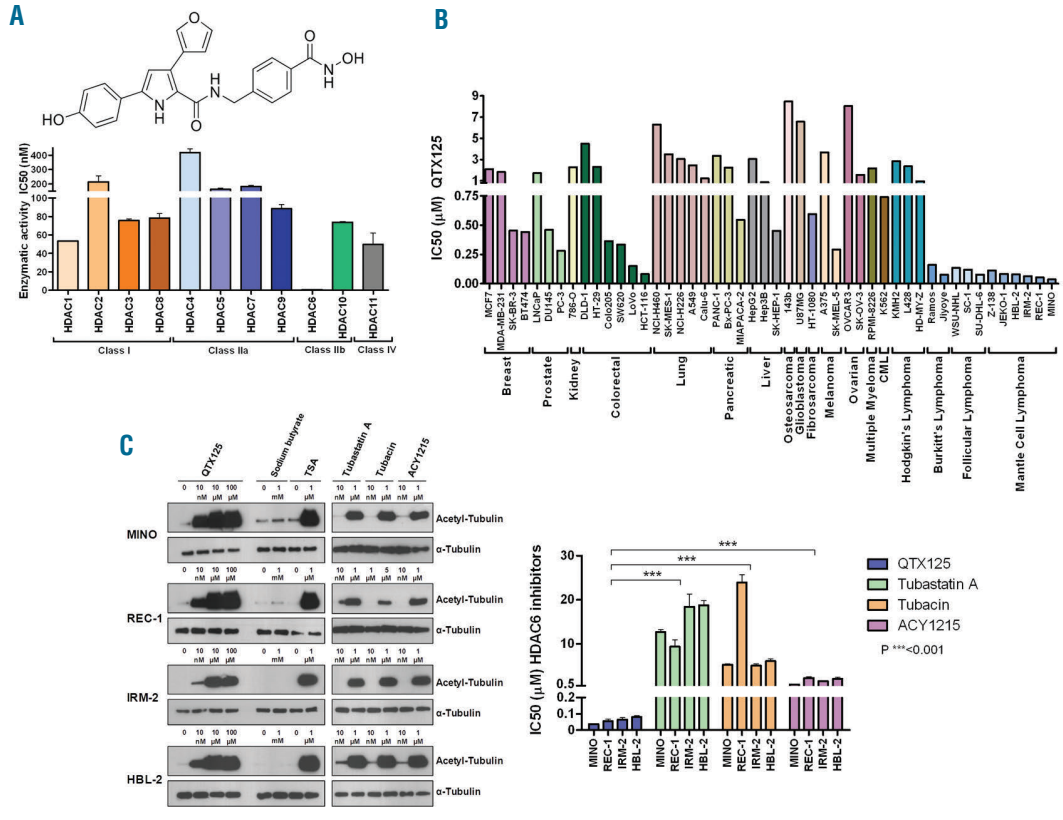

Figure 1. Chemical structure and HDAC specificity of QTX125 and its effect on α-tubulin acetylation and cell growth. (A) (Top) Chemical structure of QTX125. (Below) *In vitro* enzymatic activity of 11 HDACs upon QTX125 use. (B) Growth-inhibitory effect of QTX125 in cancer cell lines determined by the MTS assay. (C) (Left) Western-blot assays in MINO, REC-1, IRM-2 and HBL-2 cells show the induction of α-tubulin hyperacetylation upon QTX125 administration. Sodium butyrate is shown as an HDAC inhibitor that does not affect HDAC6 (negative control). TSA is shown as an HDAC inhibitor that affects all HDAC classes, including HDAC6 (positive control). The effect of the three available specific HDAC6 inhibitors (tubastatin A, tubacin, and ACY1215) is also shown. Total α-tubulin is used as a loading control. (Right) Growth-inhibitory effect of QTX125 in the mantle cell lymphoma cell lines determined by the MTS assay in comparison to the other, previously described HDAC6 inhibitors. CML: chronic myelogenous leukemia.

ion present at the active site, preventing activation of the enzyme (typically, a hydroxamic acid in HDAC6 inhibitors); ii) a hydrophobic linker region that mimics the 1,4-butylene alkyl chain of the lysine residue present in the natural substrates of HDACs; and iii) a filling-cap group, usually an aromatic or heteroaromatic ring, that binds to the substrate-binding region of the enzyme and fills the entrance to the hydrophobic channel. Variations in one or more of these regions may result in greater selectivity to one isoform than the others. Thus, the HDAC6 hydrophobic channel appears wider than that of other HDAC subtypes, suggesting that replacement of the traditional alkyl chain linker with bulkier and shorter aromatic moieties might enhance HDAC6 selectivity. Taking into account these HDAC6 inhibitor structures, the structural differences between HDAC6 and other HDAC isoforms (and also the structural information of our previously developed HDAC inhibitors[9]), a new potential HDAC6 selective inhibitor was designed and synthesized: QTX125 [3-(3-furyl)-N-{4-[(hydroxyamino)carbonyl]benzyl}-5-(4-hydroxyphenyl)-1H-pyrrole-2-carboxamide] (Figure 1A). QTX125 was synthesized by means of a 7-step synthetic procedure, starting with an aldol condensation reaction of 4-hydroxyacetophenone with 3-furaldehyde to obtain the corresponding α,β-unsaturated ketone. This ketone was then treated with ethyl nitroacetate and triethylamine, the mixture obtained being oxidized by means of the Nef reaction with sodium ethoxide to yield the corresponding γ-ketoester. Through a cyclization reaction of this ester in the presence of ammonium salts,[10] good yields of the ethyl 3-(furan-3-yl)-5-(4-hydroxyphenyl)-1H-pyrrole-2-carboxylate were obtained. Deprotection of the methyl ester group of the pyrrole, and coupling with the methyl 4-(aminomethyl)benzoate yielded the corresponding amide. Further elaboration produced the final hydroxamic acid. It is noteworthy that, as designed, the synthesis is well-suited to kilogram-scale production.

The selectivity of QTX125 for inhibiting HDAC6 function in comparison with all the other HDACs was measured by determining the *in vitro* enzymatic activity of 50 μM of each acetylated AMC-labeled peptide substrate

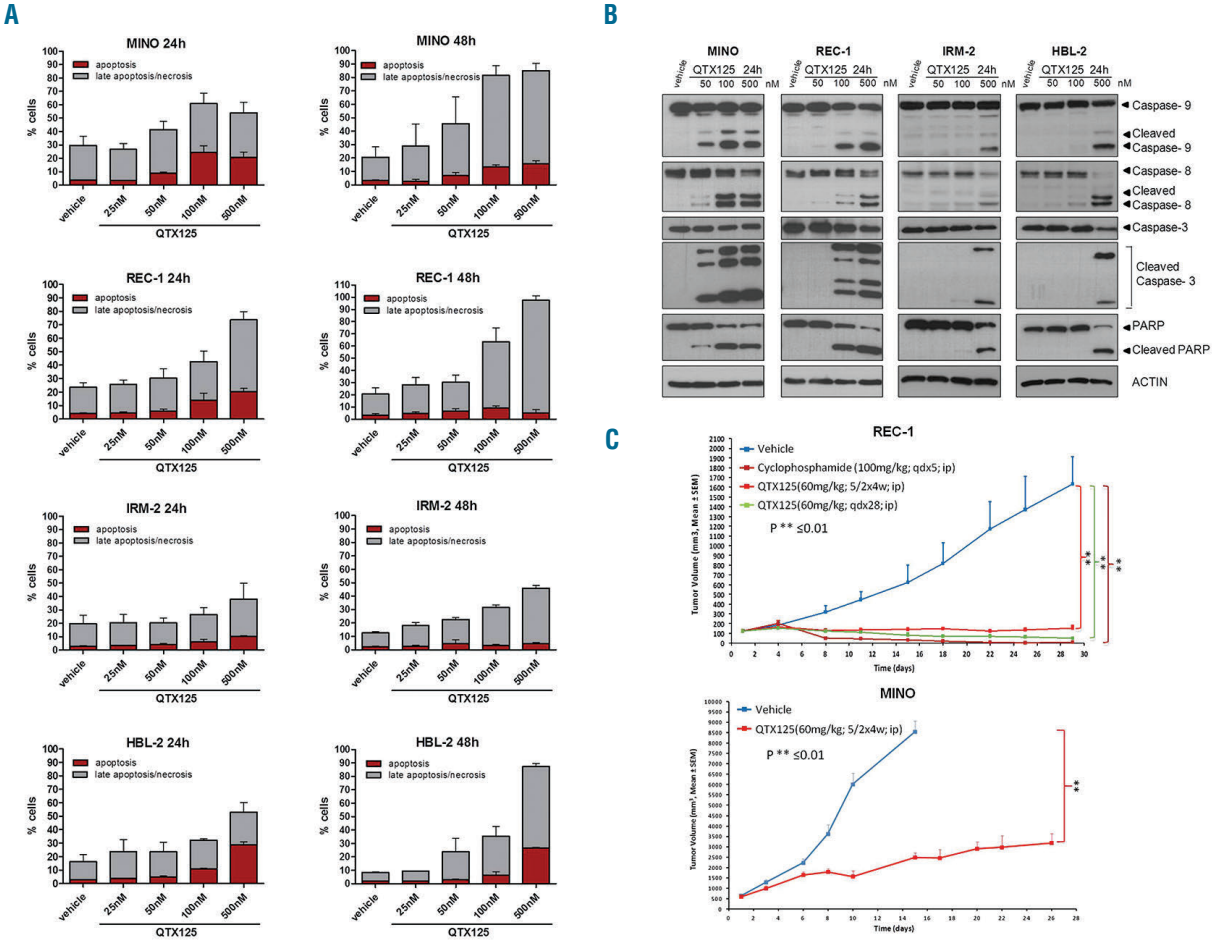

Figure 2. QTX125 use in mantle cell lymphoma (MCL) induces cell death by apoptosis and inhibits lymphoma growth in xenografted mice. (A) Quantification of the flow cytometry values of annexin V/PI incorporation (Alexa Fluor® 488 Annexin V/Dead Cell Apoptosis Kit, Invitrogen) to show the proapoptotic effect of QTX125 on the MCL cell lines MINO, REC-1, IRM-2 and HBL-2. (B) Induction of programmed cell death upon QTX125 administration shown by the cleavage of caspase-9, caspase-8, caspase-3, and PARP in the western blot assay. Actin is used as a loading control. (C) Antitumoral activity of QTX125 in REC-1 and MINO xenografts in nude mice. For REC-1, tumor volume was monitored over time in vehicle and QTX125-treated (two regimens) and cyclophosphamide-treated mice (Mann–Whitney U-test). qdx5: daily dosing for 5 days; 5/2x4w: 5 days of dosing/2 days off for 4 weeks; qdx28: daily dosing for 28 days. For MINO, tumor volume was monitored over time in vehicle and and QTX125-treated mice (5/2x4w: 5 days of dosing/2 days off for 4 weeks). The vehicle group arm was stopped at 15 days for ethical reasons.

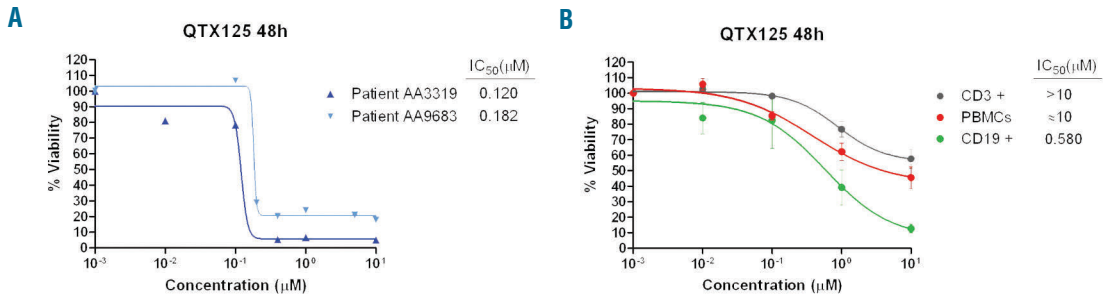

Figure 3. QTX125 use in primary mantle cell lymphoma (MCL) samples and normal blood. (A) Effect of QTX125 in cell viability determined by flow cytometry of AnnexinV/7AAD negative cells in primary MCL samples from the patients AA3319 and AA9683. IC50 values are shown for each sample. (B) Effect of QTX125 in cell viability determined by flow cytometry of AnnexinV/7AAD negative cells in peripheral blood mononuclear cells (PBMCs), $CD3^+$ and $CD19^+$ cells obtained from healthy donors (n=4). IC50 values are shown for each sample.

and an optimal concentration of the corresponding enzyme (HDAC1, HDAC2, HDAC3, HDAC4, HDAC5, HDAC6, HDAC7, HDAC8, HDAC9, HDAC10 and HDAC11) (*Online Supplementary Appendix*). QTX125 demonstrated an exceptional specificity for inhibiting HDAC6 enzymatic activity (Figure 1A). To test the capacity of QTX125 as an antitumor agent, we first determined the 72-hour IC50 values using the MTS [3-(4,5-dimethylthiazol-2-yl)-5-(3-carboxymethoxyphenyl)-2-(4-sulfophenyl)-2H-tetrazolium] assay in a panel of 48 human cancer cell lines, including solid tumors (breast, prostate, kidney, colorectal, lung, pancreas, liver, osteosarcoma, glioblastoma, fibrosarcoma, melanoma, and ovarian cancer), and hematologic malignancies [chronic myelogenous leukemia, multiple myeloma, Hodgkin lymphoma, Burkitt cell lymphoma, follicular lymphoma, and mantle cell lymphoma (MCL)] (*Online Supplementary Appendix*). We observed that QTX125 had the strongest growth-inhibitory effect in Burkitt cell lymphoma, follicular lymphoma, and MCL (Figure 1B).

Mantle cell lymphoma therapy constitutes an unmet medical need because there is no single accepted treatment approach for the disease.[11] R-CHOP (rituximab, cyclophosphamide, doxorubicin, vincristine, prednisone) is a common first-line therapeutic approach, but is of limited duration.[12] Due to the antitumoral effect of QTX125 in MCL cell lines and its specificity in blocking HDAC6 activity that we observed here, we decided to characterize in detail QTX125 in MCL, further encouraged by the finding that HDAC6 activity is essential for MCL growth.[13] The growth-inhibitory effect of QTX125 at nanomolar levels in the aforementioned MCL cell lines was confirmed by the 3-(4,5-dimethylthiazol-2-yl)-2,5-diphenyltetrazolium bromide (MTT) assay, and the cell count of alive cells by trypan blue staining and by flow cytometry of AnnexinV/PI (*Online Supplementary Figure S1*). A further analysis of the MCL cell lines MINO, REC-1, IRM-2 and HBL-2 also showed that the use of QTX125 induced dose-dependent hyperacetylation of α-tubulin (Figure 1C), the best known target of HDAC6, thus providing further validation that the drug targets this particular enzyme. Trichostatin A was used as a general inhibitor for HDAC classes I, IIa, IIB (including HDAC6) and IV, whereas sodium butyrate was used as an HDAC inhibitor that does not affect HDAC6 (Figure 1C).[14] The three available HDAC6 inhibitors (tubastatin A, tubacin, and ACY1215) were also used as specific positive controls for HDAC6-inhibition-mediated hyperacetylation of α-tubulin (Figure 1C). Importantly, QTX125 was able to induce α-tubulin acetylation even at 10 nM concentration, whereas the other HDAC6 inhibitors did not (Figure 1C). In our MCL cell lines, and with QTX125, we did not observe any increase in CD20 expression as occurs with other HDAC6 inhibitors in Burkitt and diffuse large B-cell lymphoma cell lines[15] (*Online Supplementary Figure S2*). Strikingly, QTX125 was the most powerful inhibitor of growth in the MCL cell lines compared with the other three HDAC6 inhibitors reported (Figure 1C).

We also showed that the observed inhibition of cell proliferation upon QTX125 administration was associated with the induction of subsequent apoptosis demonstrated by annexin V/propidium iodide double staining (Figure 2A) and the cleavage of caspase-9, caspase-8, caspase-3, and PARP (Figure 2B) (*Online Supplementary Appendix*). Finally, we translated our experiments from the *in vitro* assays described above to the *in vivo* setting of a mouse model. The antitumor activity of QTX125 was evaluated using REC-1 cells xenografted in nude mice (*Online Supplementary Appendix*). We randomly selected 8 mice as the control group treated with vehicle and another 8 for QTX125 treatments (intraperitoneal administration of 60 mg/kg in two different regimens). Tumor volume was monitored every two days. The use of the HDAC6 inhibitor QTX125 was significantly associated with the inhibition of lymphoma growth in comparison to the control group (Figure 2C). The extent of blockage of tumor growth was similar to that observed in xenografted lymphomas treated with cyclophosphamide, a DNA alkylating drug commonly used in MCL therapy.[11,12] Use of QTX125 was also associated with the growth inhibition of a second xenografted MCL cell line, MINO (Figure 2C). The cytotoxicity of QTX125 was also evaluated in 2 primary samples obtained from patients with MCL (see *Online Supplementary Table S1* for details of patients' samples). Incubation with QTX125 strongly reduced cell viability, with IC50 values of 0.120 and 0.182 μM. (Figure 3A). Non-malignant lymphocytes, such as peripheral blood mononuclear cells (PBMCs), $CD3^+$ cells (T cells) and $CD19^+$ (B cells) were more resistant to QTX125–mediated growth inhibition (Figure 3B) than MCL cell lines (*Online Supplementary Figure S1*) or MCL primary samples (Figure 3A).

Overall, our results show that the QTX125 compound obtained is a new HDAC6-specific inhibitor that inhibits cell-growth inhibition and causes programmed cell death in association with increased levels of acetylated α-tubulin, its most recognizable target. The antitumoral effect is particularly evident in MCL models, both in culture and *in vivo*, surpassing the efficacy of currently available HDAC6 inhibitors. We demonstrate, therefore, the effi-

cacy of QTX125 in the pre-clinical setting and suggest it warrants further assessment as a novel candidate agent for use in epigenetic lymphoma therapy.

Montserrat Pérez-Salvia,[1] Eneko Aldaba,[2] Yosu Vara,[2] Myriam Fabre,[3] Cristina Ferrer,[3] Carme Masdeu,[4] Aizpea Zubia,[5] Eider San Sebastian,[5] Dorleta Otaegui,[6] Pere Llinàs-Arias,[1] Margalida Rosselló-Tortella,[1] Maria Berdasco,[1] Catia Moutinho,[1] Fernando Setien,[1] Alberto Villanueva,[7] Eva González-Barca,[8] Josep Muncunill,[9] José-Tomás Navarro,[9] Miguel A. Piris,[10] Fernando P. Cossio,[5] and Manel Esteller[1,11,12,13]

[1]Cancer Epigenetics and Biology Program (PEBC), Bellvitge Biomedical Research Institute (IDIBELL) L'Hospitalet, Barcelona, Catalonia; [2]Quimatryx, San Sebastian; [3]Oncomatryx, Arteaga Auzoa, 43, Derio; [4]Department of Organic Chemistry I, Universidad del País Vasco/Euskal Herriko Unibertsitatea (UPV/EHU), San Sebastián; [5]Department of Organic Chemistry I, Centro de Innovación en Química Avanzada (ORFEO-CINQA), Universidad del País Vasco/Euskal Herriko Unibertsitatea (UPV/EHU), Donostia International Physics Center (DIPC), San Sebastián; [6]Mass Spectrometry Platform, CIC biomaGUNE, San Sebastian; [7]Laboratory of Translational Research, Catalan Institute of Oncology (ICO), IDIBELL L'Hospitalet, Barcelona, Catalonia; [8]Department of Hematology, ICO-Hospital Duran i Reynals, IDIBELL, University of Barcelona, L'Hospitalet, Barcelona, Catalonia; [9]Department of Hematology, ICO-Hospital Universitari Germans Trias i Pujol, Josep Carreras Leukaemia Research Institute, Universitat Autònoma de Barcelona, Badalona, Catalonia; [10]Pathology Service, Fundación Jiménez Díaz, Madrid; [11]Centro de Investigacion Biomedica en Red Cancer (CIBERONC), Madrid; [12]Physiological Sciences Department, School of Medicine and Health Sciences, University of Barcelona (UB), L'Hospitalet, Catalonia and [13]Institucio Catalana de Recerca i Estudis Avançats (ICREA), Barcelona, Catalonia, Spain

Funding: this work was supported by the Institute of Health Carlos III (ISCIII), co-financed by the European Development Regional Fund, 'A way to achieve Europe' ERDF, under I-PFIS contract no. IFI17/00006. M.P.S. was supported by a Formacion de Profesorado Universitario (FPU) fellowship from Spanish Ministery of Education.

Correspondence: mesteller@idibell.cat

doi:10.3324/haematol.2018.189241

Information on authorship, contributions, and financial & other disclosures was provided by the authors and is available with the online version of this article at www.haematologica.org.

References

1. Rodríguez-Paredes M, Esteller M. Cancer epigenetics reaches mainstream oncology. Nat Med. 2011;17(3):330-339.
2. Jones PA, Issa JP, Baylin S. Targeting the cancer epigenome for therapy. Nat Rev Genet. 2016;17(10):630-641.
3. Huertas D, Soler M, Moreto J, et al. Antitumor activity of a small-molecule inhibitor of the histone kinase Haspin. Oncogene. 2012; 318(11):1408-1418.
4. Filippakopoulos P, Knapp S. Targeting bromodomains: epigenetic readers of lysine acetylation. Nat Rev Drug Discov. 2014;13(5):337-356.
5. Pérez-Salvia M, Simó-Riudalbas L, Llinàs-Arias P, et al. Bromodomain inhibition shows antitumoral activity in mice and human luminal breast cancer. Oncotarget. 2017;8(31):51621-51629.
6. Seidel C, Schnekenburger M, Dicato M, Diederich M. Histone deacetylase 6 in health and disease. Epigenomics. 2015;7(1):103-118.
7. Govindarajan N, Rao P, Burkhardt S, et al. Reducing HDAC6 ameliorates cognitive deficits in a mouse model for Alzheimer's disease. EMBO Mol Med. 2013;5(1):52-63.
8. Lernoux M, Schnekenburger M, Dicato M, Diederich M. Anti-cancer effects of naturally derived compounds targeting histone deacetylase 6-related pathways. Pharmacol Res. 2018;129:337-356
9. Zubia A, Ropero S, Otaegui D, et al. Identification of (1H)-pyrroles as histone deacetylase inhibitors with antitumoral activity. Oncogene 2009;28(11):1477-1484.
10. Aginagalde M, Bello T, Masdeu C, Vara Y, Arrieta A, Cossío FP. Formation of γ–oxoacids and 1H-pyrrol-2(5H)-ones from α,β–unsaturated ketones and ethyl nitroacetate. J Org Chem. 2010; 75(21):7435-7438.
11. Spurgeon SE, Till BG, Martin P, et al. Recommendations for clinical trial development in mantle cell lymphoma. J Natl Cancer Inst. 2016; 109(1):djw263.
12. Howard OM, Gribben JG, Neuberg DS, et al. Rituximab and CHOP induction therapy for newly diagnosed mantle-cell lymphoma: molecular complete responses are not predictive of progression-free survival. J Clin Oncol. 2002;20(5):1288-1294.
13. Lwin T, Zhao X, Cheng F, et al. A microenvironment-mediated c-Myc/miR-548m/HDAC6 amplification loop in non-Hodgkin B cell lymphomas. J Clin Invest. 2013;123(11):4612-4626.
14. Zhang Y, Li N, Caron C, et al. HDAC-6 interacts with and deacetylates tubulin and microtubules in vivo. EMBO J. 2003;22(5):1168-1179.
15. Bobrowicz M, Dwojak M, Pyrzynska B, et al. HDAC6 inhibition upregulates CD20 levels and increases the efficacy of anti-CD20 monoclonal antibodies. Blood. 2017;130(14):1628-1638.